UNIVERSITA' DEGLI STUDI DI MILANO-BICOCCA
Facoltà di Scienze Matematiche, Fisiche e Naturali
Dottorato di Ricerca in Biologia XXIII Ciclo

CHARACTERIZATION OF HUMAN SIALIDASE NEU4: ROLE OF THE PROLINE-RICH REGION IN SIGNAL TRANSDUCTION

Tesi di Dottorato di:
Dott.ssa ALESSANDRA BIGI
Matr. 041269

Coordinatore del Dottorato: Prof. Enzo WANKE
Tutor: Dott.ssa Paola FUSI

Anno Accademico 2009/2010

Table of contents

List of abbreviations

Tables and Figures Index

Abstract

Chapter 1. Introduction 1

1.1 Sialic acids 2

1.1.1 Sialic acid structure 2

1.1.2 Sialic acid occurrence.....3

1.1.3 Sialic acid function.....3

1.1.4 Sialic acid metabolism.....6

1.2. Sialidases (EC 3.2.1.18).....9

1.2.1 Sialidase - historical.....9

1.2.2 Sialidase primary structure 10

1.2.3 Sialidase three-dimensional structure 10

1.2.4 Substrate requirements of sialidases 11

1.2.5 Catalytic mechanism of sialidases.....12

1.2.6 Sialidase gene evolution.....13

1.2.7 Sialidase substrates and their pathological roles 14

1.2.8 Biological function of sialidases.....18

1.2.9 Sialidases in disease 21

1.3. Mammalian sialidases 23

1.3.1 Introduction 23

1.3.2 Tissue and cellular distribution of mammalian sialidases.....23

1.3.3 Molecular cloning of mammalian sialidases 27

1.3.4 Molecular properties of cloned human sialidases 29

1.3.5 Expression and transfection studies.....33

1.3.6 Three-dimensional structures of human sialidases 34

1.3.7 Evolutionary aspects of sialidases 36

1.3.8 Physiological roles of human sialidases 38

1.3.9 Assembly and physiological role of multi-protein complexation of sialidase 39

1.3.10 Pathological conditions associated with sialidase deficiency 40

1.3.11 Sialidase and muscle cell differentiation 43

1.3.12 Sialidase in nervous tissue 43

1.3.13 Aberrant expression of sialidase in cancer 45

1.4. The human sialidase NEU4 51

1.4.1 Identification of human NEU4 gene 51

1.4.2 Molecular properties of human NEU4 protein 53

1.4.3 Enzymatic properties of human NEU4 sialidase 54

1.4.4 Expression of NEU4 in human tissues 55

1.4.5 Subcellular localization of human NEU4 56

1.4.6 Physiological and pathological roles of human NEU4 58

Chapter 2. Aim of the Thesis 67

Chapter 3. Materials and Methods 69

3.1 Reagents and antibodies 70

3.2 Vectors 70

3.3 Cell cultures, transfection and treatments 71

3.4 Homology molecular modeling 72

3.5 RNA isolation, RT-PCR and Q-PCR 72

3.6 Solubilzation experiments 73

3.7 Cross-linking with paraformaldehyde 74

3.8 Confocal immunofluorescence microscopy 74

3.9 Subcellular fractionation and mitochondria isolation 75

3.10 Mitoplasts isolation and protease treatment 76

3.11 Protein extraction 76

3.12 Co-immunoprecipitation experiments 77

3.13 Glycoproten analysis 77

3.14 Proliferation assays 77

3.15 Neurite outgrowth evaluation 78

3.16 Sialidase and acetylcholinesterase assays 78

3.17 SDS-PAGE and western blotting 78

3.18 Statistical analysis 79

Chapter 4. Results 81

4.1 Human sialidase NEU4 long and short are extrinsic proteins bound to outer mitochondrial membrane and the endoplasmic reticulm, respectively 82

4.1.1 NEU4 long and NEU4 short are extrinsic membrane proteins. 82

4.1.2 NEU4 long and NEU4 short are anchored to membranes through protein-protein interactions 83

4.1.3 The long form of NEU4 localizes in mitochondria, while the short form is bound to the endoplasmic reticulum 83

4.1.4 The long form of NEU4 is bound to outer mitochondrial membrane 85

4.2 The proline-rich region does not directly affect NEU4 association to membranes 98

4.2.1 Deletion mutants of NEU4 lacking the Pro-rich region show catalytic properties similar to those of corresponding wild-type enzymes 98

4.2.2 The Pro-rich region is not responsible for the intracellular distribution of both NEU4 long and short 99

4.2.3 The deletion of the Pro-rich region does not increased the solubility of NEU4 long protein 99

4.2.4 The deletion of the Pro-rich region does not affect the interaction of NEU4 long with proteins putatively involved in its anchorage to membranes 100

4.3 The proline-rich region increases cell proliferation and activity towards glycoproteins 107

4.3.1 Expression of wild-type and mutated NEU4 long in SK-N-BE cells.....107

4.3.2 The Pro-rich region of NEU4 long promotes alterations of sialoglycoprotein profile 108

4.3.3 The Pro-rich loop of NEU4 plays a role in increasing proliferation rate in SK-N-BE cells.....109

4.4 Expression of NEU4 accelerates retinoic acid incuced neuronal differentiation.....116

4.4.1 Retinoic acid treatment increases expression of myc-tagged NEU4 proteins, either wild-tyoe or mutated.....116

4.4.2 Expression of NEU4 long increased neurite outgrowth induced by retinoic acid treatment.....117

4.5 The proline-rich region mediates interaction between NEU4 and Akt in SK-N-BE cells.....124

4.5.1 NEU4 Pro-rich sequence possesses consensus motifs for both Akt and Erk1 kinases.....124

4.5.2 Involvement of NEU4 expression in both Erk1/2 MAPK and PI3K/Akt signaling pathways in SK-N-BE cells 124

4.5.3 NEU4 interacts with Akt kinase through its proline-rich region 125

4.5.4 PI3K/Akt signaling pathway is required for RA induced neuronal differentiation in SK-N-BE cells 126

Chapter 5. Discussion.....133

Chapter 6. References.....143

List of abbreviations

4MU-NeuAc, 4-methylumbelliferyl-N-acetyl-α-D-neuraminic acid
AchE, acetylcholinesterase
BSA, bovine serum albumin
Cav-1, caveolin-1
CHAPS, 3-[(3-Cholamidopropyl)dimethylammonio]-1-propanesulfonate
Cnx, calnexin
COX IV, cytochrome c oxidase
Cyt c, cytochrome c
DAKO, DakoCytomation Fluorescent Mounting Medium
DMEM, Dulbecco's Modified Eagle's Medium
DTT, dithiothreitol
ECL, enhanced chemioluminescence
EDTA, ethylenediaminetetraacetic acid
EEA1, early endosomal antigen 1
EGTA, ethylene glycol tetraacetic acid
Erk1/2, extracellular regulated kinase 1 and 2
FBS, fetal bovine serum
GPI, glycosylphosphatidylinositol
HRP, horseradish peroxidase
LAMP-1, lysosome-associated membrane protein 1
MAA, *Maackia amurensis* agglutinin
MAPK, mitogen-activated protein kinase
MTT, [3-(4,5-dimethylthiazol-2-yl)-2,5-diphenyl tetrazolium bromide]
N4L, NEU4 long
N4LnoP, mutant NEU4 long
N4S, NEU4 short
N4SnoP, mutant NEU4 short
PBS, phosphate buffered saline
PDI, protein disulfide-isomerase
PFA, paraformaldehyde
PGK, 3-phosphoglycerate kinase
PI3K, phosphatidylinositol 3-kinase
PMSF, phenylmethylsulfonyl fluoride
PVDF, polyvinylidine difluoride
Q-PCR, quantitative-polymerase chain reaction
RA, retinoic acid
RIPA, radio immunoprecipitation assay
RT-PCR, reverse transcription-polymerase chain reaction
SNA, *Sambucus nigra* agglutinin
SDS-PAGE, sodium dodecyl sulfate-polyacrylamide gel electrophoresis
SOD2, superoxide dismutase 2
TBS, tris buffered saline
TIMM50, translocase of inner mitochondrial membrane, subunit 50
TOMM22, translocase of outer mitochondrial membrane, subunit 22
VDAC1/Porin, voltage-dependent anion channel

Tables and Figures Index

Table

1-1 Sialic acid-metabolizing enzymes....6

1-2 General functions of glycosphingolipids (GSLs)....18

1-3 Distribution of mammalian sialidases....24

1-4 Comparison of the amino acid properties of mammalian sialidases....33

3-1 List of primers used for NEU4 cDNAs production....71

3-2 List of primers used for RT-PCR....73

3-3 List of human primers used for Q-PCR....73

Figure

1-1 Chemical structure of the sialic acid molecule and a list of natural substituents....2

1-2 *N*-acetylneuraminic acid (Neu5Ac)....3

1-3 The masking function of sialic acids: mechanism of binding (b) and phagocytosis (c) of sialidase-treated erythrocytes (a) by macrophages....5

1-4 Metabolism of sialic acids....7

1-5 Secondary structure model of the sialidase protein from *Salmonella typhimurium* with the bound inhibitor Neu2en5Ac....11

1-6 The pathway of biosynthesis of o-, a-, b- and c-series gangliosides....15

1-7 Structures of representative sphingolipids....16

1-8 Gene structure of the human NEU1, NEU2, NEU3, and NEU4 genes....29

1-9 Multiple amino acid sequence alignment of sialidases....32

1-10 A gene family tree of mammalian sialidases constructed from the sequences of NEU protein family members....33

1-11 Structural changes of NEU2 upon maltose and DANA binding....36

1-12 A possible mechanism of apoptosis regulation by NEU3 in cancer cells....50

1-13 Functional relationship of three sialidases in human cancer cells and a possible role of NEU3 as a potential target for cancer diagnosis and therapy

.....51

1-14 Deduced amino acid sequence of the human NEU4 sialidase 52

1-15 Alignment of the amino acid sequences of human NEU4, the putative mouse ortholog, human NEU3, and human NEU2.....53

1-16 GD3-mediated apoptosis.....62

4-1 Partition of NEU4 long and NEU4 short proteins during Triton X-114 phase separation 87

4-2 Extraction of NEU4 short and NEU4 long upon sodium carbonate treatment.....88

4-3 Cross-linking with paraformaldehyde and analysis of NEU4 long containing complexes 89

4-4 Cross-linking with paraformaldehyde and analysis of NEU4 containing complexes.....89

4-5 Subcellular localization of NEU4 long and NEU4 short determined by indirect immunofluorescence staining.....90

4-6 Time course of NEU4 long and NEU4 short expression in COS-7 cells monitored by indirect immunofluorescence staining.....92

4-7 Mitochondrial localization of NEU4 long and NEU4 short in COS-7 and HeLa cells determined by indirect immunofluorescence staining.....93

4-8 Coexpression of NEU4 long and NEU4 short in COS-7 and HeLa cells evaluated by indirect immunofluorescence staining 94

4-9 Intracellular distribution of NEU4 long and NEU4 short evaluated by subcellular fractionation 95

4-10 Recovery of NEU4 long or NEU4 short in a purified heavy mitochondrial fraction 96

4-11 Submitochondrial localization of the long form of NEU4 97

4-12 Human sialidase NEU4 possesses a proline-rich region in the sequence.....101

4-13 Homology modeling of both wild-type and mutated NEU4 long.....102

4-14 Sialidase activity of both wild-type and mutated NEU4 short.....103

4-15 Subcellular localization of NEU4 long and NEU4 short mutants determined by indirect immunofluorescence staining.....104

4-16 Submitochondrial localization of both wild-type and mutated NEU4 long 105

4-17 Extraction of both wild-type and mutated NEU4 long upon sodium carbonate treatment.....105

4-18 Cross-linking with paraformaldehyde and analysis of wild-type or mutated NEU4 long containing complexes.....106

4-19 Differential expression of both wild-type and mutated NEU4 long in stable transfected SK-N-BE clones 111

4-20 Differential expression of human sialidases in SK-N-BE clones 112

4-21 Expression of both wild-type and mutated NEU4 long in SK-N-BE clones.....113

4-22 Sialoglycoprotein profile of SK-N-BE clones 114

4-23 Effect of both wild-type and mutated NEU4 long on cell proliferation 115

4-24 Expression of wild-type and mutated NEU4 long in RA treated SK-N-BE clones.....120

4-25 Acetylcholinesterase activity during RA induced differentiation 121

4-26 Role of NEU4 Pro-rich region in neurite formation during RA induced differentiation.....122

4-27 Role of NEU4 in neurite formation during RA induced differentiation 123

4-28 Recognition motifs for both Akt and Erk1/2 kinases in NEU4 proline-rich region 128

4-29 Activation of PI3K/Akt and Erk1/2 pathways in RA treated SK-N-BE clones.....129

4-30 NEU4 long interacts with Akt kinase in SK-N-BE cells.....130

4-31 Role of PI3K/Akt pathway in RA induced neurite outgrowth 131

Abstract

Sialidases or neuraminidases are glycohydrolytic enzymes removing sialic acid residues from glycoproteins and glycolipids. They are widely distributed in nature, from microorganisms to vertebrates. In mammals, four sialidases with different subcellular localization and biochemical features have been described: a lysosomal sialidase (NEU1), a cytosolic sialidase (NEU2), and two membrane-associated sialidases (NEU3 and NEU4). NEU4, the most recently identified member of the human sialidase family, is found in two forms, long and short, differing in the presence of a 12 amino acids sequence at the N-terminus of the protein. Contradictory data are present in the literature about the subcellular distribution of these enzymes, and their membrane anchoring mechanism is still unclear.

First of all, in this work we investigated NEU4 long and NEU4 short membrane anchoring mechanism and their subcellular localization in COS-7 and HeLa cells. As observed by solubilization and cross-linking experiments, NEU4 long and short are extrinsic membrane proteins, probably associated to the lipid bilayer through protein-protein interactions. These results are in accordance with primary structure analysis that did not evidence any transmembrane sequence, nor the presence of any membrane binding motifs. Subcellular localization studies, performed through confocal immunofluorescence and subcellular fractionation, showed that human NEU4 is a membrane-bound enzyme; in particular, the long form of NEU4 localizes in mitochondria, while the short one is mainly associated with the endoplasmic reticulum. In addition, a finer submitochondrial fractionation and a protease treatment of intact mitochondria and mitoplasts provided evidence for NEU4 long location in the outer mitochondrial membrane.

Moreover, primary structure analysis showed the presence of a proline-rich region which is unique to NEU4, having no counterpart in any other human sialidase. Deletion mutants lacking this loop showed subcellular distributions similar to those of wild-type proteins in COS-7 cells, suggesting that this region does not directly affect the association of NEU4 to the membranes. We subsequently hypothesized an involvement in the interaction with signaling pathway components.

Studies in collaboration with the Department of Medical Chemistry, Biochemistry and Biotechnology (L.I.T.A.) of the University of Milano evaluated the effect of NEU4 long transfection in human neuroblastoma SK-N-BE cell line. Similarly, we produced stable SK-N-BE clones transfected with the mutated form of NEU4 long (N4LnoP). The mRNA level of both NEU4 and the other human sialidases were checked in both wild-type and mutated NEU4 clones by RT-PCR and real-time PCR. In addition, only the wild-type form of NEU4 long was able to alterate the sialoglycoprotein profile and significantly enhance the proliferative ability of SK-N-BE cells, suggesting that the Pro-rich region of NEU4 is involved in both these phenomena. Subsequently, in order to study the function of NEU4 in SK-N-BE cell line, we analyzed the effect of NEU4 expression also under retinoic acid induced differentiating conditions. Our results show that retinoic acid treatment increases the expression of NEU4, either wild-type or mutated, due to the presence of RA response elements (RARE) in the CMV promoter.

In addition, both morphological change analysis and neurite outgrowth quantification were consistent with acetylcholinesterase activity data, indicating a role for NEU4 long and its Pro-rich region in the early phases of retinoic acid induced neuronal differentiation process.

Since potential Akt and Erk1 kinase motifs were found in NEU4 proline-rich region, activation of both phosphatidylinositol 3-kinase (PI3K)/Akt and mitogen-activated protein kinase (MAPK) signaling pathways were studied in stable SK-N-BE clones. Our results demonstrate that the expression of NEU4, both wild-type and mutated, does not significantly affect retinoic acid induced activation of both Akt and Erk1/2 pathways in SK-N-BE cells, suggesting that NEU4 could be located in a downstream place in these signaling pathways. As confirmed by immunoprecipitation experiments, NEU4 long interacts with Akt kinase in SK-N-BE cells. Conversely, the lacking of the proline-rich region impaired interaction between NEU4 and Akt, indicating that the formation of NEU4-Akt complex occurs through the proline-rich region. On the contrary, no interactions between NEU4 and Erk1/2 kinase were observed, suggesting that NEU4 is not a substrate of this kinase. Finally, treatment with LY294002 PI3K inhibitor demonstrates that PI3K/Akt signaling pathway is required for neuronal differentiation induced by retinoic acid in this neuroblastoma cell line. On the whole, these data suggest that NEU4 long is a downstream component of Akt signaling pathway required for RA induced neuronal differentiation in SK-N-BE cells.

1. Introduction

1.1 Sialic acids

1.1.1 Sialic acid structure

Sialic acids are a family of about 40 derivatives of the nine-carbon sugar neuraminic acid[1,2]. The amino group at position 5 and the carboxyl group at position 1 confers a negative charge to the molecule under physiological conditions and characterizes it as a strong organic acid (pK 2.2; Figure 1-1).

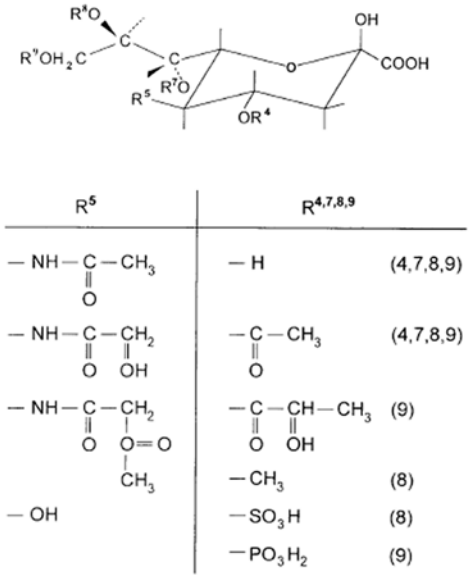

Figure 1-1 Chemical structure of the sialic acid molecule and a list of natural substituents.
(Traving, C. & Schauer, R. *Cell Mol Life Sci* 1998)

The unsubstituted form, neuraminic acid, does not exist in nature. The amino group is usually acetylated, leading to *N*-acetylneuraminic acid (Neu5Ac), the most widespread form of sialic acid (Figure 1-2). Substituting one of the hydrogen atoms in the methyl moiety of the acetyl group by a hydroxyl group results in *N*-glycolylneuraminic acid (Neu5Gc), which is common in many animal species but has been found in humans only in the case of particular cancers. Another significant modification is the esterification of the hydroxyl groups mainly at positions 7, 8 and 9 with acetic acid, whereas this so-called *O*-acetylation is more rarely found at position 4, for example in horses[3]. A number of other modifications of the sialic acid molecule are known, including introduction of a lactoyl group at position 9 and of a sulfate or a methyl group at position 8, the latter of which has been found in gangliosides from the starfish *Asterias rubens*[2]. Sialic acid molecules can be substituted in more than one position, for example in 7,8,9-tri-*O*-acetyl-*N*-acetyl- or *N*-glycolylneuraminic acid. An unusual

modification of the sugar is the deamination at position 5, leading to the C-5 deaminated sugar 2-keto3-deoxy-nonulosonic acid (KDN), that has been found in sperm and eggs of teleost fish[2]. Both sialic acids 2,3-didehydro-Neu5Ac (Neu5Ac2en) and 2,7-anhydro-Neu5Ac occur only in the 'free' state, since they lack the glycosidic linkage forming hydroxyl groups. Modifications to hydroxyl groups include methylation, acylation, phosphorylation, and sulfation, or unsaturation at C-2/C-3[4].

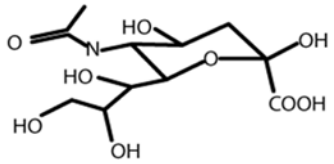

Figure 1-2 *N*-acetylneuraminic acid (Neu5Ac).

There exists a specific pattern of sialic acid derivatives depending on the tissue and the developmental stage of each individual species[2]. The variability of sialic acids is further extended by their location on cells and molecules. In humans, normally only small amounts of 'free' sialic acids are present. Sialic acids usually represent the terminal, non-reducing sugar moiety in glycoproteins or glycolipids linked to galactose (α2-3 or α2-6), *N*-acetylgalactosamine (GalNAc), or *N*-acetylglucosamine (α2-6) (GlcNAc). Sialic acids that occur as side chains are linked via C2 to position 3 or 6 of the penultimate sugar, while sialic acids that are internal to oligosaccharides, polysaccharides of glycoproteins, or glycolipids are linked to position 8 of another sialic acid molecule, as well as in bacterial capsules and gangliosides of higher animals[5]. Co-polymers of sialic acid via α2-8, α 2-9, or α 2-8/α2-9 linkages result in polysialic acids, common in embryonic tissue glycoproteins, and could play a role in cell adhesion and organogenesis[6].

1.1.2 Sialic acid occurrence

Sialic acids have been found in the animal kingdom, from the echinoderms, such as starfish[7], upwards to humans[8], whereas there is no hint of their existence in lower animals of the protostomate lineage or in plants, except for buckwheat[9]. The only known exception is the occurrence of polysialic acid in the larvae of the insect *Drosophila*[6]. In addition, there are sialic acids in some protozoa, viruses and bacteria[1,10,11]. Thus, several strains of *Escherichia coli* contain long saccharide stretches consisting of up to 200 sialic acid molecules, the so-called colominic acid. Sialoglycoconjugates are present on cell surfaces as well as in intracellular membranes (e.g., of the Golgi apparatus). In higher animals they are also important components of the serum and of mucous substances.

1.1.3 Sialic acid function

The structural diversity of sialic acid is reflected in the variety of its biological functions, including blood protein half-life regulation, variety of

toxin neutralization, cellular adhesion and glycoprotein lytic protection[5,12,13]. Sialic acids play important roles in various biological processes by influencing the conformation of glycoproteins, recognizing and masking the biological sites of the molecules and their binding sites to the cells[14]. Due to their negative charge, sialic acids are involved in binding and transport of positively charged molecules (e.g. Ca^{2+}) as well as in attraction and repulsion phenomena related to cellular and molecular recognition. Their exposed terminal position in carbohydrate chains, in addition to their size and negative charge, enable them to function as a protective shield for the subterminal part of the molecule (preventing e.g. glycoproteins from being degraded by proteases) or cell (as is the case for the mucous layer of the respiratory epithelium). In infectious processes, the colonization of bacteria is prevented by the sialic acid coat covering the host cell surface. Another phenomenon is the spreading effect that is exerted on sialic acid-containing molecules due to the repulsive forces acting between their negative charges[15]. This stabilizes the correct conformation of enzyme or cell membrane (glyco) proteins, and is important for the slimy character and the resulting protective function of mucous substances, such as on the surface of the eye or on mucous epithelia.

Another important feature of sialic acids is the masking of cells and molecules (Figure 1-3). Erythrocytes are covered by a dense layer of sialic acid molecules. During the normal life span of red blood cells, sialic acids are removed stepwise from the cell surface by the action of serum sialidase and by spontaneous chemical hydrolysis. The exposure of the penultimate galactose residues represent signals for degradation of the respective blood cells. Finally, the unmasked erythrocytes are bound to macrophages and phagocytosed[16]. Thus, sialic acids prevent erythrocytes from being degraded, because they mask the subterminal galactose residues. The same mechanism works on other blood cells (thrombocytes and leucocytes) and on various serum glycoproteins, which are bound by hepatocytes after exposure of subterminal galactose residues. However, masking of endogenous structures can also have a detrimental effect, as can be seen in the case of some tumors that are sialylated to a much higher degree than the corresponding normal tissues. Consequently, the transformed cells become ‘invisible’ to the immune defense system. The immunosuppressive effect of the higher degree of sialylation in tumors is due to an increased activity of sialyl-transferases. Thus, terminal galactose residues that would otherwise inhibit further cell growth and spreading are masked. This might be one reason for the loss of contact inhibition of cancer cells[17]. The masking effect of sialic acids also helps to hide antigenic sites on parasite cells from the host immune system. This is the case for microbial species like certain *E. coli* strains and gonococci as *Neisseria gonorrhoeae*[18].

In addition to their roles in masking subterminal sugars and preventing cell-cell interactions through nonspecific charge repulsion effects, sialic acid residues are also well suited as ligands for mediating selective recognition processes between cells and molecules[1,12]. Thus, the immune system can distinguish between self and nonself structures according to their sialic acid pattern. Sialic acid represents, for example, blood group antigenic determinants, and is a necessary component of receptors for many

endogenous substances such as hormones and cytokines. In addition, many pathogenic agents such as toxins (e.g. cholera toxin), viruses (e.g.influenza), bacteria (e.g. *Escherichia coli*, *Helicobacter pylori*) and protozoa (e.g. *Trypanosoma cruzi*) also bind to host cells via sialic acid-containing receptors[1].

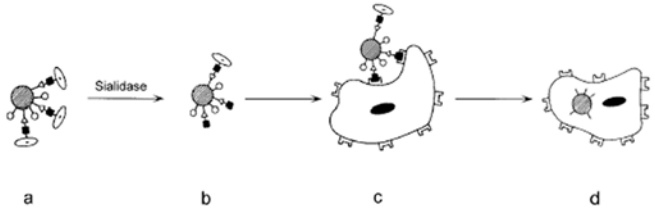

Figure 1-3 The masking function of sialic acids: mechanism of binding (b) and phagocytosis (c) of sialidase-treated erythrocytes (a) by macrophages.
(Traving, C. & Schauer, R. *Cell Mol Life Sci* 1998)

Another group of sialic acid-recognizing molecules belongs to the so-called lectins. They are usually oligomeric glycoproteins from plants, animals and invertebrates that bind to specific sugar residues. Very common sialic acid-binding lectins are wheat germ agglutinin (WGA), *Limulus polyphemus* agglutinin (LPA), *Sambucus nigra* agglutinin (SNA) and *Maackia amurensis* agglutinin (MAA), which are specific for α2-6-linked and α2-3-linked sialic acids. Plants do not have sialic acids. Therefore, these lectins might be helpful in the defense against sialic acid-containing microorganisms or plant-eating mammals. In mammals, there exist counterparts of lectins, including selectins as well as members of the sialoadhesin family ('siglecs')[19] such as sialoadhesin (Sn), CD22, CD33, myelin-associated glycoprotein (MAG) and Schwann cell myelin protein (SMP)[20]. Selectin and siglec molecules consist of several domains, one of which is responsible for sialic acid binding. Selectins play an important function in the initial stage of adhesion of white blood cells to endothelia, the so-called rolling of the cells, which may be followed by extravasation of leukocytes from the circulation into tissue sites. They are located on endothelial cells and recognize sialic acids in the sialyl Lewis $(Le)^x$ and sialyl Le^a structure on the surface of leucocytes. Because these molecules are also present on tumor cells, selectins might be involved in tumor metastasis. CD22, a member of the immunoglobulin superfamily, is a type I membrane glycoprotein expressed in B cells. It mediates binding of B cells to other B or T cells, neutrophiles, monocytes or erythrocytes. The ligand of CD22 is sialic acid bound in α2-6 linkage to branched *N*-linked oligosaccharides. Sialoadhesin was found on macrophages and is thought to be important for the development of myeloid cells in the bone marrow and trafficking of leucocytes in lymphatic tissues. Binding between these receptors and their ligands depends on the presence of only a few functional groups of the oligosaccharide. Thus, these receptors bind as well to low-affinity ligands that are presented in high density on a cell surface as to a

low number of high-affinity ligands. Thus, a better fine tuning of cell-cell interactions is possible, as required for very specific recognition processes.

1.1.4 Sialic acid metabolism

Sialic acid biosynthesis and degradation

In view of the diverse structures of sialic acids and the various biological roles attributed to these sugars, enzymes involved in the metabolism of sialic acids assume significance. Several of the sialic acid-metabolizing enzymes are listed in Table 1-1.

Table 1-1 Sialic acid-metabolizing enzymes.
(Achyuthan, K. E. & Achyuthan, A. M. *Comp Biochem Physiol B Biochem Mol Biol* 2001)

Enzyme	Catalytic activity/function	Reference
Neu5Ac aldolase	Sialic acid synthesis from pyruvic acid and *N*-acetyl-D-mannosamine	Tuppy and Gottschalk, 1972
Sialyl transferase	Transfers sialic acid to polysaccharides, glycoproteins or glycolipids. Also transfer of nucleotide-linked sialic acid to glycoconjugates	Datta and Paulson, 1997
Esterase	Hydrolyzes *O*-acetyl groups in sialic acid	Klein and Roussel, 1998
Endosialidase	Hydrolyzes sialic acid linkages internal to molecules	Long et al., 1993
Trans-sialidase	Transfers sialic acid from polysaccharides to water or with greater preference to glycan chains	Frasch, 1994
Sialidase L	Releases 2,7-anhydro-Neu5Ac from Neu5Ac-α2–3-galactose linkages	Chou et al., 1996
KDNase	Releases KDN residues from sialoglyco-conjugates; some can also hydrolyze α-ketosides of Neu5Ac	Terada et al., 1997; Pavlova et al., 1999
Bi-functional enzyme	Hemagglutinin-sialidase of paramyxoviruses; capable of hemagglutinin and sialidase activity	Taylor, 1996
Exo-α-sialidase	Hydrolyzes terminal sialic acid in glycoconjugates	References in this review

The reactions of sialic acid synthesis and degradation are distributed among different cell compartments (Figure 1-4). The *N*-acetylneuraminic acid (Neu5Ac) is synthesized from *N*-acetylmannosamine-6-phosphate and phospoenolpyruvate in the cytosol by the catalytic activity of Neu5Ac aldolase. After dephosphorylation of the reaction product, Neu5Ac-9-phosphate, the molecule is activated in the nucleus by the transfer of a cytidine monophosphate (CMP) residue from cytidine triphosphate (CTP) through CMP-Neu5Ac synthase. This sugar nucleotide is the only natural case of a *β* linkage between sialic acid and another compound, because in glycoconjugates an α is always present. CMP-Neu5Ac is then translocated into the Golgi apparatus or the endoplasmic reticulum[3,12]. There, the transfer of the activated sialic acid (nucleotide-linked sialic acid) to the oligosaccharide chain of a nascent glycoconjugate is accomplished by sialyltransferase. The bound sialic acid can then be modified by *O*-acetylation or *O*-methylation before transport of the mature glycoconjugate to the cell surface, whereas the only modification that takes place before the transfer onto the glycoconjugate is the hydroxylation of the *N*-acetyl group of CMP-Neu5Ac, which leads to CMP-Neu5Gc in the cytosol[4].

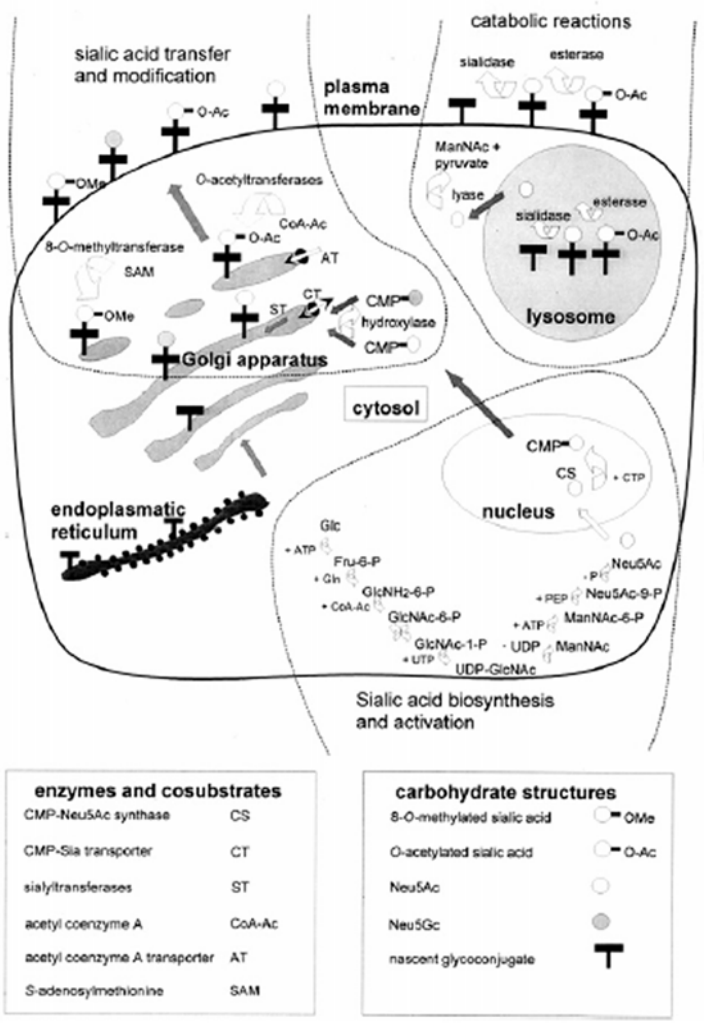

Figure 1-4 Metabolism of sialic acids.
(Traving, C. & Schauer, R. *Cell Mol Life Sci* 1998)

The key enzymes of sialic acid catabolism are sialidases, exoglycosidase that hydrolyze the glycosidic linkage between sialic acid molecules and the penultimate sugar of the carbohydrate chains of oligosaccharides and glycoconjugates. Sialic acid residues can be removed from cell surface or serum sialoglycoconjugates by membrane-bound sialidases. Usually, the glycoconjugates that are prone to degradation are taken up by receptor-mediated endocytosis in higher animals. After fusion of the endosome with a lysosome, the terminal sialic acid residues are removed by lysosomal sialidases. In contrast, the corresponding microbial enzymes are mostly secreted to get into contact with their substrates in the environment. Esterases hydrolyze the *O*-acetyl groups in sialic acids[21]. A

prerequisite for the effective action of sialidases is the removal of *O*-acetyl groups by the hydrolytic action of sialate *O*-acetyl esterases[1], whereas bound Neu5Gc is a fairly good substrate. Free sialic acid molecules (Neu5Ac or Neu5Gc) are transported through the lysosomal membrane into the cytosol, from where they can be recycled by activation and transfer onto another nascent glycoconjugate molecule in the Golgi. Alternatively, they can be retransferred onto glycoconjugates by sialyltransferases after activation to CMP-Neu5Ac or further degraded to acylmannosamine and pyruvate by acylneuraminate lyases.

Sialidase-like enzymes

We can find two types of sialidases. Endo-α-sialidase (E.C. 3.2.1.129) hydrolyzes sialic acid linkages internal to macromolecules, while exo-α-sialidase (EC 3.2.1.18) remove terminal sialic acid moieties from glycoproteins, glycopeptides, gangliosides, oligosaccharides and polysaccharides. Bacteriophage KIE endosialidase is the protein responsible for initial binding to host *Escherichia coli* K1 bacteria. Bacteriophage E expresses endosialidase activity with specificity for α2-8-linked poly-*N*-acetylneuraminic acid (polysialic acid; PSA) carbohydrate polymers of the K1 glycocalyx. Unlike exosialidases, bacteriophage E endosialidase was not inhibited by the active site-directed, transition state analog Neu5Ac2en. The protein in paramyxoviruses (parainfluenza virus, mumps virus, and Newcastle disease viruses) is bifunctional, capable of hemagglutination and sialidase activity[22].

A special sialidase subgroup is represented by the trans-sialidases, which combine the features of sialidases and sialyltransferases. In fact, trans-sialidases are capable of dual catalytic activity: 'normal' sialidase activity, as well as transferring the sialic acid to non-sialylated glycan chains[23].These enzymes preferably transfer the sialic acid molecule directly from one glycosidic linkage onto another sugar residue instead of a water molecule. The most common 'alternative' acceptor molecule is β-galactose, as a terminal component of oligosaccharides and glycoproteins. The involvement of a sialidase-like enzyme in sialylation has so far only been found in some species of the genus *Trypanosoma*[24-26]. These flagellated protozoa, responsible for several very important infectious diseases, reveal a complex life cycle, during which they are transmitted from mammalian to insect hosts and back again. The different stages in this life cycle are accompanied by significant changes in the morphology and physiology of the parasites. The American species *Trypanosoma cruzi* causes Chagas disease in humans[27], for which vectors are insects of the genus *Rhodnius* and *Triatoma*, respectively. In this case, the parasites penetrate the host cell membranes, for example of the heart muscle, thus evading the immune system. In the African species *T*. *brucei*, infection of humans and domestic animals occurs via a sting of the Tse-Tse fly *Glossina* sp. *T*. *brucei*, which is the infectious agent of sleeping sickness in humans and Nagana disease in cattle, respectively, is able to escape host immune defense by successive expression of a series of variable surface glycoproteins (VSGs), leaving the immune response of the host always one step behind. According to these different strategies for maintaining an advantage over the host, trans-

sialidase expression is restricted only to certain stages in the life cycle. In *T. cruzi*, the enzyme is present in the mammalian bloodstream form and may be involved in the invasion of host cells. On the other hand, *T. brucei* reveals trans-sialidase activity only in the procyclic form, colonizing the gut of the fly[28]. Its function in this species consists in the transfer of sialic acids from the surface of sucked mammalian blood cells or from serum glycoproteins onto the parasite's own surface glycoproteins[29]. Thereby, the trypanosome would be protected from the proteases and glycosidases of the fly's digestive tract as well as from possible immunological attack[27]. The trans-sialidase from *T. cruzi* has been found to consist of several domains, among them an N-terminal domain responsible for sialidase activity and two further domains that are involved in sialyltransferase activity[30]. Interestingly, trypanosomal species possessing trans-sialidases do not contain enzymes for sialic acid anabolism[24].

An unusual enzyme, 'sialidase L', was detected in *Macrobdella decora* leech. Sialidase L hydrolyzed Neu5Ac-α2-3-galactose linkages in glycoconjugates, leading to release of 2,7-anhydro-Neu5Ac instead of Neu5Ac[31]. Another type of sialidase, 'KDNase', identified in fish, microorganisms, and the oyster, liberated KDN residues from α2-3, α2-6, and α2-8 linkages from a range of sialoglycoconjugates. Two KDNases were recently distinguished: one specific for KDN-α-ketosides, and the second also capable of cleaving α-ketosides of Neu5Ac, although at reduced rates[32,33]. A unique feature of influenza virus sialidase was the ability to convert, at an extremely slow rate, Neu5Ac to Neu5Ac2en, that is an inhibitor of sialidase itself[34]. Several sialidase-like enzymes are listed in Table 1-1 .

1.2 Sialidases (EC 3.2.1.18)

1.2.1 Sialidase - historical

Hirst (1941) first discovered sialidase activity while investigating red cell agglutination in the presence of influenza virus. Sialidases have been called 'neuraminidases' or RDEs (receptor-destroying enzymes), because they were first described for viruses[35]. The terms 'sialidase' and 'neuraminidase' were first proposed, respectively, by Heimer and Meyer[36] and Gottschalk[37]. Currently, 'sialidase' is deemed appropriate to describe these enzymes. There is a proposal to denote prokaryotic enzymes as 'neuraminidase' and eukaryotic enzymes as 'sialidase'[38].

Sialidases or neuraminidases (EC 3.2.1.18; exo-α-sialidase; N-acylneuraminosyl glycohydrolase) are a family of exoglycosidases that catalyze the hydrolytic cleavage of nonreducing sialic acid residues ketositically linked to mono- or oligosaccharide chains of glycoconjugates. They are widely distributed in nature, from viruses, and microorganisms such as bacteria, protozoa, and fungi to avian and mammalian species among the vertebrates. Perhaps the most widely studied sialidase is from influenza virus, where the enzyme is involved in viral replication and released from infected cells. The studies on influenza virus neuraminidases

led to the development of specific inhibitors approved for therapeutical use in the treatment of human influenza[39].

1.2.2 Sialidase primary structure

The alignment of sialidase primary structures shows the existence of conserved regions. The most important conserved sequence and structure motif is the so-called Asp-box, which is a short repeat motif with consensus sequence distinguishing bacterial from influenza neuraminidases (**S**-X-**D**-X-**G**-X-**T**-**W,** where X indicates any amino acid)[40,41]. The name is due to the presence of the aspartic acid residue. The five different residues are conserved to different degrees. This motif is found four to five times throughout all microbial sequences, whereas in viral sialidases it is only found once or twice or is even absent. The third Asp box is more strongly conserved than are Asp boxes 2 and 4. Interestingly, the space between two sequential Asp boxes is also conserved between different primary structures. The Asp boxes were believed to participate in catalytic action. However, increasing insight into the three-dimensional structure of sialidases contradicts this idea, attributing to them simply a structural role[42]. In contrast to the Asp boxes, the 'FRIP' motif (X-**R**-X-**P**) is located in the N-terminal part of the amino acid sequences. In this motif, arginine and proline residues are absolutely conserved. In particular, the arginine is directly involved in catalysis by binding of the substrate molecule[43]. Also important for the catalytic reaction of sialidases is a glutamic acid-rich region, which is located between Asp boxes 3 and 4 as well as two further arginine residues. There are also several single, conserved residues dispersed throughout the sequence.

1.2.3 Sialidase three-dimensional structure

The three-dimensional structure of both the monomeric sialidase from *S. typhimurium* and the tetrameric enzyme from influenza virus are known. X-ray analysis has been performed in complex with the sialidase inhibitor 5-*N*-acetyl-2-deoxy-2,3-didehydroneuraminic acid (Neu2en5Ac)[42]. Despite of the low overall homology, the three-dimensional structure of bacterial sialidase is identical to that found in sialidase monomers of influenza virus (Figure 1-5). The enzyme is mainly β-sheet with two small α-helical segments, with a shallow active site crevice. In particular, the secondary structure consists of six four-stranded antiparallel β-sheets arranged as the blades of a propeller around an axis passing through the active site[42]. The viral tetramer is stabilized by C-terminal extensions interacting with the first and second sheets of adjacent monomers. The Asp boxes are located at equivalent positions on the surface of the protein monomers from the different species, namely at the turn between the third and fourth strands of the first four sheets. Their aromatic residues form a hydrophobic core stabilizing the turn, whereas the aspartic acid residues point into the solvent. Thus, they might represent contact sites between subunits of the protein. On the other hand, there are only one or two Asp boxes in tetrameric influenza virus sialidases. In agreement with the location of these motifs on the surface of the enzyme molecule, another possible role for these regions

might be involvement in the process of enzyme secretion. The carboxylate group of the substrate is stabilized by three arginine residues in the active center[44]. One of them descends from the FRIP region.

Figure 1-5 Secondary structure model of the sialidase protein from *Salmonella typhimurium* with the bound inhibitor Neu2en5Ac.
(Traving, C. & Schauer, R. *Cell Mol Life Sci* 1998)

1.2.4 Substrate requirements of sialidases

Exo-α-sialidases cleave the terminal, non-reducing sialic acid residue from glycoproteins, oligosaccharides, polysaccharides, glycolipids, gangliosides, and synthetic glycosides. The ketosidic bond linking sialic acid to various sialidase substrates has the α-D configuration and is equatorial to the pyranose ring, as first proposed by Kuhn and Brossmer. Only α-ketosides are susceptible to sialidase attack as demonstrated by Meindl and Tuppy[45]. Perhaps the only naturally occurring linkage of ketosidically bound Neu5Ac that is not hydrolyzed by sialidase is cytidine-5'-monophosphate-Neu5Ac. Optical studies showed that the anomeric carbon in this compound was in the β-configuration[46]. When released by sialidase catalysis, the α-D-sialic acid anomer rapidly undergoes mutarotation in solution to produce β-D-sialic acid. A small portion of sialic acid in solution exists in the thermodynamically unfavorable open-chain form. The susceptibility of a sialic acid residue to sialidase attack is greatly influenced by adjacent residues, usually a sugar such as galactose, *N*-acetylgalactosamine, *N*-acetylglucosamine, another sialic acid, or an aglycone 'reporter' group in the case of synthetic substrates. While α2-3 and α2-6 linkages of sialic acid are preferentially cleaved by sialidase, other types of linkages are known, including α2-4, α2-9[47] and α2-8 in polysialic acids[6]. Internal sialic acids are generally resistant to the action of *exo*-α-sialidase, presumably due to steric hindrance. In general, the rates of human exo-α-sialidase cleavage are as follows: α2-3 > α2-6 > α2-8. As with the chemical structure of the substrate, the susceptibility of a glycosidic linkage to hydrolysis by sialidases varies with enzyme source.

The presence of a free carboxyl group in sialic acid is essential for sialidase catalysis. Methyl esters of sialic acid are resistant to sialidase attack[48]. Modification of the hydroxyl groups of sialic acid by various *O*-substitutions affects reactivity. For example, 4-*O*-acetylation of sialic acid renders it resistant to bacterial and mammalian (including human) sialidases, but not to viral sialidases. This may be because the C-4 binding pockets in bacterial and mammalian sialidases active sites are considerably smaller compared to viral sialidases[49]. As stated above, substitution of an -OH residue at C-5, instead of the usual *N*-acetyl or *N*-glycolyl groups, resulted in KDN and KDN-glycosides that are resistant to the action of *exo*-α-sialidases. Changes in the 'natural' nitrogen group substituent of sialic acid, from *N*-acetyl or -glycolyl to *N*-formyl, -succinyl, or -propionyl, also reduced the susceptibility to sialidase hydrolysis[50]. Exo-α-sialidases generally hydrolyze the Neu5Ac linkage at a faster rate than the Neu5Gc linkage.

Various modifications to the glycerol side chains have been reported to be associated with resistance to sialidase hydrolysis. Shortening of the C7-C9 carbon chain resulted in resistance to sialidase activity. Inhibitors targeting influenza virus sialidase, but not human or bacterial sialidases, were designed through such modifications[22,49,51,52]. In addition, the nature of the aglycone has a profound influence on the susceptibility to, as well as the rates of, sialidase catalysis. Changes to the pH optimum and/or kinetic parameters (K_m, V_{max} , and k_{cat}) of sialidases are common, depending on the chemical nature of the aglycone.

The divalent cation requirements for sialidases vary with source, and Ca^{2+} is considered as either essential for sialidase activity, or at least capable of stimulating it. Several membrane-bound sialidases were reported to be stimulated by the presence of detergents, or a physiologic activator[53]. Multi-protein complexation is essential for the stable expression of placental sialidase. Chelators (ethylen-ediamine tetraacetic acid, EDTA) and metals (Cu^{2+} and/or Zn^{2+}) were reported to inhibit sialidases from certain sources, but not others. Free sialic acid is only a weak inhibitor of sialidases (IC_{50} = 1-2 mM). Transition state analogs of sialic acid have been modeled to generate potent inhibitors of influenza virus sialidases.

1.2.5 Catalytic mechanism of sialidases

Elucidation of the catalytic mechanism of sialidases is very important, as these enzymes are involved in the pathogenesis of several infectious diseases. Therefore, they are of great importance in medicine and the pharmaceutical industry for the analysis of oligosaccharides and the development of sialidase inhibitors, for example as potential drugs against influenza infections[54]. Some insight into the catalytic mechanism of these enzymes can be gained from the analysis of the corresponding primary and three-dimensional structures. These data together with mutagenesis experiments[55] provide enough information to develop a model of the catalytic process[42,43].

While much of the information regarding the catalytic mechanism has come from studies of non-mammalian sialidases, some general features of the reaction are common to all exo-α-sialidases[30]. Some of the general properties are perhaps applicable to 'sialidase-like enzymes', described

above. For example, certain KDNases can hydrolyze sialic acid-containing glycosides, although at greatly reduced rates. Furthermore, the transition state analog Neu5Ac2en, a potent inhibitor of bacterial, viral, and mammalian sialidases, was also inhibitory toward a KDNase from *Sphingobacterium multivorum*. Finally, certain features of the exo-α-sialidase catalytic mechanism are similar to those of the KDNase[32].

The recognition portion of the substrate (sialic acid) probably binds initially to the enzyme active site in a boat configuration. Depending on the source of the sialidase, the reactive substrate configuration of the sugar following binding could vary from boat, twist-boat, flattened-boat, chair, flattened-chair, or half-chair. Sugar distortion appears to be a common feature for all sialidase catalysis studied thus far.The enzyme catalysis process has four steps. The first step involves the distortion of the α-sialoside from a 2C5 chair conformer to a boat conformer when the sialoside binds to the sialidase. In the second step the glycosidic oxygen is protonated, leading to a partial positive charge at carbon atom 2 of the sialosyl cation (oxocarbonium ion intermediate), and a tetrahedral transition complex is thus formed. A water molecule, or an activated hydroxonium ion (H_3O^+), serves as the nucleophilic proton donor to the positive charge at C-2, necessary for the hydrolysis reaction. The final two steps of the enzyme mechanism are the formation and release of Neu5Ac from the active site of the sialidase. Neu5Ac is initially released as the α-anomer. It is conceivable that expulsion of product from the active site is favored by the mutarotation of the α-anomer to the thermodynamically more stable β-anomer for Neu5Ac in solution[56].

While this overall reaction mechanism seems to be generally valid for sialidases, there are also some differences[44]. Thus, there is a strong interaction between the oxygen of carbon atoms 8 and 9 of the glycerol side chain and the glutamic acid residue in influenza virus sialidase, which leads to a slow turnover of the substrate by the viral sialidase. In *Salmonella*, there exist two strong and one weak hydrogen bonds between the enzyme and O4, whereas in influenza virus there is only one weak bond. This is an important point, for most sialidases are absolutely unable to cleave 4-*O*-acetylated sialic acids. However, this is the case for the viral enzyme, although at a slow rate. Therefore, analogs of the sialidase inhibitor Neu2en5Ac have been developed, containing an amino or guanidino group at C-4. These substances are strong inhibitors of enzyme activity[54]. Especially the guanidino derivative represents a potent drug against influenza infections that is in stage III of clinical trials[57].

1.2.6 Sialidase gene evolution

Sialidases have been extensively investigated, especially in microbial species. Primary structure data enable us to draw some conclusions about the relationship and evolution of these enzymes. Close contact between the partners exchanging genetic information would be necessary, as is the case in host-parasite interactions. Other possible vehicles for horizontal gene transfer are viruses. Finally, free DNA molecules can be taken up by several naturally transformable bacterial species by the process of transfection. Gas gangrene, a bacterial infection caused by *Clostridium perfringens,*

represents a proper scenario for horizontal gene transfer with bacterial cells being in intimate contact with damaged host cells. It is also conceivable that the genetic information might have been transferred from bacteria to eucaryotes. Schauer and Vliegenthart, however, propose an exchange of information in the reverse direction[4]. For some strains of *Salmonella typhimurium* it has been shown that sialidase genes are spread between strains of this species by horizontal gene transfer[58]. To learn something about the evolution of sialidase genes, sialidase primary structures had to be elucidated. The alignment of sialidase primary structures[40] reveals that - apart from some conserved regions - the overall homology between the sequences is low. The conserved areas point to a single evolutionary origin of sialidases. The percentage of identical amino acids between each pair of sequences can be calculated and the values used to construct a dendrogram of sialidase relationships. For example, it can be seen that clostridial sialidases form a group of closely related enzymes. The highest degree of similarity was found between the 'small' sialidase isoenzyme from *C. perfringens*[59] and the enzyme from *C. sordellii*[60], whereas the close relationship between the 'large' isoenzyme from *C. perfringens*[61] and the one from *C. septicum*[62] is expected, as suggested by 16S ribosomal RNA (rRNA) analysis. According to one hypothesis[63], the genetic information for sialidases was spread by horizontal gene transfer at two time points in evolution. Genes that were acquired by microbial species at an earlier time are well adapted to their environment, as demonstrated by their broad substrate specificity and their secretion into the medium to make contact with their substrates (e.g. the 'large' isoenzyme from *C. perfringens*). On the other hand, sialidase genes that have been transferred during a more recent event reveal a limited substrate specificity and have not been fully adapted to their new 'host' because they still lack a signal for excretion of the enzyme proteins (e.g. the 'small' sialidase isoenzyme from *C. perfringens*).

1.2.7 Sialidase substrates and their pathological roles

Glycolipids constitute a large and heterogeneous family of sphingolipids constituent of cell membranes and enriched in the plasma membrane. They are anchored to the extracytoplasmic leaflet of cell membranes through their ceramide moiety. At the plasma membrane, they expose the sugar-containing hydrophilic portion to the extracellular space, contributing to the complexity of the glycocalix. Animal cells and several plant cells contain at least some glycolipid class in their membranes. Gangliosides are acidic glycosphingolipids that contain one or more sialic acid residues and are particularly prevalent on neuronal cells. Ganglioside expression is highly regulated during development and differentiation. The control relies mainly on transcriptional and post-transcriptional modulation of key glycosyltransferases acting at the branching points of the pathway of biosynthesis. The machinery for synthesis in the Golgi complex and its dynamics constitute a potential target for fine tuning of the control of ganglioside expression according to cell demands.

The synthesis of gangliosides Lactosylceramide and more glycosylated species, including gangliosides, are built up by the stepwise addition of sugar units to GlcCer, catalyzed by membrane bound

glycosyltransferases[64-67]. Different sialyltransferases (Sial-T1, Sial-T2/Sial-T3) build up the gangliosides GM3, GD3 and GT3. Gangliosides GM3, GD3 and GT3 are converted to ganglio-series forms of the a-, b- or c-pathway by sequential glycosylations catalyzed by GalNAc-T, Gal-T2 and Sial-T4 (Figure 1-6). These transferases have rather broad acceptor specificity and glycosylate the corresponding intermediates of the o-, a-, b- or c-series[68]. In addition to the *de novo* synthesis of glycolipids, recycling from the endosomal pathway through the Golgi has been well documented. The relative contribution of these two pathways has been examined in several cell lines; it has been found that the salvage or recycling pathway predominates in slowly dividing cells, while the *de novo* pathway predominates in rapidly dividing cells[69].

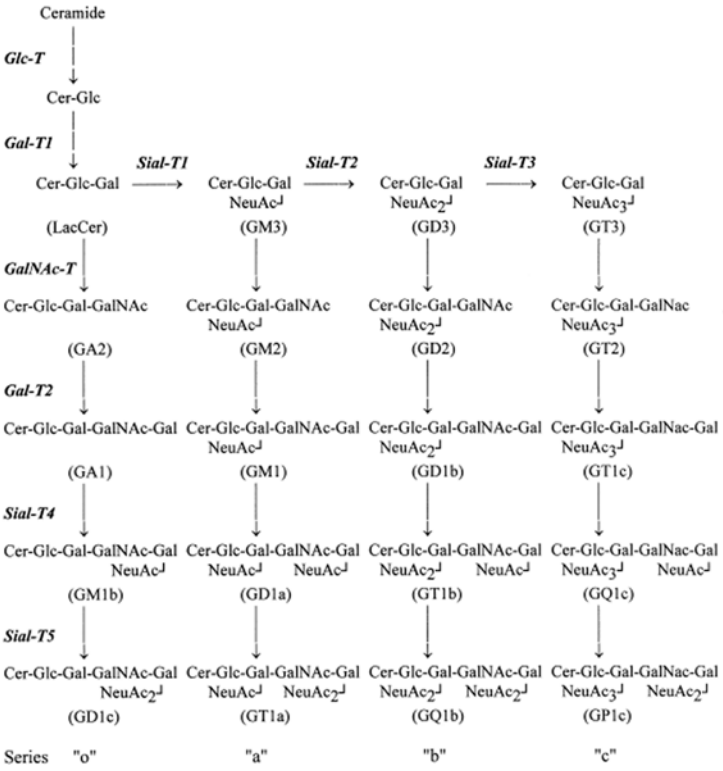

Figure 1-6 The pathway of biosynthesis of o-, a-, b- and c-series gangliosides.
(Maccioni, H. J., et al. *Biochim Biophys Acta* 1999)

Glycolipid patterns vary between different cell types and change with the differentiation of the cell[70]. Differences in glycolipid composition have even been found between different neuronal cell types[71]. The biological function of this molecular diversity is unclear, but the vital role of glycosphingolipids has been demonstrated by the fact that their complete deficiency in mice leads to early embryonic lethality. Gangliosides seem to

be involved in cell-to-cell interactions[72] and are also reported to regulate the activities of receptor tyrosine kinases in the plasma membrane such as the receptors of epidermal growth factor[73], nerve growth factor[74], and insulin[75] and in this way might regulate cell signaling.

Under most circumstances, the prevalent sphingolipids of cells are the complex sphingolipids: phosphosphingolipids such as sphingomyelins and glycosphingolipids such as ganglioside GM1 shown in Figure 1-7. Complex sphingolipids are found in all eukaryotes and some prokaryotes and viruses, mainly as components of the plasma membrane and related organelles (endosomes, lysosomes, Golgi membranes, etc.). Gangliosides are not homogeneously distributed on the cell surface; the amounts of sphingolipids in particular regions of the membrane can be considerably higher because sphingolipids are asymmetrically distributed (mainly on the exoplasmic leaflet), and some categories of sphingolipids such as sphingomyelin, ceramide, and glucosylceramide (sometimes in combination with cholesterol) spontaneously aggregate to form microdomains termed 'rafts', 'caveolae', and 'detergent-resistant membranes'[76]. These sphingolipid-rich microdomains are believed to be important in clustering proteins involved in cell signaling; for example, glycophosphatidylinositol-anchored proteins congregate in the exoplasmic region of lipid rafts while myristoylated and palmitoylated G proteins can protrude into the cytoplasmic side of rafts.

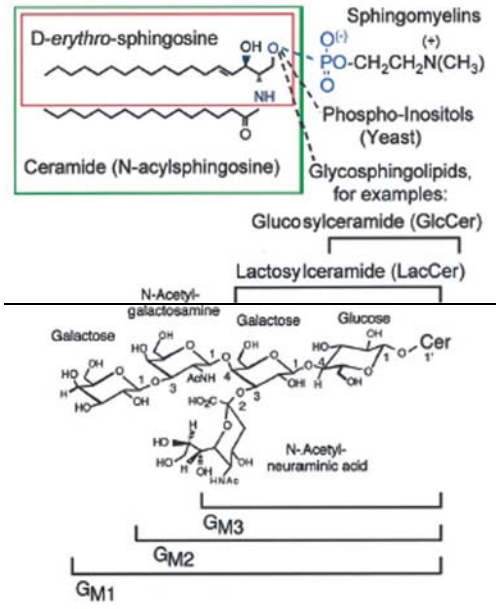

Figure 1-7 Structures of representative sphingolipids.
(Smith, W.L. & Merrill, A.H., Jr. *J Biol Chem* 2002)

Several reports indicate that physiological processes like embryogenesis and differentiation of neuronal cells and leukocytes might be

influenced by gangliosides[77]. The adult mammalian central nervous system is an inhibitory environment for nerve regeneration, partially because of specific inhibitors on myelin including myelin-associated glycoprotein (MAG), Nogo, and chondroitin sulfate proteoglycans[78-80]. Presumably, these inhibitors bind to specific nerve cell surface ligands, resulting in transmembrane signals that lead to growth cone collapse and inhibition of axon extension.

MAG (Siglec-4) is a member of the Siglec family of sialic acid (NeuAc) binding lectins (carbohydrate binding proteins)[81,82]. *In vitro* binding studies indicate that MAG binds preferentially to the 'NeuAc α3 Gal β3 GalNAc' glycan structure[83], which is prominently expressed on certain gangliosides, sialic acid-bearing glycosphingolipids that comprise major determinants on mammalian nerve cells. Mice genetically lacking the 'NeuAc α3 Gal β3 GalNAc' terminus on gangliosides demonstrate axon degeneration and dysmyelination similar to that in MAG knockout mice[84]. These findings led us to propose that the major brain gangliosides GD1a and GT1b are functional nerve cell surface ligands responsible for MAG-mediated inhibition of nerve regeneration and to probe the molecular mechanism by which inhibition is initiated.

Glycosphingolipids (GSLs), including gangliosides, have been known to function in animal cells as antigens, and receptors for microbial toxins, as well as mediators of cell adhesion and modulators of signal transduction[85-87] (see Table 1-2). At cell surface microdomains, glycosyl epitopes, carried either by glycosphingolipids, *N*- or *O*-linked oligosaccharides, are recognized by carbohydrate-binding proteins or complementary carbohydrates. Carbohydrates can mediate cell signaling leading to changes in cellular phenotype. Clustered GSLs may provide detergent-resistant properties[88,89], and interact with various functional components on cell membrane. GSL clusters at the cell surface membrane interact with functional membrane proteins such as integrins, growth factor receptors, tetraspanins (TSPs), and non-receptor cytoplasmic protein kinases (*e.g.*, Src family kinases, small G-proteins) to form microdomains, termed 'glycosynapse', controlling GSL-dependent or -modulated cell adhesion, motility and growth[90,91]. The hypothesis of signaling transduction through membrane microdomains arose when growth factor receptor tyrosine kinase (GFR) was found to be inhibited by surrounding gangliosides[92,93] and when Src kinase activity was demonstrated to be associated with GPI-anchored proteins[94]. Many adhesion molecules involved in monocyte adhesion, principally adhesion between T- or B-lymphocytes and antigen-presenting cells, are organized in microdomains on membrane, particularly TCR for T-cells, and CD15 for B-cells. Organizational framework of such membrane proteins has been thought to be similar to that of caveolae or raft, although there are many differences in size, dynamic status, and detergent-resistance properties. Thus, the term "immunological synapse" was proposed for such microdomain, which is claimed to be different from caveolae or raft[95].

Several studies have demonstrated that glycosylation plays a central role in defining tumor progression. Tumor progression is associated with overexpression of defined types of GSLs involved in GSL-dependent adhesion of tumor cells to target cells, which activates signal transducers to

enhance motility and invasiveness[96]. Glycosylation dictates the organizational status of glycosynapse, which in turn strongly affects cellular phenotype influencing tumor cell malignancy. These observations open a new possibility that malignancy is not defined by tumor-specific molecules or their genes but rather is caused by disorganization of cell membrane components. Supporting this hypothesis, a classic work demonstrates that highly malignant teratocarcinoma kills the host when intraperitoneally inoculated, but it undergoes normal development when inoculated into the blastocyst[97,98]. More recently Bisseell group demonstrated that misregulation of signaling pathways involved in epithelial cell communication with neighboring cells and ECM results in loss of tissue organization contributing to tumor formation and progression[99,100]. These works furnish an unequivocal example of malignance arising from disorganization, rather than from changes in gene structure. Therefore, modulation of glycosynapse functions can lead to new strategies in cancer therapy. Noteworthy is the inhibition of GM3-dependent adhesion[101] and EGFR signaling[101] by lyso-GM3. Elucidation of the molecular mechanism of interaction among components in glycosynaptic domain will require extensive physical studies and might bring insights into approaches to disrupt or promote such interactions.

Table 1-2 General functions of glycosphingolipids (GSLs).
(Regina Todeschini, A. & Hakomori, S.I. *Biochim Biophys Acta* 2008)

General functions of GSLs [100]		
1.	GSL antigens	
	•	blood group ABH; Lewis (Le^a, Le^b, Le^c, Le^d, etc); I/i; P, P^k and p antigens;
	•	heterogenetic Forssman; Hanganutziu-Deicher (NeuGc epitope); Galα1→3Galβ1→3GlcNAc (di-Gal);
	•	cell type specific antigens (CD15, CD76, CD75, CD71, CD57, CD65;
	•	developmentally regulated [stage-specific embryonic antigen-1 (SSEA-1), Le^x, SSEA-3, SSEA-4, etc];
	•	tumor-associated antigens [Gb3, Gal-Gb4, Globo-H, GD3,GD2, fucosyl GM1, sialosyl-Le^c, sialosyl-Le^a, etc).
2.	GSL receptors for microbial infection and toxins, *e.g.*	
	•	choleratoxin (GM1);
	•	Shigella or verotoxin (Gb3);
	•	Botulinum neurotoxin (GT1b, GD1a as co-factors of protein receptor);
	•	*E. coli* infection (globo-series GSL);
	•	*Staphylococcus* infection (Gg4; asialo-GM1).
3.	GSLs in cell adhesion/ recognition	
	i.	Mediated by GSL-binding protein, *e.g.*
	•	~~neuronal cell adhesion to myelin sheath membrane mediated by gangliosides and myelin-associated~~ glycoproteins;
	•	myeloglycan GSLs to selectin;
	•	GM1 mediating adhesion through galectin-1.
	ii.	Mediated by GSL-GSL interaction, *e.g.*
	•	GM3-LacCer/ Gg3 interaction mediating melanoma adhesion to endothelial cells (initiation of metastasis);
	•	Gb4-GalGb4/ nLc_4 interaction mediating human teratocarcinoma cell interaction (model of human embryo compaction);
	•	Le^x-Le^x interaction mediating mouse embryogenesis.
	•	Glycan-to-glycan interaction mediating species-specific sponge cell aggregation in proteoglycan [54,101];
	•	GalCer/ GalCer-sulfatide interaction in myelin membrane mediating signal transduction in oligodendrocytes [102,103];
	•	sperm (KDN)GM3 interaction with Gg3-like epitope, expressed on micropyle of vitelline envelope in egg, mediating sperm-to-egg interaction in rainbow trout fertilization [104].
4.	GSLs controlling cell motility and signal transduction	
	i.	GSL to TSP interaction, *e.g.*
	•	GM3/TSP CD9 complex [73–79]
	•	GM2/GM3/CD82 complex [86].
	ii.	GSL to GSL interaction through cis-CCI

1.2.8 Biological function of sialidases

Sialidases occur in higher animals of the deuterostomate lineage that possess the corresponding sialic acid-containing substrates as components of an autonomous sialic acid metabolism. However, they have also been

found in a variety of microorganisms, such as viruses, bacteria and protozoa[15,102]. Some of the latter organisms do not contain or produce sialic acid themselves. Microbial species often live in close contact with higher animals as hosts, for example as parasites. Then, in these microbial species these enzymes may have a nutritional function, enabling their owners to scavenge host sialic acids for use as a carbon and energy source. For some microbial pathogens, sialidases are believed to act as virulence factors, allowing successful competition with the host by alleviating their spread in host tissue[103]. The Gram positive anaerobic species *Clostridium perfringens* causes gas gangrene. This severe or even fatal disease develops when deep wounds are becoming increasingly anoxious due to damage to the surrounding blood vessels and are contaminated with these bacteria or their spores. In the absence of oxygen, the bacteria begin to divide rapidly. During propagation they excrete a cocktail of enzymes with different substrate specificities, that is composed of proteases, hyaluronidases, collagenases, phospholipases, lecithinases and also a sialidase, which degrade a variety of host structures. Sialidases play a crucial role in this scenario, as they remove the first line of host defense by cleaving the terminal sialic acid residues[104]. Thus, subterminal molecules including proteins become easily accessible. Multiplication and spread of the bacteria in the tissues can be very rapid (10 cm per hour). A possible role for sialidases is that of spreading factors which facilitate the propagation of bacteria and their invasion of host tissue[104,105]. Another effect of sialidase overflow is anemia: red blood cells are covered by a dense coat of sialic acid molecules that is removed by this dysregulated sialidase action. As a consequence, the galactose residues are demasked on the blood cell surface after removal of sialic acids, presenting a signal for degradation by liver hepatocytes[13]. Due to the resulting lack of negative charge on the erythrocyte surface, the cells tend to aggregate, which leads to thrombosis[15,106]. Additionally, enzymes, hormone and serum glycoproteins are inactivated by high sialidase levels[15]. Another possible role of sialidases from parasites is the demasking of subterminal host cell structures, which then serve as receptors for the parasites and toxins, as in the case of cholera[15,107]. The pathophysiological significance of sialidases can also be seen from infection of humans with influenza A or B. Here, the sialidase function is analogous to that of *O*-acetylesterase in influenza C virus and thus represents another ‘receptor-destroying enzyme’. The sialidase enables release of the viral progeny, and by cleavage of host sialic acids leads to impairment of the viscosity of the protective mucous layer of the upper respiratory apparatus.

Nevertheless, the role of sialidases as factors in pathogenesis is controversial. On the one hand, they confirm the impact of pathogenic microbial species like *Clostridium perfringens*. On the other hand, these enzymes are factors common in the carbohydrate catabolism of many nonpathogenic species, including higher animals. They do not, however, exert a direct toxic effect. Instead, their detrimental effect depends on the massive amount of enzyme that is released[106] into the host together with other toxic factors upon induction[15] by host sialic acids under nonphysiological conditions, which leads to a variety of cell damage. In summary, sialidases are common enzymes in sugar catabolism that become

dangerous only when they improve the parasitic or pathogenic potential of a microorganism with respect to its environment. Also for these species, however, the enzyme has an additional nutritional function.

Certain bacterial sialidases reveal a more complex structure consisting of several domains with special functions. Thus, the enzyme from *Vibrio cholerae*, which has also been crystallized[108], proved to contain two lectin-like domains flanking the central catalytic domain. These domains reveal a sandwich-like structure composed of seven and six antiparallel β sheets, respectively, and probably serve in binding of carbohydrates. The actual ligands, however, are so far unknown. A galactose-binding pocket was identified as a part of a jelly roll domain in the sialidase from *Micromonospora viridifaciens*[109]. It is linked via an immunoglobulin-like domain to the catalytic part of the molecule. The galactose-binding pocket is only 30 Å away from the sialic acid binding site. So each of the two domains seems to interact with a different part of the sialoside substrate.

Although microbial sialidases that have been purified and characterized reveal a high degree of variability with respect to their properties, they can be classified into two groups according to their size[110]: 'small' proteins of around 42 kDa and 'large' ones of 60 to 70 kDa. The primary structures of the 'large' sialidases contain extra stretches of amino acids between the N-terminus and the second Asp box as well as between the fifth Asp box and the C-terminus. It is believed that they contribute to the broader substrate specificity of the 'large' sialidases.

On the other hand, it is tempting to assume that the sequence areas that are additionally present in some primary structures encode extra domains such as the galactose binding domain of the *M. viridifaciens* enzyme[109]. The 'small' sialidases are not Ca^{2+}-dependent in contrast to some of the 'large' enzymes. The only common feature of all sialidase proteins is a slightly acidic pH optimum. Remarkably, trans-sialidases operate best under neutral conditions. Usually sialidases are specific for Neu5Ac that is α2-3, α2-6 or α2-8 linked to the subterminal sugar chain of poly- and oligosaccharides, glycoproteins and gangliosides. Neu5Ac-bound α2-3 in most cases is hydrolyzed at the highest rate[1]. The endosialidase of bacteriophage E acts exclusively upon α2-8 bound Neu5Ac and Neu5Gc. Ganglioside GM1 is a substrate only for the enzyme from *Arthrobacter ureafaciens*. With the exception of *S. typhimurium*, the first reaction product of the sialidase reaction is the form of Neu5Ac, which then mutarotates to the more stable β form. Finally, an enzyme has been identified that splits KDN instead of Neu5Ac, a so-called KDNase, in the loach *Misgurnus fossils*, in the ovary of rainbow trout and in *Sphingobacterium multivorum*[111,112].

Less knowledge exists so far about sialidases from higher animals, although this is a very interesting and important field. The first phylum in the animal kingdom to contain sialidases is the echinoderms. The enzyme from *Asterina pectinifera* ovary has a pH optimum of 3 to 4 and hydrolyzes a broad spectrum of substrates, including sialyloligosaccharides, glycoproteins and gangliosides, and is also found in human placenta[113]. Mammalian sialidases with different substrate specificities were found in lysosomes (specific for sialyloligosaccharides, glycoproteins, gangliosides), the Golgi,

the plasma membrane and the cytosol (sialyloligosaccharides and glycopeptides).

The significance of sialidases for mammals can be seen from the severe consequences of genetic diseases concerning sialidases. Deficiency of the human lysosomal sialidase leads to sialidosis, an autosomal recessive genetic disorder that can be classified into type I (late onset) and type II (infantile onset) cases[114]. Frame-shift and missense mutations have been found to be responsible for sialidosis. The lysosomal sialidase gene was localized on chromosome 6 in proximity to the human lymphocyte antigen (HLA) locus, which corresponds to the localization of this gene in the major histocompatibility complex (MHC) of rat and mouse. The lysosomal enzyme is most similar to the sialidase from *S. typhimurium* but has three glycosylation sites. The lysosomal as well as the cytosolic mammalian sialidases share the presence of Asp boxes, the FRIP region and even the same fold with their microbial counterparts, pointing to a single evolutionary origin of all sialidases[114]. Another inherited lysosomal storage disease is galactosialidosis with sialidase and β-galactosidase being deficient secondary to the lack of cathepsin A:protective protein[115]. All these components are part of a 1.27-MDa complex. Normally, sialidase is synthesized as a 45.5-kDa precursor, including a signal peptide of 47 amino acids. Removal of the latter and glycosylation leads to the mature protein of 48.3 kDa that is found in lysosomal and plasma membranes. In addition, the enzyme is only active in association with cathepsin A, which is important for the correct conformation of the sialidase and protects against intralysosomal proteolysis. The same is true for β-galactosidase. In galactosialidosis, the missing interaction with cathepsin A leads to sialidase and galactosidase deficiency due to abnormal proteolytic cleavage and rapid degradation of the two proteins.

A sialidase with unique features has been described for *Macrobdella decora*[31]. It releases 2,7-anhydro-Neu5Ac and is absolutely specific for Neu5Aca2.3 Gal. The calculated mass is 83 kDa. Like the enzyme from *A. pectinifera*, it is similar to the enzyme from *S. typhimurium*, and shares the presence of Asp boxes and the FRIP region with microbial sialidases, but the similarity with other, especially mammalian sialidases, is only slight.

1.2.9 Sialidases in disease

Hemagglutinin-neuraminidases (HNs), sialidases (NAs), and trans-sialidases (TSs) are also implicated as virulence factors in a range of diseases.

The influenza type A and B viruses have two surface glycoproteins: hemagglutinin (HA), which recognizes sialic acid for attachment but is also involved in the fusion of viral and cell membranes, and neuraminidase (NA). The role of the neuraminidase is to process progeny virus particles when they bud from an infected cell, removing viral sialic acids to halt self-agglutination of viruses. The neuraminidase forms tetramers on the viral surface, anchored by N-terminal transmembrane regions. The paramyxoviruses also possess sialidase activity in the dual-function HN molecule. Indeed, they have two surface glycoproteins: the fusion protein (F), which is involved in the fusion of viral and host cell membranes, and

hemagglutinin-neuraminidase (HN), which recognizes for cell attachment and also cleaves sialic acid. There is evidence that both F and HN are required for fusion[116]. Human parainfluenza viruses, one of the major causes of infant respiratory disease, have several serotypes, making vaccination an unattractive route, in contrast to the mumps virus, for which an effective vaccine exists. The HN molecule also forms on the viral surface tetramers comprising two disulphide-linked dimers (in most strains), anchored via N-terminal transmembrane segments[117]. No sequence similarity between the influenza and paramyxovirus enzymes is evident, although modeling has suggested that they share a common fold[118].

Sialidases are produced by a wide range of bacteria, and are often one of several virulence factors secreted by bacteria involved in important diseases[105,119,120]. Many pathogenic and nonpathogenic sialidase-producing bacteria can use sialic acid as a carbon and energy source, and possess both permeases to transport the sugar inside the cell, and the enzymes for its catabolism. In certain cases the enzyme also has a defined role in disease. For example, *Vibrio cholerae* sialidase removes sialic acid from higher order gangliosides to create GM1 , the binding site for cholera toxin[107].

Bacterial sialidases vary in size from 40kDa to 120kDa. Most exist as monomers, but higher oligomeric states have been reported. Most are secreted as soluble proteins, others are tethered to the bacterial surface (e.g. in *Streptococcus pneumoniae*[121], and some are not secreted (e.g. the small sialidase of *Clostridiurn perfringens*, which also secretes a larger, quite distinct sialidase[110]. The bacterial sialidases share little sequence identity, typically 30%, but contain two conserved sequence motifs: the first is the RIP/RLP motif (Arg-Ile/Leu-Pro), the second is the Asp-box motif (Ser/Thr-X-Asp-[X]-Gly-X-Thr-Trp/Phe; where X represents any amino acid), which can occur several times along the chain[41].

Sialidases transfer carbohydrate-linked sialic acid to water, but certain parasites possess trans-sialidases (TSs) that transfer carbohydrate-linked sialic acid to other carbohydrates. Many trypanosome species possess trans-sialidases on their surfaces. The appearance of the enzyme is developmentally regulated, such that in *Trypanosoma cruzi* the enzyme shows highest activity in the infective trypomastigote stage of the parasite[122]. In contrast, the TS of *Trypanosoma brucei* is more active in the insect form of the parasite[123]. The *T. cruzi* TS (TCTS) is part of a large gene family, some members of which do not have any enzyme activity[124]. The role of TCTS in cell attachment does not required enzymatic activity[125]. The enzymatically active members transfer sialic acid from host cells to the parasite's own surface glycoproteins, the parasite being unable to synthesize sialic acid itself. This sialylation appears to be important for cell invasion and evasion of the immune system.

TCTS is a multidomain protein: a catalytic N-terminal domain (containing an RIP motif and two Asp boxes) is followed by one or two other domains, one of which may have a fibronectic type III fold, which in turn is/are followed by a 12-amino-acid motif that is repeated 44 times before a GPI anchor links the molecule to the parasite's surface[126]. In the trypomastigote form, TCTS appears to form a trimeric structure through

association of the repeat sequences. TCTS has a high substrate specificity for sialic acid linked α2-3 to β-galactose[127]. Finally, TCTS is also shed from the parasite surface in a soluble form, that enhances virulence via inflammatory cells[128]. Trans-sialidases and sialidases have been found in several *Trypanosoma* species, but not in many other parasites, such as *Leishmania*[28] and *Plasmodium falciparum*[129].

Several pathogenic bacteria and various tumour cells express poly-α2-8-linked sialic acid on their surfaces. One such bacterium is *Escherichia coli* K1, which can cause high mortality rates in cases of neonatal meningitis. An endosialidase that binds to and hydrolyzes such polysialic acid substrates has been isolated from bacteriophage K1E[130] and K1F[131]. The enzyme is a trimer of 74kDa monomers that contain two Asp boxes. The enzyme may find a use in the diagnosis and therapy of K1 meningitis.

1.3 Mammalian sialidases

1.3.1 Introduction

In mammals, sialidases have been proved to be involved in several cellular phenomena, including cell proliferation and differentiation, membrane function, and antigen masking. The enzyme involvement in this complex net of biological phenomena could be either direct or secondary to desialylation of various substrate(s). Lysosomal sialidase is clearly implicated in two lysosomal storage disorders: sialidosis (OMIM 256550) and galactosialidosis (OMIM 256540)[132].

Compared to bacterial or viral sialidases, there is less information regarding mammalian sialidases in general, and human sialidases in particular, as nothing is known of their structures[22]. Indeed, the detailed study of mammalian sialidases has been hampered for a long time because of both their low cellular concentration and their lability during the classic purification procedures. The small number of information regarding human sialidases is due also to many factors intrinsic to human sialidases, such as thermal instability, low abundance in the cell, particulate nature, different subcellular requiring the isolation of subcellular organelles, molecular heterogeneity (isoenzymes), membrane association, and often the interaction of human sialidase with other proteins and enzymes to form multi-protein complexes.

1.3.2 Tissue and cellular distribution of mammalian sialidases

Warren and Spearing[133] first demonstrated a human exo-α-sialidase activity in a commercial preparation of human plasma glycoprotein, Cohn fraction VI. The enzyme had a pH optimum of 5.5, was stimulated by Ca^{2+} and inhibited by EDTA. Early reports of human sialidase also include the brain[134] and intestinal mucosa[135].

Sialidase activity was detected in various human cells, tissues, and body fluids, as shown in Table 1-3. Human tissue or body fluids must be rigorously examined to exclude bacterial contamination as a source for the observed sialidase activity. This is especially true with bacteria-rich

specimens, such as oral cavity swab specimens, where *Staphylococcus* or *Streptococcus* could result in spurious 'human sialidase' activity.

Table 1-3 Distribution of mammalian sialidases.
(Traving, C. & Schauer, R. *Cell Mol Life Sci* 1998)

Organ/tissue	Body fluid	Cells
Brain	Semen	Fibroblasts
Kidney	Plasma	Macrophages
Liver	Serum	Platelets
Thyroid	Saliva	B & T lymphocytes
Leucocytes		Monocytes
Mammary gland		Endothelial cells
Placenta		Erythrocytes
Salivary gland		Epithelial cells
Skin		K562 erythroleukemia cells
Intestine		Epithelial cells
Chorion		Hepatocytes
Testis		Neuroblastoma cells
Pulmonary parenchyma		Granulocytes
		Amniotic cells
		Thymocytes

Human tissue sialidases

There have been several studies on sialidase activity in various human tissues, as well as salivary glands, brain, liver, and placenta (Table 1-3). Fukui et al.[136] detected two types of sialidase activities in human saliva: soluble and particulate-bound. Sialidase activity detected in the submandibular and sublingual secretions of human volunteers, originated from leukocytes or epithelial cells in the oral cavity, or from minor salivary glands. The human salivary sialidase was closely related to human liver sialidase, but was distinct from bacterial sialidases.

The first report of sialidase activity in human brain was by Ohman et al.[137]. The enzyme located in the particulate fraction of human brain homogenate was complexed with endogenous substrates and other glycosidases. Both α2-3 and α2-8 sialosyl linkages were hydrolyzed by the enzyme, and GD1a, GD1b, and GM3 gangliosides were the preferred substrates. Sialidase in human brain appeared to be developmentally regulated, since the activity was not detected before the fetal age of 15-20 weeks and adult level activity was reached by approximately 5 years of age[138]. Several other investigators subsequently demonstrated the presence of both soluble and particulate-bound sialidase activity in human brain homogenates[139,140]. Both forms of sialidase had an acid pH optimum (pH 3.0-4.5) and utilized brain gangliosides and α2-3- and α2-6-linked synthetic sialic acid substrates[141]. Cantz and colleagues[142-144] have recently investigated sialidase activity, both in brain homogenates and neuroblastoma cells in culture. They reported that the human brain gray matter had a three-fold higher GM3 ganglioside hydrolyzing sialidase activity compared to the white matter. Kopitz et al.[142,144] also showed that the human neuroblastoma cells SK-N-MC contained a cell surface sialidase that

cleaved terminal sialic acids from gangliosides, leading to a decrease in GM3 content and an increase in GM1 and lactosylceramide in these cells. Such alterations in ganglioside profiles, could lead to changes in cellular morphology, release of cells from contact inhibition of growth, and loss of differentiation markers in neuronal cells. It was also concluded that gangliosides on the external side of the plasma membrane of these cells are important modulators of cellular functions[142]. Miyagi et al.[145] reported the partial gene sequence of human brain sialidase: the human brain sialidase had approximately 24% sequence identity to human major histocompatibility-related sialidases and 83% identity to bovine brain sialidase. Tay-Sachs disease is a severe, inherited disorder of the nervous system in which there is an accumulation of the brain lipid, GM2 ganglioside. Transfection of human sialidase cDNA into neuroglia cells derived from a Tay-Sachs fetus showed a dramatic reduction in the levels of GM2, leading the authors to conclude that pharmacological induction or activation of human sialidase could offer a treatment for Tay-Sachs disease[146].

Sialidase activity in human liver was demonstrated using Neu5Ac-Lac (α2-3 and α2-6)[141] and 4-MU-Neu5Ac. An exception to the α2-3 linkage preference was exhibited by human liver sialidase, which was more active toward α2-6-linked sialic acids of glycoproteins, such as mucin or colominic acid. Schauer and coworkers demonstrated two types of activity in human liver mitochondrial-lysosomal fractions[147]. One of these activities hydrolyzed gangliosides and the synthetic substrate Neu5Ac-Lac, whereas the second type of sialidase was active toward fetuin and sialylhexasaccharides[148,149]. Spaltro and Alhadeff[150] demonstrated the existence of multiple isoenzymes of sialidase in human liver, with different isoelectric point (pI) and substrate specificity. Whether the various isoforms of human sialidases represent various post-translationally modified forms of the same gene product, or genetically distinct enzymes, is not yet clear.

Verheijen et al.[151,152] partially purified and characterized a placental sialidase and demonstrated that the 76-kDa human enzyme existed in a complex with two other proteins: a 64 kDa β-galactosidase, and a 32 kDa protein named ‘protective protein’. They showed that placental sialidase was lysosomal and, furthermore, that the multi-protein complexation was essential for expressing sialidase activity. Two types of sialidases with nearly identical biochemical and enzymatic properties were identified in human placental tissue[153]. Both had a molecular mass of approximately 65 kDa, and hydrolyzed 4-MU-Neu5Ac, as well as sialyllactose and the ganglioside GD1a. The only major difference between the two was that one type of sialidase activity was soluble, whereas the second was pellet-bound.

There have also been attempts to link the levels of sialidase activity in various human tissues as a diagnostic tool or of prognostic value to diseases. Den Tandt et al.[154] described an intestinal sialidase activity toward 4-MU-Neu5Ac, that was inhibited by Neu5Ac, glycoprotein, and oligosaccharide substrates, but not by gangliosides. A sialidase activity in human skin was also described by Mier and coworkers[155]. The sialidase activity was elevated in a few, but not all, psoriatic biopsy specimens, and therefore was of no diagnostic value. Sialidase activity was also detected in human renal tissue, but with no clear correlation between activity levels and

renal infections[156]. On the other hand, sialidase activity levels in breast milk were considered as a prognostic test for intrauterine fetal death[157]. Sialidase activity was also reported in human chorion tissue and amniotic fluid. For this reason chorion biopsy specimens could be used for prenatal diagnosis of sialidosis[158]. Serum and breast tissue sialidase levels were elevated in patients with breast cancer, than sialic acid and sialidase levels could be a possible marker for breast cancer[159]. However, additional studies are necessary to confirm this theory.

Human cellular sialidases

Sialidase activity was detected in several human cells (Table 1-3). However, few of these cellular sialidases have been well characterized to date. Marchesini et al.[160] used 4-MU-Neu5Ac to identify sialidase activity in human lymphocytes, granulocytes, erythrocytes, and platelets. The pH optimum for all these was reported to be between 4.0 and 4.8. The various blood cells showed different relative specific activities. The higher sialidase activity was detected in lymphocytes, while a lower level was observed in granulocytes and platelets. On the other hand, erythrocytes possess the lowest sialidase activity among the blood cells. An endogenous monocyte sialidase activity was implicated in the regulation of hyaluronic acid receptors[161].

Sialidase activity was detected in cultured human erythroleukemia K562 cells. Treatment of K562 cells with the anticancer drug adriamycin resulted in a 40% decrease in sialidase activity compared to untreated control cells[162]. Partial desialylation of aged erythrocyte-membrane sialoglycoproteins could constitute a signal for phagocytosis. Venerando et al.[163] identified two types of sialidases in human erythrocyte membranes based on the type of membrane anchor, pH optimum, and effects of the detergent Triton X-100 on enzyme activity. The neutral sialidase was probably responsible for the desialylation of erythrocyte membranes during the physiological aging of erythrocytes in circulating blood. The mechanism(s) of neutral sialidase activation is still unknown. A glycosylphosphatidyl-inositol (GP-I)-anchored sialidase activity on human erythrocyte surface was also reported by Chiarini et al.[164]. This sialidase hydrolyzed ganglioside substrates and possessed a pH optimum of 4.2, similar to the other acidic sialidases.

A membrane-bound sialidase activity with an acidic pH optimum was also detected in human thymocyte lysates[165]. No differences were observed in the levels of sialidase activity between immature and mature thymocytes, demonstrating that this enzyme did not play a role in T-cell maturation. However, since changes in sialidase activity, along with changes in cell surface sialylation profile, were demonstrated during T cell activation, the sialidase could play a role in cell physiology by regulating T cell activation.

A neutrophil sialidase activity that redistributed to different subcellular fractions on activation was demonstrated by Cross and Wright[166]. Neutrophil sialidase was initially associated with lysosomes and the plasma membrane. Following neutrophil activation, there was a redistribution of sialidase activity to the cell surface. The inhibition of neutrophil aggregation, as well as

neutrophil adhesion to plastic surfaces, by Neu5Ac2en suggests a role for the sialidase in neutrophil adhesion and aggregation.

A particulate, acid sialidase was detected in the sedimentable fraction of leukocyte homogenates with an optimum pH of 4.0 toward Neu5AcLac[167]. Two different types of sialidases (A and B) were identified in human leukocytes by Waters et al.[168]. The two sialidases were distinguished based on differences in optimum pH, effects of detergents, as well as temperature lability. The labile sialidase activity was found in the lysosomal fraction of leukocyte homogenates, whereas the temperature-stable activity was exclusively associated with the plasma membranes.

A Sialidase activity was also detected in the lymphocytes of a patient with adult-type sialidosis and partial β-galactosidase deficiency[169,170]. Sialidase activity in patient lymphocytes was compared to the activity in lymphocytes from normal subjects. Two types of sialidase activity were detected: a sonication-labile activity, which preferentially hydrolyzed the hydrophilic substrates, 4-MU-Neu5Ac and Neu5AcLac, and a second type of activity that was stable to sonication and hydrolyzed both hydrophilic substrates and gangliosides[170]. In addition, the authors demonstrated that only the sonication-labile lysosomal sialidase activity was deficient in sialidosis, whereas the sonication-stable sialidase was unaffected.

Warner and O'Brien[171] first demonstrated the presence of sialidase in human skin fibroblasts using 4-MUNeu5Ac. Most significantly, they found that sialidase activity was reduced to less than 2.5% of normal activity in fibroblasts of sialidosis patients, and to approximately 50% of normal levels in fibroblasts of obligate heterozygotes. This was the first indication that fibroblast sialidase could be used for the clinical diagnosis of sialidosis. These studies were followed by Ben-Yoseph et al.[172] reporting altered levels of sialidase activity in cultured skin fibroblasts from sialidosis and galactosialidosis patients. At least two genetically distinct sialidases were found in human skin fibroblasts. Despite certain differences in their properties, both enzymes were bound to membranes and both were thermally labile[173], similar to the oral, liver, and placental sialidases discussed above. One type of sialidase was glycolipid and ganglioside substrate-specific and the second was oligosaccharide substrate-specific. During sialidosis, there is a deficiency of this activity, whereas the ganglioside-specific sialidase activity remains unaltered.

Two distinct types of sialidases, with different subcellular localization (lysosomal and plasma membrane-associated), were found in the cultured human fibroblasts[174]. Both types of activity hydrolyzed the ganglioside GM3, but with different pH optima: pH 4.5 (lysosomal) and 6.5 (membrane-associated)[175]. In contrast, Fingerhut et al.[53] reported only one lyosomal sialidase activity in human fibroblasts that hydrolyzed hydrophilic and membrane sialoglycoconjugates.

1.3.3 Molecular cloning of mammalian sialidases

Starting from the amino acid sequences of tryptic peptides of the purified enzyme, in 1993 the first mammalian sialidase was cloned: it was the rat skeletal muscle cytosolic sialidase[176]. The primary structure of the protein revealed interesting homologies with the amino acid sequences of

the microbic counterparts. In fact, as already reported for viral and bacterial sialidases[41], the mammalian sialidase contains the F(Y)RIP domain in the amino-terminal portion of the protein, followed by a series (two) of so-called 'Asp-boxes' (SxDxGxxT/W). The following year, the cloning of the cDNA encoding the soluble sialidase secreted in the culture media by Chinese hamster ovary (CHO) cells was reported[177]. The two cDNA sequences show a high level of identity and encode highly homologous polypeptides. Then, in the late 1990s, three independent groups of investigators[114,178,179] reported the cloning of the first human sialidase (GenBank numbers, R13552, X78687, U84246, respectively), that is located in lysosomes. The cDNA encoding the sialidase in all three reports was approximately 1.9 kb in size and comprised of 1245 nucleotides. The gene was named NEU1 and mapped to the histocompatibility locus on the chromosome 17[180,181], which is sintenic to the human histocompatibility region on chromosome 6p21. These mapping data were supported by the identification of the combined deficiency in sialidase and cytochrome P450 steroid 21-hydroxylase activities[182], an enzyme encoded by a gene also located in the histocompatibility locus on chromosome 6p21. The human NEU1 gene (G9 sialidase gene) spans about 3.7 kb of DNA on chromosome 6p21.3 and is organized in six exons[179]. The position of the introns in the murine gene corresponds exactly to those in the human gene, although there is some variation in intron size. The human NEU1 gene was also identified by two other groups[114,178] using an '*in silico* cloning approach' searching for sequences containing F(Y)RIP motif and Asp boxes in the Expressed Sequence Tags database (dbEST)[183]. Identification of several mutations in sialidosis patients has demonstrated that the isolated cDNA encoded a lysosomal sialidase. Using the human cDNA as a probe, the mouse gene was isolated and the mutation responsible for the neuraminidase deficiency in SM/J mouse strain was identified[184,185].

In 1999, using a sequence homology-based approach, a novel human cDNA named NEU2 and encoding for a sialidase that mapped to chromosome band 2q37 was reported[186] (GenBank number Y16535). The open reading frame was composed of 380 amino acids being shorter than the sialidases reported previously[114,178,179]. The human NEU2 gene is organized in two exons separated by one intron on chromosome 2q37.1[186]. The rat orthologue shows a similar simple organization[145]. The promoter region of both the human[186] and rat[187] genes contain a classic TATA box and four E-boxes (-CAxxTG-), that are described as the DNA binding motif recognized by several nuclear factors belonging to the basic helix-loop-helix family of DNA binding protein.

Starting from the peptide sequences obtained from digestion of the purified NEU2 enzyme[188], in the same year the cloning of the cDNA encoding the membrane-associated sialidase from bovine brain was published[145], followed by the identification of the human ortholog[189]. A human brain ganglioside sialidase gene (GenBank number AB008185) was localized to chromosome band 11q13.5. Searching for entries showing homologies with the human cytosolic sialidase NEU2, a fragment of the same cDNA was identified in the dbEST[183]. This EST was used as a probe to isolate, from a human skeletal muscle cDNA library, the complete

transcript of this membrane-associated sialidase, named NEU3[190]. The human NEU3 gene (GenBank number Y18563) is located on chromosome 11q13.4 and comprehends 4 exons. Sequence analysis of the 58 untranslated regions reveals the presence of several Sp1-binding sites and the absence of TATA and CAAT box sequences, in agreement with the Northern blot analysis that shows a ubiquitous expression pattern. The identification of the mouse brain sialidase cDNA from a mouse embryo cDNA library was reported by Fronda and collaborators[191]. The molecular cloning of mouse cytosolic and plasma-associated sialidase cDNAs was obtained from the sequence information of previously cloned sialidase enzymes[192]. The same approach was used to clone the lysosomal and membrane-associated sialidase from a rat brain cDNA library[193].

Finally, Monti et al.[194] have recently identified a fourth human sialidase gene, NEU4, by the bioinformatics analysis of the sequences generated by the Human Genome Project (GenBank AF048727). The NEU4 gene, identified by searching sequence databases for entries showing homologies to the human cytosolic sialidase NEU2, maps in the telomeric region of the long arm of chromosome 2 (2q37), and is organized in four exons.

Figure 1-8 summarizes the schematic genomic organization of the four human sialidase genes cloned so far based on the analysis of the nucleotide sequences generated by the Human Genome Project.

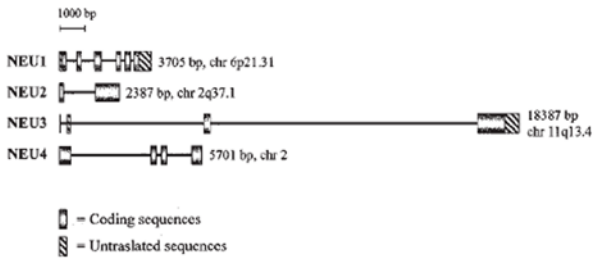

Figure 1-8 Gene structure of the human NEU1, NEU2, NEU3, and NEU4 genes.
(Monti, E. et al. *Neurochem Res* 2002)

1.3.4 Molecular properties of cloned human sialidases

The cDNA for human lysosomal sialidase (NEU1) was cloned and sequenced by three groups of investigators[114,178,179]. The translated protein was 415 amino acids long, corresponding to a molecular mass of approximately 45.5 kDa. The amino-terminal 45 amino acid residues had the characteristic signal sequence and three potential *N*-glycosylation sites. Following cleavage of the signal sequence and glycosylation, the mature protein was 370 amino acids long with a molecular mass of approximately 45 kDa. This sialidase contained a 'F/YRIP' motif and between three and five conserved and/or degenerate 'Asp-boxes'. Milner et al.[179] also mapped five intron/exon boundaries in the cloned G9 sialidase (NEU1) gene sequence.

The open reading frame of human NEU2 was composed of 380 amino acids, being shorter than NEU1 sialidases reported previously[114,178,179]. The primary amino acid sequence of this enzyme shared approximately 43% identity with the three lysosomal sialidases described above. NEU2 sialidase, however, showed a high degree of identity (72-74%) with the cytosolic sialidases from rat and hamster[186,195]. NEU2 sialidase was also found to be similar to a cosmid sequence, presumably coding for sialidase (GenBank accession AF048727). This sialidase contained one potential *N*-glycosylation site, two 'Asp-boxes' and an 'F/YRIP' motif in the primary sequence. NEU2 has a molecular mass of 42.2 kDa and an isoelectric point of 6.8. As confirmed by the absence of signal sequence or transmembrane domain, human NEU2 sialidase showed a cytosolic localization.

A human brain ganglioside sialidase cDNA was cloned and sequenced[189]. There were similarities and differences between the ganglioside and lysosomal sialidases. The cDNA was 3.0 kb in size and encoded an open reading frame comprising 436 amino acids with a molecular mass of 48.3 kDa, significantly longer than the lysosomal sialidases[114,178,179]. Similar to lysosomal sialidases, the ganglioside sialidase had three 'Asp-boxes' and an 'F/YRIP' motif, in addition to a presumptive transmembrane domain, but had only approximately 19% identity to human lysosomal sialidases[189]. A ganglioside sialidase, designated NEU3, which also localized to human plasma-membrane was cloned independently by Monti et al.[190]. The open reading frame consisted of 428 amino acids with a calculated molecular mass of 48.25 kDa and a theoretical pI of 6.78. NEU3 sialidase contained three 'Asp-boxes', an 'F/YRIP' motif, one potential *N*-glycosylation site, a putative transmembrane domain, and a ubiquitous tissue distribution. Despite small differences in amino acid length and composition, it is likely that the ganglioside sialidase cloned by Wada et al.[189] and NEU3[190] are either the same gene product, or at least highly similar enzymes.

The recently identified NEU4 gene encodes a 484-residue protein, as reported by Monti and coworkers[194]. The predicted protein, NEU4, contains all the typical sialidase amino acid motifs and, apart from an amino acid stretch that appears unique among mammalian sialidases, shows high sequence homology with the cytosolic (NEU2) and the plasma membrane-associated (NEU3) enzymes.

All the mammalian sialidases cloned so far show high degree of homology and share amino acid blocks of highly conserved residues, F(Y)RIP motif and Asp boxes in topologically equivalent positions throughout the primary structure (Figure 1-9). In addition, 8 or 9 of 12 of the amino acid residues that form the catalitic site of *S. thypimurium* enzyme[42] are conserved in mammalian sialidases. Overall, the protein family can be separated into three main groups: the lysosomal sialidases that are characterized by a leader sequence of 45 (human), 40 (mouse and rat) amino acid long, the soluble or cytosolic sialidase and the (plasma) membrane associated enzymes. Within these groups, the differences in terms of amino acid sequences are very low, with similarity values ranging roughly from 75% to 90%. Interstingly, NEU4 shows a characteristic stretch

of about 80 amino acid residues (aa 294-373) that appears unique among mammalian sialidases[132]. Data obtained from multiple sequence alignment were used by Monti et al.[132] to construct a gene family showing the relationships between the different mammalian sialidases cloned so far (Figure 1-10). The higher the percent similarity between sequences, the closer they are on the philogenetic tree. The lengths of the branches give an estimate of how distantly related the sequences represented by those branches are. The Kyte-Doolittle hydrophobicity plot of the human proteins does not show typical transmembrane domains, suggesting that the polypeptides are soluble. The association to the membrane of the NEU3 enzymes should involve different mechanism(s) of anchorage to the lipid bilayer[132].

Table 1-4 summarizes the general characteristics of the different members of the mammalian sialidase family. The differences in molecular weight are modest, as well as the isoelectric points that generally have values below 7, except in the case of MmNEU2 and HsNEU4. All the polypeptides have potential *O*-glycosylation sites and a great number of amino acid residues that can be covalently modified by phosphorylation[132].

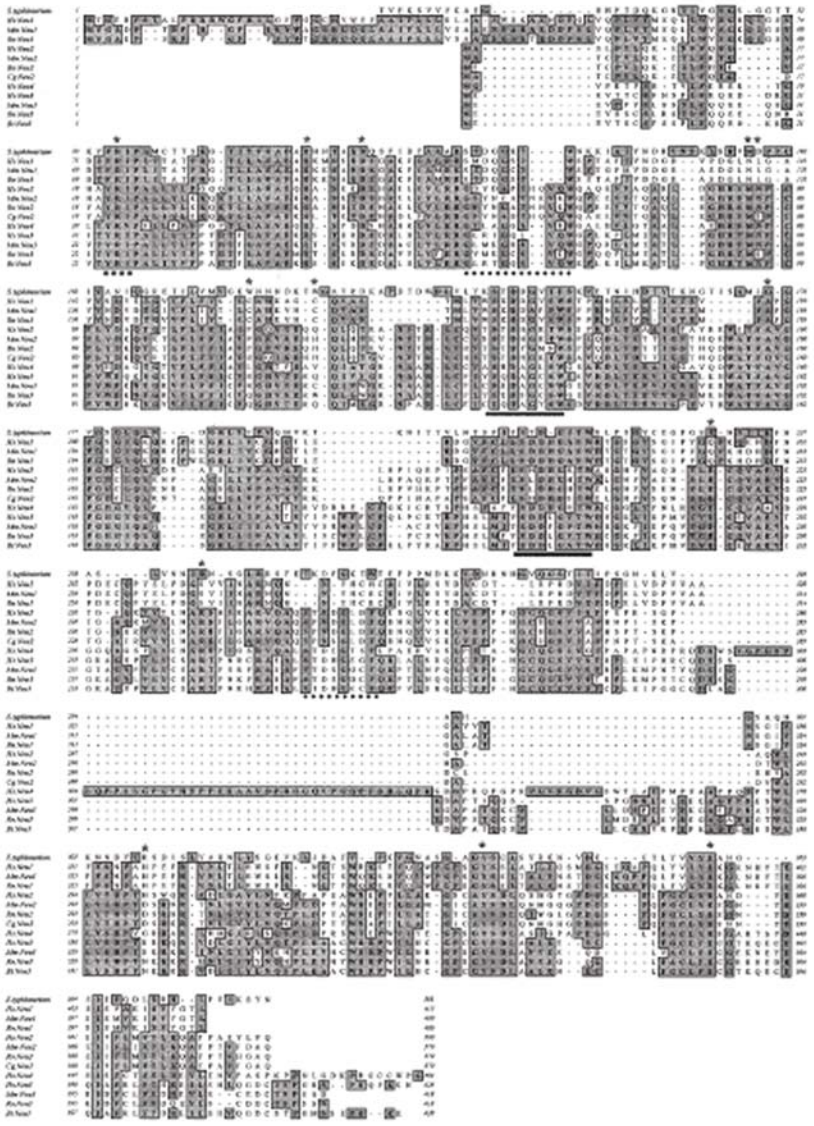

Figure 1-9 Multiple amino acid sequence alignment of sialidases.
(Monti, E. et al. *Neurochem Res* 2002)

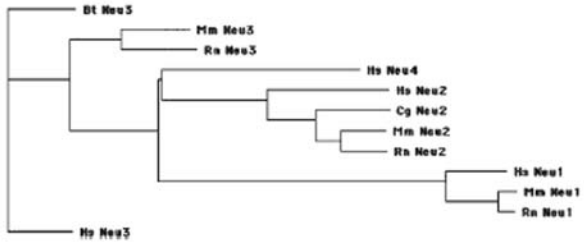

Figure 1-10 A gene family tree of mammalian sialidases constructed from the sequences of NEU protein family members.
(Monti, E. et al. *Neurochem Res* 2002)

Table 1-4 Comparison of the amino acid properties of mammalian sialidases.
(Monti, E. et al. *Neurochem Res* 2002).

	Homo sapiens (Hs)	*Mus musculus* (Mm)	*Rattus norvegicus* (Rn)	*Cricetulus griseus* (Cg)	*Bos taurus* (Bt)
Neu1					
Amino acids	415	409	409		
Molecular mass	45.47 kDa	44.59	44.69		
Theoretical pI	5.59	5.67	5.66		
O-Glycosylation sites	T:3, S:1	T:3	T:3		
Phosphorylation sites	S:16, T:8, Y:3	S:13, T:6, Y:1	S:13, T:8, Y:1		
Neu2					
Amino acids	380	379	379	379	
Molecular mass	42.23 kDa	42.40	42.38	41.96	
Theoretical pI	6.35	7.65	6.80	6.45	
O-Glycosylation sites	T:1, S:1	T:2	T:2	T:1	
Phosphorylation sites	S:10, Y:3	S:8, T:2, Y:3	S:9, T:3, Y:4	S:7, T:3, Y:3	
Neu3					
Amino acids	428	418	418		428
Molecular mass	48.25 kDa	48.85	46.98 kDa		47.92
Theoretical pI	6.78	6.28	5.79		6.38
O-Glycosylation sites	T:1, S:3	T:2	T:3		S:2
Phosphorylation sites	S:12, T:10	S:10, T:6, Y:3	S:16, T:4, Y:1		S:12, T:8, Y:3
Neu4					
Amino acids	484				
Molecular mass	51.63 kDa				
Theoretical pI	7.97				
O-Glycosylation sites	T:1, S:2				
Phosphorylation sites	S:21, T:7, Y:3				

Note: The target amino acids for *O*-glycosilation and phosphorilation are indicated with the single letter code.

1.3.5 Expression and transfection studies

The expression levels in different tissues of NEU1, NEU2, and NEU3 were assessed by Northern blot analysis. Human NEU1 gene is expressed in a single transcript of about 1.9 kb in all tissue tested. The transcript appeared to be the most abundant in pancreas, followed, in decreasing order, by skeletal muscle and kidney, heart and placenta, liver, lung, and, finally, at relatively low levels, brain[178]. Conversely, the mouse gene is expressed in two major and two minor transcripts, with a length from 1.8 to 4.0 kb. The mRNAs levels appeared to be the most abundant in kidney and epididymis, a moderate expression is detected in brain and spinal cord, followed by liver, adrenal gland, lung, heart, smooth muscle, testis and finally spleen which shows low expression levels[184,196].

Human NEU2 is transcribed, among the different members of the gene family, at a rather poor level. The transcript detectable in skeletal muscle is about 4 kb long[186]. The low expression level of NEU2 is confirmed by the absence of ESTs corresponding to the transcript in dbEST[183].

Human NEU3 shows by Northern analysis two transcripts, one of about 7.4 kb appears to be the major form, and the other one, with a molecular weight of about 2 kb, is present only in certain tissues[189]. Overall the gene is expressed in a ubiquitous manner, with the higher expression detectable in adrenal gland, skeletal muscle, testis, and thymus[189,190]. In addition, NEU3 is expressed in human fetal tissues[190]. As revealed by northern blot analysis, the mouse gene is expressed most highly in the heart and, at a lower level, also in brain, spleen, lung, kidney and testis, showing a unique transcript of about 3.4 kb[192].

Expression analysis of human NEU4 gene reveals the presence of transcripts in all the human tissue tested. Besides a well detectable expression in several CNS districts, colon, small intestine, and kidney, the highest expression is detected in liver. In addition, NEU4 is expressed with a roughly similar pattern in fetal tissues[194].

Transfection studies with human sialidases offer great potential for investigating the *in vivo* functions of the enzyme[197]. For example, Meuillet et al.[198] found that human epidermoid carcinoma cell line (A431) transfected with human sialidase cDNA grew faster than control cells, displayed increased receptor kinase sensitivity and tyrosine autophosphorylation, and lower levels of the ganglioside GM3. The authors proposed that modulation of ganglioside expression by human sialidases might represent an approach to alter tumor growth. The role of 'protective protein' in sialidosis or galactosialidosis was also elucidated using gene transfection studies, regardless of whether the sialidase gene being transfected was of human or rodent origin[184,197]. Transient expression of lysosomal sialidase cDNA into sialidase-deficient fibroblasts restored sialidase activity to these cells[178]. Immunofluorescence studies with COS-7 cells expressing recombinant NEU1 sialidase showed that the enzyme was localized to the endoplasmic reticulum[179], although its role in this subcellular compartment is not clear. Transfection of NEU2 sialidase cDNA into COS-7 cells resulted in enhancement of sialidase activity, and also assigned a cytoplasmic localization, demonstrating the particulate nature of this sialidase[195]. In contrast, immunofluorescence of COS-7 cells transfected with NEU3 sialidase cDNA showed a plasma membrane localization for this sialidase[190]. By transfecting normal and mutant cDNA for human lysosomal sialidases into COS-7 cells and sialidase-deficient human fibroblasts, Lukong et al.[199] and Bonten et al.[200] have identified the effects of specific gene mutations on sialidase activity and its correlation with sialidosis. Transfection of human sialidase cDNA into neuroglia cells suggested a pharmacological role for the activation of sialidase in the treatment of Tay-Sachs disease[146].

1.3.6 Three-dimensional structures of human sialidases

As already mentioned, the primary structures of all mammalian sialidases cloned so far have shown significant homologies with bacterial sialidases whose three-dimensional structure has been solved. Thus, a

computer modeling approach can be used to predict the structure of the mammalian sialidases based on the structures of bacterial enzymes. In the case of the human lysosomal sialidase NEU1 the modeling was performed using the structures from *S. typhymurium*, *V. cholerae*, and *M. viridifaciens* as templates. The resulting structural model indicates that NEU1 shares the same fold of bacterial and viral sialidases. The typical sialidase structure consists of six four-stranded antiparallel β-sheets arranged as the blades of a propeller[201-203].

Similar results were obtained for the human cytosolic sialidase NEU2, based on the atomic coordinates of the homologous bacterial enzyme from *S. thypimurium*[195]. The overall predicted structure of NEU2 shows again the six-bladed β-propeller fold typical of viral and bacterial sialidases. Despite the low sequence identity between the viral and the bacterial sialidases (about 15%) and among different bacterial enzymes (about 30%), the topology of the active site and the residues involved in its formation are strictly conserved in these proteins. The main differences are located in the amino acid residues that in the microbic enzymes form a hydrophobic pocket that accommodates the *N*-acetil group of sialic acid. These discrepancies could reflect peculiar substrate specificity of mammalian sialidases.

Afterwards, Chavas and coworkers[204] reported the first high resolution X-ray structures of mammalian sialidase, human NEU2, in its apo form and in complex with an inhibitor, 2-deoxy-2,3-dehydro-*N*-acetyl neuraminic acid (DANA). The structure shows the canonical six blade β-propeller observed in viral and bacterial sialidases with its active site in a shallow crevice. In the complex structure, the inhibitor lies in the catalytic crevice surrounded by ten amino acids. In particular, the arginine triad, aids in the positioning of the carboxylate group of DANA within the active site region. The tyrosine residue, Y334, conserved among mammalian and bacterial sialidases as well as in viral neuraminidases, facilitates the enzymatic reaction by stabilizing a putative carbonium ion in the transition state. The loops containing E111 and the catalytic aspartate D46 are disordered in the apo-form. Upon binding of DANA, the loops become ordered to adopt two shirt α-helices to cover the inhibitor, illustrating the dynamic nature of substrate recognition (Figure 1-11). The *N*-acetyl and glycerol moieties of DANA inhibitor are recognized by NEU2 residues not shared by bacterial sialidases and viral neuraminidases, which can be regarded as a key structural difference for potential drug design against bacterial, influenza and other viruses.

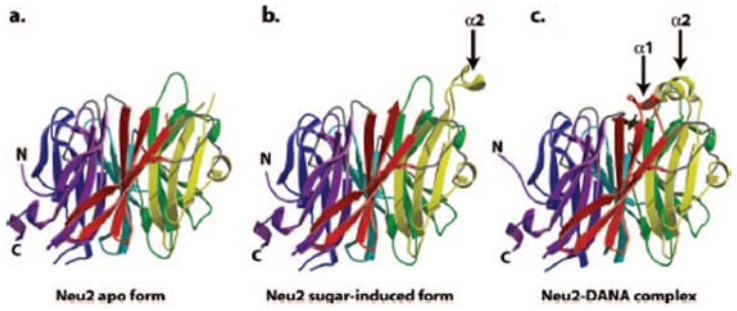

Figure 1-11 Structural changes of NEU2 upon maltose and DANA binding.
(Chavas, L.M. et al. *J Biol Chem* 2005)

Since human sialidase enzymes have low homology with their viral, bacterial and protozoal counterparts, the models built with them may not be accurate. Moreover human NEU2 is the only human sialidase whose crystal structure is available so far, and this sialidase has a high level of sequence identity with NEU3 (42%) and NEU4 (44%) and low but significant identity with NEU1 (28%).

Recently, three-dimensional structures of NEU1, NEU3 and NEU4 were modeled based on the experimental crystal structure of human NEU2, using the homology modeling program MODELER[205]. The amino acid sequences of NEU1, NEU3 and NEU4 were aligned with sequence of NEU2 extracted from its crystal structure, using a multiple sequence alignment method based on the CLUSTAL W program, named Align123. The alignment of sequences showed the common motif F/YRI/VP near N-terminal and the highly conserved amino acids residues that form the active site of NEU2 enzyme. The refined final alignments of human sialidase enzymes were used for constructing homology models of human sialidase enzymes using the MODELER program. Predicted structures and the experimental protein-ligand complex of NEU2 were compared to identify similarities and differences among the active sites. Comparison between the modeled structures and crystal structure of NEU2 showed similarity in active site topology and overall folding of enzymes. Despite these similarities, some differences at the active site and its vicinity emphasize the differences in the experimental substrate specificity. Molecular electrostatic potential calculations revealed the differences in the charge distributions around the putative substrate entry site, which can account for differential substrate recognition and binding. Thus results of this study supply useful information in better understanding of the structural differences at the active site among the human sialidase enzymes and the present work constitutes the first step in the structure-based design of selective NEU3 inhibitors.

1.3.7 Evolutionary aspects of sialidases

The apparent lack of sialic acid or sialidases among plants raises interesting evolutionary questions[40,206]. Sialidase activity is increased in the tissues and blood of humans as a result of certain viral or bacterial

infections. However, thus far an unmistakable correlation between the presence of sialic acid and microbial or viral pathogenicity has not been established. This raises the intriguing possibility of whether the sialidases were acquired by microorganisms from their hosts during evolution. Many bacteria expressing sialidase do not synthesize sialic acids. Sialidases might have been acquired by such bacteria only to assist their spread among mammalian hosts. The frequent occurrence of sialidases among pathogens and the structural similarities between animal and microbial sialidases are evidence for such a hypothesis. It also supports the argument that the various sialidases originated from a common ancestral gene and for the existence of a sialidase superfamily[40]. Miyagi et al.[145] also postulated a common ancestry for the human, bacterial and mammalian sialidases based on amino acid sequence identities. There is, of course, the possibility that the biosynthesis of sialic acid and sialidases arose early during evolution and that the microorganisms lost sialic acid biosynthetic ability, while retaining the sialidase gene in order to assist in their spread among mammalian hosts.

Viral, microbial, and animal (including human) sialidases share common structural motifs[40]. One is the so-called ‘Asp-box’ motif, comprising the consensus amino acid sequence: S/W-X-D-X-G-X-S/T-W/F. There are two-five-fold repeats of this motif in the amino acid sequence of sialidases from various sources. There are four separate types of ‘Asp-boxes’, designated I-IV. ‘Asp-boxes’ II and IV are more degenerate than I and III. The precise role of the ‘Asp-box’ motif in sialidase activity is unknown. It was proposed that the sequence might be involved in the secretion of the sialidases, or that it might be important for protein folding, or help to maintain the structure of the catalytic domain in sialidases[22]. The last suggested role seems likely, because Lukong et al.[199] and Bonten et al.[200] identified several mutations affecting the ‘Asp-box’ residues or those flanking the ‘Asp-box’ of human lysosomal sialidase. Several mutations in sialidosis patients, affecting the ‘Asp-box’ residues or those flanking the ‘Asp-box’ of human lysosomal sialidase, resulted in a deficiency of sialidase activity. Because these motifs are distantly located from the catalytic site, it is unlikely that the ‘Asp-box’ is directly involved in sialidase catalysis. A second conserved motif is the ‘F/YRIP’ motif, comprising the amino acid sequence: X-P-R-P[40]. This sequence is located amino-terminally from the ‘Asp-box’ motif. The arginine in the ‘F/YRIP’ sequence is one of the catalytic triad of arginine residues that interact with the carboxylate group of sialic acid during substrate binding and catalysis. Two additional conserved regions are evident from an examination of the amino acid sequences of all human sialidases: the AFAE and the FLF-Y/F amino acid sequences. The structural or biological significance of these two conserved regions for human sialidase is currently unknown.

Amino et al.[207] proposed that the blood-sucking insect *Triatoma infestans* might have evolved from plant-sucking hemiptera by switching to blood-sucking. During the switch, *Triatoma* could have acquired a sialidase gene from a vertebrate host. The authors believe that such an acquisition could also explain the similarities in the substrate preferences (for α2-3 linkage) common to viral, trypanosomal and bacterial sialidases. However, trypanosomal trans-sialidases could have evolved as a group distinct from

bacterial sialidases. Identification of the genes encoding the various sialidases will be essential for an understanding of the evolutionary linkages among the prokaryotic and eukaryotic sialidases. The data emphasize the need for eliminating pathogens as a source of sialidase activity while studying human tissues.

A horizontal gene-transfer mechanism for the spread of the sialidase gene was proposed to explain the existence of structurally similar sialidases among evolutionarily distinct creatures, as well as for a common origin for all sialidases[40,58]. When evolutionarily distant microorganisms are in ecologically close proximity to their host tissues, gene transfer between the organisms could be facilitated by viruses, plasmids, or transposons. For example, amino acid and nucleotide sequence analyses and secondary structure predictions indicated that the sialidases in *Salmonella typhimurium* (Gram-negative) and *Clostridium perfringens* (Gram-positive) are homologous. These sialidases were also similar to other microbial (*C. sordellii*, *Bacterioides fragilis*, and *T. cruzi*) and viral (influenza virus) sialidases[58]. This hypothesis would, of course, imply that the mammalian sialidase is the ancestor of pathogenic microbial sialidases, suggesting a monophylogeny for these enzymes. When a gene is acquired from a foreign source by bacteria, the gene is usually adapted for bacterial purposes, or else the gene is eliminated. Sialidases in *S. typhimurium* and *C. perfringens* are cytosolic and cannot utilize the sialoglycoconjugate substrates occurring extracellularly in their hosts. In order to utilize these types of substrates, the sialidases would have to acquire a signal peptide sequence and become secreted sialidases. However, the lack of such an adaptation in these bacteria argues that the acquisition of the sialidase gene in these microorganisms is a recent event[58]. The fact that NEU2, the first human sialidase whose structure has been characterized, also adopts the same active site architecture reinforces the notion of a common ancestor of sialidases despite the low sequence homologies between bacterial and their viral counterparts[204].

1.3.8 Physiological roles of human sialidases

Sialidases are involved in the metabolism of sialic acids, and could therefore regulate cellular processes by modifying the expression of sialic acid. Striking differences were found in cellular sialylation patterns during growth, development, activation, aging, and oncogenesis. For example, desialylated erythrocytes, lymphocytes, and platelets were shown to be rapidly bound and phagocytosed by macrophages and eliminated from the blood stream[13]. Sialylation also protects proteins against proteolytic attack, and desialylation by sialidases could render these proteins susceptible to proteolysis[208]. Sialidase activity was supposed to play a role in the assembly of tropoelastin into elastic fibers, based on results with cultured fibroblasts from patients with sialidosis or galactosialidosis[209]. The presence of sialic acid in glycoproteins was responsible, at least in part, for binding and transport of molecules, masking of cellular antigens, cells surface charge, cells aggregation, and cells shape[210]. Involvement of sialic acids, and therefore of sialidases, seemed likely in such cellular phenomena as malignant transformation, contact inhibition, cell growth, cell proliferation, cell

differentiation, cell-cell interactions, cell membrane functions, and cell migration[102,211]. Other functions of sialidases include catabolism of glycoproteins and glycolipids (lysosomal sialidase), catabolism of gangliosides in lysosomes, plasma membrane, and myelin (ganglioside sialidase), and the remodeling of polysialic acids (endosialidase)[212].

The physiological roles of human sialidases during ganglioside catabolism were explored. Ganglioside catabolism occurred primarily at the plasma membrane level, catalyzed by sialidase. Human fibroblasts in culture released two or more distinct sialidases into the 'conditioned medium', and these sialidase(s) may be of lysosomal origin[175,213,214]. GM3 ganglioside plays a role in modulating the phosphorylation status of growth factors. Sialidases, by hydrolyzing GM3 to lactosylceramide, could therefore play a role in cell proliferation. Lactosylceramide might also cycle back to GM3, due to sialyltransferase[175,215,216]. Neu5Ac2en strongly and specifically inhibited both fibroblast sialidase activity and cell growth and proliferation when added to cells in culture[214]. On the other hand, addition of *C. perfringens* sialidase to human skin fibroblasts in culture resulted in the stimulation of cell growth, thereby providing some evidence of a role for sialidase during cell proliferation[217]. Sweeley and colleagues have therefore suggested a role for the extracellular sialidases in modulating transmembrane signaling events[175,215].

1.3.9 Assembly and physiological role of multi-protein complexation of sialidase

The human enzyme often existed in a multi-protein complex. Mammalian lysosomal sialidase is unique in requiring multi-protein complexation in order to stably express enzymatic activity. It turned out that the multi-protein complexation has major implications, not only in structure-function relationships of human placental (lysosomal) sialidase, but also in human diseases associated with the deficiency of one or more proteins of the complex.

Perhaps the first report of multi-protein complexation was by Ohman et al.[137], who reported that human brain sialidase existed in a complex with glycosidases. The high (approx. 240 kDa) molecular mass assigned to human leukocyte and fibroblast sialidases[218] could also be due to multi-protein complexation. Human lymphocyte sialidase was shown to form a complex with β-galactosidase by Verheijen et al[219]. Human lysosomal membrane-bound sialidase was also shown to exist in a 600-700 kDa high molecular mass aggregate due to complexation of human sialidase (76 kDa) with β-galactosidase (64 kDa) and a 'protective protein' (32 kDa)[220,221]. The high molecular-mass aggregate consisted of multimers of all three proteins[151,152]. Molecular mass of sialidases could change due to the glycosylated nature of the enzyme, as was demostrated for the mature form of human placental sialidase[222]. Multi-protein complex formation was essential to conferred stability to the sialidase activity. The human placental multi-protein complex, designated 'NGC' (neuraminidase-galactosidase-carboxypeptidase), was extensively characterized by Potier et al.[223]. They proposed a model in which the 'NGC' consists of a core hexamer of sialidase (66 kDa) and β-galactosidase (63 kDa) in unknown proportions.

The hexamer is surrounded by five 52 kDa carboxypeptidase heterodimers that act as a bridge between the sialidase and β-galactosidase protomers in the 'NGC' complex.

The availability of the cDNA encoding the lysosomal sialidase NEU1 allowed a detailed study of the process of its catalitic activation. In mammalian tissues, NEU1 is present as a high-molecular-weight multi-enzyme complex with the protective protein/cathepsin A (PPCA) and β-galactosidase and copurifies with these proteins[224,225]. A much larger (1.27 MDa) multi-protein complex that included sialidase, cathepsin A, β-galactosidase, and *N*-acetylgalactosamine-6-sulfate sulfatase was described in human placenta and cultured human skin fibroblasts[224]. The multi-protein complex of sialidase, β-galactosidase, and protective protein-cathepsin A (PPCA) was expressed in insect cells and isolated as a multimer of 1350 kDa[226]. Direct binding of β-galactosidase, as well as the 20 kDa subunit of PPCA, to the sialidase was also demonstrated. These authors showed that lysosomal sialidase was activated following multimerization at acidic pH in the presence of PPCA. The interactions of sialidase with PPCA were essential for the lysosomal routing and localization. Probably, the association with PPCA allowed the correct folding and oligomerization of the sialidase and also prevented the aggregation of the partially or completely unfolded enzyme.

The exact mechanism(s) by which multi-protein complexation takes place and the precise physiological role(s) of the resulting complex are not fully understood. It is clear that multi-protein complexation at some level is essential for expressing sialidase activity[220,222]. In this respect, human lysosomal sialidase is unique in being the only member of the sialidase superfamily that needs other protein(s) in order to be catalytically active. Multi-protein complexation was thought to protect the sialidase against degradation by lysosomal proteases[223,224], as well as to provide control mechanisms for sialidase activity[226]. These types of mechanism(s) might also serve in a larger sense, to regulate the metabolism (biosynthesis and degradation) of sialoproteins, complex sialooligosaccharides, and gangliosides.

A genetic deficiency of the 'protective protein' was associated with the rapid degradation of β-galactosidase and sialidase, leading to sialidosis or galactosialidosis[220,223]. First of all, the complex was absent in fibroblasts from galactosialidosis patients[224]. However, recombinant 'protective protein' in the culture medium was taken up by the mannose-6-phosphate receptor system of the deficient fibroblasts[227]. Once internalized, the 'protective protein' was routed to the lysosomes and processed into the mature 32-20 kDa heterodimeric form that restored cathepsin A, sialidase, and β-galactosidase activity to the deficient fibroblasts[227]. Electroporation of sialidase cDNA into fibroblasts cultured from sialidosis patients was also able to restore sialidase activity to these cells[178].

1.3.10 Pathological conditions associated with sialidase deficiency

It is believed that lysosomal sialidase is involved in the degradation of sialoglycoproteins. Two human diseases, sialidosis and galactosialidosis, are clearly associated with a deficiency or defect of lysosomal sialidase.

Analysis of the molecular defects in the sialidase NEU1 gene in sialidosis patients with various degree of disease penetrance shows a characteristic spectrum of mutations. In fact, most of the sialidosis patients studied so far had amino acid substitutions but not frameshift or splicing defects[114,178,197,199,200,228]. Transgenic expression of the missence mutants allowed the study of their residual enzymatic activities, subcellular distribution. Overall, three mutation groups can be constructed: a) catalytically inactive and not lysosomal; b) catalitically inactive but with lysosomal localization; and c) catalytically less active than wild-type.

Sialidosis

Sialidosis is an inherited, autosomal, recessive lysosomal storage disease associated with lysosomal acid sialidase deficiency and subsequent lysosomal storage[229]. There are two major clinical manifestations: sialidosis type I (non-dysmorphic, late, adult onset) and type II (early, infantile onset); the latter being the more severe condition. Sialidosis types I and II share certain clinical manifestations. Sialidosis type I can be detected in patients within the age group of 8-25 years. This condition manifests as cherry-red spot myoclonus, seizures, neuropathy, corneal clouding and difficulties in walking[229]. Sialidosis type II is manifested as coarse face, myoclonus, mental retardation, cherry-red spots, psychomotor retardation, bone abnormalities, progressive neurological disorders, vacuolated lymphocytes, and hepatosplenomegaly, with severe cases being fatal[229].

Sialyloligosaccharides, sialylglycoproteins, glycolipids, and GM3 are all substrates for lysosomal acid sialidases. Lieser et al.[230] reported two distinct lysosomal sialidases: one that utilized sialylglycoproteins and sialyloligosaccharides as substrates, was cytosolic; the second type was membrane-bound, and utilized glycolipids and the ganglioside GM3 as substrates. Only the cytosolic (lysosomal) sialidase was deficient in sialidosis, whereas the membrane-bound sialidase was normal. Consequently, there was an accumulation and excessive urinary excretion of sialyloligosaccharides during sialidosis, whereas the levels of polysialogangliosides or GM3 were normal.

Several investigators have identified a number of mutations in the lysosomal sialidase gene isolated from sialidosis types I and II patients. It is important to note a correlation between residual sialidase activity and the clinical severity of sialidosis[200]. A case in point is the $Tyr^{370} \rightarrow Cys$ mutation in sialidosis type II that abolished enzymatic activity. A tyrosine has been identified as the catalytic site residue for viral, bacterial, and, presumably, the human sialidase, explaining the severe enzyme deficiency associated with this mutation[200].

Measurement of sialidase activity in freshly isolated fibroblasts or leukocytes using 4-MUNeu5Ac as substrate offers a diagnostic test for sialidosis patients. Less than 15% of normal sialidase activity was detected in the leukocytes of sialidosis patients[168,218]. It is difficult to distinguish between sialidosis and galactosialidosis, since sialidase activity is deficient in both diseases. However, carboxypeptidase activity is additionally deficient only in the cells from patients with galactosialidosis and will help to distinguish the two types of patients. Using synthetic substrates, Mueller and

Wenger[231] reported less than 10% of the normal levels of sialidase activity in fibroblasts or leukocytes from amniotic fluid of sialidosis patients, potentially enabling this to be a prenatal diagnostic test. No treatment is currently available for sialidosis patients.

Galactosialidosis

Galactosialidosis is an autosomal, recessively inherited, lysosomal storage disease in which there are depressed levels of sialidase activity in afflicted patients[232-234]. This disease was also referred to as Goldberg syndrome, I-cell disease, mucolipidosis II, cherry-red-spot myoclonus syndrome, and GM1-gangliosialidosis type 4[231]. Certain clinical manifestations and biochemical features of galactosialidosis are similar to those of sialidosis. Like sialidosis, patients with galactosialidosis also accumulate and excrete large amounts of a complex carbohydrate mixture of glycopeptide fragments rich in sialic acid. Galactosialidosis also manifests heterogeneous clinical phenotypes: an early-onset, severe, infantile form of the disease and a late-onset, slowly progressive, adult form of the disease[233]. Neurological signs of galactosialidosis include cherry-red spots, myoclonus, and mental retardation. There is skeletal dysplasia, corneal clouding, hepatosplenomegaly, hernia, coarse face, and hearing loss. Foam cells appear in the bone marrow. Endothelial cells and lymphocytes are vacuolated. The breakdown of vascular cell adhesion molecules in vacuolated endothelial cells appeared to promote brain infarctions in galactosialidosis patients[235].

In galactosialidosis, there is a combined deficiency of sialidase and β-galactosidase[229]. The primary molecular defect in galactosialidosis is with the 'protective protein' (expressing cathepsin A, serine protease, carboxypeptidase, and C-terminal deamidase activities). In fibroblasts of galactosialidosis patients, the levels of both sialidase and β-galactosidase were severely deficient compared to the levels in normal fibroblasts[236]. A 'corrective factor' (later identified as 'protective protein') present in normal fibroblasts, when added to defective fibroblasts, restored both sialidase and β-galactosidase activity to near normal levels in the defective cells. A combined β-galactosidase-sialidase deficiency was caused by a defective 32 kDa protein ('protective protein'), which was required for the protection of sialidase and β-galactosidase against intralysosomal degradation[236].

The genetic defect was a mutant form of the 'protective protein' gene that was localized to chromosome 20q13.1[234,237] using the *in situ* hybridization technique[238]. Fibroblasts obtained from galactosialidosis patients transfected with the chimeric cDNAs for 'protective protein' and green fluorescent protein resulted in restoration of intracellular levels of cathepsin A, sialidase, and β-galactosidase activity[239]. Vinogradova et al.[115] found that there was a five-fold decrease both in the sialidase levels and sialidase half-life in fibroblasts from galactosialidosis patients compared to normal cells. In the fibroblasts of galactosialidosis patients, the sialidase was also degraded into 38 kDa and 24 kDa catalytically inactive fragments.

The combined deficiencies of β-galactosidase and sialidase in lymphocytes and in cultured skin fibroblasts will help to diagnose galactosialidosis patient. Similar combined deficiencies in the amniotic fluid

could help in the prenatal diagnosis of galactosialidosis[240,241]. Only the activity that is predominant in lymphocytes is deficient in galactosialidosis patients. Sialidase activity is similarly deficient in sialidosis. For diagnostic purposes therefore, it is important to measure sialidase activity in both isolated lymphocytes and cultured skin fibroblasts of patients clinically diagnosed with galactosialidosis[234]. It is equally important to also demonstrate β-galactosidase deficiency in patients in order to confirm the diagnosis of galactosialidosis and exclude sialidosis. No therapy currently exists for the treatment of galactosialidosis patients.

1.3.11 Sialidase and muscle cell differentiation

The enhancer/promoter sequence of rat cytosolic sialidase (RnNEU2) contains four E-boxes and a classic TATA box[187]. E-boxes are involved in the development- and tissue-specific regulation of muscle gene transcription[242]. A similar organization of the 58-upstream region was reported for human NEU2 gene[186], indicating that at least the rat and human genes are preferentially expressed in muscle tissues. In addition, the rat 58-upstream region was better characterized following its ability to drive the transcription of a reported gene in transient transfection experiments[187]. The promoter region is active in rat myogenic cells, and its transcriptional activity was increased after induction of myoblast differentiation. Further studies demonstrated that during myoblast differentiation NEU2 mRNA levels as well as enzyme-specific activity increase, and myotube formation can be blocked by the addition of a specific antisense oligomer[243]. Finally, the presence of RnNEU2 in rat skeletal muscle cells was demonstrated using both fluorescence and electron microscopy[244]. The enzyme appears to be diffusely distributed in the muscle fibers and also found in the perimysium and blood vassels. In addition, many immunogold particles were also found in the cytosolic compartment of axons, Schwann cells, and cells of endomysium and, again, blood vessels, indicating that NEU2 is also present in cells other than skeletal muscle fibers. Overall, these data provide direct evidence for the involvement of RnNEU2 in the complex series of events leading to myoblast differentiation.

1.3.12 Sialidase in nervous tissue

Sialylated molecules are abundant in the nervous system, suggesting that this might be a location where sialidases could play an important regulatory role. Sialidases in nervous tissue have been extensively studied in the last three decades[45]. The plasma membrane-associated sialidase (NEU3), together with sialyltransferase, is thought to play a pivotal role in the regulation of the sialic acid levels of membrane-bound sialyl glycoconjugates. Among these compounds, gangliosides are the most abundant in the plasma membrane of vertebrate cells and are involved in several important biological processes[245]. In human neuroblastoma cells, NEU3 acted specifically on gangliosides with terminal sialic acids, yielding to GM1 and lactosylceramide[246,247]. Recently, using a water-soluble GD1a-neoganglioprotein substrate on intact neuroblastoma cells, it was proved that NEU3 is cell surface oriented[248]. In addition, NEU3 cofractionates with

markers of lipid rafts, membrane functional microdomains where gangliosides and other glycosphingolipids are arranged together with signaling proteins[76,249]. Moreover, recent researches suggest the involvement of NEU3 in neuritogenesis and axonal growth and regeneration. The general mechanism by which gangliosides promote neuritogenesis has not been elucidated yet, but a massive desialylation of the cell surface carried out by endogenous as well as exogenous sialidases has been suggested as a critical event for myelination[250], neuronal differentiation[246,247,251,252], synaptogenesis, and synaptic function[253]. In this perspective, the molecular cloning of the plasma membrane associated sialidases (PMS, NEU3) has provided several research tools to better investigate the role of the enzyme. For example, expression studies of mouse NEU3 demonstrated its involvement in Neuro2a cell differentiation[192]. *In situ* hybridization of adult mouse brain demonstrates NEU3 expression in the cerebral cortex, in the granule cell layer Purkinje cells and deep cerebellar nucleus of the cerebellum. In addition, NEU3 level is increased during Neuro2a cell differentiation, and stable transfection of the enzyme resulted in accelerated neurite arborization. Among sphingolipids, ganglioside GM1 plays a role in axonal growth and neuronal differentiation but most of the data obtained in this field depended on addition of exogenous GM1 or GM1 blockers (i.e., antibodies, cholera toxin) to cultures of neuron-like cell lines. The molecular cloning of the plasma membrane-associated sialidase (NEU3)[145,189,190,192,193] allowed a modification of the enzyme level in cultured cells. Since NEU3 is able to hydrolyse a mixture of gangliosides into GM1 *in vitro*, an enhancement of the plasma membrane associated sialidase probably leads to an enrichment of the membrane GM1 *in vivo*. A recent paper provides several information about the biological role of this membrane enzyme[254]. NEU3 mRNA level is high at early developmental stages of the hippocampus while it is lower in the adulthood. The protein level follows a temporal correlation with neuritogenesis, and its inhibition with the sialidase competitive inhibitor NeuAc2en diminishes neurite growth. Conversely, an increase of NEU3 enzyme activity, obtained by transfecting hyppocampal neurons in culture, accelerates axonal growth and the polarization of citoskeletal proteins. NEU3 overexpression increases the regeneration capacity of the initial axon in response to axotomy. NEU3 induces TrkA-mediated signaling, leading to actin depolymerization and axonal growth. The mechanism by which NEU3 affects TrkA is likely through changes in cells' ganglioside composition, such as desialylation of GD1a to produce increased levels of GM1. NEU3 has been shown to cause increases in ganglioside GM1, which is capable of enhancing TrkA dimerization and potentiating the effect of nerve growth factor (NGF)[255]. Overall, these experimental evidences imply that NEU3, through the modulation of GM1 plasma membrane content, is involved in the complex machinery controlling the axonal growth and regeneration.

To understand the role of NEU3 in neuronal differentiation, Proshin et al.[256] studied the relationship between neurite outgrowth and NEU3 expression in human neuroblastoma NB-1 cells. Induction of neurite outgrowth by dibutyryl cAMP increased NEU3 expression, and this event was probably attributable, in part, to transactivation of the NEU3 gene

through cAMP responsive elements in the 5'-upstream region. While treatment with dibutyryl cAMP alone enhanced the outgrowth of dendrite-like processes, transfection of the NEU3 gave rise to a more prominent outgrowth of neurites with axon-like characteristics, even in the absence of stimulus. These results indicate that NEU3 regulates neurite formation in NB-1 cells, and suggest that this effect may be enhanced by dibutyryl cAMP via a cAMP-dependent pathway. Recently, Valaperta et al.[257] showed that a reduction of the plasma membrane-associated sialidase NEU3 activity upon NEU3 siRNA caused neurite elongation in Neuro2a murine neuroblastoma cells. The differentiation process was accompanied by an increase of the acetylcholinesterase activity, a moderate increase of the c-Src expression and by the presence of the axonal marker tau protein on the neurites. Characterization of the sphingolipid pattern and turnover in transduced and control cells revealed that the total ganglioside content remained quite similar in NEU3 silenced cells, however GM2 increased by 54%, GM3 remained constant and GM1 and GD1a decreased by 66% and 50%, respectively. In addition, ceramide decreased by 50%, whereas the sphingomyelin content did not change in NEU3 silenced cells.

NEU3 activity can also affect cellular proliferation and neurite outgrowth in neuroblastoma cells, but the details of these changes remain unclear. Both NEU3 silencing[257] and NEU3 overexpression[256] have been shown to stimulate neurite outgrowth. This apparent discrepancy may reflect the differences present in the cholinergic and adrenergic neuroblastoma cell lines in which these experiments were performed[258]. NEU3 activity is enriched in membrane microdomains of neuroblastoma cells and cosegregates with GM1 and other lipid raft markers such as flotillin, Src family kinases, and glycosylphosphatidylinositol (GPI)-anchored proteins[259]. The localized distribution of NEU3 within a particular neurite specifies the site of axon generation[260]. Intriguingly, a bacterial sialidase can have a similar effect in living animals: delivery of *Clostridium perfringens* sialidase to a spinal cord injury site in a rat dramatically enhanced spinal axon outgrowth and might represent a therapy to improve recoveries from central nervous system injuries[261].

1.3.13 Aberrant expression of sialidase in cancer

Aberrant sialylation in cancer cells is thought to be a characteristic feature associated with malignant properties including invasiveness and metastatic potential. In the 1960’s and early 1970’s, the subject of cell surface sialic acids in malignant cells received attention. A large number of studies suggested the increase in negative surface charge to be correlated with reduced adhesiveness of tumor cells. On the other hand, incubation of tumor cells with bacterial sialidase resulted in decreased surface charge followed by suppression of malignancy, probably due to the increased immunogenicity of the cells. Investigations into biochemical properties of the cell surface were pursued extensively, and characteristic features of the changes in cancer cells were identified[211,262-264]. Carbohydrate portions of glycoproteins and glycolipids undergo neoplastic alterations, and the changes in glycoprotein carbohydrates include an increase in sialylation. Aberrant sialylation is closely associated with the malignant phenotype of

cancer cells including metastatic potential and invasiveness. In fact, altered glycosylation of functionally important membrane glycoproteins may affect tumor cell adhesion or motility, resulting in invasion and metastasis[265-267]. A general increase in sialylation is often found in cell surface glycoproteins of malignant cells[268], and altered sialylation of glycolipids is also observed as a ubiquitous phenotype, leading to the appearance of tumor-associated antigens, aberrant adhesion, and blocking of transmembrane signaling[263]. Despite the number of reports describing involvement of sialic acids in cancer, it is still uncertain what the causes of such aberrant sialylation are and what the consequences of these changes are. Cellular sialic acid contents are mainly controlled metabolically by sialidases in cooperation with sialyltransferases. Sialidase, which cleave sialic acids from gangliosides and glycoproteins, have been suggested to play important roles in many biological processes through regulation of cellular sialic acid contents, through changing the conformation of glycoproteins, and through recognition and masking of biological sites of functional molecules. In fact, sialidases of mammalian origin have been implicated not only in lysosomal catabolism but also in regulation of important cellular events including cell differentiation, cell growth, and apoptosis. However, drawing definite conclusions regarding physiological links between sialic acid contents and malignant properties is difficult due to controversial experimental results.

Several observations on the changes in the sialidase of cancer cells suggested that these enzymes might be related to tumorigenic transformation and tumor invasiveness. Increased sialidase activity toward gangliosides were described to be associated with malignant transformation in BHK-transformed cells[269] and also in 3T3-transformed cells, where loss of cell density-dependent suppression of membrane-bound sialidase activity for gangliosides was observed[270]. Bosmann et al.[271] observed elevated sialidase activity in human cancer tissues with fetuin as a substrate. In the human promyelocytic leukemia cell line HL-60, stimulation of sialidase activity toward 4MU-NeuAc occurs during cell differentiation into granulocytes by retinoic acid or DMSO[272].

The four types of human sialidases identified to date (NEU1, NEU2, NEU3, and NEU4) were found to behave in different manners during carcinogenesis. Different sialidases have been observed to promote or oppose malignant phenotypes. Recent advances in the molecular cloning of mammalian sialidases has facilitated elucidation of the molecular mechanisms and significance of these alterations. Using a differential assay procedure for each form, it was observed that intra-lysosomal and membrane-bound sialidase activities were elevated, whereas cytosolic sialidase activity was reduced in rat hepatomas as compared with normal liver[273]. In mouse epidermal JB6 cells exposed to TPA and in their anchorage-independent transformants, lysosomal sialidase activity was decreased while plasma membrane-associated sialidase activity was increased as compared with corresponding activities in the untreated JB6 cells[274]. When the levels of sialidase activity were assayed in transformed rat 3Y1 cells, lysosomal sialidase activity was found to be inversely correlated with the metastatic potential of the cells[275]. As compared with control 3Y1 cells, src-transformed cells exhibited decreased lysosomal-type sialidase

activity, and v-fos transfer to these transformed cells induced an even more severe decrease in the sialidase activity with acquisition of high lung metastatic ability. Various lysosomal enzymes other than sialidase were not appreciably affected by the transformation, suggesting that the alteration occurs specifically in sialidase. Since metastatic potential did not parallel the sialic acid levels or the levels of sialyltransferases, it is likely that altered sialidase expression is more important for metastasis in transformed cells[275]. Sialidases are indeed closely related to malignancy and are thus potential targets for cancer diagnosis and therapy.

Sialidases NEU1 and NEU2 in cancer

A good inverse relationship between NEU1 expression level and matastatic ability was found in both mouse adenocarcinoma colon cells of different metastatic potential[276], as well as in the rat 3Y1 transformants described above[275]. Then, it was investigated how sialidase expression influences metastasis by introducing NEU2 cDNA into a B16-BL6 mouse melanoma variant subclone derived from B16 melanoma known to be highly invasive and metastatic[277]. Intravenous injection of stable transfectants into syngenic mice resulted in a marked decrease of experimental pulmonary metastasis, invasiveness and cell motility but no change in cell growth or cell attachment to fibronectin, collagen type VI or laminin. Sialidase overexpression did not lead to any significant changes in cell surface or intracellular glycoproteins, while there were a decrease in ganglioside GM3 and an increase in lactosylceramide as assessed by thin layer chromatography. When the sialidase gene was transfected into highly metastatic mouse colon 26 adenocarcinoma cells, changes in the sialyl Le^x level were observed in addition to marked suppression of metastasis[276]. Stable transfection of NEU2 in NL17 cells showed marked inhibition of lung metastasis, invasion and cell motility with a concomitant decrease in sialyl Le^x and GM3 levels. The results together indicate that the sialidase level is a determining factor affecting metastatic ability, irrespective of the sialic acid contents. In addition, NEU2 may participate in cell apoptosis, Tringali et al.[278] reporting that NEU2 gene introduction into leukemic K562 cells induced increased sensitivity to apoptotic stimuli by impairing Bcr-ABl/Src kinase signaling.

To investigate whether overexpression of NEU1 sialidase can reverse metastatic ability, rat lysosomal sialidase gene was introduced into Bl6-BL6 melanoma cells[279]. As expected, sialidase overexpressing cells showed suppression of experimental pulmonary metastasis and tumor progression. In contrast to the case with NEU2 sialidase, the NEU1 transfectants exhibited reduced anchorage-independent growth and increased sensitivity to apoptosis, induced by suspension culture or serum depletion *in vitro*, but no significant alterations in invasiveness, cell motility, or cell attachment. The results indicate that the sialidase affects malignant properties including the metastatic ability of cancer cells, in a manner different from that of NEU2. Expression levels of human ortholog NEU1 decreased in human colon cancer tissues as compared with that in the adjacent non-cancerous mucosa[280]. Human NEU1 overexpression suppressed cell migration and invasion in human colon adenocarcinoma HT-29 cell, whereas its knock

down resulted in the opposite effects. When NEU1-overexpressing cells were injected transsplenically into mice, the *in vivo* liver metastatic potential was significantly reduced[281].

Sialidase NEU3 in cancer

Investigation of plasma membrane-associated sialidase accomplished by Kakugawa et al.[282] revealed that NEU3 mRNA levels were increased up to 100-fold in human colon cancer tissues compared to adjacent non-tumor mucosa, and significant elevation of sialidase activity in the tumors was also observed. NEU3 level was downregulated by sodium butyrate treatment while NEU1 was upregulated. Transfection of the NEU3 gene into cancer cells inhibited apoptosis accompanied by increased Bcl-2 and decreased caspase expression, while knock down of this gene with a short interfering RNA (siRNA) resulted in enhanced apoptosis, indicating that high expression of NEU3 in cancer cells leads to protection against programmed cell death. In colon cancer cells, NEU3 differentially regulates cell proliferation through integrin-mediated signaling depending on the extracellular matrix[283]. The sialidase further causes increased adhesion to laminins and consequent cell proliferation, but rather decrease in cell adhesion to fibronectin, collagen I and IV. Triggered by laminins, NEU3 can clearly stimulate phosphorylation of focal adhesion kinase (FAK) and extracellular signal-related kinase (ERK), without any activation of fibronectin. NEU3 markedly enhances tyrosine phosphorylation of intergrin β4 only on laminin-5, with recruitment of Shc and Grb-2, and is coimmunoprecipitated by anti-integrin β4 antibody, suggesting that the association of NEU3 with integrin β4 might facilitate promotion of integrin-derived signaling on laminin 5.

NEU3 is also overexpressed in renal cell carcinomas (RCCs), correlating with elevation of interleukin IL-6, a pleiotropic cytokine that has been implicated in immune responses and the pathogenesis of several cancers, including RCCs[284]. In human RCC ACHN cells, IL-6 treatment has been shown to enhance NEU3 promotor luciferase and endogenous sialidase activity significantly. NEU3 gene transfection or IL-6 treatment both result in suppression of apoptosis and promotion of cell motility, exerting synergistic effects in combination. NEU3 was found to hardly affect MAPK or IL-6-induced STAT3 activation but promoted the PI3K/Akt cascade in both IL-6 dependent and independent ways. Furthermore, IL-6 promoted Rho activation and the effect was potentiated by NEU3, leading to increased cell motility that was affected by LY294002, a PI3K inhibitor. NEU3 silencing by siRNA resulted in the opposite: decreased Akt phosphorylation and inhibition of Rho activation. As also described for colon tumors, gycolipid analysis showed decrease in ganglioside GM3 and increase in lactosylceramide after NEU3 transfection. Thus, NEU3 activated by IL-6 stimulates IL-6-mediated signaling largely via the PI3K/Akt cascade in a positive feedback manner and contributes to expression of a malignant phenotype in RCCs. In ovarian clear cell adenocarcinomas, a high level of NEU3 expression is significantly correlated with the T3 factor (T: tumor size) of the pTNM classification (cancer stage classification[285].

To define further the molecular mechanisms of NEU3 effects and its possible targets, the encoding gene was silenced by siRNA or overexpressed in human cancer cells[286]. NEU3 silencing caused apoptosis without specific stimuli, accompanied by decreased Bcl-XL and increased mda7 and GM3 synthase mRNA levels in HeLa cells, whereas overexpression resulted in the opposite. Human colon and breast carcinoma cell lines, HT-29 and MCF-7 cells, appeared to be similarly affected by treatment with the NEU3 siRNA, but interestingly non-cancerous human WI-38 and NHDF fibroblasts and NHEK keratinocytes showed no significant changes. NEU3 siRNA was found to inhibit Ras activation and NEU3 overexpression to stimulate it with consequent influence on ERK and Akt. Ras activation by NEU3 was largely abrogated by PP2 (a src inhibitor) or AG1478 (an EGFR inhibitor), and in fact, siRNA introduction reduced phosphorylation of EGFR while overexpression promoted its phosphorylation in response to EGF (Figure 1-12). To summarize, NEU3 sialidase activates molecules including EGFR, FAK, ILK, Shc, integrin β4 and also Met, often upregulated in carcinogenesis, and may thus cause accelerated development of malignant phenotypes in cancer cells.

Immunohistochemical analysis of surgical specimens using anti-NEU3 monoclonal antibody confirmed NEU3 upregulation in several human cancers, for example in colon and prostate cancer. In the latter case, a positive relationship with the pathological progression stage was found. These results indicate that the sialidase could indeed be a useful target for cancer diagnosis and therapy.

NEU3 expression causes cell-type specific effects on cell proliferation, apoptosis and motility. These effects are probably due, at least in part, to NEU3's ability to desialylate glycolipids: overexpression of NEU3 leads to decreased levels of certain sialylated glycolipids, such as GM3, and an increased level of the unsialylated glycolipid LacCer. In the leukemic cell line K562, NEU3 silencing leads to slowed cell growth, increased susceptibility to apoptosis, and increased propensity to differentiate[287]. The mechanisms by which NEU3 suppresses apoptosis are still being deciphered, but existing evidence suggests that this protein functions both by interacting directly with signaling molecules and by exerting its enzymatic activity on ganglioside substrates, which in turn interact with signaling molecules. One substrate of NEU3, GM3, interacts directly with the EGF receptor and reduces its ability to respond to EGF ligand, possibly by sequestering EGFR in specialized membrane microdomains[288]. In the presence of NEU3, GM3 is hydrolyzed to LacCer, relieving the inhibition of EGF signaling. In this way, NEU3 activity leads to increased EGF signaling and cell proliferation[289]. NEU3 also modulates integrin signaling pathways, leading to increased proliferation and motility[283]. NEU3-mediated depletion of GM3 has been shown to block integrin-mediated adhesion to fibronectin, consistent with other work that showed functional and physical interactions between α5β1 integrin and GM3[290,291]. NEU3 activity also promotes integrin-mediated adhesion to laminin[283]. The net effect of these changes in adhesive properties is to stimulate cell proliferation. Additional work will be needed to clarify the molecular details of GM3's and LacCer's roles in these processes.

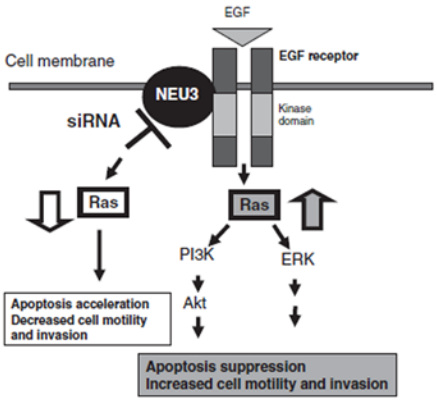

Figure 1-12 A possible mechanism of apoptosis regulation by NEU3 in cancer cells.
(Miyagi, T. *Proc Jpn Acad Ser B Phys Biol Sci* 2008)

Sialidase NEU4 in cancer

When NEU4 mRNA levels were compared between human colon cancer and adjacent non-cancerous tissues, a marked decrease in its expression was noted in the tumors[292], in clear contrast to the NEU3. In these cultured cancer cells, the enzyme was upregulated in the early stage of apoptosis induced by either the death ligand TRAIL, or serum-depletion. Transfection of NEU4 gene into DLD-1 and HT-15 colon adenocarcinoma cells resulted in acceleration of apoptosis and a decreased invasiveness and cellular motility. On the other hand, siRNA-mediated NEU4 targeting caused a significant inhibition of apoptosis and promotion of cellular invasiveness and motility. Lectin blot analyses revealed that desialylated forms of approximately 100-kDa glycoproteins were prominently increased in the NEU4-transfectants, whereas only slight changes in glycolipids were. These results suggest that NEU4 plays important roles in the maintenance of normal mucosa, mostly through desialylation of glycoproteins and that downregulation may contribute to invasive properties and protect against programmed cell death in colon cancers.

Future perspectives

In conclusion, investigation of mammalian sialidases has clarified some of the molecular bases of aberrant sialylation. In particular, it has been shown that the expression level of NEU1 is a critical factor for metastasis, and NEU3 upregulation is essential for survival of cancer cells, and that alteration in sialidase expression may be a defining factor for cancer progression, irrespective of sialic acid contents. Sialidase alterations, therefore, open up potential applications in cancer cure and diagnosis. As illustrated in Figure 1-13, downregulation of NEU3 expression by treatment with the specific siRNA, antibody or inhibitor may lead to prevention of cancer progression. In particular, taking advantage of its limited effects on

normal cells, NEU3 siRNAs causing apoptosis in cancer cells could offer a useful tool for cancer therapy.

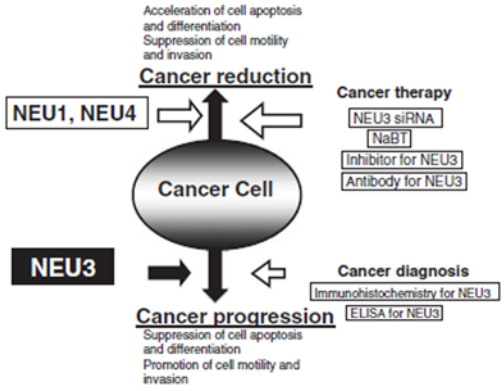

Figure 1-13 Functional relationship of three sialidases in human cancer cells and a possible role of NEU3 as a potential target for cancer diagnosis and therapy.
(Miyagi, T. *Proc Jpn Acad Ser B Phys Biol Sci* 2008)

1.4 The human sialidase NEU4

1.4.1 Identification of human NEU4 gene

A search of the UniGene database using the conserved sequence information of sialidases has revealed the existence of a cluster (Hs.302024) of sequences designated human NEU4 based on sequence homology. These sequences contain five open reading frames coding for proteins of different length. Three of them (AJ277883, NM_080741, AK091038) are 100% identical in their regions of overlap[132]. A similar search was conducted by Comelli and coworkers starting from the Celera murine gene database[293]. The search revealed a gene with an open reading frame highly homologous to the human NEU4 sialidase, designated as murine neuraminidase 4 (NEU4). The complete gene contains four exons and an open reading frame of 501 amino acids. It shows significant homology to the previously cloned neuraminidases with characteristic conserved motifs ascribed to the neuraminidase active site. Of all known murine sialidases, it is the most similar to NEU3 (42%). A cDNA encoding the entire coding sequence was isolated from mouse brain and expressed as a recombinant protein in COS-7 cells. The expressed recombinant protein is an active sialidase and is found to be predominantly expressed in brain.

At the same time, Monti et al.[194] identified and expressed a new member of the human sialidase gene family (NEU4). The corresponding gene, identified by searching sequence databases for entries showing homologies to the human cytosolic sialidase NEU2, maps in the telomeric region of the long arm of chromosome 2 (2q37), as already reported for the

NEU2 gene, and encodes a 484-residue protein. The polypeptide contains all the typical sialidase amino acid motifs and, apart from an amino acid stretch that appears unique among mammalian sialidases, shows a high degree of homology for NEU2 and the plasma membrane-associated (NEU3) sialidases. As already indicated by data obtained from the UCSC Genome Browser (Human November 2002 Freeze), the human NEU4 gene spans a region of 6663 bp on chromosome 2q37.3 (position 239447224-239453886) and consists of four exons. All splice sites agree with the GT/AG consensus sequence. The codon for the translation-initiator methionine (Met^1) is located in exon 2, whereas the termination codon, TAA, is located in exon 4. NEU4 is flanked on the telomeric side by the glycoprotein β-Gal 3'sulfotransferase gene (GP3ST, position 239455556-239489719) and on the centromeric side by the deoxythymidylate kinase gene (DTYMK, position 239389244-239400264).

Based on the human cDNA sequence predicted to represent the NEU4 sialidase gene in public databases, a cDNA covering the entire coding sequence was isolated from human brain and expressed in mammalian cells[280]. A search of the GenBank™ databases revealed the existence of six NEU4-related sequences (BC012899, AJ277883, AK091038, AK096992, NM 080741, and NT005416), completely identical in their overlapping regions. Based on these sequences, two cDNAs from the human brain were isolated by PCR. As shown in Figure 1-14, the two isoforms differed only in their length at the N-terminus. The long form encoded an additional 12 amino acid sequence at the N-terminus, which was predicted to be a mitochondrial targeting sequence by the MitoProt II, PSORT II server and TargetP v 1.0 prediction programs; the short form did not have this N-terminal sequence. It was also predicted that the long form can be cleaved at the 19th amino acid from the N-terminus[294] (Figure 1-14), although at present there are not evidence that the targeting sequence of the long form is processed on import. One of the characteristic features of the NEU4 cDNA sequence is the very high content of GC (70%). Comparison of the nucleotide sequence with those of other mammalian sialidases revealed significant identity: 40% with NEU3[189], 35% with NEU2[186] and 24% with NEU1[179].

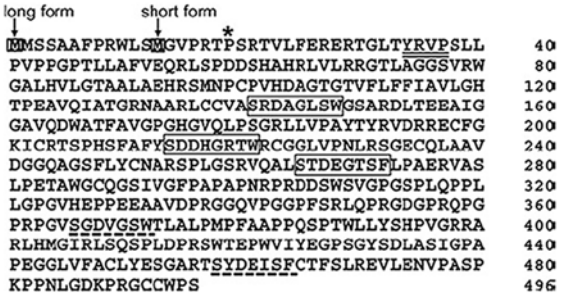

Figure 1-14 Deduced amino acid sequence of the human NEU4 sialidase.

(Yamaguchi, K. et al. *Biochem J* 2005)

1.4.2 Molecular properties of human NEU4 protein

The predicted NEU4 protein is 484 amino acids long, with a calculated molecular weight and a theoretical pI of 51.57 kDa and 7.97, respectively (Figure 1-15). The primary structure analysis of NEU4 revealed, as already reported for the other human and mammalian sialidases cloned so far[132], the presence of two canonical Asp boxes and one YRVP motif. In the case of NEU4, The F/YRIP motif, which is highly conserved in all of the sialidase enzymes and occurs near the N-terminus of these polypeptides, is slightly varied and contains a V residue instead of the canonical I (YRVP, amino acids 22-25). Moreover, NEU4 contains two classical Asp blocks, both in agreement with the consensus sequence (SRDAGLSW, amino acids 129-136; SDDHGRTW, amino acids 202-209). In addition, most of the amino acid residues possibly involved in the active site architecture are localized in topologically equivalent positions along the protein sequence.

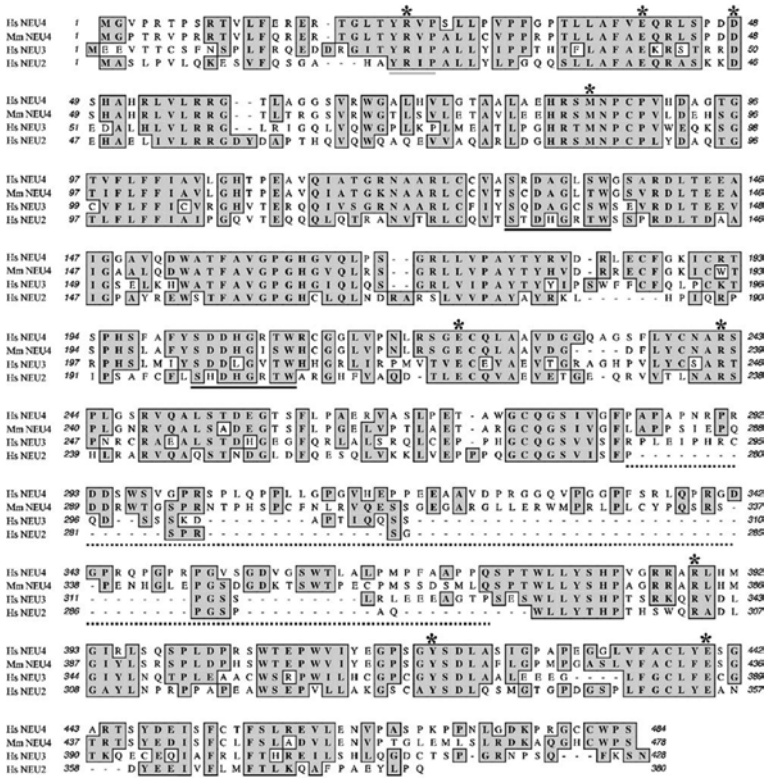

Figure 1-15 Alignment of the amino acid sequences of human NEU4, the putative mouse ortholog, human NEU3, and human NEU2.
(Monti, E. et al. *Genomics* 2004)

As already reported for the other members of the mammalian sialidase family characterized so far, 9 of 12 of the amino acid residues that form the catalytic site of the *Salmonella typhimurium*[42] enzyme are

conserved in NEU4 sialidase. The differences, as already reported for *Vibrio cholerae* sialidase[108] and all the other mammalian enzymes cloned so far, are concentrated in the hydrophobic residues (W121, W128, and L175) that in the *S. typhimurium* enzyme form the hydrophobic pocket accommodating the N-acetyl group of the sialic acid.

A characteristic feature of NEU4 is a long stretch of 79 amino acid residues (amino acids 284-373) that appears unique among mammalian sialidases. Recently, a sequence corresponding to the putative mouse ortholog of NEU4 (Accession No. XM_136821) was predicted by the National Center for Biotechnology Information by computational analysis of the mouse genome sequence using a gene prediction method (GenomeScan), supported by EST evidence (RIKEN clone 9330166I04 and NIH BMAP clone UI-M-BG1-aie-c-03-0-UI). Overall, the two proteins show a high level of sequence identity (70%) with the exception of an 87-amino-acid stretch (amino acids 287-372) where the identity drops to about 36%. In addition, a putative NEU4 rat protein sequence has been predicted (Accession No. XP_237421), derived from the analysis of the genomic sequences without further cDNAs and/or EST evidence. The rat protein also contains the long amino acid stretch with very low sequence identity with the human counterpart. As for human NEU4, both the mouse and the rat proteins contain a slightly modified YRIP motif in which the canonical I residue is substituted by the smaller V amino acid residue.

A Kyte-Doolittle hydrophobicity plot of NEU4 did not show long stretches of hydrophobic amino acids. The analysis for putative transmembrane regions using the TMpred program revealed two stretches of 18 (amino acids 90-107) and 20 residues (amino acids 353-372) that apparently divide the proteins into separate segments located on the opposite sides of the membrane. From these results the suggested model for transmembrane topology is the N-terminus outside (aa 1-89), a segment of 245 amino acid residues inside (amino acids 108–352), and the C-terminus outside (amino acids 373-484). In addition, the protein showed three potential *O*-glycosylation sites, together with several S, T, and Y amino acid residues that are identified as potential phosphorylation sites. Moreover, neither potential GPI-modification sites nor myristoylation sites were detected. Secondary-structure prediction performed by the PSIPRED prediction server at University College London revealed the presence of 21 putative H-strand regions, a characteristic common to all the sialidases studied so far.

The deduced protein for the long form of NEU4 comprises 496 amino acids,with a molecular mass of 52937 Da, and the sequence includes an Arg-Ile(Val)-Pro sequence and three typical and two atypical Asp boxes[41], the consensus sequence for sialidases, but no potential *N*-glycosylation site[280].

1.4.3 Enzymatic properties of human NEU4 sialidase

Another feature that differentiates NEU4 from the other human sialidases characterized so far is its substrate preference. Preliminary experiments, carried out using standard assay conditions, demonstrate that COS-7 cells transiently transfected with NEU4 showed enzymatic activity

only towards the fluorescent substrate 2'-(4-methylumbelliferyl)-α-D-*N*-acetylneuraminic acid (4MU-NeuAc), with a pH optimum of 3.2[194]. Sialidase activity is roughly doubled upon NEU4 transfection and, as already reported for NEU3, the enzyme protein acts in the acidic range of pH. NEU4 enzyme failed to remove sialic acid residues from the oligosaccharide α2,3-sialyllactose, gangliosides GD1a and GM3 (bearing both sialic acid residues linked with α2,3 sialosyl linkage), and glycoproteins of human (transferrin) and bovine (α1-acid glycoprotein, fetuin, and mucin) origin (bearing the α2,3 and α2,6 sialosyl linkages). Interestingly, a 57 kDa membrane-bound sialidase from pig liver microsomes can effectively hydrolyze 4MU-NeuAc, whereas, as we found in the case of NEU4, it failed to remove sialic acid residue(s) significantly from oligosaccharides, glycoproteins, and gangliosides[295].

On the contrary, according to Yamaguchi and coworkers[280], when the expression vectors for the two forms were introduced into COS-1 or HEK-293T cells, both forms of NEU4 exhibited marked sialidase activity against 4MU-NeuAc, and also against gangliosides. Although the two forms of NEU4 did not differ significantly from each other in terms of their enzymatic properties, comparisons with other human sialidases revealed marked differences in substrate specificity. Over 70% of the activity of the expressed sialidase in the crude extract was recovered in the particulate fraction, with less than 20% of the activity remaining in the cytosolic fraction, suggesting that the enzyme is probably almost entirely membrane-bound. The sialidase acted efficiently on glycoproteins and oligosaccharides as well as on 4MU-NeuAc and gangliosides, unlike the NEU1 and NEU3 sialidases. Both isoforms of NEU4 revealed this broad substrate specificity, in that all substrates tested except ganglioside GM1 were hydrolysed effectively. In particular, submaxillary mucins were cleaved to a significant degree, which seems to be a unique characteristic of this sialidase among the mammalian sialidases. The relative rates of hydrolysis of GD1a and GM3 compared with GD3 by the enzyme were similar to those of NEU3, which almost specifically hydrolyses gangliosides and scarcely showed any activity towards sialyllactose, fetuin or α1-acid glycoprotein.

Similarly, by using the synthetic fluorescent substrate 4MU-NeuAc, Seyrantepe et al.[296] demonstrated that the NEU4 gene product indeed had sialidase activity. The pH-optimum was 3.5, i.e. close to that of NEU1 and NEU3 but in contrast to those enzymes NEU4 retained almost 40% of its maximal activity at higher pH. Although all mammalian sialidases show activity against 4MU-NeuAc, they differ in their specificity against natural substrates, NEU1 being most active on oligosaccharides and NEU2 and NEU3 on glycolipids[178,297,298]. Human NEU4 showed broad substrate specificity, being almost equally active on glycoproteins (mucin), oligosaccharides (sialyllactose), 4MU-NeuAc, and sialylated glycolipids (mixed bovine gangliosides).

1.4.4 Expression of NEU4 in human tissues

To ascertain the expression level of NEU4 gene, an RNA dot-blot analysis was performed with an RT-PCR product spanning the entire NEU4 ORF, by using a dot-blot containing poly(A)$^+$ RNA extracted from 50 different

human tissues[194]. NEU4 gene appears to be widely expressed at low level in human tissues. The highest expression of NEU4 was detected in liver tissue, although the enzyme was also expressed in a well detectable level in all the CNS districts spotted, colon, small intestine, and kidney. In addition, this liver specific expression is detectable in the fetal tissue analyzed. Information about the expression profile can be also derived from NEU4 ESTs present in dbEST[183]. In this case, 22 of 24 are of CNS origin with 19 entries derived from cDNA libraries of oligodendroglioma, a rare glial tumor.

In addition, the relative abundance of NEU4 mRNAs in human tissues was determined by Northern blotting[280]. The human NEU4 sialidase gene was expressed predominantly in the liver, and at relatively low levels in the kidney, heart and brain. Expression of the isoforms is tissue-specific, as assessed by RT-PCR. Brain, muscle and kidney contained both isoforms of NEU4 gene; liver showed the highest expression, and the short form was predominant in this organ. The liver, that showed the highest levels of NEU4 transcripts, expressed the short form predominantly, and the long form was barely detectable in the colon. The long form/short form ratio was nearly 1 in brain, lower in kidney and muscle, and extremely low in liver and colon, as determined by quantification of the relative expression levels of the two forms of NEU4. When the expression of all sialidases was analysed comparatively, NEU4 appeared to be expressed at a lower level than NEU3, and at below one tenth the level of NEU1.

Northern blot analysis performed by Seyrantepe and colleagues[296] showed that similarly to NEU1, NEU4 is a ubiquitously expressed housekeeping gene found in all tissues studied. However, the expression profiles of NEU1 and NEU4 do not completely coincide. High expression of both NEU1 and NEU4 is detected in skeletal muscle, heart, placenta, and liver, whereas NEU1 is expressed at a much higher level in kidney, spleen, thymus, colon, brain, lung, and small intestine.

1.4.5 Subcellular localization of human NEU4

Although the two isoforms of human NEU4 were not distinguishable with regard to substrate specificity, they exhibited differential subcellular localizations. As reported in the case of the plasma membrane-associated sialidase NEU3[190], expression experiments in COS7 cells demonstrate that the short form of NEU4 enzyme is found associated with the rough membrane structures pelleted by ultracentrifugation[194]. These results, obtained by measuring the enzyme activity using the artificial substrate 4MU-NeuAc, were confirmed by Western blot analysis using the fusion protein carrying the hemagglutinin (HA) epitope in the N-terminal region (HA-NEU4), with the tagged protein detectable in the 100,000g-pelleted material only. Immunofluorescence localization of the tagged HA-NEU4 protein further demonstrates the membrane association of the enzyme. In addition, no significant colocalization with lysosomes was detected and, apparently, the tagged enzyme is not present at the cell surface. From the analysis of the hydropathic profile calculated using the Kyte-Doolittle method and as already reported for NEU3[190], no multiple stretches of hydrophobic amino acids were detected along the primary structure. The analysis of the NEU4 amino acid sequence carried out using the TMpred algorithm predicted a

model with the N- and C-terminus outside and two strong transmembrane helices that encompass the central portion of NEU4. In this spatial arrangement, the highly conserved amino acid residues possibly involved in the active site formation within this protein portion (E222 and R242) are exposed to the cytosol and separated by the lipid bilayer from the others (R23, E41, D48, M85, R389, Y419, and E439). Since from the three-dimensional data collected so far it is unlikely that a sialidase with this structural feature shows enzyme activity, a substitute model(s) must be found. In this perspective, because no potential GPI modification or myristoylation site was found, a stretch of hydrophobic residues exposed near the C-terminus at the protein surface could be responsible for membrane association.

With regard to subcellular localization, it has been reported that the major localization sites of the three sialidases previously cloned are the lysosomes, cytosol and plasma membranes for NEU1, NEU2 and NEU3 respectively. Immunofluorescence studies accomplished by Yamaguchi et al.[280] with HA-tagged NEU4 revealed that the long form is localized in the mitochondria in several human cell types, including DLD-1 and A431 cells. Analyses using EGFP fused to the N-terminus of the long form and point mutation of the signal sequence provided evidence that the N-terminus contains a potential mitochondrial targeting sequence. In contrast, the ubiquitously expressed short form showed a diffuse localization probably in the intracellular membranes, as already demonstrated by Monti et al.[194], indicating that the sequence comprising the N-terminal 12 amino acid residues acts as a targeting signal for mitochondria. Furthermore, substitution of arginine (at position 17) by alanine near the putative cleavage site at the long-form N-terminus prevented the mitochondrial targeting, supporting evidence that the N-terminus of the long form of NEU4, covering the putative cleavage site, contains a mitochondrial targeting signal[280]. Thus, NEU4 is possibly involved in regulation of apoptosis by modulation of ganglioside GD3, which accumulates in mitochondria during apoptosis and is the best substrate for the sialidase.

Consistent with the immunofluorescence data, localization of the long form of NEU4 in mitochondria was also confirmed by recovery of most of sialidase activity in a purified fraction of mitochondria, devoided of contaminating organelles such as lysosomes fractionation, indicating that the long form of NEU4 is localized to mitochondria[280]. On the other hand, the short form did not co-localize with any of the marker proteins tested, including an endoplasmic reticulum protein, calnexin. After a submitochondrial fractionation performed in colon cancer DLD-1 cells transfected with NEU4 long form,sialidase activity was detected primarily in the inner and outer membrane fractions, but to a lesser extent in the matrix. These biochemical data were supported by electron microscopy showing that immunogold particles were located along and/or in the mitochondrial inner and outer membranes[280].

Inconsistent with these findings is a report that exogenous NEU4 was localized in the lysosomal lumen in COS-7 cells and human fibroblasts[296], when using a cDNA probably corresponding to the long form. In fact, confocal fluorescent microscopy showed that in COS-7 cells and human

fibroblasts NEU4 was targeted to cytoplasmic organelles colocalizing with the lysosomal markers LysoTracker Red or LAMP-2. Moreover, the majority of NEU4-related sialidase activity in the COS-7 cells transfected with NEU4 was found in the light mitochondrial fraction-enriched in lysosomes and containing most of the lysosomal β-hexosaminidase activity. In addition, their fractionation data suggested that NEU4 is a soluble hydrolase located in the lysosomal lumen, in contrast to the integral lysosomal membrane protein NEU1, which cannot be solubilized without detergent[299]. Finally, the authors demonstrated that NEU4 was targeted by the mannose 6-phosphate receptor, a mechanism involved in the transport of precursors of lysosomal luminal proteins[296].

Whatever reasons may exist for the discrepancy, it is possible that the localization of NEU4 is not fixed and can be changed under different physiological conditions. Although previous studies on mammalian sialidases have revealed a close relationship between their subcellular localization and function, these enzymes may be expected to be targeted to other organelles in response to a variety of cellular events, as reported previously[299]. It is therefore important to observe the localization of NEU4 under various cellular conditions.

1.4.6 Physiological and pathological roles of human NEU4

NEU4 and lysosomal storage

Seyrantepe and coworkers[296] have examined the lysosomal storage in the cells of a sialidosis patient (line WG0544) transfected with NEU4 expressing plasmids. They found that transfection with NEU4 expression vector resulted in clear improvement of lysosomal storage, as observed by electron microscopy. In fact, cells transfected with NEU4 or NEU1 presented small electron-dense granules typical of normal lysosomes. Both NEU4 and NEU1 therefore conferred normal lysosomal morphology to sialidosis fibroblasts, suggesting that NEU4, similarly to NEU1, is active on undigested substrates containing neuraminic acid.

Several laboratories reported[174,300,301] that NEU1 is able to catalyze the hydrolysis of gangliosides in the presence of bile salts or the sphingolipid activator protein saposin B. However, the analysis of storage products in sialidosis and galactosialidosis patients or in the knock-out mouse model of galactosialidosis[302] did not show storage of gangliosides, suggesting that NEU1 is not essential for their catabolism. Although NEU2 and NEU3 desialylate glycolipids *in vitro*, they cannot account for ganglioside catabolism because they are not present in the lysosome. Seyrantepe et al.[296] found that NEU1 has very little activity toward mixed gangliosides even in the presence of bile salts. In contrast, mixed bovine gangliosides are desialylated by NEU4 at a rate compatible to that of 4MU-NeuAc, suggesting that NEU4 is the enzyme responsible for the catabolism of sialylated glycolipids. *In vitro*, the reaction requires a detergent, but in the cell, gangliosides could probably be hydrolyzed in the presence of sphingolipid activator proteins. Other experiments, in particular those involving NEU4 knock-out models, are required to define the biological role of NEU4 and to prove that it acts on gangliosides in lysosomes.

Their data also showed that NEU4 is active against a majority of NEU1 endogenous substrates[296]. Being expressed in NEU1-deficient sialidosis fibroblasts, NEU4 completely eliminated undigested substrates of NEU1 and restored normal morphological phenotype of the lysosomal compartment, thus offering therapeutic potential. The strategy for treatment of lysosomal storage disorders (enzyme replacement therapy, bone marrow transplantation, or gene therapy) relies on the principle of 'cross-correction' where precursors of missing enzymes secreted from donor cells or exogenously supplied are internalized by other cells through the receptor-mediated endocytosis[303]. Therefore, the therapeutic success for a particular disorder depends on the molecular properties of the deficient enzyme as follows: its solubility and stability, mechanism of its lysosomal targeting, whether it has to be post-translationally modified, etc. In this respect disorders caused by inherited sialidase deficiency did not have much perspective because NEU1 is an integral membrane protein that cannot be secreted from donor cells[299] and requires coexpression with cathepsin A for activation and stabilization[114,178]. In contrast, NEU4 is a soluble enzyme, whose precursor is targeted to the lysosome by the mannose 6-phospate receptor and can be potentially taken up by the cells from the medium. In accordance with this hypothesis, the authors observed a complete elimination of storage materials in 55% of sialidosis cells and in 25% of galactosialidosis cells, whereas only 3-5% of cells were transfected with NEU4 plasmid[296]. An explanation of this fact could be that the NEU4 released from the transfected cells enters cells neighboring and corrects their phenotype. Therefore, recombinant human NEU4 might be of potential use for enzyme replacement therapy in sialidosis and galactosialidosis. However, enzyme replacement rarely achieves superphysiologic levels of the enzyme in target tissues, and because patients with NEU1 deficiency but with two normal NEU4 alleles still develop the disease, physiologic levels of NEU4 are likely not sufficient to prevent accumulation of sialylated compounds. Much more attractive, therefore, would be to induce the expression of the endogenous NEU4 gene to compensate for NEU1 deficiency. Since NEU4 seems to be expressed in every human tissue, this approach may have a general effect throughout the whole organism, including the central nervous system, which is presently beyond the scope of the enzyme replacement therapy.

Tay-Sachs disease is a severe lysosomal disorder caused by mutations in the Hexa gene coding for the α-subunit of lysosomal β-hexosaminidase A, which converts GM2 to GM3 ganglioside by removing N-acetyl-glucosamine residue from GM2 ganglioside. This causes accumulation of GM2 ganglioside in neurons of affected patients with subsequent neuronal death, resulting in progressive neurologic degeneration that is fatal in early childhood. To investigate whether NEU4 is involved in ganglioside catabolism, Seyrantepe et al.[304] transfected β-hexosaminidase-deficient neuroglia cells from a Tay-Sachs patient with a NEU4 expressing plasmid and demonstrated the correction of the storage impairement due to the clearance of accumulated GM2 ganglioside. HeLa cells stably transfected with NEU4 siRNA, as well as mice with targeted disruption of the NEU4 gene, showed partially impaired catabolism and lysosomal storage of

gangliosides, suggesting that NEU4 is a critical functional component of the ganglioside metabolizing system, contributing to the postnatal development of the brain and other vital organs.

The larger lamellar bodies observed in the NEU4 knock-out animals may indicate a potential induction of surfactant synthesis in the type II pneumocytes due to the absence of NEU4. By *in situ* hybridization, NEU4 mRNA was shown to be strongly expressed in cells that are scattered in the mouse brain. The distribution of these cells is reminiscent of that of microglial cells, which infiltrate the developing CNS after P5 and participate in axon growth, vasculogenesis and apoptosis. The time course of the migration of microglial cells into the brain is consistent with that of NEU4 expression, which sharply increases several days after birth and reaches a peak at several weeks of age. However, while the predominant expression is in microglia, NEU4 appears to be expressed at low levels ubiquitously in the brain, so we cannot exclude the possibility that it is also produced at lower levels in other cell types, such as neurons, given its impact in diseases such as sialidosis and galactosialidosis where as we previously showed exogenous NEU4 eliminated undigested substrates and restored a normal morphological phenotype of the lysosomal compartment *in situ*[296].

An additional lysosomal disease which may be ameliorated by the lysosomal presence of NEU4 activity is the knockout mouse model of Tay-Sachs disease[305,306]. The human disorder, is caused by mutation of the Hexa gene coding for the α-subunit of lysosomal β-hexosaminidase A, enzyme that converts GM2 to GM3 ganglioside. $Hexa^{-/-}$ mice, depleted of β-hexosaminidase A, remain asymptomatic to at least 1 year of age[307], owing to the ability of these mice to catabolize stored GM2 ganglioside via a lysosomal sialidase into glycolipid GA2. GA2 is further processed by β-hexosaminidase B, to yield lactosylceramide[306], thereby completely bypassing the β-hexosaminidase A defect. Since this bypass is not effective in humans, infantile Tay-Sachs disease is fatal in the first years of life. The tissue levels of NEU4 mRNA may provide an explanation for the difference in Tay-Sachs disease severity in humans and mice. Comelli et al.[293] showed NEU4 to be expressed at high level in mouse brain with only trace expression in other tissues. In contrast, expression in human tissues was more widely distributed, with brain levels lower than in other tissues[194,280,296]. Transfection of human Tay-Sachs neuroglia cells with NEU4 produces a similar catabolism through GA2, effectively 'treating' the disease through the same metabolic bypass that is so effective in the mouse model[304]. For these reasons, the authors speculated that stimulation of human NEU4, perhaps through drug-mediated induction or activation, could activate the bypass in human Tay-Sachs disease or could substitute for NEU1 in human sialidosis and galactosialidosis and provide treatment for these devastating diseases.

Recently, other studies performed by Seyrantepe et al.[308] demonstrated that mice depleted of both ganglioside NEU4 and Hexa genes ($NEU4^{-/-}$ and $Hexa^{-/-}$) show epileptic seizures with 40% penetrance correlating with polyspike discharges on the cortical electrodes of the electroencephalogram observed in Tay-Sachs patients. Single Hexa or NEU4 knockout mice ($Hexa^{-/-}$ or $NEU4^{-/-}$) do not show such symptoms. Further, double-knockout but not single-knockout mice have multiple

degenerating cortical and hippocampal neurons and multiple layers of cortical neurons accumulating GM2 ganglioside[308]. Together, these data suggest that NEU4 depletion exacerbates the disease in Hexa$^{-/-}$ mice, supporting the view that NEU4 is one of the modifier genes in the mouse model of Tay-Sachs disease, reducing the disease severity through the metabolic bypass. However, while disease severity in the double mutant is increased, it is not profound suggesting that NEU4 is not the only sialidase contributing to the metabolic bypass in Hexa$^{-/-}$ mice.

This mouse model with a double Hexa/NEU4 deficiency progresses toward the neuropathological abnormalities of Hexb$^{-/-}$ mice or of human Tay-Sachs patients. While other sialidases also may contribute to the bypass pathway, it is important to note that transfection of NEU4 in cultured fibroblasts from patients with sialidosis or galactosialidosis and of neuroglia cells from a patient with Tay-Sachs disease resulted in increased sialidase activity and normalization of lysosomal morphology[296,304]. Also, correction was observed in cells not receiving the targeting vector, suggesting that secretion and reuptake of NEU4 might also contribute to disease amelioration. According to their findings, the authors affirmed that, because NEU4 targets to the lysosome but does not require formation of a multienzyme complex and appears to participate in secretion and reuptake by nearby cells, it might act as an optimal pharmacologic modifier, perhaps through pharmacologic induction, for the treatment of human Tay-Sachs disease.

NEU4 and mitochondrial apoptosis

Interestingly, in contrast to the short form which is ubiquitously expressed, NEU4 long is specifically expressed in brain[280]. Although the physiological roles of NEU4 long in brain is still unclear, its substrate specificity and intracellular localization suggest that it may be involved in the mitochondrial apoptotic pathway in neuronal cells[280,309-311].

Previous observations[309] indicate that mitochondrion is a key destination for the apoptogenic ganglioside GD3 (Figure 1-16), as shown by the reports that apoptosis induced by ceramide exposure[312] and tumour necrosis factor-α[313] caused targeting of GD3 to the mitochondria.

In line with these observations, NEU4 may regulate the level of mitochondrial GD3, the best substrate for this sialidase. Especially in the nervous system, where the long form is enriched, it may function as a mitochondrial targeting sialidase in apoptosis. The possible involvement of NEU4 long and its substrate ganglioside GD3 in the apoptotic cell death under the existence of catechol-oxidized metabolites generated by tyrosinase was investigated[314]. The authors demonstrated that overexpression of tyrosinase causes apoptotic neurodegeneration in SH-SY5Y cells, and that the apoptotic phenotype is characterized by a cytochrome c release concomitant with the trafficking of GD3 to mitochondria. Furthermore, the expression level of NEU4 long is dramatically decreased in the early course of apoptosis, thus providing evidence that the long form of NEU4 and its substrate GD3 may be implicated in the mitochondrial apoptotic pathway in neuronal cell death.

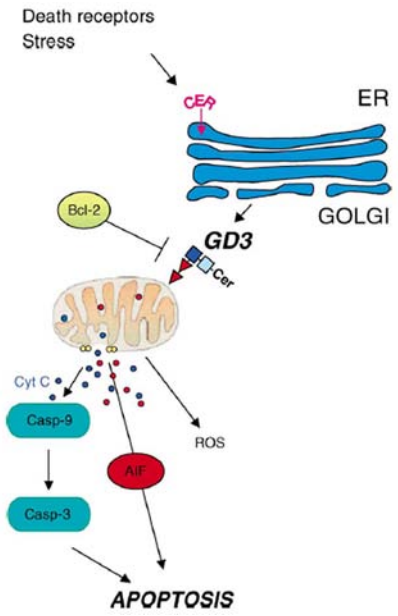

Figure 1-16 GD3-mediated apoptosis.
(Malisan, F. & Testi, R. *Biochim Biophys Acta* 2002)

NEU4 and immune system

Circulating peripheral blood monocytes play a key role in potentiating diverse immune activities and can differentiate into either macrophages or dendritic cells by exposure to specific stimuli[315]. The function of monocytes changes from antigen recognition and processing to antigen presentation in macrophages and dendritic cells. Desialylation of glycoconjugates on the surface of freshly isolated monocytes using an exogenous bacterial neuraminidase activated the extracellular signal-related kinase 1/2 (ERK1/2), enhanced the production of specific cytokines, and promoted the responsiveness of monocytes to bacterial lipopolysaccharide[316]. Stamatos, et al.[317] demonstrated that endogenous sialidase activity of freshly isolated human monocytes is upregulated during their differentiation into macrophages. They showed that NEU1 and NEU3 are present in both monocytes and macrophages, and that the specific activity of only NEU1 is upregulated during differentiation. On the other hand, NEU4 is also expressed in monocytes as evidenced by the presence of NEU4 RNA, but the amount of this RNA declines during monocyte differentiation.

A recent paper associates NEU4 sialidase activity to the anti-inflammatory properties of thymoquinone (TQ), which is derived from the nutraceutical black cumin oil[318]. Although the medicinal properties of TQ have been extensively studied, the precise molecular mechanism(s) of anti-inflammatory effects of TQ is not well understood. Using a newly developed assay to detect sialidase activity in live macrophage cells, Finlay and coworkers[318] showed that TQ has no inhibitory effect on endotoxin lipopolysaccharide (LPS) induced sialidase activity in live BMC-2

macrophage cells. Instead, TQ induced a vigorous sialidase activity in live BMC-2 macrophage cells, live DC-2.4 dendritic cells, TLR-deficient HEK293 cells, HEK-TLR4/MD2 cells, SP1 mammary adenocarcinoma cells, human WT and 1140F01 and WG0544 type I sialidosis fibroblast cells, as well as in primary bone marrow (BM) macrophage cells derived from WT and NEU1-deficient mice, but not from NEU4 knock-out (NEU4KO) mice. The neuraminidase inhibitor Tamiflu (oseltamivir phosphate), as well as neutralizing antibodies against NEU4 and MMP-9, completely blocks TQ-induced sialidase activity in human THP-1 monocyte cells, which express NEU4 and MMP-9 on the cell surface. This TQ-induced NEU4 sialidase activity hydrolyzes sialic acids not only from the artificial 4MU-NeuAc substrate but also natural gangliosides and mucins. In addition, RT-PCR and western blot analyses reveal no correlation between mRNA and protein values for NEU3 and NEU4 in human monocytic THP-1 cells, suggesting for the first time a varied post-transcriptional mechanism for these two mammalian sialidases even when they have similar functions. The cell may tightly control the rates of degradation or synthesis for NEU3 and NEU4 and this is not dependent on thymoquinone activation[318]. Taken together, these findings establish an unprecedented activation of NEU4 sialidase on the cell surface by thymoquinone. The potentiation of GPCR-signaling by TQ via membrane targeting of Gαi subunit proteins and matrix metalloproteinase-9 activation may be involved in the activation process of NEU4 sialidase on the cell surface of live cells.

More recently, in a new report[318] the same authors demonstrated that TQ-induced NEU4 activity facilitates MyD88/TLR4 complex formation and subsequent NFκB activation and nuclear localization in HEK-TLR4/MD2 cells and primary BM macrophages from WT and NEU1-deficient mice, HEK-TLR4/MD2 cells an BMC-2 macrophage cell line but not in primary macrophage cells from NEU4-knockout mice. Tamiflu, Gαi-sensitive pertussis toxin (PTX), and the broad range inhibitor of matrix metalloproteinase (MMP) galardin applied to live HEK-TLR4/MD2 cells and primary BM macrophage cells completely block TQ-induced MyD88/TLR4 complex formation. Coimmunoprecipitation experiments reveal for the first time that NEU4 forms a complex with MMP-9, which is already bound to TLR4. This tripartite alliance would make TQ-induced NEU4 activity readily available to target sialyl residues of TLR4 receptors. In addition, NEU4-knockout mice respond poorly to TQ in producing pro-inflammatory cytokines and chemokines after 5-h treatment compared to the wild-type or hypomorphic cathepsin A mice with a secondary 90% NEU1 deficient mice[318]. The findings in this report suggest that MMP-9 forms an important molecular signaling platform in complex with TLR4 receptors at the ectodomain and acts as the intermediate link for TQ-induced NEU4 sialidase in generating a functional receptor, with subsequent NFκB activation and pro-inflammatory cytokine production *in vivo*.

NEU4 and neuronal cell differentiation

Sialidase NEU4 is reported to be dominantly expressed in the mouse brain, but its functional significance is not fully understood. To clarify the physiological functions of NEU4, Shiozaki et al.[319] examined NEU4

expression in the mouse brain and observed a possible involvement in neural differentiation in connection with another sialidase, NEU3, which greatly increases during differentiation of neuroblastoma cells and causes acceleration of neurite formation[192,254,256,260].

Comelli et al.[293] reported that murine NEU4 is dominantly expressed in brain, and a cDNA cloned from the brain encoded a protein with low sialidase activity. NEU4 was found to be expressed not only in brain but also in other mouse tissues including lung and spleen, sites shown by Seyrantepe et al.[304] to exhibit vacuolization in NEU4 knock-out mice. They also showed that murine NEU4 possesses two splicing variants. The shorter form (NEU4b) expresses sufficient sialidase activity toward various substrates, but the long one (NEU4a), particularly highly expressed in the brain, shows weak sialidase activity as reported by Comelli et al.[293]. From the predicted three-dimensional structure of human NEU4, the 23-N-terminus amino acid residues in NEU4a are not likely to be related to the active site[205].

Recently, Shiozaki and coworkers[319] reported that murine NEU4 was found to possess two isoforms differing in expression levels, developmental pattern, and enzymatic properties. Distinct from the human isoforms, the murine forms, to a different extent, both catalyzed the removal of sialic acid from gangliosides as well as glycoproteins, and NEU4a isoform seemed to hydrolyze polysialylated NCAM more efficiently than NEU4b, despite the low activity toward ordinary substrates. *In situ* hybridization showed NEU4 mRNA mainly in hippocampus, in which polysialylated NCAM is rich and decreases after birth. As NEU4 expression increases in the postnatal period, NEU4, especially NEU4a, may participate in the NCAM decrease. NEU4 expression was relatively low in the embryonic stage and then rapidly increased at 3-14 days after birth, whereas NEU3 mRNA showed high levels in the embryonic stage and downregulation in the postnatal period. The authors previously observed that hippocampus neurons have enhanced axonal growth with an increase in NEU3 expression, and this can be suppressed with NeuAc2en, a NEU3 inhibitor[254]. Directly contrasting with NEU3, NEU4 was downregulated during retinoic acid-induced differentiation in Neuro2a cells. Overexpression of NEU4b resulted in suppression of neurite formation, and its knock-down showed the acceleration. Thin layer chromatography of the glycolipids from NEU4-transfected cells showed ganglioside compositions to be only slightly affected, although lectin blot analysis revealed desialylation of a 95 kDa glycoprotein during cell differentiation[319]. These results suggest that mouse NEU4b, plays an important role in the negative regulation of neurite formation, possibly through desialylation of glycoproteins.

NEU4 and cancer

In mammalian cells, all four types of sialidase have been described and found to behave in different ways during carcinogenesis. As previously described, murine sialidases NEU1 and NEU2 exhibit altered expression, playing important roles in cancer development[276,277,279]. Furthermore, increased expression of human plasma membrane-associated sialidase NEU3 in colon[282] and renal[284] cancers and its involvement in apoptosis

suppression was also documented. However, human NEU1 and NEU4 have not been extensively investigated.

Expression of the isoforms of NEU4 is tissue specific; both isoforms were expressed in the brain, muscle, and kidney, and predominantly the short form was expressed in the liver and colon. In clear contrast to the case for NEU3, a marked decrease of NEU4 expression was detected in tumors as compared with the adjacent noncancerous mucosa[292], although diverse values were obtained especially for expression levels in noncancerous tissues. A greater than 80% reduction of the expression level of the noncancerous tissues was observed in tumors.

A study of Yamanami et al.[292] reported altered expression of human sialidase NEU4 and evidence of its influence on the malignant phenotype in colon cancers. Human colon mucosa was relatively rich in NEU4, which has been observed to possess short and long isoforms, but hardly contained the latter form. In clear contrast to the NEU3[282], NEU4 mRNA levels were found by quantitative RT-PCR to be markedly decreased in colon cancers.

Upregulation was evident with the early stage of apoptosis induced by TRAIL treatment or serum-depletion in the cancer cells, and NEU4 overexpression in DLD-1 and HT-15 colon adenocarcinoma cells resulted in acceleration of apoptosis accompanied by caspase-3 activation, decreased invasiveness and cellular motility[14]. An essential involvement of NEU4 in apoptosis was confirmed by siRNA-mediated NEU4 targeting, that caused a significant inhibition of apoptosis and promotion of invasion and motility. In addition, an early increase of endogenous NEU4 during apoptosis suggests that NEU4 itself seems to induce apoptosis for maintenance of normal mucosa and thus, the decrease of NEU4 in colon cancer might lead to protection against programmed cell death[14]. The molecular mechanism of the NEU4 effect on apoptosis in response to TRAIL and serum depletion is uncertain at present, but it is possible that NEU4 might downregulate the MEK/ERK signaling pathway because both of the stimuli lead to apoptosis via decreasing ERK phosphorylation[320]. The NEU4 reduction rate was statistically correlated only with venous invasion but not with histological differentiation or pathological stages, even the clear NEU4 effects were observed in the cells. It is unclear why the NEU4 effects do not always reflect on the clinical features, but one of the factors for this ambiguity is possibly due to the participation of NEU1 level influencing malignancy, as suggested in a previous work[279]. NEU4 and NEU1 would collaborate together in the same direction towards reduced invasive properties of cancer cells. These data suggest that the combined activity assays for NEU1 and NEU4 in surgical specimens may be useful for the diagnosis and clinical prognosis of colon cancer.

Lectin blot analyses revealed that desialylated forms of nearly 100 kDa glycoproteins were prominently increased with peanut agglutinin (PNA) in NEU4 transfectants, whereas only slight changes in glycolipids were detected as assessed by thin layer chromatography[292]. The results on sialic acid analysis and lectin blotting suggest that effects of NEU4 on cell motility, invasiveness as well as cell apoptosis are mostly through desialylation of *O*-glycosylated proteins, rather than hydrolysis of gangliosides. It seems likely that the desialylated *O*-glycosylated proteins of about 100 kDa are possibly

some types of mucins that are known to establish a selective molecular barrier at the epithelial cell surface and conduct signals in response to external stimuli as cell surface receptors[321]. Since aberrant alteration in mucin expression or glycosylation has been implicated in the development of cancer and is known to influence various cellular phenomena including proliferation, differentiation, apoptosis, adhesion invasion and immune surveillance[321,322], desialylation of mucins by NEU4 might cause changes in cell apoptosis, motility and invasion. These results on apoptosis induction provide an important clue to the biological significance of NEU4 expression in colon cancer. The opposing alteration expression patterns of NEU3 and NEU4 in colon cancer and during cell apoptosis suggest opposite influences on the malignant phenotype with reference to apoptosis, cell motility and invasion. Recent studies revealed that NEU3 upregulation plays a role in determining malignant properties of cancer cells[284,323]. In contrast, NEU4 appears to be involved in maintaining the normal mucosa, possibly through desialylation of glycoproteins, and its downregulation may contribute to invasive properties of colon cancers and protection against programmed cell death of colon cancers. The functional difference between the two sialidases might be due to the difference in their substrate specificities. NEU4 seems to be a positive regulator for cell death, possibly through desialylation of *O*-glycosylated proteins, whereas NEU3 could play a role as a negative regulator by modulation of gangliosides[292]. Although molecular mechanisms underlying NEU4 effects on apoptosis, cell invasion and motility have yet to be fully elucidated, this study points to elucidating the biological role of NEU4 in cell homeostasis, which can explain its downregulation in human cancer cells.

2. Aim of the Thesis

Sialidases or neuraminidases are glycohydrolytic enzymes removing sialic acid residues from glycoconjugates, such as glycoproteins, glycolipids, gangliosides, and polysaccharides. They are widely distributed amongst all living organisms, from microorganisms to vertebrates. In mammals, several sialidases with different subcellular localizations and biochemical features have been described: a lysosomal sialidase (NEU1), a cytosolic sialidase (NEU2), and a membrane-associated sialidase (NEU3). NEU4 is the most recently identified member of the human sialidase family. This enzyme is found in two forms, long and short, differing in the presence of a 12 amino acids sequence at the N-terminus of the protein.

In literature, different and contrasting subcellular localizations had been previously suggested for both NEU4 long and NEU4 short[194,280,296]. Yamaguchi and colleagues demonstrated a mitochondrial localization for the long form of NEU4 and an intracellular membrane distribution for the short one[280]. Conversely, Seyrantepe and colleagues[296] suggested a lysosomal localization for this sialidase and demonstrated that mice deficient in NEU4 exhibit abnormal ganglioside catabolism and lysosomal storage[304].

The alignment of human sialidases amino acid sequences showed the presence in NEU4 of a long proline-rich region, which is non-homologous to the other human sialidases. Since NEU4 folds into an active sialidase, it seems likely that this amino acid stretch represents a separate domain providing unique functionality to this sialidase, as previously suggested[293]. Since proline-rich sequences are well known to play an important role in the assembly of multi-protein complexes[324], we hypothesized an involvement of NEU4 Pro-rich region in the protein-protein interactions involved in the mechanism of anchorage to the membranes of this sialidase.

Therefore, in this work we attempted to understand the function of the proline-rich region of human NEU4.

Specific aims:

1. To investigate membrane anchoring mechanism and subcellular localization of NEU4 long and NEU4 short.
2. To analyze the effect of Pro-rich region deletion on both subcellular localization and membrane association of NEU4.
3. To study the role of NEU4 Pro-rich region in cell proliferation and activity towards glycoproteins in SK-N-BE neuroblastoma cells.
4. To examine the function of NEU4 in retinoic-acid induced neuronal differentiation of SK-N-BE cells.
5. To determine the role of NEU4 Pro-rich region in protein-protein interactions in PI3K/Akt and Erk1/2 MAPK signaling pathways in SK-N-BE cell line.

3. Materials and Methods

3.1 Reagents and antibodies

Mouse anti-c-myc mAb and rabbit anti-Caveolin-1 pAb, for western blotting experiments, were purchased from Santa Cruz Biotechnology. Mouse anti-PDI mAb was from Stressgene and mouse anti-EEA1 mAb from BD Biosciences. Rabbit anti-Calnexin, anti-VDAC1/Porin, anti-COX IV and anti-Superoxide Dismutase 2 pAbs, goat anti-TIMM50 pAb and mouse anti-TOMM22 mAb were obtained from Abcam. Mouse anti-PGK mAb was purchased from Molecular Probes. p44/42 MAPK (Erk1/2), phospho-p44/42 MAPK (Erk1/2) (Thr202/Tyr204), phospho-Akt (Ser473), Akt (pan), and PTEN rabbit mAbs were from Cell Signaling Technology. Mouse anti-vinculin was obtained from Sigma. Goat anti-mouse and rabbit anti-goat IgG HRP-conjugated antibodies were from Calbiochem. Goat anti-rabbit IgG HRP-conjugated antibody was from Biorad. For immunofluorescence staining, mouse anti-cytochrome *c* mAb was purchased from Promega Corporation, mouse anti-LAMP1 and anti-Calnexin mAbs from BD Biosciences, and rabbit anti-class III beta-tubulin from Covance. Mouse anti-HA mAb was obtained from Santa Cruz Biotechnology, and rabbit anti-c-myc pAb from Sigma. Donkey anti-rabbit Cy3- and anti-mouse Cy2-conjugated antibodies were purchased from Jackson ImmunoResearch Laboratories, whereas donkey anti-rabbit IgG Alexa Fluor® 488 conjugated antibody was purchased from Molecular Probes. Dulbecco's Modified Eagle's Medium (DMEM), RPMI 1640, fetal bovine serum (FBS), L-glutamine, penicillin and streptomycin were obtained from Lonza. Genetic (G418) was obtained from Invitrogen. Poly-D-lysine and retinoic acid were from Sigma, LY294002 (PI3 Kinase Inhibitor) was from Cell Signaling Technology. All other reagents were purchased from Sigma.

3.2 Vectors

cDNA encoding the long form of NEU4 was amplified by PCR using oligonucleotide primers NEU4-EcoRI F and NEU4-XbaI R, *Pfu* Turbo DNA-polymerase (Stratagene) and NEU4 long in pCDNA3x(+)HA (Invitrogen) as template. The resulting PCR product was subcloned into pcDNA3.1/*myc*-His expression vector (Invitrogen) to obtain NEU4 long fused in C-terminal with c-myc epitope and a poly-histidine tag. NEU4 short cDNA was generated by PCR deletion of the sequence encoding the additional 12 amino acid residues at N-terminal of NEU4 long. Mutagenesis was performed using Quick-Change Site-directed Mutagenesis Kit (Stratagene), according to the manufacturer's guidelines; NEU4S primers were used, together with pcDNA3.1/*myc*-His-NEU4 long vector as template, in order to obtain NEU4 short fused in C-terminal with c-myc epitope and a poly-His tag. NEU4 short fused in N-terminal with HA epitope was kindly supplied by prof. Monti[194]. NEU4 long (N4L) and NEU4 short (N4S) sequences were confirmed by automated sequencing using vector and gene-specific primers (T7 and BGH for plasmid and NEU4-INT for NEU4 insert).

The deletion mutant of NEU4 long lacking the Pro-rich region was obtained by the following steps. First of all, the amplification of the regions located both upstream and downstream of the proline-rich region was

performed by PCR using NEU4 long vector as template and NEU4-N and NEU4-C primers, respectively. Each cDNA fragment, coding for the N- or C-terminal portion of NEU4 long, was subcloned in a pCR-BLUNT vector (Invitrogen). Subsequently, NEU4 cDNA fragments have been ligated to one another and the resulting cDNA, coding a NEU4 deleted in the proline-rich region, was subcloned into pcDNA3.1/*myc*-His vector. Finally, in order to obtain the cDNA coding for NEU4 long mutant (N4LnoP), the insertion of the corresponding NEU2 sequence was carried out. This cloning procedure was accomplished in two steps by subsequent PCR reactions using NEU4noP Step1 and NEU4noP Step2 as primers. The mutant form of NEU4 short was made by a deletion PCR using NEU4S primers and N4LnoP vector as template.

All NEU4 long and NEU4 short sequences, either wild-type and mutated, were confirmed by automated sequencing using vector and gene-specific primers (T7 and BGH for plasmid and NEU4-INT F for NEU4 insert). The sequences of primers used for PCR are listed in Table 3-1.

Table 3-1 List of primers used for NEU4 cDNAs production.

Primer Name	Primer Sequence
NEU4-EcoRI F	5' - GGAATTCATGATGAGCTCTGCAGCCTTCC - 3'
NEU4-XbaI R	5' - GTCTAGAGGAGGGCCAGCAGCACCC - 3'
NEU4-INT F	5' - CGCCGCGCGCCTCTGCTG - 3'
NEU4S F	5' - GGTACCGAGCTCGGATCCATGGGGGTCCCTCGTACCCC - 3'
NEU4S R	5' - GGGGTACGAGGGACCCCCATGGATCCGAGCTCGGTACC - 3'
NEU4-N-BamHI F	5' - CGCCGCGGATCCATGATGAGCTCTGCAGCCTTCCCA - 3'
NEU4-N-XbaI R	5' - GCTCTAGAGAAGCCCACGATGCTGCCCTG - 3'
NEU4-C-XbaI F	5' - GCTCTAGATGGCTGCTGTACTCCCACCC - 3'
NEU4-C-EcoRI R	5' - CCGGAATTCGGAGGGCCAGCAGCACCC - 3'
NEU4noP Step1 F	5' - CAGCATCGTGGGCTTCCCCAGTCCTCGCTCGTCTAGATGGCTGCTG - 3'
NEU4noP Step1 R	5' - CAGCAGCCATCTAGACGAGCGAGGACTGGGGAAGCCCACGATGCTG - 3'
NEU4noP Step2 F	5' - CCCAGTCCTCGCTCGGGGCCTGGCTCCCCAGCTAGATGGCTGCTG - 3'
NEU4noP Step2 R	5' - CAGCAGCCATCTAGCTGGGGAGCCAGGCCCCGAGCGAGGACTGGG - 3'

3.3 Cell cultures, transfection and treatments

COS-7 and HeLa cells were cultured using DMEM supplemented with 10% (v/v) FBS, 4 mM L-glutamine, 100 U/ml penicillin and 100 µg/ml streptomycin and maintained at 37°C in a humidified 5% CO_2 incubator. Cells, cultured in 100 mm cell culture dishes (seeded at 6 x 10^5 cells/dish) or onto glass coverslips (seeded at 2.5 x 10^4 cells/coverslip), were transiently transfected with NEU4 expressing vectors in serum-free medium using FuGene6 reagent (Roche), according to the manufacturer's instructions. After transfection, cells were grown for 24-36 h in complete medium and then processed for NEU4 expression analysis. Cell viability before and after transfection was carried out using MTT assay (Sigma), according to the manufacturer's instructions. Transfection efficiency was evaluated with beta-galactosidase assay, according to the manufacturer's protocol.

Human SK-N-BE neuroblastoma cells were cultured in RPMI 1640 medium supplemented with 10% FBS and 2 mM L-glutamine and

maintained at 37°C in a humidified 5% CO_2 incubator. cDNAs encoding human NEU4 long, either wild-type and mutated, cloned into the pcDNA3.1/*myc*-His expression vector were used for transfection in SK-N-BE cells. Transfection was carried out in a serum-free medium using FuGene6 reagent (Roche), according to the manufacturer's instructions. After transfection, stable clones were isolated and maintained with 200 µg/ml geneticin (G418) in the culture medium.

Under differentiating conditions, SK-N-BE cells were cultured in low serum (1% FBS) medium, with or without addition of retinoic acid (RA) at a concentration of 10 µM. For inhibition of PI3K/Akt pathway, cells were pretreated with LY294002 one hour before and during the RA stimulation. RA and LY294002 were reconstituted in ethanol and DMSO, respectively, and stock solutions were diluted in the culture medium at the indicated working concentrations.

3.4 Homology molecular modeling

The homology models of NEU4, both wild-type and mutated, were generated with HHpred[325] using the method of HMM-HMM comparison of the queried protein and the templates deposited in the PDB database. The generated models were visualized using pyMol and the images were imported.

3.5 RNA isolation, RT-PCR and Q-PCR

Total RNA was isolated by SK-N-BE cells using RNeasy Mini Kits (Qiagen) according to manufacturer's instructions, adding a DNase digestion step to eliminate possible genomic DNA contamination. Subsequently, 1 µg RNA from each sample was reverse-transcribed using 200 U SuperScript® II RT (Invitrogen) and random primers (Invitrogen) in a total volume of 20 µl, according to the manufacturers' protocol.

For RT-PCR analysis, one µl (50 ng) of cDNA was amplified by PCR using DreamTaq™ DNA Polymerase (Fermentas) and specific pairs of primers. The expression of myc-tagged NEU4 long cDNAs in stable SK-N-BE clones was performed using two different forward primers, NEU4 F and NEU4 long F, and a common reverse primer, Myc R, annealing to the myc region. As internal control, amplification of housekeeping beta-actin gene was performed. The primers used for RT-PCR are listed in Table 3-2.

For real time PCR (Q-PCR), one µl (50 ng) of cDNA was amplified using the SYBR Green PCR Master Mix (Applied Biosystem) and specific primers of interest. Real time PCR was carried out using a 7500 Real-Time PCR System (Applied Biosystem) and the amplification was performed with 40 cycles of 15 s at 95°C and 60 s at 59°C. Our samples were analyzed for the expression of NEU1, NEU2, NEU3, and NEU4. To normalize each sample for total RNA content, control housekeeping gene (beta-actin) was used under similar PCR conditions. The relative expression level was calculated with the $2[-\Delta\Delta C(T)]$ method and was expressed as a fold change. All PCR experiments were performed in triplicate and the standard deviations were calculated and displayed as error bars. The accuracy was

monitored by the analysis of melting curves. The primers used for real time PCR are listed in Table 3-3.

Table 3-2 List of primers used for RT-PCR.

Primer Name	Primer Sequence
NEU4 long F	5' - CTCTGCAGCCTTCCCAAG - 3'
NEU4 F	5' - ACCGCCGAGAGTGTTTTGG - 3'
Myc R	5' - TCCTCTTCTGAGATGAGTT - 3'

Table 3-3 List of human primers used for Q-PCR.

Gene	Forward Primer	Reverse Primer
NEU1	5' - CCTGGATATTGGCACTGAA - 3'	5' - CATCGCTGAGGAGACAGAAG - 3'
NEU2	5' - AGAAGGATGAGCACGCAGA - 3'	5' - GGATGGCAATGAAGAAGAGG - 3'
NEU3	5' - TGAGGATTGGGCAGTTGG - 3'	5' - CCCGCACACAGATGAAGAA - 3'
NEU4	5' - ACCGCCGAGAGTGTTTTGG - 3'	5' - CGTGGTCATCGCTGTAGAAGG - 3'
beta-actin	5' - CGACAGGATGCAGAAGGAG - 3'	5' - ACATCTGCTGGAAGGTGGA - 3'

3.6 Solubilization experiments

Membrane solubilization with Triton X-114 was performed as described (Bordier 1981). Briefly, 24 h after transfection, COS-7 cells were washed twice with cold PBS, harvested by scraping and collected at 800 g for 10 min at 4°C. Cells were lysed by 5 sec probe sonication (Bandelin Sonoplus 2070 sonicator) in 10 mM Tris-HCl, pH 7.4, 150 mM NaCl, supplemented with protease inhibitors, and then centrifuged at 800 g for 10 min at 4°C. The resulting crude extract was diluted in 100 µl of the above buffer to yield a final protein concentration of 1.0 mg/ml. Protein extraction was performed by addition to the sample of a corresponding volume of 2% (v/v) precondensed Triton X-114 in 10 mM Tris-HCl, pH 7.4, 150 mM NaCl, followed by incubation for 1 h on ice. Detergent-extracted samples (200 µl) were then layered onto a cushion of 6% (w/v) sucrose, 10 mM Tris-HCl, pH 7.4, 150 mM NaCl, 0.06% Triton X-114 (300 µl), incubated 3 min at 30°C and centrifuged at 300 g for 3 min at room temperature. After centrifugation, the upper aqueous phase was removed and treated again with 1% fresh Triton X-114. A second phase separation was then performed as above using the same sucrose cushion. Finally, the detergent and aqueous phases were adjusted to the same final volume with 10 mM Tris-HCl, pH 7.4, 150 mM NaCl. Aliquots of the starting sample and separated phases were subjected to sialidase activity assay and analyzed by western blotting for detection of NEU4 and endogenous protein markers, Caveolin-1 (as an integral membrane protein) and PDI (as a soluble protein).

Sodium carbonate extractions were performed as described[326]. Briefly, 36 h after transfection, COS-7 cells were washed twice with cold PBS, harvested by scraping and then collected by centrifugation at 800 *g* for 10 min at 4°C. Cells were suspended in ice-cold 10 mM Tris-HCl, pH 7.5, containing protease inhibitors, and sonicated at the minimum setting for 5 sec. After centrifugation at 800 *g* for 10 min at 4°C, the supernatant (crude

extract) was centrifuged at 100,000 *g* for 1 h at 4°C to collect total cell membranes. The pellet was resuspended in lysis buffer and then split into identical aliquots. To obtain peripheral protein extraction, membrane samples were then treated with an equal volume either of ice-cold 0.2 M Na_2CO_3, pH 12.0 or 10 mM Tris-HCl, pH 7.5, 3 M NaCl or lysis buffer alone, as a control, and incubated for 30 min on ice. After centrifugation at 100,000 *g*, pellets were resuspended in the appropriate buffer to yield the membrane fractions, while the supernatants represented the soluble fractions. Samples containing sodium carbonate were quickly brought to pH 7.5 by the addition of acetic acid. Finally, soluble and membrane fractions were adjusted to the same final volume and then subjected to sialidase activity assay and western blotting for detection of NEU4 and endogenous markers, Caveolin-1 (as an integral membrane protein) and EEA1 (as a peripheral membrane protein).

3.7 Cross-linking with paraformaldehyde

Paraformaldehyde cross-linking was performed in transfected cells as described[327]. Briefly, 24 h after transfection, COS-7 cells were treated with 0.25-1.0% (w/v) paraformaldehyde (PFA) in PBS for 5-60 min at 37°C. The cross-linking reaction was quenched with glycine to a final concentration of 125 mM, for 5 min at room temperature. Cells harvested by scraping were collected at 800 *g* for 10 min at 4°C, washed twice with PBS and resuspended in lysis buffer (50 mM Tris pH 7.5, 150 mM NaCl, 10% glycerol, 1% NP-40, 5 mM EDTA) containing protease inhibitors. After an incubation of 30 min on ice, cell lysate was centrifuged at 18,000 *g*, to pellet cell debris. Prior to SDS-PAGE, cell extract was heated in sample buffer for 10 min at 65°C for complexes analysis or boiled for 20 min at 95°C to reverse the formaldehyde cross-links. Aliquots of PFA-treated cell extracts, before and after subjecting them to cross-link reversal condition, were analyzed by western blotting with anti-c-myc antibody for detection of NEU4.

3.8 Confocal immunofluorescence microscopy

For colocalization studies, COS-7 and HeLa cells were cultured onto glass-coverslips and transfected with NEU4 expressing vectors; 24 h after transfection, cells were briefly washed in PBS, fixed with 3% (w/v) paraformaldehyde (PFA) in PBS for 20 min at room temperature or in methanol for 5 min at -20°C. PFA reaction was quenched by treatment with 50 mM NH_4Cl in PBS for 30 min. Fixed cells were washed three times with PBS and then permeabilized with 0.3% Saponin (w/v) in PBS (PBS-Sap) for 20 min and double-stained at room temperature with anti-c-myc and anti-cytochrome *c*, anti-LAMP1 or anti-Calnexin antibodies at appropriated dilutions in PBS-Sap for 1 h. After incubation, cells were washed three times in the same buffer and then double-stained with Cy2- and Cy3-conjugated secondary antibodies as above. After washes with PBS-Sap and PBS, coverslips were mounted using DakoCytomation Fluorescent Mounting Medium (DAKO).

For neuronal differentiation analysis, SK-N-BE cells were plated on poly-lysine-coated glass-coverslips (5 x 10^3 cells/coverslip) and treated with retinoic acid as described above. After 1 and 2 days of treatment, cells were briefly washed in PBS and fixed with 3% PFA in PBS for 20 min at room temperature. After three washes in PBS, fixed cells were blocked and permeabilized with 1% (w/v) BSA in PBS-Sap (PBS-Sap-BSA) for 20 min and stained at room temperature with anti-class III beta-tubulin antibody in PBS-Sap-BSA for 1 h. After incubation, cells were washed three times in the PBS and stained with anti-rabbit 488 AlexaFluor antibody for 1 h. After three washes with PBS, nuclei were stained with far red-fluorescent TO-PRO-3 dye in PBS for 15 min, prior to final washes in PBS and treatment with DAKO mounting medium.

Slides were examined with a Leica Mod. TCS-SP2 (Leica Microsystem) confocal microscopy and images were processed with Leica Confocal software (LCS.EXE) and Adobe Photoshop software.

3.9 Subcellular fractionation and mitochondria isolation

For subcellular fractionation experiments, 36 h after transfection COS-7 cells were washed twice with cold PBS and lysed on plate using fractionation buffer (20 mM HEPES, pH 7.4, 250 mM sucrose, 10 mM KCl, 1.5 mM $MgCl_2$, 1 mM EDTA and 1 mM EGTA), containing protease inhibitors and 1 mM DTT. Cell lysate was then passed through a 25 G needle 10 times, leaved for 20 min on ice and centrifuged at 800 *g* for 5 min at 4°C to remove nuclei and unbroken cells. The post-nuclear supernatant was centrifuged at 10,000 *g* for 15 min at 4°C to collect mitochondria and then at 100,000 *g* for 1 h to obtain microsomal and cytosolic fractions. Mitochondrial and microsomal pellets were washed with fractionation buffer, resuspended by pipetting, passed through a 25 G needle 10 times and then recentrifuged as above. After centrifugation, wash buffer was removed and pellets were resuspended in buffer containing 10% glycerol and 0.1% SDS. Mitochondrial, microsomal and cytosolic fractions were subjected to western blotting for detection of NEU4 and endogenous markers, COX IV (as mitochondrial protein), Calnexin (as ER protein) and PGK (as cytosolic protein).

For mitochondria isolation, 24 h after transfection COS-7 cells (2 x 10^7) were washed twice with cold PBS, harvested by scraping and collected at 800 *g* for 10 min at 4°C. Mitochondria isolation was performed using Mitochondria Isolation Kit for Cultured Cells (Pierce) following the reagent-based method, according to the manufacturer's instructions. Briefly, the post-nuclear supernatant (total extract), obtained after cell lysis, was centrifuged at 3,000 *g* for 15 min at 4°C to collect a purified fraction of mitochondria. The mitochondrial pellet was lysed with 2% (w/v) CHAPS in PBS by vortexing and centrifuged at maximum speed to obtain membrane (pellet) and soluble (supernatant) fractions. Aliquots of the post-nuclear supernatant, total mitochondria and submitochondrial fractions were analyzed by western blotting for detection of NEU4 and mitochondrial markers, VDAC1/Porin (outer membrane), COX IV (inner membrane) and

SOD2 (matrix). To assess the purity of the mitochondrial fraction, lysosomal α-mannosidase was assayed as described[328].

3.10 Mitoplasts isolation and protease treatment

Submitochondrial fractionation was performed as described[329]. For preparation of mitoplasts (mitochondria devoid of their external membrane), intact mitochondria were subjected to osmotic shock, by resuspension in 20 mM Hepes/KOH, pH 7.4 followed by incubation for 30 min on ice. Mitoplasts were recovered by centrifugation at 4,000 *g* and then resuspended in 10 mM Hepes/KOH, pH 7.4, 220 mM mannitol, 70 mM sucrose. As a control, whole mitochondria were incubated in an isotonic buffer (10 mM Hepes/KOH, pH 7.4, 220 mM mannitol, 70 mM sucrose) for 30 min on ice and centrifuged as described above. Samples of mitochondria and mitoplasts were treated with trypsin at a final concentration of 0, 10 and 25 µg/ml for 20 min on ice. Reactions were stopped by adding PMSF at a final concentration of 0.4 mg/ml and protease inhibitors. After incubation for 5 min on ice, the samples were centrifuged at 12,000 *g* for 10 min at 4°C, and the pellets were analyzed by western blotting for detection of NEU4 and mitochondrial markers, TOMM22 (outer membrane), TIMM50 (inner membrane) and SOD2 (matrix).

3.11 Protein extraction

To determine NEU4 sialidase expression and analyze glycoproteins profile, SK-N-BE cells were usually seeded in 100 mm dishes at a density of 1 x 10^6 cells/dish and grown for 24 h. Then, cells were harvested by centrifugation and resuspended in PBS containing protease inhibitors and lysed by sonication, following by a centrifugation at 800 *g* for 10 min to eliminate unbroken cells and nuclear components. Subsequently, supernatant (total extract) was centrifuged at 200,000 *g* for 20 min on TL100 Ultracentrifuge (Beckman) to obtain a cytosolic fraction and a membrane fraction. Aliquots of both cytosolic and membrane fractions were used to analyze glycoprotein content, as described below. Aliquots of the membrane fractions were also used for NEU4 sialidase activity determination, as well as for NEU4 detection by western blotting.

For analysis of Akt and Erk1/2 signaling pathways, SK-N-BE cells were plated in 60 mm dishes at 1.5 x 10^5 cells/dish and grown in untreated and RA treated conditions for 1 and 2 days. At different time points, cells were washed with ice-cold PBS and lysed in RIPA buffer, containing both protease and phosphatase inhibitors, and 1mM PMSF. After an incubation on ice for 30 min, cells were centrifuged at 18,000 *g* for 15 min, and supernatants (total extract) analyzed for protein content. Equal amount of protein were separated on SDS-PAGE, transferred onto a PVDF membrane, and probed with antibodies against Akt, phospho-Akt (p-Akt), Erk1/2, phospho-Erk1/2 (p-Erk1/2), PTEN, and vinculin. Detection of vinculin was used as internal control to ensure equal loading and transfer of proteins.

To measure the activity of acetylcholinesterase and to perform co-immunoprecipitation experiments, SK-N-BE cells were washed with ice-cold

PBS and lysed in Nonidet-P40 buffer, containing both protease and phosphatase inhibitors, on ice for 30 min. Supernatants obtained after a centrifugation at 18,000 *g* for 15 min were used for immunoprecipitation analysis or acetylcholinesterase activity assay, as described below.

3.12 Co-immunoprecipitation experiments

For co-immunoprecipitation (co-IP) experiments, SK-N-BE cells were plated at a density of 8 x 10^5 cells in 100 mm dishes, transiently transfected with NEU4 cDNAs and then cultured in normal growth conditions for 2 days. Then, cells were lysed in Nonidet-P40 buffer as described above. An amount of 1 mg of total cellular protein was incubated overnight with rabbit anti-c-myc, anti-Akt or anti-Erk1/2 antibodies at 4°C. Subsequently, samples were incubated with protein A-Sepharose (Amersham Pharmacia Biotech) for 4 h at 4°C. After three washes in lysis buffer containing both protease and phosphatase inhibitors, immunoprecipitates were collected by centrifugation, resuspended in 30 µl of 2x SDS-sample buffer. After boiling, samples were subjected to electrophoresis followed by western blot analysis.

3.13 Glycoprotein analysis

For analysis of sialoglycoproteins profile, 30 µg of proteins derived from both membrane and cytosolic fractions of mock, N4L, and N4LnoP expressing SK-N-BE cells were separated on 10% SDS-PAGE and transferred onto a PVDF membrane. Sialoglycoproteins detection was carried out employing the DIG Glycan Differentiation Kit (Roche), according to the manufacturer's instructions. Glycoproteins with α2-6-linked sialic acid were identified using SNA (*Sambucus nigra* agglutinin) lectin while α2-3-linked sialic acid was detected using MAA (*Maackia amurensis* agglutinin) lectin. Protein levels were quantified by densitometry using ImageJ Software from NIH Image and the results are represented as a plot profile.

3.14 Proliferation assays

For Trypan blue exclusion assay, mock, N4L, and N4LnoP transfected SK-N-BE cells were seeded in 6-well culture plates at a density of 5 x 10^4 cells/well and grown for 4 days. At each time point, cells were collected by trypsinization, resuspended in PBS and then mixed with 0.4% trypan blue dye. After a 3 min incubation time, unstained viable cells were counted in a hemacytometer.

To assess viability of stable transfected SK-N-BE clones, cells were analyzed using *in vitro* toxicology assay kit, MTT based (Sigma), in accordance to manufacturer's protocols. Briefly, SK-N-BE cells were seeded in 96-well microtiter plates at a density of 3 x 10^3 cells/well in 100 µl of complete RPMI without phenol red and cultured for 4 days. At each time point, reconstituted MTT was added to the cells in an amount equal to 10% of the culture medium volume. After a 4 h incubation time, absorbance upon

solubilization was measured at 570 nm using a BioRad microplate reader. The results are expressed as mean values ± standard deviation.

3.15 Neurite outgrowth evaluation

Analysis of neurite outgrowth in RA treated SK-N-BE cells was carried out measuring both the percentage of cells bearing neurites and neurite length using NeuronJ, an ImageJ plugin for neurite tracing and quantification. More than 10 arbitrarily chosen fields were imaged under a confocal microscope in transmission or fluorescence mode. About 500 cells were examined for each experimental condition. The number of cells bearing neurites were expressed as percentage of the total cell number in each field. The neurite length were expressed as fold respect to the cell body diameter. All data are presented as means ± standard deviation.

3.16 Sialidase and acetylcholinesterase assays

NEU4 sialidase activity was determined with 4MU-NeuAc (Sigma) as a substrate[194]. Briefly, reactions were set up in triplicate using 30-50 µg of total proteins in 50 mM Na citrate/phosphate buffer, pH 3.2, 0.1 mM 4MU-NeuAc, 6 mg/ml BSA, in a final volume of 100 µl. Reactions were stopped by adding 1.5 ml of 0.2 M Glycine/NaOH, pH 10.8, after incubation at 37°C for 30 or 60 min. The amount of sialic acid released was evaluated by spectrofluorimetric measurement of the 4-methylumbelliferone released.

In order to measure acetylcholinesterase activity, SK-N-BE cells were plated in 100 mm dishes (1.5×10^5 cells/dish) for 24 h and then treated with RA in a low serum medium. After 2 and 5 days of RA treatment, SK-N-BE cells were lysed in Nonidet-P40 buffer, as described above, and total extracts obtained were used for enzymatic assay. Acetylcholinesterase activity was assayed according to the spectrophotometric procedure described by Ellman et al.[330]. Briefly, the reaction mixture was prepared in 200 mM sodium phosphate buffer, pH 7.5, containing 0.6 mM DNTB and 1 mM acetylthiocholine iodide. One unit of achetylcholinesterase activity is defined as the amount of enzyme liberating 1 nmol of product per min.

3.17 SDS-PAGE and western blotting

Protein concentration of samples was determined by the Bradford assay[331] using Coomassie Plus - The Better Bradford™ Assay Kit (Pierce). SDS-PAGE and western blotting were carried out by standard procedures. PVDF Immobilon-P (Millipore) membranes were blocked with 5% (w/v) dried milk in TBS, 0.1% (v/v) Tween20 (TBS-T) for 30 min at room temperature and then incubated overnight at 4°C with appropriate dilutions of antibodies in 5% dried milk in TBS-T (for anti-c-myc, anti-EEA1, anti-Cav-1, anti-PDI, and anti-vinculin antibodies) or 5% (w/v) bovine serum albumin (BSA) in TBS-T (for anti-Cnx, anti-PGK, anti-VDAC1, anti-SOD2, anti-COX IV, anti-TOMM22, anti-TIMM50, anti-Akt, anti-phospho-Akt, anti-Erk1/2, anti-phospho-Erk1/2, anti-PTEN antibodies). After three washes with TBS-T,

membranes were incubated for 1 h with anti-mouse, anti-rabbit or anti-goat HRP-conjugated IgG antibodies, diluted in 5% dried milk in TBS-T. After final washes in TBS-T, detection was performed using ECL plus detection system (Millipore). Protein levels were quantified by densitometry of immunoblots using ImageJ software from NIH Image.

3.18 Statistical analysis

Values are presented as means ± standard deviation (SD). Statistical analyses were usually performed using Student's t-test comparing mock cells data with treated cells data. Sometimes comparisons among different stimulations were performed. Significance was defined as *, $p<0.05$; **, $p<0.01$; ***, $p<0.001$.

4. Results

4.1 Human sialidase NEU4 long and short are extrinsic proteins bound to outer mitochondrial membrane and the endoplasmic reticulum, respectively

4.1.1 NEU4 long and NEU4 short are extrinsic membrane proteins

Transmembrane regions prediction methods, such as TMpred and TMHMM, suggest the existence of a potential transmembrane domain in NEU4 primary structure. However, the presence of such a domain is not compatible with the typical sialidase β-propeller three dimensional structure, yielded by homology modeling[205]. Conversely, no membrane anchoring motifs, such as GPI anchors, palmitoylation or myristoylation sites, are present on NEU4 aminoacidic sequence. In order to gain insight into the mechanism through which NEU4 long and NEU4 short bind to the membranes, we undertook protein extraction with Triton X-114 followed by temperature-induced phase separation, as previously performed for sialidase NEU3[332]. This detergent allows protein solubilization with phase-separation of hydrophilic from amphiphilic membrane proteins. Crude extracts, obtained from COS-7 cells transiently expressing either NEU4 long or short form as fusion proteins carrying a C-terminal c-myc epitope, were initially treated with Triton X-114 and then subjected to aqueous/detergent phase separation. Western blot analysis showed that both forms of NEU4 were totally extracted in the aqueous phase (Figure 4-1), as well as Protein Disulfide Isomerase (PDI), which is a hydrophilic protein loosely bound to ER membranes. On the contrary Caveolin-1 (Cav-1), a protein associated to the lipid bilayer by a hydrophobic domain and palmitoylation, was extracted by Triton X-114 and then totally recovered in the detergent phase. These phase-partitioning results prompted us to affirm that both forms of NEU4 are hydrophilic proteins, as already suggested by primary structure analysis. Moreover, no sialidase activity was detected in both aqueous and detergent fractions (data not shown).

In order to assess whether NEU4 is a peripheral membrane protein, the membrane fractions obtained from COS-7 cells expressing either NEU4 long or NEU4 short were brought to pH 11.5 with sodium carbonate and incubated for 30 min on ice. A subsequent ultracentrifugation yielded a soluble fraction and a membrane fraction, which were brought to pH 7.5 and subjected to SDS-PAGE followed by western blotting (Figure 4-2 A). NEU4 detection was performed with an anti c-myc antibody. In addition, Early Endosome Antigen 1 (EEA1) and Caveolin-1 (Cav-1) were used as controls for peripheral and intrinsic membrane proteins, respectively. As expected, both the long and the short form of NEU4 were found in the particulate fraction of untreated samples, as confirmed by sialidase activity assay using 4MU-NeuAc as a substrate (Figure 4-2 C). Partial recovery of both NEU4 long and NEU4 short in the soluble fraction in control samples is due to minor protein release during collection and manipulation of membranes samples. Both long and short forms of NEU4 were partially solubilized by sodium carbonate treatment. A densitometric analysis of the bands showed that about 30% and 50% of NEU4 short and NEU4 long, respectively, were solubilized upon carbonate treatment (Figure 4-2 B). As expected, after

treatment with sodium carbonate, the peripheral membrane protein EEA1 was completely recovered in the soluble fraction, while Cav-1, an integral membrane protein, was not solubilized at all, thus demonstrating that carbonate treatment extracts peripheral proteins without affecting membrane integrity. After sodium carbonate treatment no appreciable sialidase activity could be recorded in any fraction (data not shown), presumably due to alkaline denaturation or inactivation of the enzyme, as previously reported for sialidase NEU3[332]. In addition, treatment of the membrane fraction prepared from COS-7 expressing either NEU4 long or NEU4 short with a high ionic strength buffer, containing 1.5 M NaCl, did not cause any NEU4 release (data not shown), suggesting that this sialidase is a peripheral protein strongly associated to membranes.

4.1.2 NEU4 long and NEU4 short are anchored to membranes through protein-protein interactions

Since our data showed that both forms of NEU4 are extrinsic membrane proteins, we performed cross-linking experiments in order to assess whether these sialidases might be anchored to the membrane via protein-protein interactions. The lack of any motif for membrane anchoring through prenylation, acylation or GPI on NEU4 aminoacidic sequence suggested protein-protein interactions as the most likely membrane associating mechanism. Paraformaldehyde (PFA) is known to form covalent bonds between chemical groups not further apart than 2 Å, which can readily be reversed by heat treatment at 95°C. COS-7 cells transiently expressing either NEU4 long or NEU4 short were supplemented in the medium with PFA, as reported in Material and Methods. Crude cell extracts were then subjected to SDS-PAGE and western blotting in order to assess the presence of NEU4 complexes. Both NEU4 forms and their complexes were detected with an anti-c-myc antibody. Initially, COS-7 cells expressing either long or short form of NEU4 were treated with various concentrations of PFA for different times (Figure 4-3). These preliminary tests showed that 20 min incubation with 0.25% (w/v) PFA was sufficient to obtain cross-linking of NEU4 to adjacent membrane proteins; higher PFA concentrations (Figure 4-3 A) or longer incubation times (Figure 4-3 B) resulted in smeared electrophoretic bands, indicative of aspecific cross-linking. As shown in Figure 4-4, after PFA treatment, NEU4 was detected only as a high Mr complex (higher than 250 kDa), which hardly entered into the running gel. Cross-linking reversion, obtained by incubation at 95°C for 20 min, led to the disappearance of NEU4 complex and to the reappearance of the bands corresponding to NEU4 long and NEU4 short. This experiment confirmed that both forms of NEU4 interact with other proteins likely involved in their anchorage to membranes.

4.1.3 The long form of NEU4 localizes in mitochondria, while the short form is bound to the endoplasmic reticulum

The existence of contradictory data in literature[194,280,296] about NEU4 subcellular localization prompted us to further investigate this issue, both through confocal microscopy and subcellular fractionation studies.

Colocalization experiments were carried out in COS-7 cells, transiently expressing either NEU4 long or NEU4 short as fusion proteins carrying a C-terminal c-myc epitope. Markers of different cellular compartments, such as cytochrome c (cyt c) for mitochondria, Lysosome-Associated Membrane Protein-1 (LAMP-1) for lysosomes and Calnexin (Cnx) for endoplasmic reticulum, were also used. 24 h after transfection, cells were fixed, permeabilized and analyzed by confocal microscopy. Results, reported in Figure 4, showed that NEU4 long colocalizes with the mitochondrial marker cyt c (Figure 4-5 A panel f), as reported by Yamaguchi and colleagues[280], but not with the lysosomal marker LAMP-1 (Figure 4-5 B panel f), as claimed by Seyrantepe and coworkers[296]. Moreover, while colocalization of NEU4 short with either of these markers could not be observed (Figure 4-5 A panel c and 4-5 B panel c), superimposition with Cnx diffused fluorescent signal, shown in Figure 4-5 C panel c, suggested that NEU4 short can be bound to the endoplasmic reticulum. Colocalization of NEU4 long or NEU4 short with the subcellular markers was confirmed by Z-stack analyses, performed on confocal microscopy images (data not shown).

In order to check the possibility that the observed subcellular localization of both NEU4 forms might be an artifact due to protein transient overexpression, NEU4 subcellular localization was evaluated at different post-transfection times. No differences in subcellular localization of both NEU4 forms was observed when fixing and analyzing the cells 5, 10, 24 and 36 h after transfection (Figure 4-6). NEU4 short appeared to be diffusely localized inside the cells at all times, its signal only slightly superimposing with cyt c. On the contrary, NEU4 long exhibited the already observed complete colocalization with the mitochondrial marker. Moreover, a total and partial mitochondrial colocalization of NEU4 long and NEU4 short, respectively, was also observed in HeLa cells, demonstrating that this subcellular distribution is not restricted to a particular cell type (Figure 4-7).

Finally, to assess the difference in subcellular localization between the short and long form of NEU4, we performed cotransfection experiments with both c-myc-tagged NEU4 long and HA-tagged NEU4 short expressing vectors. Results are shown in Figure 4-8: NEU4 short showed a diffused intracellular label both in COS-7 and in HeLa cells, while a more localized distribution, closely mirroring the one observed in single transfection experiments, was found for NEU4 long in both cell types. The overlay confirms the results obtained by separate transfections, showing only a partial colocalization for NEU4 long and NEU4 short.

Results obtained by confocal microscopy were confirmed in subcellular fractionation experiments, shown in Figure 4-9, yielding a mitochondrial, a microsomal and a cytosolic fraction. NEU4 long was found only in the mitochondrial fraction, while the short form was found also in the microsomal fraction, enriched in endoplasmic reticulum membranes. As expected, none of the two proteins was found in the cytosolic fraction. Detection of COX IV, Cnx and 3-phosphoglycerate kinase (PGK) confirmed fractionation efficiency. In order to quantify the relative abundance of NEU4 long and NEU4 short in mitochondria, these organelles were purified from crude extracts transiently expressing each form of NEU4, as described in Materials and Methods. This procedure allowed to obtain a highly purified

fraction containing heavy mitochondria; only 3.5% of total lysosomes were found in this fraction, as confirmed by activity assay of the lysosomal α-mannosidase (Figure 4-10 C). Western blot analysis performed with an anti c-myc antibody, showed that only NEU4 long is abundantly recovered in the mitochondrial fraction (Figure 4-10 A). A densitometric analysis showed that 66% of NEU4 long is found in mitochondria, while only 13% of NEU4 short is recovered in this fraction (Figure 4-10 B). The partial recovery of NEU4 long is accounted for by the fact that most of the small mitochondria are normally lost in the supernatant during the centrifugation. The inner mitochondrial membrane complex COX IV was used as a loading control for mitochondrial fraction and to normalize densitometric data. The apparently high content of NEU4 short in the mitochondrial fraction shown in Figure 6 is due to the fact that the same quantities of total proteins of all subcellular fractions were loaded onto the gel. However, when the same volumes of total extract and purified mitochondria were evaluated for both the short and the long form, as done in the experiment reported in Figure 7, results clearly showed that most NEU4 long is found in mitochondria, while only a small fraction of NEU4 short localizes in these organelles. The different amount of mitochondria analyzed in these two experiments was also indicated by intensity of COX IV band, which is higher in Figure 6 than in Figure 7.

4.1.4 The long form of NEU4 is bound to the outer mitochondrial membrane

To further analyse the submitochondrial localization of NEU4 long, heavy mitochondria from COS-7 cells expressing this sialidase were purified as described above and then lysed with 2% CHAPS, yielding a pellet containing the mitochondrial membranes and a supernatant representing the soluble fraction. These samples were subsequently subjected to SDS-PAGE, followed by western blotting with an anti c-myc antibody. Results, reported in Figure 4-11 A, showed that NEU4 long form is bound to mitochondrial membranes. The presence of VDAC1, a porin which is found inside the outer mitochondrial membrane, demonstrated that mitochondria are purified undamaged, carrying both outer and inner membranes. Moreover, sialidase activity performed on the same mitochondrial fractions showed that about 95% of the total enzyme activity is membrane associated (Figure 4-11 B).

In order to assess in which of the two mitochondrial membranes NEU4 long is located, isolated intact mitochondria were subjected to osmotic shock (OS) and treated with trypsin at different concentrations. This treatment partially removes the outer mitochondrial membrane, as previously demonstrated[329]. Crude extracts obtained from whole mitochondria (- OS) and mitoplasts (+ OS) were subjected to SDS-PAGE followed by western blotting (Figures 4-11 C and D). The peripheral outer membrane protein TOMM22, the peripheral inner membrane protein TIMM50 and the mitochondrial matrix enzyme SOD2 were used as controls. As expected for a peripheral outer membrane protein, Figure 4-11 D shows that there is a decrease in intensity for TOMM22 band already in the presence of 10 µg/ml trypsin in intact mitochondria (- OS) as well as in mitoplasts (+ OS). Moreover, a fragment is also detectable in the case of TOMM22 as a result

of a partial trypsin digestion. NEU4 long was proteolysed in the same manner in intact (- OS) as well as in osmotically shocked (+ OS) mitochondria, highlighting a behaviour similar to TOMM22.

On the other hand, peripheral inner membrane protein TIMM50, due to its localization, appeared to be less susceptible to trypsin treatment in intact mitochondria, showing a decrease in band intensity only at 25 µg/ml trypsin. When trypsin treatment was performed on mitoplasts, TIMM50 became more accessible to the protease and was found to be already degraded at 10 µg/ml trypsin. Moreover, in agreement with its localization in the matrix, SOD2 was found to be unaffected by tryptic digestion in all conditions. Finally, as shown in Figure 4-11 C, both TOMM22 and NEU4 long showed the same behaviour in being partially released during osmotic shock and recovered in the supernatant, unlike TIMM50. On the whole NEU4 long behaviour closely mirrored that of the outer membrane protein TOMM22, strongly suggesting an outer mitochondrial membrane localization for this sialidase.

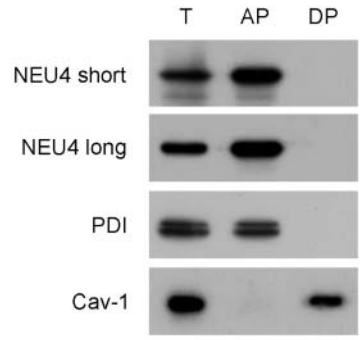

Figure 4-1 Partition of NEU4 long and NEU4 short proteins during Triton X-114 phase separation. COS-7 cells expressing NEU4 long or short were lysed and total cell extracts were subjected to phase separation with Triton X-114. Aliquots of total extract (T), aqueous phase (AP), and detergent phase (DP) were separated by SDS-PAGE and analyzed by western blotting. Both NEU4 forms were detected using an anti-c-myc antibody. To check separation, antibodies directed against hydrophilic protein disulfide isomerase (PDI) and integral membrane protein Caveolin-1 (Cav-1) were used. Blots are representative of two independent experiments.

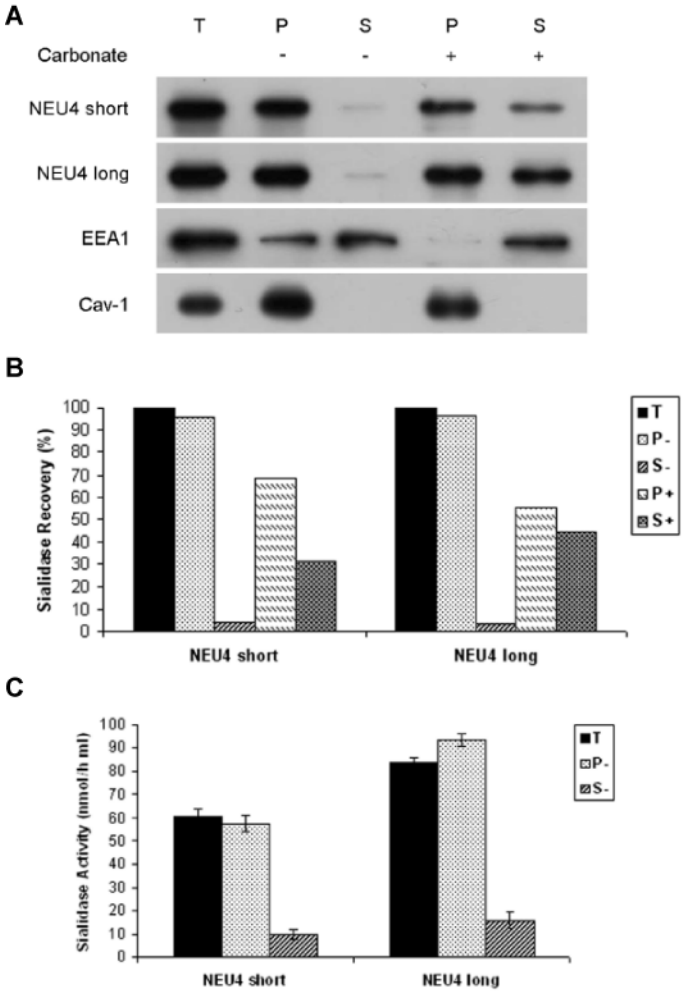

Figure 4-2 Extraction of NEU4 short and NEU4 long upon sodium carbonate treatment. COS-7 cells expressing NEU4 long or short were lysed and cell membranes were treated with the Tris buffer (Carbonate -) as a control or with sodium carbonate (Carbonate +). (**A**) Equal volumes of input cell membranes (T), membranes (P), and soluble (S) fractions were separated by SDS-PAGE and subjected to western blot analysis. NEU4 was detected using an anti-c-myc antibody. To assess the accuracy of extraction, antibodies directed against peripheral membrane protein early endosomal antigen 1 (EEA1) and integral membrane protein Caveolin-1 (Cav-1) were used. Blots are representative of three independent experiments. (**B**) Relative quantification of the NEU4 protein level in each fraction compared with input sample. Densitometric analysis was performed using NIH Image-based software ImageJ. Quantification data are representative of three independent experiments. (**C**) Sialidase activity determined with 4MU-NeuAc under control condition. Values are means ± SD of three independent experiments.

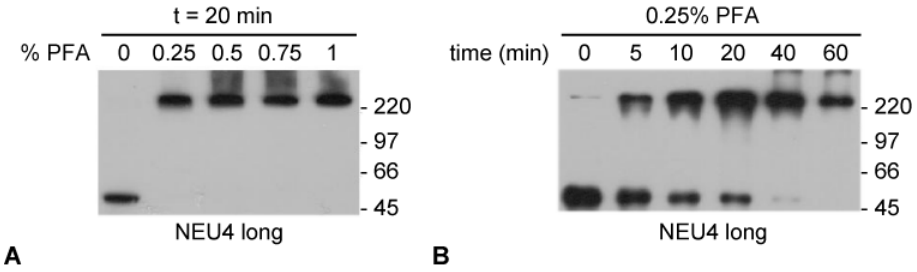

Figure 4-3 Cross-linking with paraformaldehyde and analysis of NEU4 long containing complexes. COS-7 cells expressing NEU4 long were treated with various concentrations of paraformaldehyde (PFA) for 20 min (**A**) or with 0.25% PFA for different times (**B**). In order to assess the presence of NEU4 complexes, cell lysates were separated by SDS-PAGE and analyzed by western blotting with an anti-c-myc antibody. Blots are representative of two independent experiments.

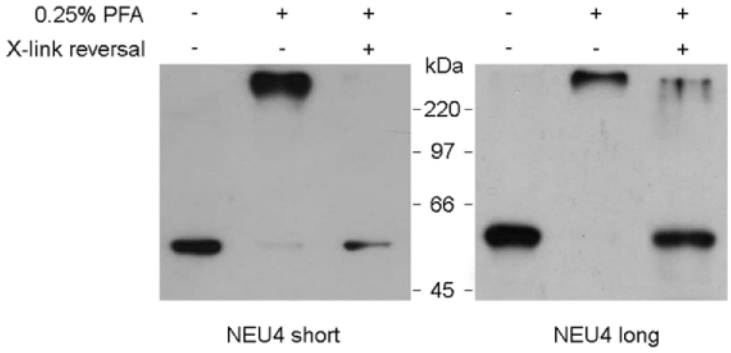

Figure 4-4 Cross-linking with paraformaldehyde and analysis of NEU4 containing complexes. COS-7 cells expressing NEU4 long or short were treated with 0.25% paraformaldehyde (PFA) for 20 min. In order to assess the presence of NEU4 complexes, cell lysates were separated by SDS-PAGE, before and after subjecting them to cross-link reversal condition, and then analyzed by western blotting with an anti-c-myc antibody. Blots are representative of three independent experiments.

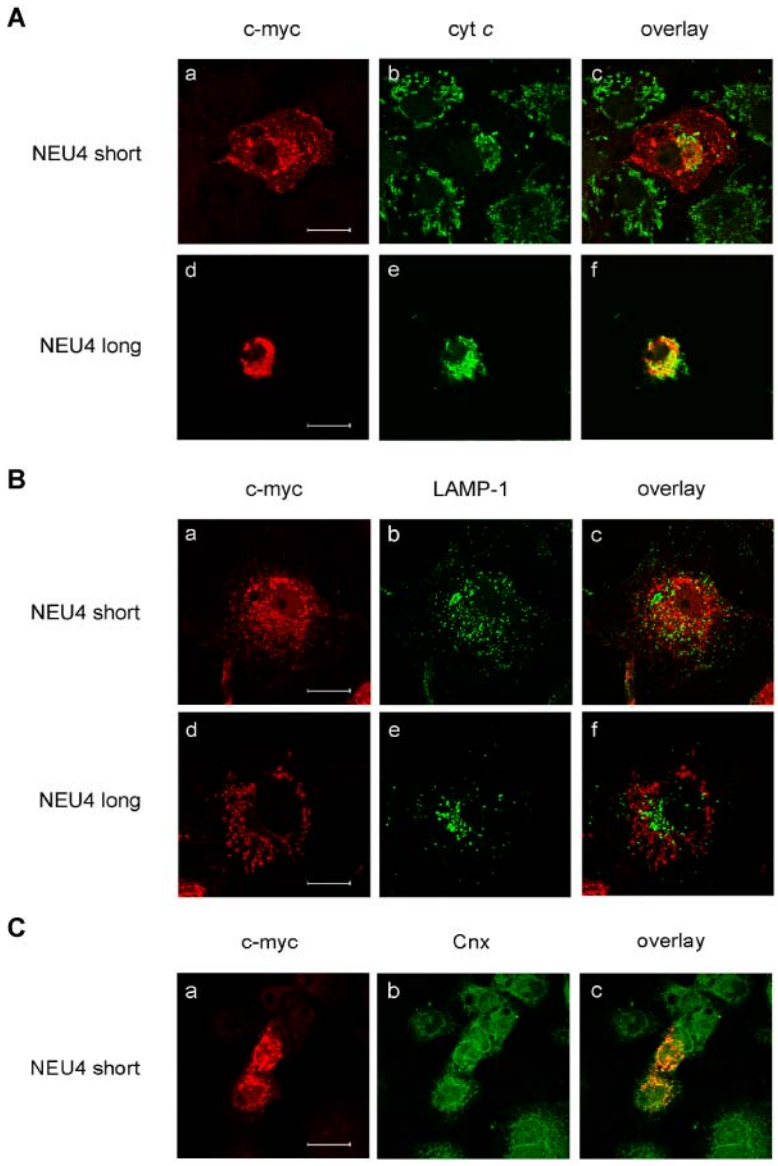

Figure 4-5 Subcellular localization of NEU4 long and NEU4 short determined by indirect immunofluorescence staining. COS-7 cells were transiently transfected with NEU4 long or short and subjected to immunofluorescence staining and confocal microscopy analysis. Images are representative of three independent experiments. (**A**) To analyze mitochondrial localization, COS-7 cells were double-stained with an anti-c-myc antibody, for detection of NEU4 short (panel a) or long (panel d), and an anti-cytochrome c (cyt c) antibody (panels b and e) as a mitochondrial marker. Overlay images are shown in panels c and f. Scale bars: 20 µm (panel a) and 25 µm (panel d). Data are representative of three independent

experiments. (**B**) To analyze lysosomal localization, COS-7 cells were double-stained with an anti-c-myc antibody, for detection of NEU4 short (panel a) or long (panel d), and an anti-LAMP-1 antibody (panels b and e) as a lysosomal marker. Overlay images are shown in panels c and f. Scale bars: 30 µm (panel a) and 15 µm (panel d). (**C**) COS-7 cells were double-stained with an anti-c-myc antibody for detection of NEU4 short (panel a) and an anti-Calnexin (Cnx) antibody (panel b) as an ER marker. Overlay image is shown in panel c. Scale bar: 25 µm.

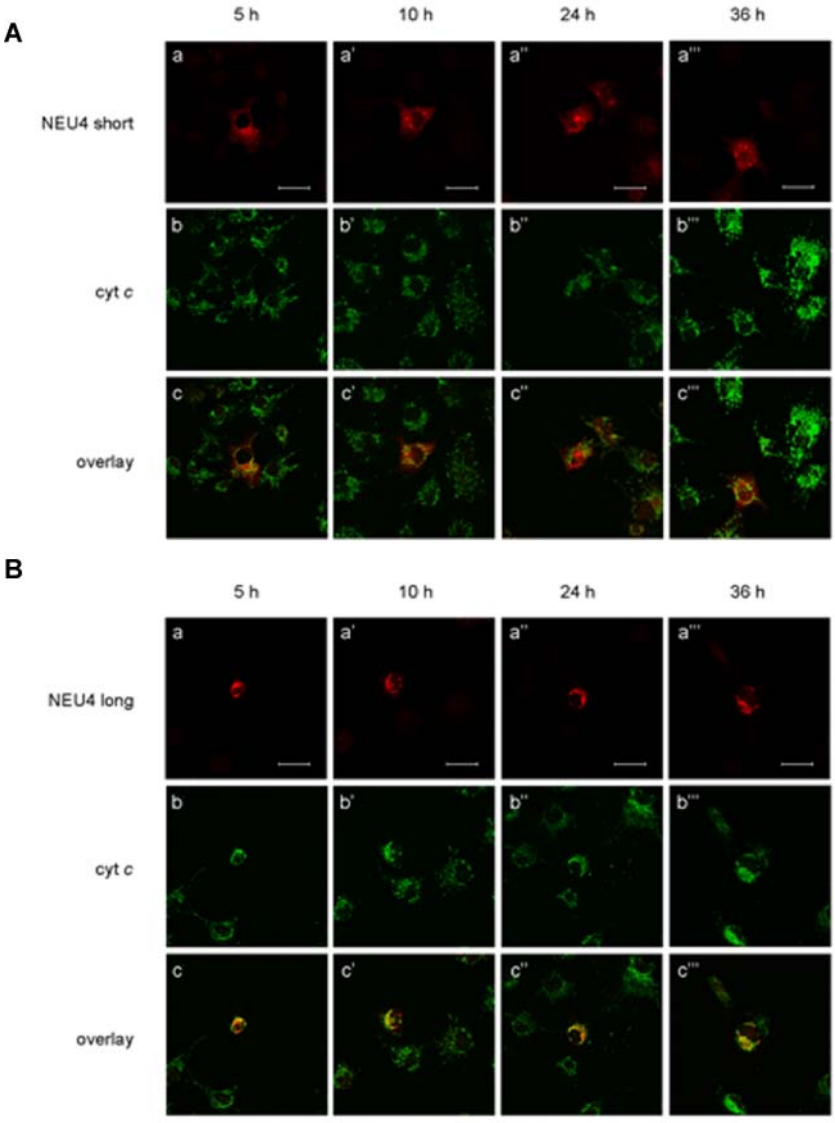

Figure 4-6 Time course of NEU4 long and NEU4 short expression in COS-7 cells monitored by indirect immunofluorescence staining. COS-7 cells were transiently transfected with NEU4 short (**A**) or long (**B**) and subjected to immunofluorescence staining and confocal microscopy analysis at 5, 10, 24 and 36 h after transfection. Cells were double-stained with anti-c-myc antibody, for detection of NEU4 long or short (panels a-a'''), and anti-cytochrome c (cyt c) antibody (panels b-b''') as mitochondrial marker. Overlay images are shown in panels c, c', c'' and c'''. Scale bars: 45 µm (panel a), 30 µm (panel a'), 35 µm (panel a''), 25 µm (panel a''') in (**A**), 35 µm (panels a-a''') in (**B**). Images are representative of three independent experiments.

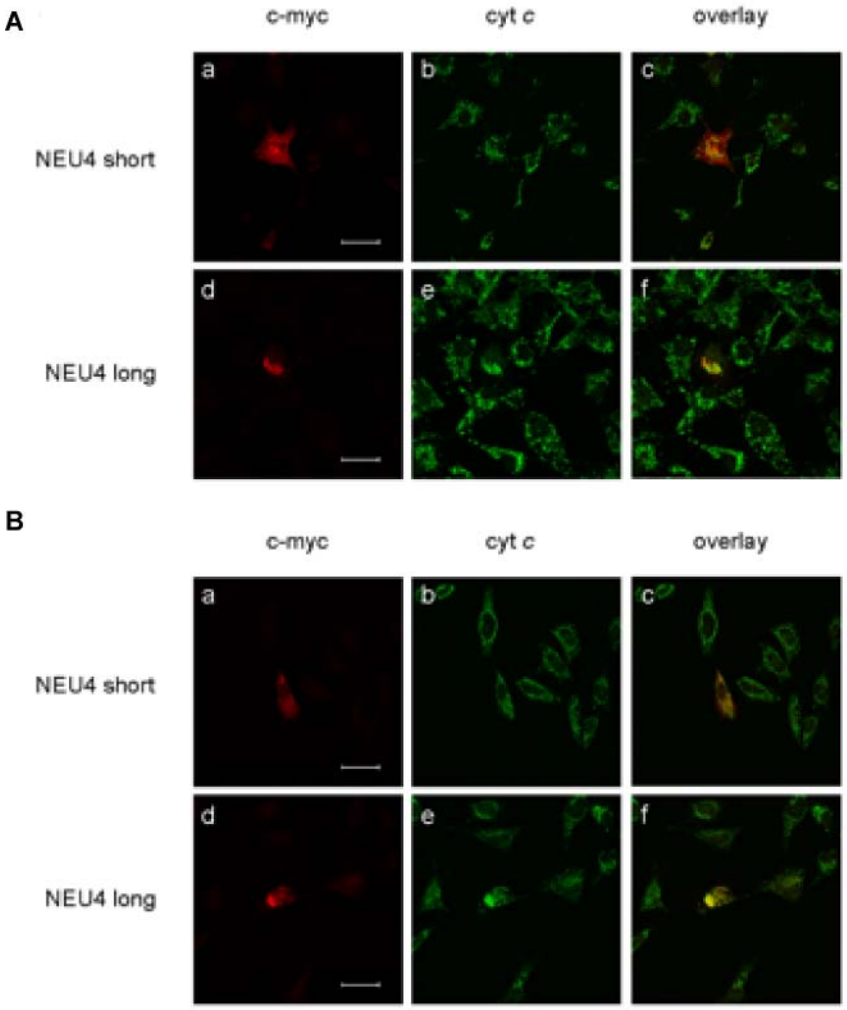

Figure 4-7 Mitochondrial localization of NEU4 long and NEU4 short in COS-7 and HeLa cells determined by indirect immunofluorescence staining. COS-7 (**A**) and HeLa (**B**) cells were transiently transfected with NEU4 long or short and subjected to immunofluorescence staining and confocal microscopy analysis. Cells were double-stained with anti-c-myc antibody, for detection of NEU4 short (panel a) or long (panel d), and anti-cytochrome c (cyt c) antibody (panels b and e) as mitochondrial marker. Overlay images are shown in panels c and f. Scale bars: 35 µm (panel a), 30 µm (panel d) in (**A**), 40 µm (panel a), 35 µm (panel d) in (**B**). Images are representative of three independent experiments.

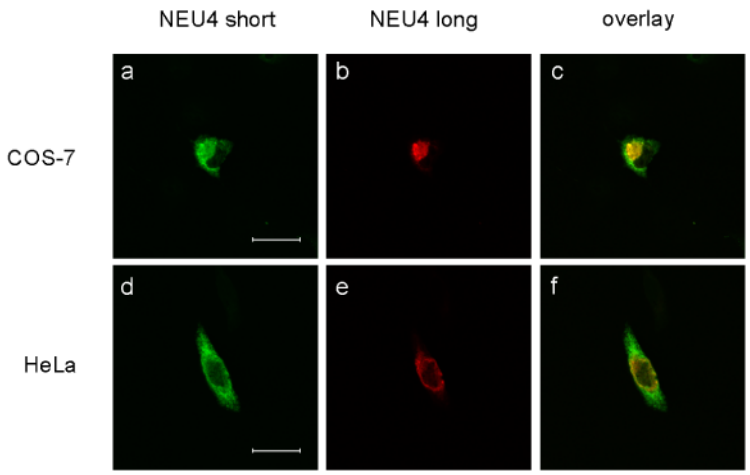

Figure 4-8 Coexpression of NEU4 long and NEU4 short in COS-7 and HeLa cells evaluated by indirect immunofluorescence staining. COS-7 and HeLa cells were transiently cotransfected with c-myc-tagged NEU4 long and HA-tagged NEU4 short and subjected to immunofluorescence staining, followed by confocal microscopy analysis. Cells were double-stained with anti-HA and anti-c-myc antibodies, for detection of NEU4 short (panels a and d) or long (panel b and e), respectively. Overlay images are shown in panels c and f. Scale bars: 30 µm (panel a) and 25 µm (panel d). Images are representative of three independent experiments.

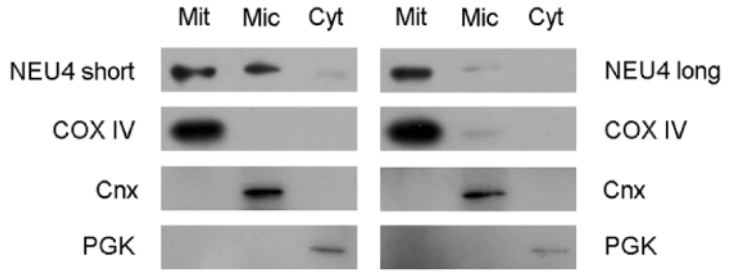

Figure 4-9 Intracellular distribution of NEU4 long and NEU4 short evaluated by subcellular fractionation. COS-7 cells expressing NEU4 long or short were lysed and subfractionated in mitochondrial (Mit), microsomal (Mic), and cytosolic (Cyt) fractions. Equal amount of protein were subjected to SDS-PAGE and western blotting. Both NEU4 forms were detected using an anti-c-myc antibody. Antibody directed against cytochrome c oxidase (COX IV), Calnexin (Cnx), and 3-phosphoglycerate kinase (PGK) were used as mitochondrial, microsomal, and cytosolic marker, respectively. Blots are representative of three independent experiments.

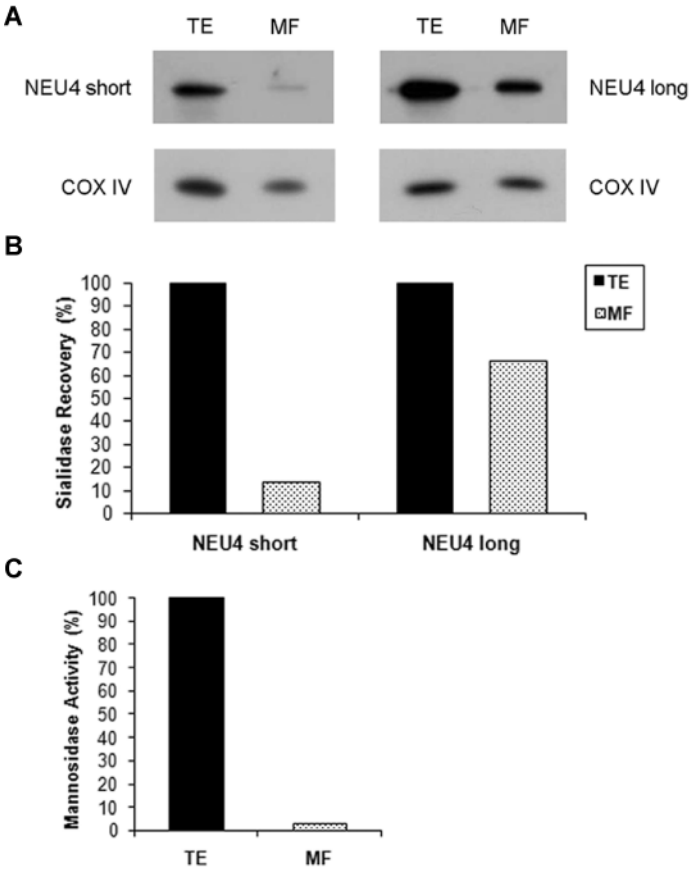

Figure 4-10 Recovery of NEU4 long or NEU4 short in a purified heavy mitochondrial fraction. COS-7 cells expressing NEU4 long or short were lysed and processed to isolate heavy mitochondrial fraction. (**A**) Aliquots of total extract (TE) and mitochondrial fraction (MF) were subjected to SDS-PAGE and western blotting. NEU4 short and long were detected using an anti-c-myc antibody. COX IV was used as mitochondrial loading control. Blots are representative of three independent experiments. (**B**) Relative quantification of the NEU4 protein level in the mitochondrial fraction compared with total cell extract. NEU4 levels in each fraction were normalized to the corresponding COX IV level. Densitometric analysis was performed using NIH Image-based software ImageJ. Quantification data are representative of three independent experiments. (**C**) Lysosomal α-mannosidase activity assayed in total extract (TE) and mitochondrial fraction (MF). Values are expressed as a percentage of enzyme activity as compared with the input crude extract. Data are representative of three independent experiments.

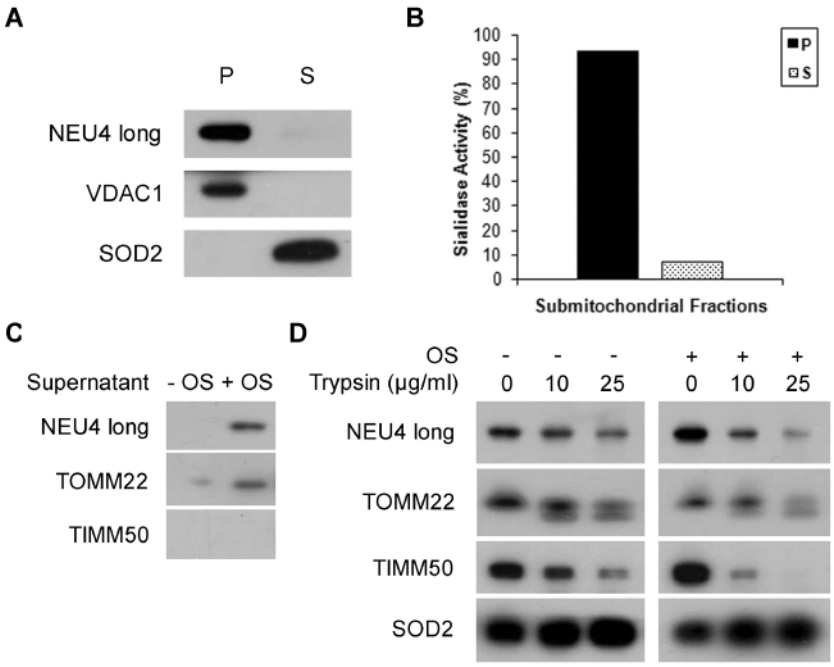

Figure 4-11 Submitochondrial localization of the long form of NEU4. (**A**) COS-7 cells expressing NEU4 long were lysed and processed to isolate heavy mitochondrial fraction. Intact mitochondria were lysed with 2% CHAPS in PBS and then subfractionated to obtain a membrane (P) and a soluble (S) fraction. Aliquots of fractions were subjected to SDS-PAGE and western blotting with an anti-c-myc antibody, for NEU4 detection. To control subfractionation, antibodies directed against outer mitochondrial membrane protein VDAC1 and mitochondrial matrix protein SOD2 were used. Blots are representative of three independent experiments. (**B**) Sialidase activity using 4MU-NeuAc as a substrate assayed in the above submitochondrial fractions. Values are expressed as a percentage of enzyme activity recovered in each fraction as compared with the input sample of mitochondria. Data are representative of three independent experiments. (**C**) Intact heavy mitochondria isolated from COS-7 cells expressing NEU4 long were subjected to osmotic shock (OS) in 20 mM Hepes/KOH, pH 7.4, as reported in Material and Methods. Mitochondria (−OS) or mitoplasts (+OS) are collected through centrifugation and supernatants were analyzed by immunoblotting, performed with an anti-c-myc antibody. TOMM22 and TIMM50 were used as outer and inner mitochondrial membrane markers, respectively. (**D**) Aliquots of intact (−OS) and osmotically shocked (+OS) mitochondria were treated with various concentrations (0, 10, and 25 µg/ml) of trypsin. After centrifugation, samples were analyzed by SDS-PAGE and western blotting with an anti-c-myc antibody for NEU4 long detection. TOMM22, TIMM50, and SOD2 were also probed with specific antibodies and used as outer membrane, inner membrane, and matrix protein controls, respectively. Blots are representative of three independent experiments.

4.2 The proline-rich region does not directly affect NEU4 association to membranes

4.2.1 Deletion mutants of NEU4 lacking the Pro-rich region show catalytic properties similar to those of the corresponding wild-type enzymes

A multiple alignment of NEU2, NEU3, and NEU4 amino acid sequences, performed with T-COFFEE, showed the presence in NEU4 of a long stretch of 81 amino acids (amino acids 284-375 in NEU4 short, amino acids 296-387 in NEU4 long), that appears unique among mammalian sialidases (Figure 4-12 A). Since conserved sialidase sequences are found on both sides of this 'insert' and since NEU4 folds into an active sialidase, it is likely that this sequence represents a separate domain that provides unique functionality to this sialidase, as previously proposed by Comelli et al.[293]. In addition, this sequence was identified as a proline-rich region by Motif Scan program (Figure 4-12 B). This region is absent both in NEU3 and in soluble NEU2 sialidases. In the latter, it is substituted by a much shorter loop, containing few prolines. Since proline-rich sequences are well known to play an important role in the assembly of multi-protein complexes[324], we hypothesized an involvement of NEU4 Pro-rich region in the protein-protein interactions involved in the mechanism of anchorage to the membranes of human sialidase NEU4.

In order to verify this hypothesis, we decided to produce NEU4 long and NEU4 short mutants lacking the proline-rich region, which was replaced by the 11 amino acids of the corresponding loop of the cytosolic sialidase NEU2. Figure 4-13 shows the results of NEU4 structure prediction obtained by using HHpred server, selecting the homologous sequences with highest scores and known structure as template. As expected, both wild-type and mutated NEU4 fold as a six-blade β-propeller (Figure 4-13 A and B, respectively). The Pro-rich region of NEU4 is located in an external loop connecting two β-strands of adjacent blades (β-strand D of blade IV and β-strand A of blade V), in a way that it does not affect the overall structure of the enzyme.

Both NEU4 long and NEU4 short mutants (named N4LnoP and N4SnoP, respectively) were transiently expressed in COS-7 cells as fusion proteins carrying a C-terminal c-myc epitope, as well as the corresponding wild-type proteins. To rule out the possibility that the deletion of the Pro-rich region could affect the NEU4 enzymatic properties, sialidase activity was evaluated in transfected COS-7 cell lysates using the synthetic fluorescent substrate 4MU-NeuAc. As shown in Figure 4-14, NEU4 short mutant (N4SnoP) is able to hydrolyze 4MU-NeuAc, although a slight reduction of specific sialidase activity compared to the wild-type form (N4S) was observed. However, the pH profile remains similar to the wild-type enzyme, with an extremely acidic pH optimum, showing a maximum around pH 3.2. In both cases, the enzyme retained a partial activity also at higher pH values.

4.2.2 The Pro-rich region is not responsible for the intracellular distribution of both NEU4 long and short

As already performed for the wild-type forms of NEU4 sialidase, subcellular localization of NEU4 mutants was investigated in transfected COS-7 cells both through confocal microscopy and subcellular fractionation. Immunofluorescence results showed that NEU4 long mutant colocalizes with the mitochondrial marker cyt c (Figure 4-15 A), as already observed for the corresponding wild-type enzyme. The short form mutant also showed an intracellular distribution similar to the corresponding wild-type protein (Figure 4-15 A); in particular, N4SnoP mutant exhibited only a partial colocalization with mitochondria, showing instead a more diffused distribution due to the association with intracellular membranes like the endoplasmic reticulum. Conversely, colocalization experiments performed using the lysosomal marker LAMP-1 demonstrated that both NEU4 mutants, as well as the corresponding wild-type enzymes, did not localized in lysosomes (Figure 4-15 B). Overall, immunofluorescence data indicated that the Pro-rich region is not directly responsible for the subcellular localization of both NEU4 long and NEU4 short and their membrane associated nature.

4.2.3 The deletion of the Pro-rich region does not increased the solubility of NEU4 long protein

In order to determine whether the absence of the Pro-rich region was able to increase the solubility of NEU4 sialidase, mitochondria from COS-7 cells transiently transfected with mutated form of NEU4 long were subfractioned into soluble and membrane fractions. VDAC1 and SOD2 were used as control for mitochondrial membranes and mitochondrial matrix, respectively. As shown in Figure 4-16, NEU4 long mutant was totally recovered in mitochondrial membranes, exactly as observed with the non-mutated form. In both cases, no band corresponding to NEU4 was observed in the soluble fraction. These results demonstrate that the deletion of the Pro-rich region and its replacement with NEU2 loop is not sufficient to increase the NEU4 solubility, which was found still anchored to the membranes as before.

In addition, COS-7 cells transfected with the deletion mutant of NEU4 long were subjected to sodium carbonate treatment, in a similar way to that previously performed with both forms of NEU4 (see above). As shown in Figure 4-17, the mutated form of NEU4 long was recovered in the particulate fraction under untreated conditions, exactly as the wild-type enzyme. The association of N4LnoP to membranes was also confirmed by the repartition of sialidase activity towards 4MU-NeuAc substrate (Figure 4-17 B). In contrast with the wild-type protein, NEU4 long mutant was not solubilized upon sodium carbonate treatment, demonstrating that this sialidase is strongly associated to membranes even in the absence of its Pro-rich loop (Figure 4-17 A). These data are in agreement with the results of colocalization studies, confirming that the proline-rich region is not essential for the attachment of NEU4 to the membranes.

4.2.4 The deletion of the Pro-rich region does not affect the interaction of NEU4 long with proteins putatively involved in its anchorage to membranes

Finally, in order to establish whether the proline-rich region of NEU4 could be important in the formation of protein-protein interactions, we decided to perform cross-linking experiments also with the mutated form of NEU4 long. For this purpose, transfected COS-7 expressing N4LnoP were subjected to PFA treatment, in a similar way to what was carried out with the wild-type proteins (see above). Results show that, exactly as wild-type NEU4 long, NEU4 long deletion mutant seems to interact with other proteins, as demonstrated by the formation of a multi-protein complex in PFA-treated cells (Figure 4-18). As expected, N4LnoP complex disappeared after cross-linking reversion, with the simultaneous detection of a protein band corresponding to the only NEU4 long mutant protein. In both cases, cross-linking with PFA results in the assembly of multi-protein complexes with similar molecular masses, thus demonstrating that the absence of Pro-rich region does not significantly affect the ability of NEU4 to interact with other proteins.

Figure 4-12 Human sialidase NEU4 possesses a proline-rich region in the sequence. (**A**) Alignment of the amino acid sequences of human NEU2 (Hs NEU2, Accession No. NM_005383), NEU3 (Hs NEU3, Accession No. Y18563), and NEU4 (Hs NEU4, Accession No. AJ277883) is shown. The alignment was performed with the T-COFFEE program. Colors legend: Red-orange: good alignment; yellow-green: average alignment; blue: bad alignment. (**B**) Representation of the proline-rich region found in NEU4 sequence with Motif Scan program.

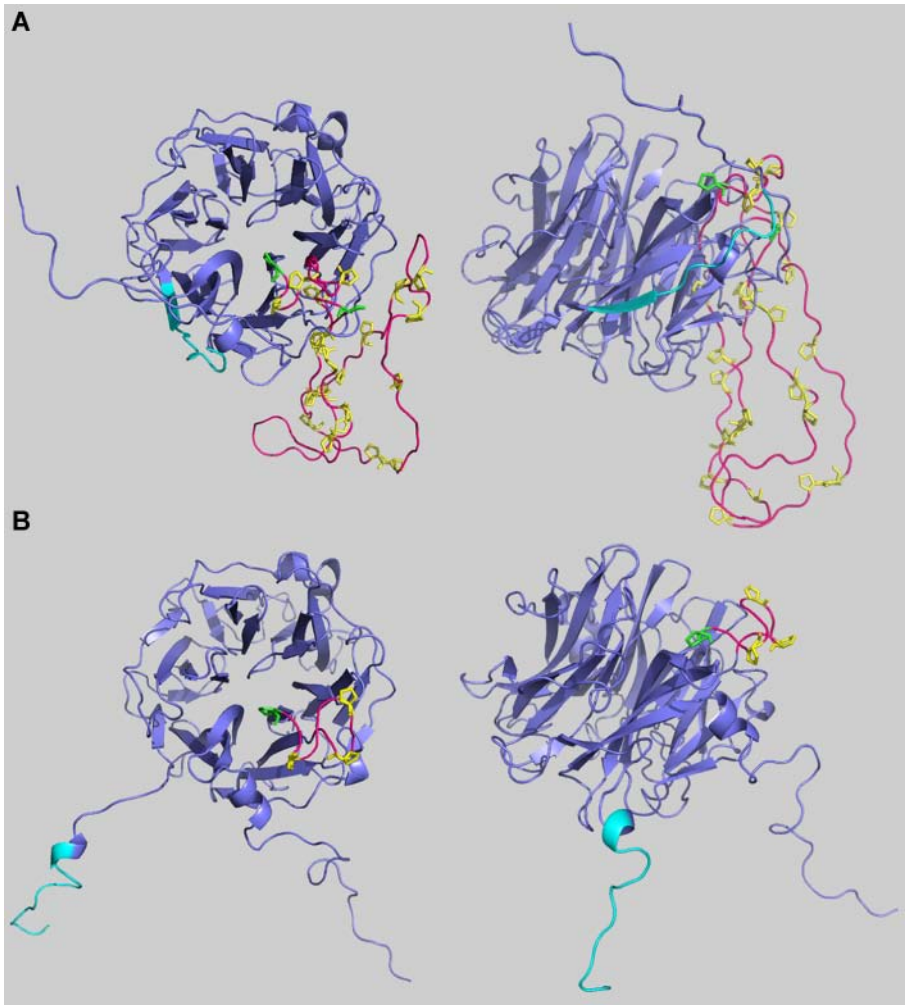

Figure 4-13 Homology modeling of both wild-type and mutated NEU4 long. Three dimensional structures of NEU4 long, either wild-type or mutated, obtained by homology modeling, as described in Material and Methods. The proline-rich loop is colored in pink, proline residues are in yellow, the N-terminal sequence of NEU4 long is in sky blue. (**A**) Predicted structures of wild-type NEU4 long, viewed into the active site (left) and from the side (right). (**B**) Predicted structures of NEU4 long mutant, viewed into the active site (left) and from the side (right).

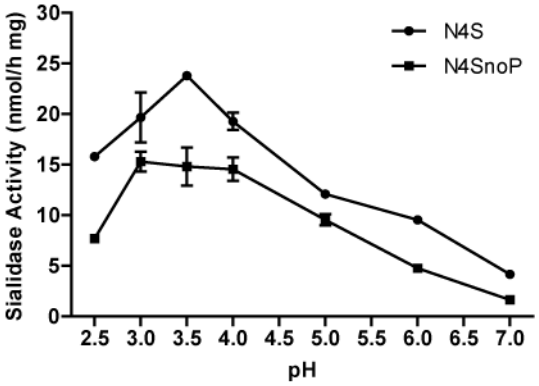

Figure 4-14 Sialidase activity of both wild-type and mutated NEU4 short. COS-7 cells expressing NEU4 short, either wild-type or mutated, were lysed, and their sialidase activity towards 4MU-NeuAc was measured at varius pH in total extracts. Values represent the mean ± SD of three independent experiments.

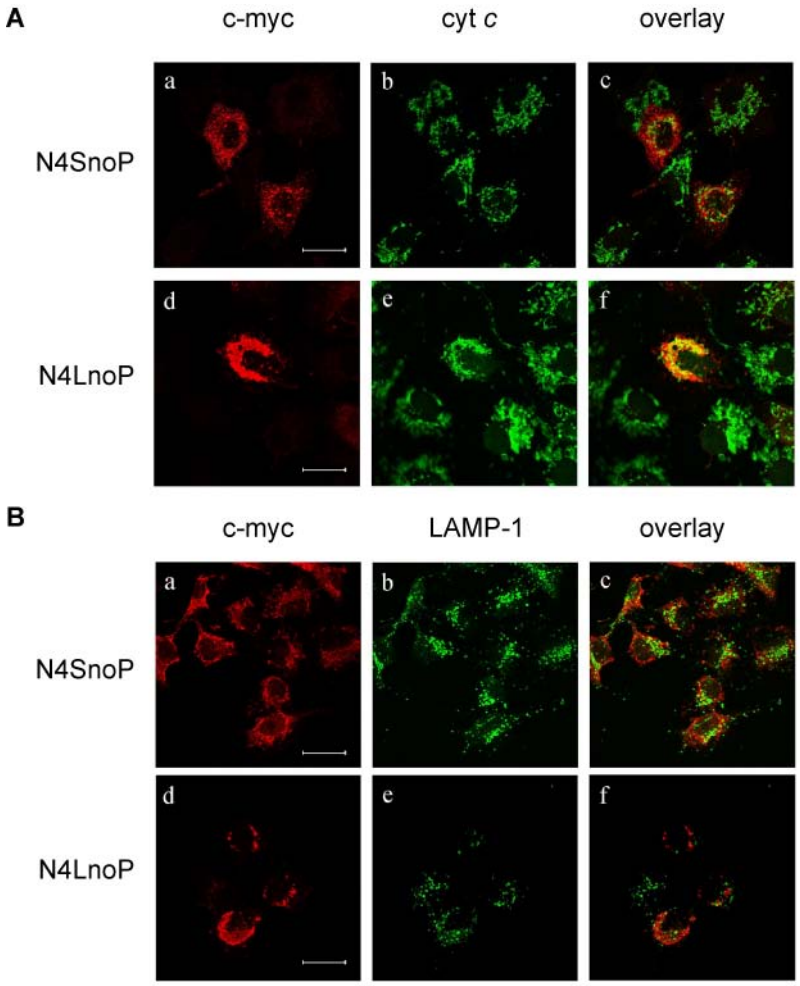

Figure 4-15 Subcellular localization of NEU4 long and NEU4 short mutants determined by indirect immunofluorescence staining. COS-7 cells were transiently transfected with N4LnoP or N4SnoP and subjected to immunofluorescence staining and confocal microscopy analysis. (**A**) To analyze mitochondrial localization, COS-7 cells were double-stained with an anti-c-myc antibody, for detection of N4SnoP (panel a) or N4LnoP (panel d), and an anti-cytochrome c (cyt c) antibody (panels b and e) as a mitochondrial marker. Overlay images are shown in panels c and f. Scale bars: 30 µm (panel a) and 25 µm (panel d). Images are representative of three independent experiments. (**B**) To analyze lysosomal localization, COS-7 cells were double-stained with an anti-c-myc antibody, for detection of N4SnoP (panel a) or N4LnoP (panel d), and an anti-LAMP-1 antibody (panels b and e) as a lysosomal marker. Overlay images are shown in panels c and f. Scale bars: 30 µm (panel a and d). Images are representative of three independent experiments.

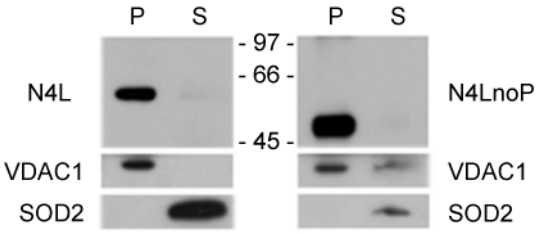

Figure 4-16 Submitochondrial localization of both wild-type and mutated NEU4 long. COS-7 cells expressing NEU4 long, either wild-type or mutated, were lysed and processed to isolate heavy mitochondrial fraction. Intact mitochondria were lysed with 2% CHAPS in PBS and then subfractionated to obtain a membrane (P) and a soluble (S) fraction. Aliquots of fractions were subjected to SDS-PAGE and western blotting with an anti-c-myc antibody, for NEU4 detection. To control subfractionation, antibodies directed against outer mitochondrial membrane protein VDAC1 and mitochondrial matrix protein SOD2 were used. Blots are representative of three independent experiments.

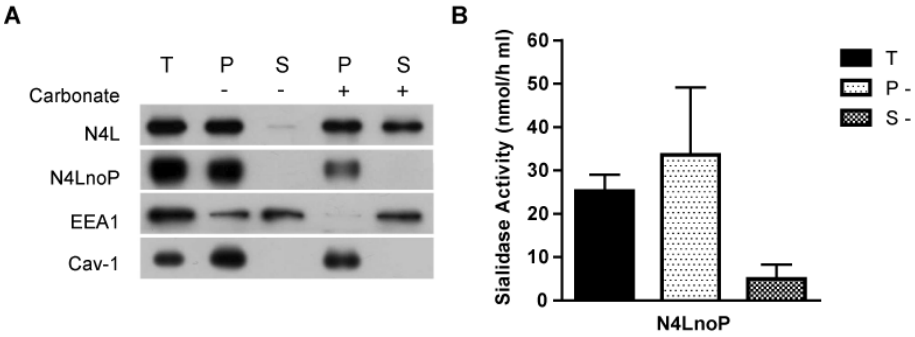

Figure 4-17 Extraction of both wild-type and mutated NEU4 long upon sodium carbonate treatment. COS-7 cells expressing NEU4 long, either wild-type or mutated, were lysed and cell membranes were treated with the Tris buffer (Carbonate -) as a control or with sodium carbonate (Carbonate +). (**A**) Equal volumes of input cell membranes (T), membranes (P), and soluble (S) fractions were separated by SDS-PAGE and subjected to western blot analysis. NEU4 was detected using an anti-c-myc antibody. To assess the accuracy of extraction, antibodies directed against peripheral membrane protein early endosomal antigen 1 (EEA1) and integral membrane protein Caveolin-1 (Cav-1) were used. Blots are representative of three independent experiments. (**B**) Sialidase activity determined with 4MU-NeuAc under control condition. Values are means ± SD of three independent experiments.

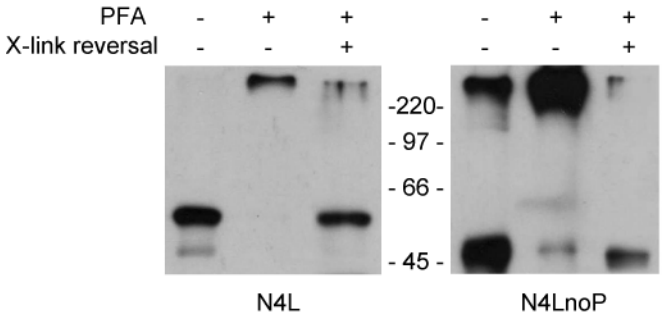

Figure 4-18 Cross-linking with paraformaldehyde and analysis of wild-type or mutated NEU4 long containing complexes. COS-7 cells expressing NEU4 long, either wild-type or mutated, were treated with 0.25% paraformaldehyde (PFA) for 20 min. In order to assess the presence of NEU4 complexes, cell lysates were separated by SDS-PAGE, before and after subjecting them to cross-link reversal condition, and then analyzed by western blotting with an anti-c-myc antibody. Blots are representative of three independent experiments.

4.3 The proline-rich region increases cell proliferation and activity towards glycoproteins

4.3.1 Expression of wild-type and mutated NEU4 long in SK-N-BE cells

As described above, deletion mutants lacking the proline-rich loop showed subcellular distributions similar to those of wild-type proteins in COS-7 cells. These evidences suggested that this region does not directly affect the association of NEU4 to the membranes. We therefore decided to investigate whether it could be involved in the interaction with signalling pathway components. Studies performed in collaboration with Department of Medical Chemistry, Biochemistry and Biotechnology (L.I.T.A.) of the University of Milano evaluated the effect of NEU4 long expression in human neuroblastoma SK-N-BE cell line, known to possess MYCN (myc myelocytomatosis viral related oncogene, neuroblastoma derived) amplification.

Similarly, we decided to produce stable SK-N-BE cell clones transfected with cDNA coding for the mutated form of NEU4 long (N4LnoP). SK-N-BE cells were transfected with the N4LnoP vector carrying neomycin resistance and a CMV promoter. Clones resistant to G418 were isolated and analyzed for mRNA content of NEU4 long, wild-type or mutated, by RT-PCR and Q-PCR. All N4LnoP clones selected were compared to the clone transfected with wild-type NEU4 long (N4L) cDNA or vector alone (mock). In order to distinguish between exogenously expressed N4L and N4LnoP, RT-PCR analyses were performed using two different pairs of NEU4 primers, with a common reverse primer annealing to the C-terminal myc epitope. Conversely, the forward primers, NEU4 long F and NEU4 F, were designed to be complementary either to the N-terminal 12 amino acid sequence or to an internal region of NEU4 template, respectively. Thus, RT-PCR reaction led to amplification bands of different sizes depending on the forward primer and the template (N4L or N4LnoP vector) used, as shown in Figure 4-19 A. Using this strategy, we performed RT-PCR starting from cDNAs of N4L and N4LnoP cell clones. In each reaction, beta-actin was used as housekeeping gene for normalization of cDNA content. Among the cell clones obtained, the higher N4LnoP level was observed in clones number 2 and 5, as demonstrated by RT-PCR performed using the two combination of primers described above (Figure 4-19 B).

In order to better quantify the expression of N4LnoP or N4L in all clones selected, we analyzed NEU4 mRNA levels by real time PCR (Q-PCR). In this case, the primers pairing to an internal region of NEU4 were used, leading to the amplification of both endogenous and exogenous NEU4, both mutated and wild-type forms. The expression of NEU4 gene was normalized to the housekeeping beta-actin mRNA level. As reported in Figure 4-19 C, all cell clones expressed N4LnoP mRNAs, except for clone number 4 expressing a level of NEU4 similar to the mock sample. In particular, clones number 2 and 5 strongly expressed the mutated NEU4 long, in accordance with previous RT-PCR analyses. The results were also expressed as fold changes respect to NEU4 mRNA level of the mock clone,

as shown in Figure 4-19 D. In particular, in four of the six N4LnoP clones analyzed we could observe an approximately 4-fold increase in NEU4 transcript, that it is supposed to correspond to a significant increase in protein level. In particular, N4LnoP clone number 5 showed an increase in mRNA level of about 10-fold compared to mock cells, as observed upon transfection of wild-type NEU4. Thus, on the basis of these Q-PCR results, this N4LnoP cell clone was selected and used for all the subsequent studies.

In order to understand the effect of stable transfection of NEU4 cDNA, either wild-type or mutated, in SK-N-BE cells, we decided to evaluate mRNA levels of the other sialidases. To this purpose, cDNA samples derived from mock, N4L, or N4LnoP SK-N-BE clones were subjected to Q-PCR analysis (Figure 4-20 A). The expression of each gene was normalized to the housekeeping beta-actin mRNA. As shown in Figure 4-20 A, SK-N-BE cell line expressed detectable levels of NEU1, NEU3, and NEU4 sialidases. On the contrary, NEU2 sialidase was not expressed in this neuroblastoma cell line. Among all sialidases detected in SK-N-BE mock cells, NEU1 was found to be expressed to a higher extent, compared to the level of both NEU3 and NEU4 mRNAs. As expected, cell clones stably overexpressing N4L or N4LnoP showed an increase of about 10-fold in NEU4 mRNA levels, due to exogenous transfection as described above. Stable transfection with wild-type form of NEU4 long cDNA caused slight changes in NEU3 mRNA only. On the contrary, upon transfection with NEU4 long mutant we observed not only a significant decrease in NEU1 expression, but also a downregulation of NEU3 mRNA. Figure 4-20 B shows Q-PCR results expressed as fold-change respect to control mock cells. Transfection of SK-N-BE with NEU4 long cDNA caused a reduction of about 1.5-fold in NEU3 transcript. However, in N4LnoP expressing cells, the mRNA levels of both NEU1 and NEU3 were 2-fold downregulated respect to their levels in mock cells. Although reduction of NEU1 and NEU3 transcription is significant, we cannot assume that these mRNA changes observed in N4L or N4LnoP expressing clones cause a significant decrease in NEU1 and NEU3 protein level as well. Further experiments using NEU1 and NEU3 antibodies will be necessary.

4.3.2 The Pro-rich region of NEU4 long promotes alterations of the sialoglycoprotein profile

In order to confirm Q-PCR results described above, protein level analysis of transfected cDNAs was performed. To this purpose, membrane fractions of all SK-N-BE clones were subjected to SDS-PAGE and western blotting. Expressed myc-tagged NEU4 proteins, either wild-type or mutated, were detected using an anti-c-myc antibody. As expected, protein bands with a molecular mass of 56 kDa and 48 kDa were detected in N4L and N4LnoP cell clones, respectively (Figure 4-21 A).

Moreover, to characterize the enzymatic properties of our SK-N-BE cell clones, we decided to evaluate the activity towards the artificial fluorescent 4MU-NeuAc substrate. Sialidase activity assays were performed on membrane fractions obtained from SK-N-BE cells transfected with the vector alone, N4L or N4LnoP cDNA. Results were normalized onto the endogenous NEU4 activity of mock cells, as shown in Figure 4-21 B. In

particular, expression of NEU4 long caused a significant 1.5-fold increase in sialidase activity, compared to the mock sample. On the contrary, no significant increase in sialidase activity was observed following stable expression of NEU4 long mutant lacking the proline-rich region. However, such a low activity in N4LnoP cells might be explained by low expression levels of myc-tagged proteins in the stable clones. In fact, as previously observed in COS-7 cells, the mutant overexpressed in SK-N-BE cells showed a good sialidase activity, although it was 2-fold lower than activity of wild-type NEU4 long (data not shown).

Interestingly, these results suggest that the Pro-rich region of NEU4 is important to modulate the activity of this sialidase in SK-N-BE neuroblastoma cells. Thus, we can hypothesize a role for the Pro-rich loop in the interaction with NEU4 substrates. To check this hypothesis, we examined the modifications induced by N4L or N4LnoP expression to their putative endogenous substrates. In particular, since we supposed an involvement of the proline-rich region in protein-protein interactions, we focused our attention on sialoglycoproteins. The ability of NEU4, either wild-type or mutated, to hydrolyze sialylated glycoproteins was assessed on both membrane and cytosolic proteins separated by SDS-PAGE and transferred onto PVDF membranes. In order to perform sialylation analysis, we used *S. nigra* agglutinin (SNA) and *M. amurensis* agglutinin (MAA) lectins, which are specific for α2-6 and α2-3 sialic acid linkage respectively. As shown in Figure 4-22 A and C, in membrane protein fractions we did not find any significant difference in the glycoproteins pattern among all SK-N-BE clones, with both types of agglutinin lectins. By contrast, pattern changes were observed in cytosolic proteins containing both α2-3- and α2-6-linked sialic acid residues in the cell clone expressing wild-type NEU4 long. On the contrary, N4LnoP expression did not cause any change in sialylation levels in proteins of the same subcellular fraction. In fact, it showed a sialylation pattern similar to that of control mock cells, both with *S. nigra* agglutinin (SNA) and *M. amurensis* agglutinin (MAA) lectins (Figure 4-22).

In particular, in N4L expressing cells glycoproteins with a molecular weight of about 70-75 kDa underwent a marked loss of sialic acid, with both α2-3- and α2-6-linkage, compared with mock and N4LnoP cell clones. Plot profiles obtained through a densitometric analysis of protein bands showed that NEU4 long expression caused a decrease of about 2-fold decrease in sialylation respect to mutant NEU4 long (Figure 4-22 B and D). The loss of activity on glycoproteins observed in mutant NEU4 long indicates that the proline-rich loop may be essential for NEU4 sialidase activity towards these cytosolic glycoproteins. Thus, we can postulate a role for NEU4 Pro-rich region in protein-protein interactions involving its possible glycoprotein substrates.

4.3.3 The Pro-rich loop of NEU4 plays a role in increasing proliferation rate in SK-N-BE cells

With the aim of investigating the effects of NEU4 long overexpression in SK-N-BE cells, we decided to check the growth potential of our stable transfected cell clones. First, the determination of cell growth was done by counting viable cells after staining with trypan blue vital dye. As shown in

Figure 4-23 A, already after 3 days of culture the viable cells of N4L clone were significantly increased as compared to mock cells. By contrast, at all the time points tested, overexpression of N4LnoP did not determine any increase in the proliferation rate of SK-N-BE cells, similar to that observed for the cells transfected with the vector alone.

To confirm the proliferation increase in cells expressing NEU4 long, observed with trypan blue exclusion assay, we tested the proliferation rate of cell clones using MTT viability test. As above, mock, N4L, and N4LnoP cells were grown for 4 days and checked for viability every day. As shown in Figure 4-23 B, results obtained with this method are similar to those obtained with trypan blue staining. In fact, cells expressing NEU4 long showed a significant increase in cellular proliferative activity, as compared to control cells. Increased proliferation of N4L cells was clearly observed at all the time points tested. On the contrary, stable transfection with NEU4 long deleted in the Pro-rich region showed only a slight increase in cell proliferation that was not significantly different from that observed in mock cells, except for early time points.

Overall, proliferation data indicate that only the wild-type form of NEU4 long is able to significantly enhance the proliferative ability of SK-N-BE cells, suggesting that the increase in cell proliferation rate is directly linked to the proline-rich region.

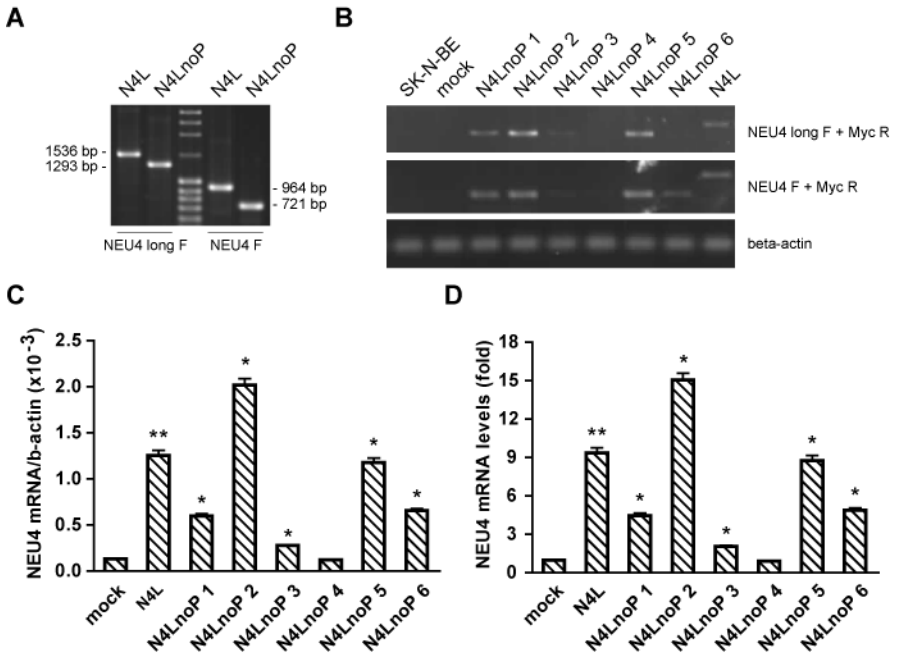

Figure 4-19 Differential expression of both wild-type and mutated NEU4 long in stable transfected SK-N-BE clones. (**A**) Amplification bands obtained by PCR using wild-type or mutated NEU4 long vector as a template, two different forward primers (NEU4 long F and NEU4 F) and a common reverse primer (Myc R), as described in Material and Methods. (**B**) Expression of NEU4 long, either wild-type or mutated, in selected SK-N-BE clones was determined by semi-quantitative RT-PCR using primers described in **A**. Expression of beta-actin was also measured as a reference gene. Gels are representative of three independent experiments. (**C**) Real-time PCR analysis of NEU4 mRNA contents normalized to the housekeeping beta-actin mRNA. Data represent the mean ± SD and are representative of three independent experiments. Significance according to Student's t-test: *p<0.05, **p<0.01 and ***p<0.001. (**D**) Real-time PCR analysis of NEU4 mRNA levels expressed as fold change compared to mock cells. Data represent the mean ± SD of three independent experiments. Significance according to Student's t-test: *p<0.05, **p<0.01 and ***p<0.001.

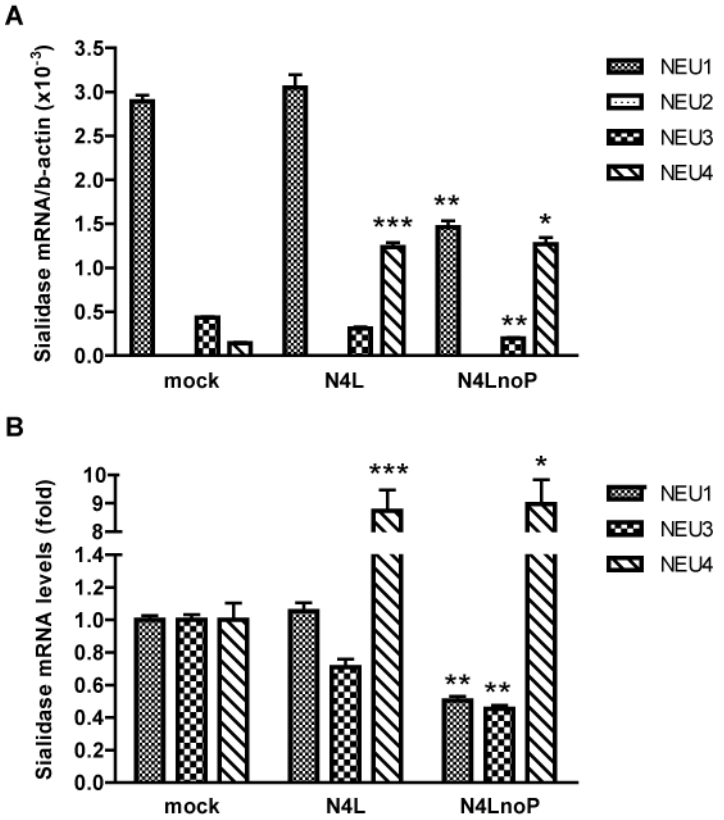

Figure 4-20 Differential expression of human sialidases in SK-N-BE clones. (**A**) Real-time PCR analysis of NEU1, NEU2, NEU3, and NEU4 mRNA contents in mock, N4L, and N4LnoP SK-N-BE cells normalized to the housekeeping beta-actin mRNA. Data represent the mean ± SD of three independent experiments. Significance according to Student's t-test: *p<0.05, **p<0.01 and ***p<0.001. (**B**) Real-time PCR analysis of NEU1, NEU3, and NEU4 mRNA levels expressed as fold change compared to mock cells, in mock, N4L, and N4LnoP SK-N-BE cells. Data represent the mean ± SD of three independent experiments. Significance according to Student's t-test: *p<0.05, **p<0.01 and ***p<0.001.

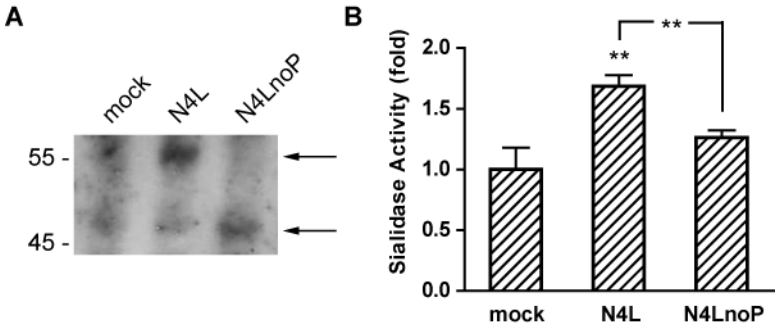

Figure 4-21 Expression of both wild-type and mutated NEU4 long in SK-N-BE clones. (**A**) Western blot analysis was performed in the membrane fractions of SK-N-BE clones (mock, N4L, and N4LnoP), using an anti-c-myc antibody. Blot is representative of three independent experiments. (**B**) Sialidase activity using 4MU-NeuAc as a substrate assayed in the membrane fractions of mock, N4L, and N4LnoP total cell extracts. Values are expressed as fold change compared to mock cells. Data represent the mean ± SD of three independent experiments. Significance according to Student's t-test: *p<0.05, **p<0.01 and ***p<0.001.

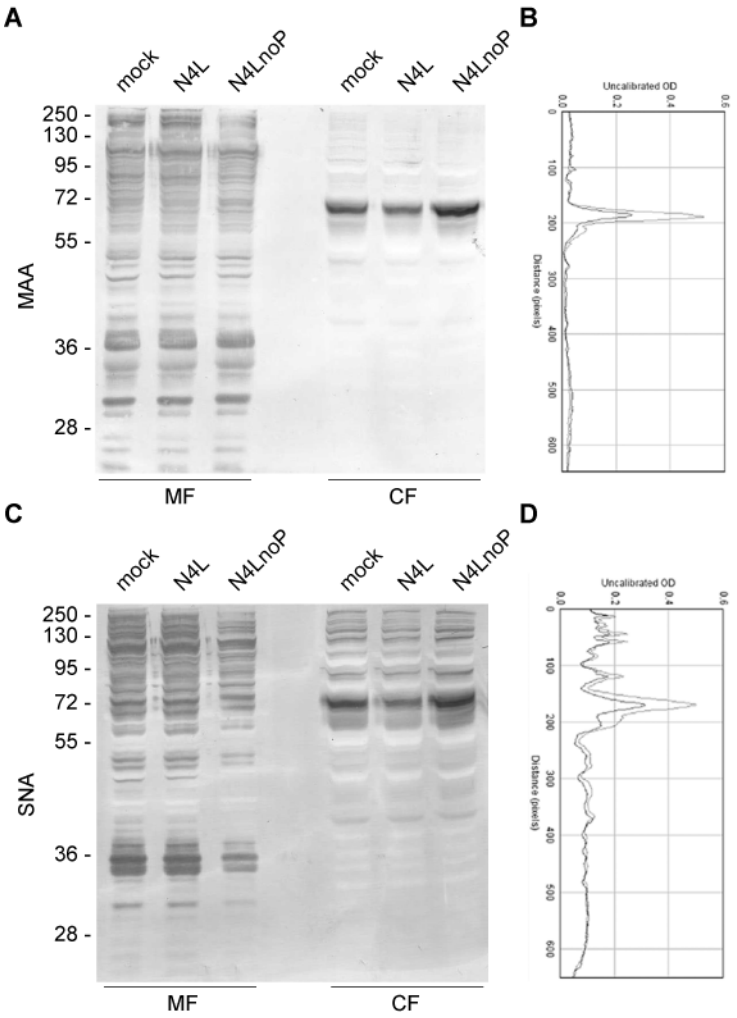

Figure 4-22 Sialoglycoprotein profile of SK-N-BE clones. Membrane and cytosolic proteins from mock, N4L, and N4LnoP SK-N-BE cells were separated by SDS-PAGE and transferred onto PVDF membranes. Sialoglycoproteins were revealed by western blotting employing the *M. amurensis* agglutinin (MAA) lectin (**A**) or *S. nigra* agglutinin (SNA) lectin (**C**). Densitometric profile (N4L in grey and N4LnoP in light grey) of western blots was obtained using *M. amurensis* agglutinin (MAA) lectin (**B**) or *S. nigra* agglutinin (SNA) lectin (**D**), and determined by NIH Image-based software ImageJ. Data are representative of three independent experiments.

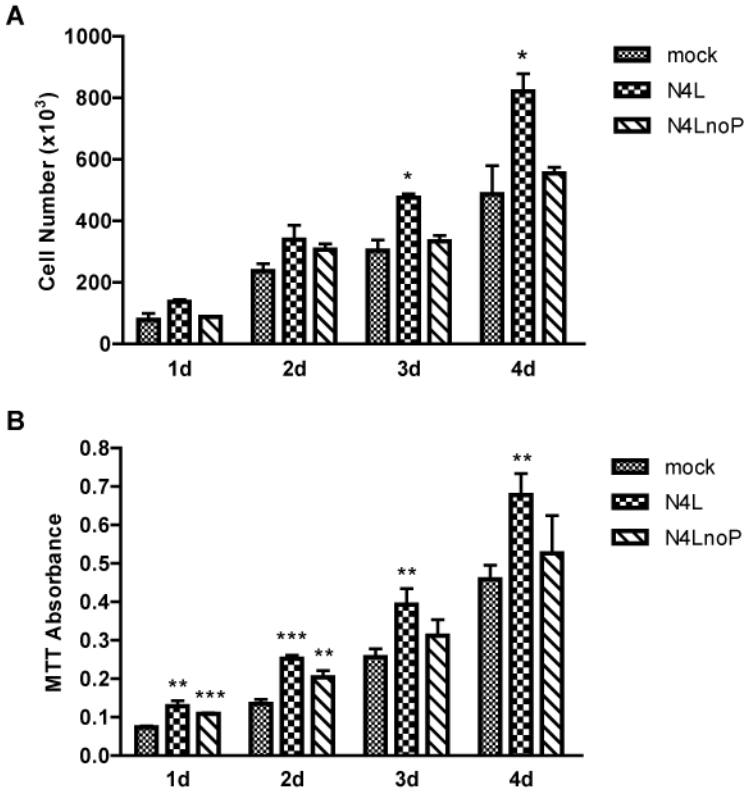

Figure 4-23 Effect of both wild-type and mutated NEU4 long on cell proliferation. (**A**) Trypan blue exclusion assay performed on mock, N4L, and N4LnoP SK-N-BE clones. Cells were cultured for 4 days and at each time point the number of unstained viable cells was measured. Data represent the mean ± SD of three independent experiments. Significance according to Student's t-test: *p<0.05, **p<0.01 and ***p<0.001. (**B**) MTT viability assay performed on mock, N4L, and N4LnoP SK-N-BE clones. Cells were cultured for 4 days and at each time point the absorbance at 570 nm was measured. Data represent the mean ± SD of three independent experiments. Significance according to Student's t-test: *p<0.05, **p<0.01 and ***p<0.001.

4.4 Expression of NEU4 accelerates retinoic acid induced neuronal differentiation

4.4.1 Retinoic acid treatment increases expression of myc-tagged NEU4 proteins, either wild-type or mutated

Subsequently, in order to study the function of NEU4 in SK-N-BE neuroblastoma cell line, we decided to analyze the effect of NEU4 overexpression also under differentiating conditions. To induce cell differentiation, SK-N-BE neuroblastoma cells were treated with retinoic acid (RA) at a concentration of 10 μM in a low serum medium (1% FBS). As controls, SK-N-BE cells were left untreated in a low serum medium. Then, we analyzed NEU4 mRNA level by real time PCR after 1 and 2 days of treatment. The results are expressed as fold changes and normalized to the mRNA content of untreated mock cells at 1 day time point, as shown in Figure 4-24 A. After 1 day of RA treatment, control mock cells showed a 6-fold increase in NEU4 mRNA levels, respect to mRNA content of untreated cells. The increase in NEU4 expression in control mock cells was slightly lower after 2 days of treatment. As expected, untreated N4L and N4LnoP expressing clones showed an higher basal level of NEU4 mRNA, due to stable transfection of the corresponding cDNAs. In both cases, under non-differentiating conditions we observed an about 2-fold increase in NEU4 mRNA levels at 2 days of treatment, which was also observed in control mock cells. Interestingly, a stronger upregulation in NEU4 mRNA level was detected in both N4L and N4LnoP clones upon stimulation with retinoic acid. In particular, in treated NEU4 long expressing cells NEU4 transcription increased up to 135-fold compared to NEU4 mRNA of mock cells. In N4L cell clone, the maximum peak (190-fold) in NEU4 mRNA content was reached after 2 days of RA exposure. In a similar way, SK-N-BE cells expressing the mutated form of NEU4 showed a strong increase in NEU4 mRNA content under differentiating condition, both at 1 and 2 days of treatment. In this case, the highest level (340-fold) was obtained already after 1 day RA stimulation, although a very high level (265-fold) was maintained after 2 days of treatment. To determine the amount of NEU4 transcription induced by retinoic acid, Q-PCR data were normalized to mRNA content of each corresponding untreated cells. As shown in Figure 4-24 B, in both N4L and N4LnoP expressing cells 1 day RA treatment caused an upregulation in NEU4 mRNA levels of about 17- and 64-fold, respectively. In all SK-N-BE clones analyzed, the higher induction in NEU4 transcription in response to RA stimulation was obtained after 1 day of treatment.

On the whole, Q-PCR analysis clearly indicates that in selected SK-N-BE clones both N4L and N4LnoP expression largely increases under differentiating conditions. The strong upregulation of both exogenous N4L and N4LnoP transcripts upon RA treatment was also confirmed by RT-PCR analysis, leading to selective amplification of myc-tagged N4L or N4LnoP cDNAs. As shown in Figure 4-24 C, bands corresponding to myc-tagged NEU4, either wild-type or mutant, were obtained from cDNA extracted from N4L and N4LnoP clones treated with RA for 1 or 2 days. According to the

real time PCR results, the expression of mutated form of NEU4 is induced more than that of the wild-type form.

Furthermore, in order to confirm these results, we decided to analyze also the N4L and N4LnoP protein levels. To this purpose, SK-N-BE cells treated with retinoic acid for 2 days were processed and analyzed through western blotting, using an anti-c-myc antibody. Consistent with our previous Q-PCR and RT-PCR results, western blot analysis revealed that the presence of RA in the culture medium strongly increased expression of both myc-tagged NEU4 proteins in stable transfected SK-N-BE clones (Figure 4-24 D). As expected, no bands corresponding to myc-tagged proteins were observed in the total extract of RA treated mock cells.

Overall, these results demonstrate that retinoic acid treatment increases both the transcription and the expression of NEU4 in SK-N-BE cells. A possible explanation of this induction may be the presence of RA response elements (RARE) in the CMV promoter[333] contained in the vector.

4.4.2 Expression of NEU4 long increased neurite outgrowth induced by retinoic acid treatment

In order to check the ability of SK-N-BE cells to acquire a differentiated neuronal-like phenotype in response to retinoic acid, we measured acetylcholinesterase activity after 2 and 5 days of treatment. As expected, the RA induced differentiation process was associated with a significant increase in acetylcholinesterase activity, from 5 nmol/min mg protein in 2 day treated cells to 9 nmol/min mg protein in 5 day treated cells. (Figure 4-25 A). Moreover, a significant increase in acetylcholinesterase activity was also observed in RA treated cells respect to the corresponding untreated cells at all tested time points. Conversely, the activity level remained unchanged in untreated conditions. In a similar way, acetylcholinesterase assay was subsequently performed on stable SK-N-BE clones, cultured for 2 or 5 days in the presence of retinoic acid. A strong upregulation of acetylcholinesterase activity was observed after 5 days of treatment, as compared to the early time point. No significant differences were observed among SK-N-BE clones at this time of differentiation. In contrast, we could observe a significant increase in acetlycholinesterase levels only in NEU4 long expressing cells after 2 days of treatment (Figure 4-25 B). Interestingly, the activity of this enzyme in SK-N-BE cells expressing NEU4 mutant is similar to control mock cells, suggesting a possible role for NEU4 Pro-rich region in neuronal differentiation.

The induction of neuronal phenotype accomplished by RA treatment was also evaluated as morphological changes in SK-N-BE cells. For detection of neurite outgrowth, both untreated and RA treated cells were fixed and stained with an anti-class III beta-tubulin antibody at 1 or 2 days after RA addition in the culture medium. In differentiated cells, neuron-specific class III beta-tubulin is known to be redistributed in neurons to both axons and dendrites. For all cell clones analyzed, a signal corresponding to beta III tubulin was detected in the cell also in the absence of any treatment, due to partial neuronal nature typical of undifferentiated neuroblastoma cells (Figure 4-26 A). Cells left in low serum medium without RA stimulation maintained a similar undifferentiated morphology at all times analyzed (data

not shown). On the contrary, already after 1 or 2 days of RA exposure we clearly observed neurite formation in all SK-N-BE cells, as expected upon stimulation with retinoic acid (Figure 4-26 A). These morphological changes seemed to be more pronounced in NEU4 long expressing cells, also at early time points. Quantification of the neurite outgrowth process in stable SK-N-BE clones was performed measuring both number and length of neurites (Figure 4-26 B). Retinoic acid induced the same extent of neurite outgrowth both in mock and in N4LnoP cells after 1 day of treatment (Figure 4-26 B). In mock cell clone, the number of cells bearing neurites remained unchanged even after 2 days culture under RA induced differentiating conditions. In contrast, in NEU4 mutant expressing cells we observed an about 2-fold increase in the percentage of cells bearing neurites after 2 days of stimulation. Interestingly, wild-type NEU4 expressing cells showed an increased formation of neurites even in absence of RA treatment. In this case, RA is able to increase the number of cells bearing neurites up to about 65% when it was maintained in the culture medium for 2 days. In these conditions, these cells reached a level of differentiation that was not significantly different to the one observed in NEU4 mutant cell clone at the same time. In addition, the neurite lengths were measured and expressed as fold respect to the cell body diameter. As shown in Figure 4-26 C, exposure of NEU4 long expressing cells to retinoic acid resulted in a significant increase in neurite length already after 1 day of treatment. On the other hand, no or very scant neurite outgrowth was observed in both mock and N4LnoP cells at this time point. However, in NEU4 mutant expressing cells, a significant increase in the neurite length was detected after 2 days of RA stimulation. In particular, at this time point both N4L and N4LnoP expressing cells reached a similar increase in neurite outgrowth. Interestingly, both morphological change analysis and neurite outgrowth quantification were consistent with the level of acetylcholinesterase activity, indicating a role for NEU4 long in retinoic acid induced neuronal differentiation process. In particular, these results suggest that the Pro-rich region of NEU4 may be responsible for the promotion of early differentiation in SK-N-BE cells.

Finally, to further analyze the differentiation process in SK-N-BE cells, we decided to extend the RA induction also up to 7 days. Morphological changes were quantified as above, in both treated and untreated cells. It is well known that deprivation of serum in the culture medium induces a differentiated phenotype in some neuroblastoma cells, even if the process is accomplished in a longer time respect to RA stimulation. Accordingly, control mock cells maintained in low serum conditions started to extend neurites after 7 days even in the absence of retinoic acid (Figure 4-27 A). As shown in Figure 4-27 B and C, both the number and the length of neurites in untreated mock cells remained lower than after RA treatment. Interestingly, the expression of exogenous NEU4, either wild-type or mutated, seemed to reduce the ability of SK-N-BE cells to spontaneously extend neurites after 7 days in a low serum medium, although the percentage of cells bearing neurites did not significantly change. Conversely, neuroblastoma differentiation was clearly visible after 7 days of treatment with retinoic acid for all cell clones analyzed (Figure 4-27 A). Accordingly, we observed a strong increase in both the number of cells bearing neurites and neurite

length, compared with 1% FBS treatment alone (Figure 4-27 B and C). Since we did not find any significant differences among stable transfected SK-N-BE clones, after such a long treatment with RA, we assume a role for NEU4 long mainly in the early phases of neuronal differentiation process.

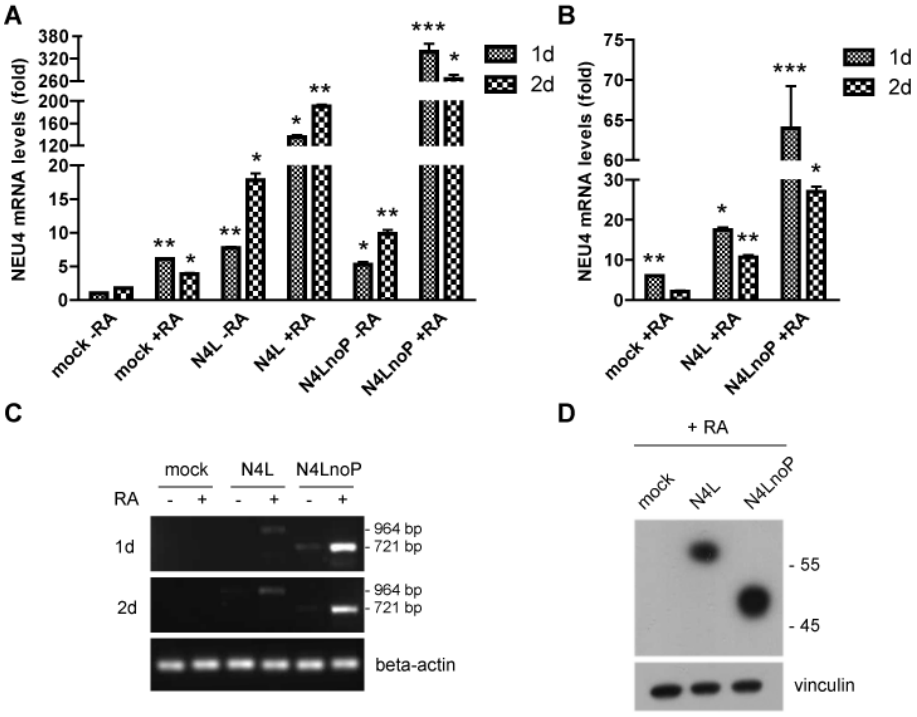

Figure 4-24 Expression of wild-type and mutated NEU4 long in RA treated SK-N-BE clones. (**A**) Real-time PCR analysis of NEU4 mRNA levels in both untreated (-RA) and RA treated (+RA) cells, in comparison with 1 day untreated mock cells. Mock, N4L, and N4LnoP SK-N-BE cells were cultured in the presence or in the absence of 10 μM RA in a low serum medium and analyzed after 1 and 2 days of RA induction. Data represent the mean ± SD of two independent experiments. Significance according to Student's t-test: *p<0.05, **p<0.01 and ***p<0.001. (**B**) Real-time PCR analysis of NEU4 mRNA levels in RA treated cells, in comparison with corresponding untreated (-RA) cells at each time point. Mock, N4L, and N4LnoP SK-N-BE cells were analyzed 1 and 2 days after RA induction. Data represent the mean ± SD of two independent experiments. Significance according to Student's t-test: *p<0.05, **p<0.01 and ***p<0.001. (**C**) Expression of NEU4 long, either wild-type or mutated, in SK-N-BE clones was determined by semi-quantitative RT-PCR using NEU4 F and Myc R primers. Expression of beta-actin was also measured as a reference gene. Gels are representative of two independent experiments. (**D**) Expression of myc-tagged NEU4 proteins in mock, N4L, and N4LnoP SK-N-BE cells after 2 days of RA treatment (10 μM). Western blot analysis was performed in total extract of SK-N-BE clones, using an anti-c-myc antibody. Vinculin was used as loading control. Data are representative of three independent experiments.

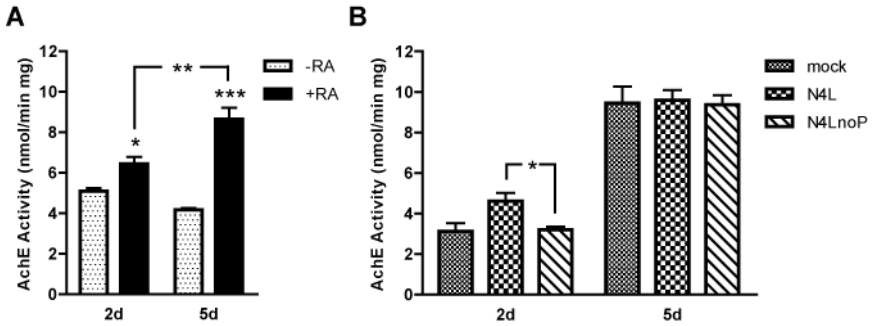

Figure 4-25 Acetylcholinesterase activity during RA induced differentiation. (**A**) AcetyIcholinesterase activity asay performed on SK-N-BE cells cultured in the presence or in the absence of 10 µM RA in a low serum medium for 2 and 5 days. Data represent the mean ± SD of three independent experiments. Significance according to Student's t-test: *p<0.05, **p<0.01 and ***p<0.001. (**B**) Mock, N4L, and N4LnoP SK-N-BE cell clones were cultured in the presence or in the absence of 10 µM RA in a low serum medium for 2 and 5 days. Data represent the mean ± SD of three independent experiments. Significance according to Student's t-test: *p<0.05, **p<0.01 and ***p<0.001.

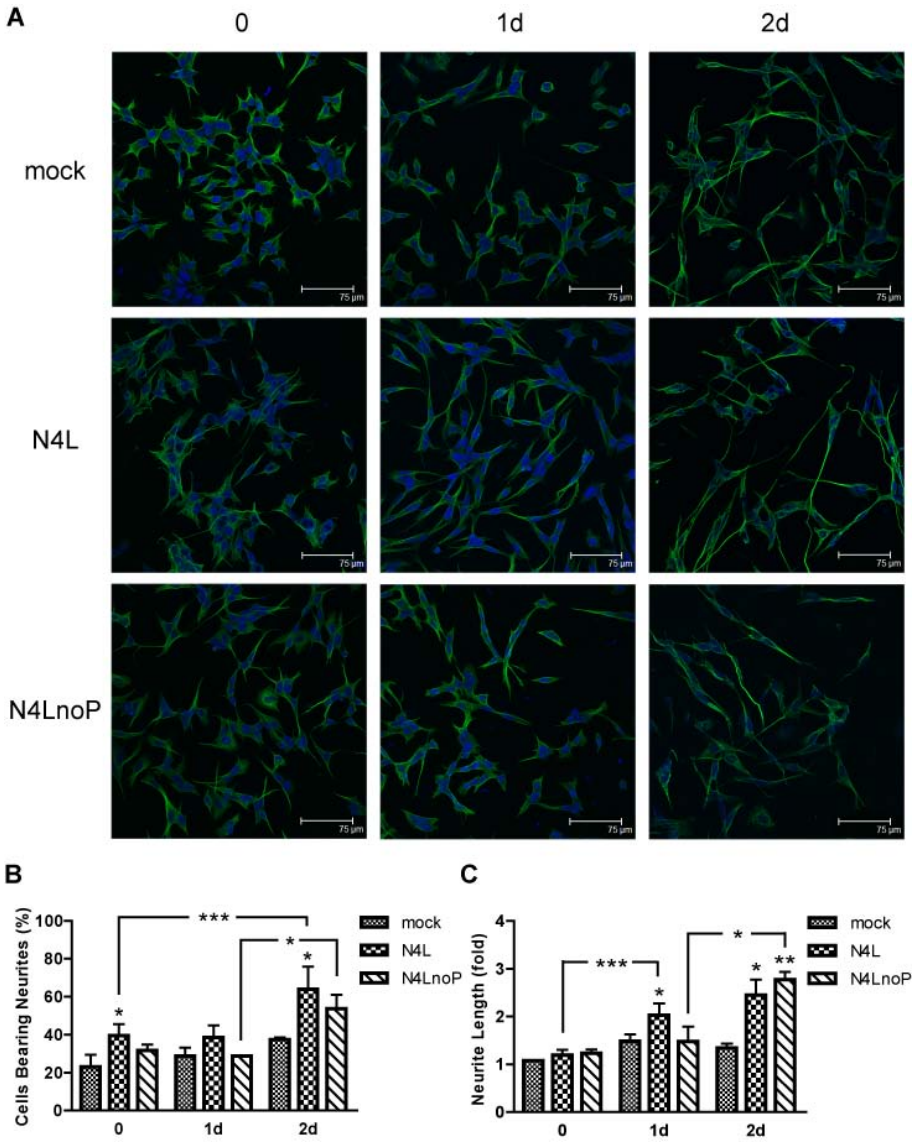

Figure 4-26 Role of NEU4 Pro-rich region in neurite formation during RA induced differentiation. Mock, N4L, and N4LnoP SK-N-BE cell clones were cultured in the presence or in the absence of 10 µM RA in a low serum medium and analyzed after 1 and 2 days of RA induction. (**A**) Immunofluorescence staining of both untreated and RA treated cells with an anti-class III beta-tubulin antibody (green) and the nuclear dye TO-PRO-3 (blue). Data are representative of three independent experiments. (**B**) Quantification of cells bearing neurites number. Analysis was performed using NeuronJ program. Values are expressed as percentage compared to the total cell number. Data represent the mean ± SD of three independent experiments. Significance according to Student's t-test: *p<0.05, **p<0.01

and ***p<0.001. (**C**) Quantification of neurite length. Analysis was performed using NeuronJ program. Values are expressed as fold compared to the cell body diameter. Data represent the mean ± SD of three independent experiments. Significance according to Student's t-test: *p<0.05, **p<0.01 and ***p<0.001.

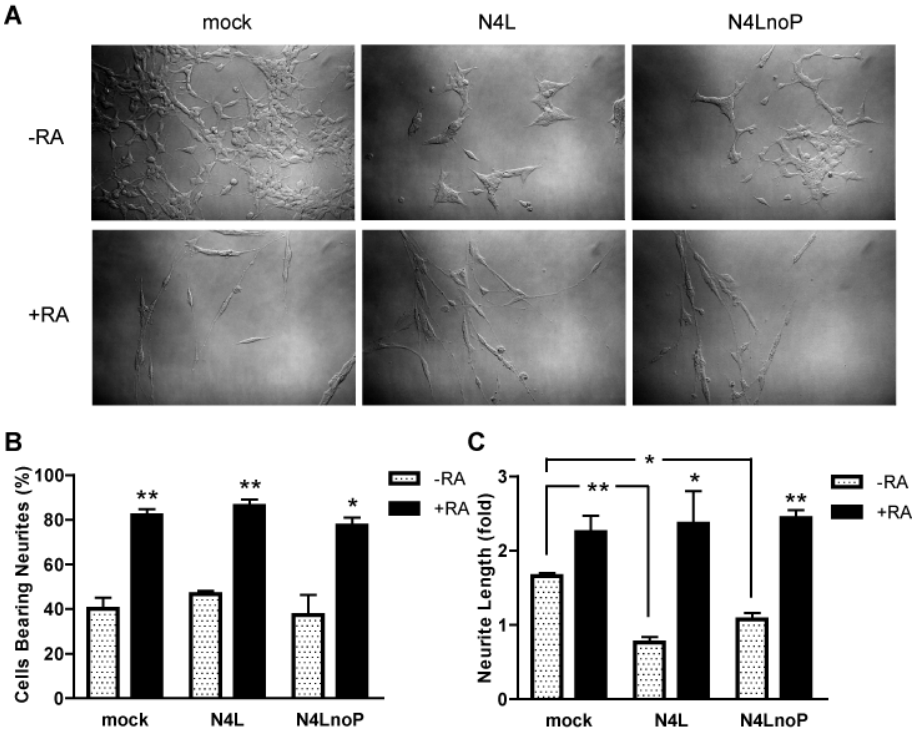

Figure 4-27 Role of NEU4 in neurite formation during RA induced differentiation. Mock, N4L, and N4LnoP SK-N-BE cells were cultured in the presence or in the absence of 10 μM RA in a low serum medium and analyzed after 7 days of RA induction. (**A**) Cells visualized in transmission mode. Images are representative of two independent experiments. (**B**) Quantification of cells bearing neurites number performed using NeuronJ program. Values are expressed as percentage compared to the total cell number. Data represent the mean ± SD of two independent experiments. Significance according to Student's t-test: *p<0.05, **p<0.01 and ***p<0.001. (**C**) Quantification of neurite length performed using NeuronJ program. Values are expressed as fold compared to the cell body diameter. Data represent the mean ± SD of two independent experiments. Significance according to Student's t-test: *p<0.05, **p<0.01 and ***p<0.001.

4.5 The proline-rich region mediates interaction between NEU4 and Akt in SK-N-BE cells

4.5.1 NEU4 Pro-rich sequence possesses consensus motifs for both Akt and Erk1 kinases

In order to check the involvement of NEU4 Pro-rich region in protein-protein interactions, we analyzed NEU4 amino acid sequence with the Scansite Motif Scanner program. Scansite searches for motifs within proteins that are likely to bind to specific protein domains such as 14-3-3, SH2, and SH3, or likely to be phosphorylated by specific protein kinases such as Src and Akt. The scanning of NEU4 amino acid sequence was performed at a high stringency level for all know domains and motifs. Patterns with a high probability of occurrence in NEU4 long protein are listed in Figure 4-28 A. In particular, two types of motifs are present in the proline-rich region of NEU4: the Akt kinase motif and the Erk1 kinase motif, that belong to basophilic serine/threonine kinase and proline-dependent serine/threonine kinase group, respectively (Figure 4-28 B). The consensus RXRXX(S/T) substrate motif for Akt kinase (PNRPRDD**S**WSVGPGS) was predicted to be phosphorylated at S307 along NEU4 sequence, whereas the Erk1 motif (SWSVGPG**S**PLQPPLL) was potentially phosphorylated by Erk1 kinase at S314. As shown in Figure 4-28 B, both Akt and Erk1 motifs are partially superimposed in NEU4 sequence and located in the upstream region of the Pro-rich loop.

4.5.2 Involvement of NEU4 expression in both Erk1/2 MAPK and PI3K/Akt signaling pathways in SK-N-BE cells

Since potential Akt and Erk1 kinase motifs were found in NEU4 proline-rich region, we decided to study both phosphatidylinositol 3-kinase (PI3K)/Akt and mitogen-activated protein kinase (MAPK) signaling pathways in N4L and N4LnoP expressing SK-N-BE cells. The activation of PI3K/Akt and Erk1/2 signaling pathways was detected by western blotting using phosphorylation-specific Akt and Erk1/2 antibodies, respectively. These analyses were carried out in both untreated and RA treated cells. As previously performed, the induction of neuronal differentiation was accomplished by RA administration in a low serum medium. First of all, we investigated whether the reduction of serum in the culture medium was able to affect the activation of these main proliferative pathways in SK-N-BE neuroblastoma cells. For this purpose, SK-N-BE clones were cultured in a low serum medium up to 2 days and analyzed at various time points. As shown in Figure 4-29 A, untreated SK-N-BE cells cultured under normal growth conditions (10% FBS) showed a basal activation of both PI3K and Erk1/2 signaling pathways. In particular, specific phosphorylation of p44 and p42 MAP kinases in Thr_{202}/Tyr_{204} and phosphorylation of Akt kinase in Ser_{473} were observed in SK-N-BE clones at time zero. Moreover, no significant differences in the basal level of both phosphorylated Akt and Erk1/2 kinases were observed among all cell clones. On the other hand, the switching to a serum starved condition (1% FBS) caused a decrease in the activation of both these pathways in a time-dependent manner. Interestingly, the

decrease in Akt phosphorylation upon serum starvation correlated with an upregulation of PTEN level in SK-N-BE cells. The main substrates of PTEN are inositol phospholipids generated by the activation of the phosphoinositide 3-kinase (PI3K)[334]. Thus, the reduction of Akt activation observed in low serum conditions might be partially due to the action of PTEN, a major negative regulator of the PI3K/Akt signaling pathway. In addition, SK-N-BE cells after 1 and 2 days of culture in a low serum medium showed a reduction in Erk1/2 phosphorylation to a similar extent in all clones analyzed.

Subsequently, the activation of signaling pathways was evaluated in SK-N-BE cells upon neuronal differentiation. To this purpose, RA was administrated in a low serum medium for 1 and 2 days (Figure 4-29 B). The activation of the PI3K pathway was observed already after 1 day of treatment, as detected by western blotting using a phosphorylation-specific Akt antibody. Although it was slightly pronounced respect to untreated cells at the early time point, the activation of PI3K/Akt pathway in response to retinoic acid was very clear after 2 days of treatment. At this time point, RA stimulation caused a partial downregulation of PTEN protein level in all SK-N-BE clones, compared to the corresponding untreated cells. Thus, the PTEN decrease might contribute to the strong Akt phosphorylation observed in RA induced differentiated cells. Activation of signaling pathways by retinoic acid appeared not to be restricted to PI3K/Akt. In fact, also the Erk1/2 MAPK pathway was rapidly activated in RA induced neuroblastoma cells, as shown in Figure 4-29 B. Specific phosphorylation of Erk1/2 kinase after RA addition was detected within 1 day, reaching a maximum level when retinoic acid was left in the culture medium for 2 days. Finally, the expression of total Akt and total Erk1/2 did not significantly change in all conditions analyzed.

Overall, these results demonstrate that the expression of NEU4, both wild-type and mutated, does not significantly affect RA induced activation of both PI3K/Akt and Erk1/2 MAPK pathways in SK-N-BE cells. This suggests a downstream localization for NEU4 in these signaling pathways during neuronal differentiation. In particular, NEU4 might be a target for both Akt and Erk1/2 kinases, working as a downstream effector for these signaling pathways.

4.5.3 NEU4 interacts with Akt kinase through its proline-rich region

Since NEU4 could be potentially phosphorylated by both Akt and Erk1/2 kinases in its proline-rich loop, interactions between these kinases and NEU4 long have been investigated using co-immunoprecipitation (co-IP), followed by western blotting detection. To this purpose, SK-N-BE cells were transiently transfected with cDNA coding for NEU4 long, either wild-type or mutated, and cultured under normal growth conditions for 2 days. As a control, SK-N-BE cells were transfected with the empty vector. Immunoblot analysis of the input total extracts showed that myc-tagged NEU4 proteins were everexpressed upon a 2 day post-transfection time. Moreover, both Akt and Erk1/2 kinases were expressed also in a phosphorylated state in all conditions (Figure 4-30 A). Starting from these cell lysates, co-immunoprecipitation of myc-tagged NEU4 proteins, Akt and Erk1/2 was

performed. After immunoprecipitation of wild-type NEU4 long using an anti-myc antibody, we did not find any interaction with Erk1/2 kinase (data not shown). Conversely, when wild-type NEU4 long was immunoprecipitated with anti-myc antibody from whole-cell lysates of N4L expressing cells, Akt was identified by western blotting. Vice versa, immunoprecipitation with anti-Akt antibody allowed the detection of myc-tagged N4L (Figure 4-30 B). On the other hand, no interactions between Akt and the mutated form of NEU4 were observed when the same immunoprecipitations were carried out from N4LnoP expressing cells. Based on this result, we can state that the formation of NEU4-Akt complex occurs through the proline-rich region. Thus, we assume that Akt kinase interacts with NEU4 and likely phosphorylates it on S307 within the Akt consensus motif located in the Pro-rich region, as previously predicted by *in silico* analysis (see above). On the contrary, the absence of an interaction between NEU4 long and Erk1/2 kinase suggests that NEU4 is not a substrate of this kinase, at least in the tested experimental conditions. However, further experiments will be necessary to confirm these hypotheses.

4.5.4 PI3K/Akt signaling pathway is required for RA induced neuronal differentiation in SK-N-BE cells

Our data demonstrated that NEU4 expression is able to improve neuronal differentiation induced by retinoic acid treatment. Since co-immunoprecipitation results indicate NEU4 long as a possible substrate of Akt kinase, we investigated whether Akt activation was able to mediate RA induced neuronal differentiation in SK-N-BE cells. In the following experiments, cells expressing NEU4 long were treated with LY294002, a specific inhibitor of the phosphatidylinositol 3-kinase, before and during RA stimulation in low serum conditions. As a control, PI3K inhibitor was tested in cells cultured in 1% FBS without RA, a condition with a low basal activation of PI3K/Akt pathway, as suggested by previous western blot results (see above). Figure 4-31 A shows that the block of Akt phosphorylation in response to LY294002 occurs in untreated serum-deprived SK-N-BE cells, as well as in cells growing in the presence of retinoic acid. Although in RA treated cells Akt phosphorylation basal levels were higher than in untreated cells, in both cases PI3K inhibitor was able to block Akt phosphorylation in a dose-dependent manner. In particular, pretreatment of SK-N-BE cells with a 50 μM concentration of LY294002 resulted in a total inhibition of Akt phosphorylation. As shown in Figure 4-31 B, pretreatment with LY294002 followed by a 2 day serum deprivation allows the cells to maintain a morphology typical for undifferentiated cells at all the doses tested. Conversely, treatment with the specific PI3K inhibitor LY294002 significantly blocked the neurite outgrowth in RA stimulated SK-N-BE cells. The inhibition of neurite extension was dependent on the concentration of inhibitor used, as also confirmed by quantification analysis of neurite length in treated cells (Figure 4-31 C). Although no significant reduction was observed at the lower dose tested (10 μM), pretreatment with higher concentrations of LY294002 inhibitor was able to prevent RA induced neurite extension in NEU4 long expressing cells. Consistent with the previous results, the maximal block of neurite outgrowth was accomplished using an inhibitor concentration of 50

μM. Treatment of both mock and N4LnoP SK-N-BE cells with LY294002 inhibitor showed cellular responses similar to those described above for NEU4 expressing cells (data not shown). Taken together, these results suggest that the PI3K/Akt signaling pathway is required for neuronal differentiation induced by retinoic acid in SK-N-BE neuroblastoma cells.

A

Site	Domain	Sequence
T18	p38 MAPK	LSMGVPR**T**PSRTVLF
T18	Cdc2 Kinase	LSMGVPR**T**PSRTVLF
Y34	Abl Kinase	RERTGLT**Y**RVPSLLP
V42	Erk D-domain	RVPSLLP**V**PPGPTLL
P43	Cortactin SH3	VPSLLPV**P**PGPTLLA
T72	Protein Kinase A	RLVLRRG**T**LAGGSVR
S96	PKC mu	AALAEHR**S**MNPCPVH
S280	14-3-3 Mode 1	LPAERVA**S**LPETAWG
S307	Akt kinase	PNRPRDD**S**WSVGPGS
S314	Erk1 Kinase	SWSVGPG**S**PLQPPLL
T419	14-3-3 Mode 1	PLDPRSW**T**EPWVIYE
Y459	Src SH2	ESGARTS**Y**DEISFCT
Y459	Fyn SH2	ESGARTS**Y**DEISFCT
Y459	Fgr SH2	ESGARTS**Y**DEISFCT

B

```
1   MMSSAAFPRW LSMGVPRTPS RTVLFERERT GLTYRVPSLL PVPPGPTLLA
51  FVEQRLSPDD SHAHRLVLRR GTLAGGSVRW GALHVLGTAA LAEHRSMNPC
101 PVHDAGTGTV FLFFIAVLGH TPEAVQIATG RNAARLCCVA SRDAGLSWGS
151 ARDLTEEAIG GAVQDWATFA VGPGHGVQLP SGRLLVPAYT YRVDRRECFG
201 KICRTSPHSF AFYSDDHGRT WRCGGLVPNL RSGECQLAAV DGGQAGSFLY
251 CNARSPLGSR VQALSTDEGT SFLPAERVAS LPETAWGCQG SIVGFPAPAP
301 NRPRDDSWSV GPGSPLQPPL LGPGVHEPPE EAAVDPRGGQ VPGGPFSRLQ
351 PRGDGPRQPG PRPGVSGDVG SWTLALPMPF AAPPQSPTWL LYSHPVGRRA
401 RLHMGIRLSQ SPLDPRSWTE PWVIYEGPSG YSDLASIGPA PEGGLVFACL
451 YESGARTSYD EISFCTFSLR EVLENVPASP KPPNLGDKPR GCCWPS
```

Figure 4-28 Recognition motifs for both Akt and Erk1/2 kinases in NEU4 proline-rich region. (**A**) Analysis of NEU4 amino acid sequence with the Scansite Motif Scanner program. Patterns with a high probability of occurrence in NEU4 long protein are listed in table. The motifs located in the proline-rich region are highlighted in yellow. (**B**) Amino acid sequence of NEU4 long. Proline-rich region is highlighted in yellow. Both Akt and Erk1/2 motifs, as well as their putative phosphorylation sites, are highlighted by red and green rectangles, respectively.

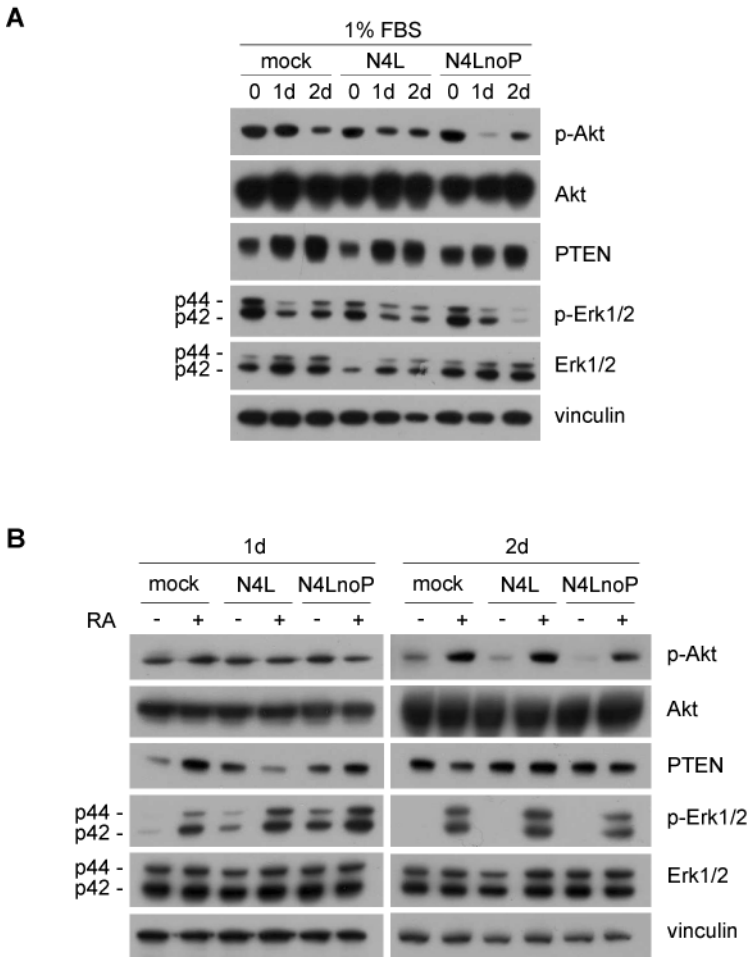

Figure 4-29 Activation of PI3K/Akt and Erk1/2 pathways in RA treated SK-N-BE clones. (**A**) Mock, N4L, and N4LnoP SK-N-BE clones were cultured in a low serum medium for 2 days and western blot analysis of Akt, phospho-Akt, PTEN, Erk1/2, and phospho-Erk1/2 was performed at each time point. Vinculin was used as loading control. Blots are representative of three independent experiments. (**B**) Mock, N4L, and N4LnoP SK-N-BE clones were cultured in the presence or in the absence of 10 μM RA in a low serum medium for 2 days. Western blot analysis of Akt, phospho-Akt, PTEN, Erk1/2, phospho-Erk1/2 was performed at each time point. Vinculin was used as loading control. Blots are representative of three independent experiments.

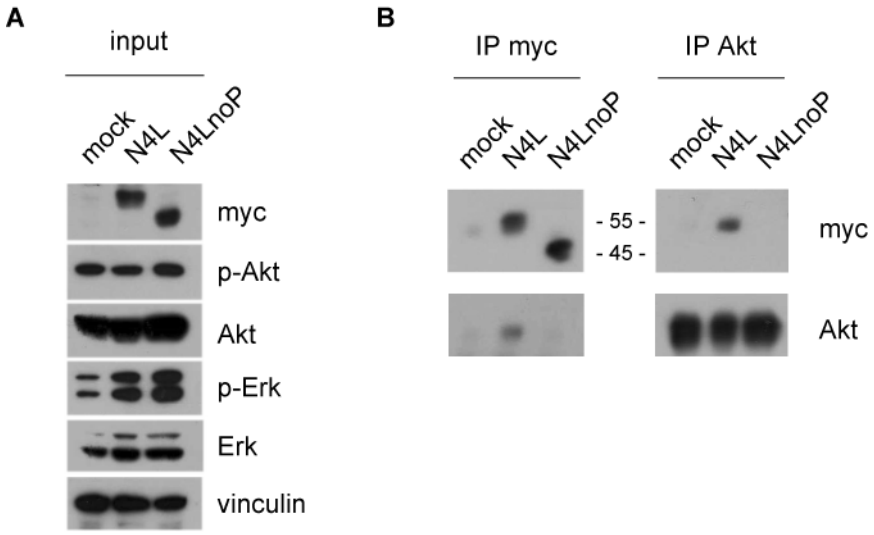

Figure 4-30 NEU4 long interacts with Akt kinase in SK-N-BE cells. Mock, N4L, and N4LnoP SK-N-BE clones were lysed and subjected to co-immunoprecipitation experiments. (**A**) Western blot analysis of myc-tagged NEU4 proteins, Akt, phospho-Akt, Erk1/2, and phospho-Erk1/2 performed onto total protein extracts (input). Vinculin was used as loading control. Blots are representative of three independent experiments. (**B**) Western blot analysis of myc-tagged NEU4 proteins and Akt after immunoprecipitation with either anti-myc or anti-Akt antibodies (left and right panels, respectively). Blots are representative of two independent experiments.

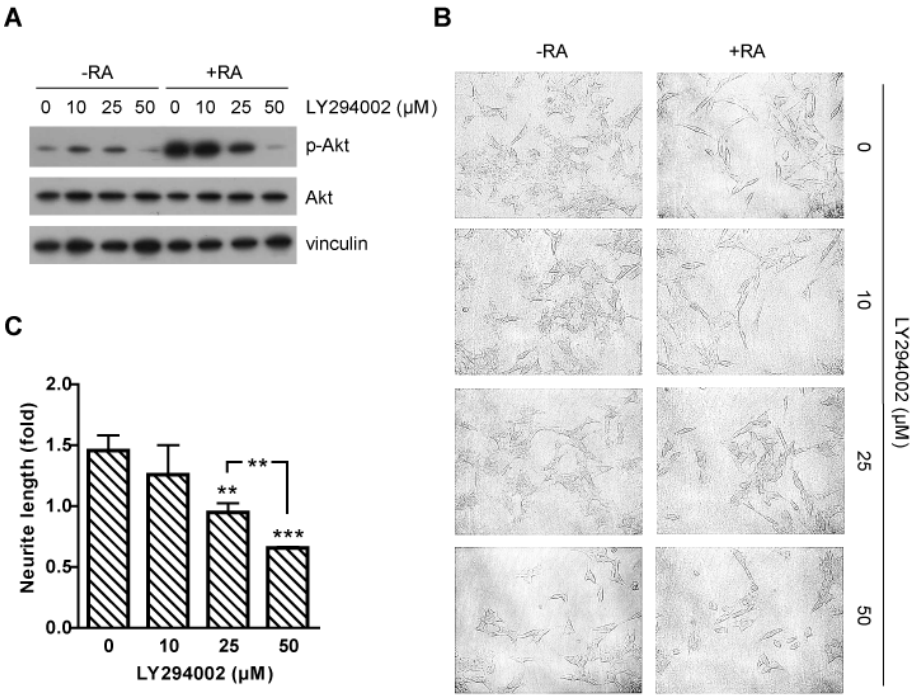

Figure 4-31 Role of PI3K/Akt pathway in RA induced neurite outgrowth. N4L SK-N-BE cells were pretreated with different doses of LY294002 inhibitor, cultured in the presence or in the absence of 10 μM RA in a low serum medium for 2 days. (**A**) Western blot analysis of Akt and phospho-Akt performed onto N4L SK-N-BE protein cell extracts. Vinculin was used as loading control. Blots are representative of three independent experiments. (**B**) Cells visualized in transmission mode. Images are representative of two independent experiments. (**C**) Quantification of neurite length. Analysis was performed using NeuronJ program. Values are expressed as fold compared to the cell body diameter. Data represent the mean ± SD of two independent experiments. Significance according to Student's t-test: *p<0.05, **p<0.01 and ***p<0.001.

5. Discussion

Although all human sialidases share a high primary structure similarity (ranging from 42 to 70%), some (the lysosomal sialidase NEU1 complex and the cytosolic sialidase NEU2) are soluble, while others (NEU4 and NEU3) are membrane associated. However, no apparent structural differences account for their different subcellular localizations and solubilities. No membrane binding motives, such as GPI anchors, miristoylation or palmitoylation sites, are evident from NEU4 and NEU3 primary structure analysis. Moreover, a potential transmembrane domain, predicted in NEU4 primary structure by TMPred and TMHMM servers, cannot fit into the β-propeller three dimensional structure, yielded by homology modeling[205], performed using NEU2 crystallographic structure as a template[204]. Therefore the mechanism through which sialidases NEU3 and NEU4 are anchored to the membrane is still unclear. Moreover, as regards human sialidase NEU4, different and contrasting subcellular localizations had been previously suggested for its two forms[194,280,296]. Yamaguchi and colleagues demonstrated mitochondrial localization for NEU4 long and intracellular membrane localization for NEU4 short[280]. On the other hand Seyrantepe and colleagues[296] claimed that NEU4 is a lysosomal enzyme and recently showed that mice deficient in NEU4 exhibit abnormal ganglioside catabolism and lysosomal storage[304].

First of all, in this work we investigated membrane anchoring and subcellular localization of NEU4 long and NEU4 short to gain some insight into the function of this sialidase. In the first part of this work, we showed that NEU4 is recovered in the aqueous phase after treatment with Triton X-114, clearly ruling out the possibility of it being an integral membrane protein. This result indirectly confirms that NEU4 folds into a β-propeller structure, which disrupts the only possible transmembrane domain. Moreover, NEU4 complete solubilization in the aqueous phase also rules out any possible interaction with membrane lipids, in accordance with primary structure analysis, suggesting that membrane proteins are involved in NEU4 anchoring. This is well in agreement with NEU4 partial solubilization obtained after alkaline treatment with sodium carbonate, that shows it to be, at least in part, an extrinsic membrane protein, as already demonstrated for NEU3[332]. However its interaction with the membrane is apparently stronger than that of the EEA1 protein, which is readily and completely solubilized by carbonate treatment. Reversible cross-linking experiments with PFA strongly suggests that both forms of NEU4 are associated to the membrane through protein-protein interactions. All these experiments yielded the same results for both NEU4 long and NEU4 short, showing that both forms interact with the membrane through the same anchoring mechanism, despite their different subcellular localizations. This in turn shows that the first 12 amino acids, which are lacking in NEU4 short, are not responsible for membrane anchoring, although they might play a role in cellular sorting.

The confocal microscopy studies on COS-7 cells transiently transfected with NEU4 long, reported in this work, clearly show that this enzyme colocalizes with mitochondria, as previously suggested by Yamaguchi and coworkers[280]. Instead, in contrast to what reported by Seyrantepe[296,304], no appreciable colocalization with lysosomes was observed in our experiments. Using the same experimental approach, we

also showed that NEU4 short is found in intracellular membranes, but does not colocalize with lysosomes. A diffused intracellular fluorescence, well superimposing with Calnexin fluorescence strongly suggests that this enzyme is located in the endoplasmic reticulum, as previously suggested[194,280]. The different subcellular localizations of the two forms is not restricted to a single cellular type, as shown by experiments performed on HeLa cells. Moreover, it not due to an overexpression artifact, as demonstrated by the fact that it does not change when both NEU4 forms are coexpressed, nor when each of them is expressed at lower levels, after shorter post-transfection times.

Our subcellular fractionation experiments confirmed confocal microscopy results: NEU4 long was found in the mitochondrial fraction, while NEU4 short was also detected in the microsomal fraction. None of these two sialidases was detected in the cytosolic fraction. In order to remove contaminating lysosomes as much as possible, western blot analyses were performed also on isolated mitochondria. The employed fractionation procedure has been reported to yield a highly purified mitochondrial fraction and control enzyme activity assays showed the presence of only 3.5% contaminant lysosomes. Thus, although NEU4 long presence in lysosomes cannot be completely ruled out, its predominant localization is beyond any doubt in mitochondria. Our data are therefore in contrast with those of Seyrantepe and coworkers[296,304], who found a predominantly lysosomal localization of NEU4, although their activity assays performed after subfractionation of transfected COS-7 cells, also showed a partial colocalization with mitochondrial and microsomal fractions. These authors also found[304] that transfection of cells from sialidosis patients with NEU4 expression vectors decreased lysosomal storage, yielding a 25% of transfected cells with normal lysosomes. Moreover they observed a reduction of only 30% of sialidase activity in lysosomes from NEU4 knock-out mice and a lysosomal storage phenotype only in lungs and spleen cells. Although these results may suggest a role for NEU4 in lysosomal degradation of gangliosides, the lack of NEU1 involvement in the process cannot be easily explained. In fact, NEU4 knock-out mice still possess a functional lysosomal NEU1 complex, actively degrading sialic acid containing compounds. Moreover, mutations of this enzyme only have been demonstrated beyond any reasonable doubt to cause sialidosis[335].

Although our data suggest that NEU4 short is found primarily in the endoplasmic reticulum, a partial localization at mitochondrial level is also apparent; the first 12 amino acids seem likely to be involved in mitochondrial sorting, as already suggested[280], although a longer tract, approximately 30 amino acids from the N-terminus, would be required for this localization, according to the prediction programs MITOPROT and signalP. On the whole it can be said that the sequence required for correct mitochondrial localization is probably longer than 12 amino acids, but the lack of the first 12 amino acids is sufficient to impair translocation to mitochondria.

When isolated mitochondria were subfractionated into a soluble fraction and a membranes containing pellet, NEU4 long was found only in the pellet, confirming its features of membrane bound enzyme. In addition, the application of a further mitochondrial subfractionation provided evidence

for NEU4 long localization in the outer mitochondrial membrane, since this enzyme behaves exactly as the outer mitochondrial membrane protein TOMM22. When mitoplasts were prepared through osmotic shock removing the outer mitochondrial membrane, both proteins were partially solubilized. Moreover, the fact that they were degraded by trypsin to the same extent in whole mitochondria and in mitoplasts suggests that NEU4 long accessibility to this protease does not change upon removal of the outer mitochondrial membrane. Moreover, incomplete degradation of NEU4 long by trypsin both in whole mitochondria and in mitoplasts suggests that this sialidase is tightly anchored to the membrane and only partially accessible to trypsin. On the contrary, a different behaviour was observed in the case of the inner mitochondrial membrane protein TIMM50, which, unlike fully accessible TOMM22, was found to be susceptible to trypsin treatment only when the outer membrane was partially destroyed after osmotic shock. Our data are consistent with those obtained by Yamaguchi and coworkers[280] in Percoll density gradient centrifugation, where about 70% of sialidase activity was recovered in the outer mitochondrial membrane fraction. Cross-linking experiments, performed in this work, will be the basis for a future purification and characterization of membrane proteins interacting with NEU4.

Another issue still to be elucidated is the role of NEU4 sialidase. It seems likely that this lowly expressed, selectively located sialidase must have a specific function, different from the main degradative role of the lysosomal sialidase NEU1. A role in signal transduction connected to apoptosis has been already proposed for mitochondrial NEU4[280], as a modulator of GD3 levels. Moreover, Hasegawa and coworkers[314] demonstrated that in SH-SY5Y cell lines NEU4 long expression was decreased prior to catechol metabolites induced apoptosis, that ganglioside GD3 was targeted to mitochondria during apoptosis and that an inhibitor of glucosylceramide synthase was able to partially recover cell viability. The same research group found that NEU4 expression was markedly decreased in colon cancer, while it was subjected to an early upregulation during apoptosis[292]. More recently, a paper has been published showing that mouse NEU4 plays an important regulatory role in neurite formation, likely through desialylation of glycoproteins[319]. All these data suggest a role in apoptosis for NEU4, through its action on GD3 ganglioside, as well as in neurite differentiation. Still obscure is the role of the short form of this enzyme. An accurate characterization of the kinetic properties of both the short and the long form of the enzyme, when affecting gangliosidic and glycoproteic substrates, will be necessary to shed light on this point.

The multiple alignment of human sialidases amino acid sequences, performed with T-COFFEE, showed the presence in NEU4 of a long stretch of 81 amino acids, which is unique to NEU4, having no counterpart in all other human sialidases. This sequence, already reported by Monti et al.[190,194], is also present in the mouse NEU4 sequence[293]. Since conserved sequences are found on both sides of this ‘insertion’ and since NEU4 folds into an active enzyme, it is likely that this sequence represents a separate domain that provides unique functionality to this sialidase, as previously proposed by Comelli et al.[293]. Moreover, this sequence was identified as a proline-rich region by Scansite program. Interestingly, this region is totally

absent in soluble NEU2 sialidase, in which it is substituted by a much shorter loop, containing few prolines. Since proline-rich sequences are well known to play an important role in the assembly of multi-protein complexes[324], we hypothesized an involvement of NEU4 Pro-rich region in the protein-protein interactions involved in the mechanism of anchorage to the membranes of human NEU4.

In order to verify this hypothesis, we produced two NEU4 mutants (NEU4 long and NEU4 short, called N4LnoP and N4SnoP, respectively) lacking the proline-rich region, which was replaced by the corresponding 11 amino acids sequence of cytosolic sialidase NEU2. NEU4 structure prediction obtained by using HHpred server, selecting the homologous sequences with known structure and the highest scores as template, confirmed that NEU4 fold as a six-blade β-propeller, as previously reported[205]. The Pro-rich region of NEU4 is located in a loop connecting two β-strands of adjacent blades (β-strand D of blade IV and β-strand A of blade V), in a way that it does not affect the overall structure of the enzyme. For this reason the structure prediction of the mutated form of NEU4 suggested a six blades β-propeller structure typical to sialidases. In order to test the function of this loop in subcellular distribution and membrane anchoring, both NEU4 long and NEU4 short mutants were transiently expressed in COS-7 cells as fusion proteins carrying a C-terminal c-myc epitope. As confirmed by sialidase activity assays on 4MU-NeuAc, the deletion of the Pro-rich region does not affect the enzymatic properties of NEU4, although a reduction of specific sialidase activity compared to the wild-type forms was observed. As already performed for the wild-type forms of NEU4 sialidase, subcellular localization of NEU4 mutants was investigated both through confocal microscopy and subcellular fractionation. Immunofluorescence results showed that NEU4 long mutant colocalizes with the mitochondrial marker cyt c, as already observed for the corresponding wild-type enzyme. N4SnoP also showed an intracellular distribution similar to the corresponding wild-type protein, exhibiting only a partial colocalization with mitochondria. Conversely, no colocalization with the lysosomal compartment was detected, as previously observed for the corresponding wild-type enzymes. Moreover, consistent with results obtained with its wild-type form, subfractionation of mitochondria purified from COS-7 cells transfected with N4LnoP confirmed the association of this enzyme to mitochondrial membranes. In addition, sodium carbonate treatment showed that NEU4 long is strongly associated to membranes even in the absence of its Pro-rich region. Overall, these findings indicate that the Pro-rich region is not directly responsible neither for the subcellular localization of both NEU4 long and NEU4 short forms nor for their ancorage to the membranes.

Finally, in order to establish whether the proline-rich region of NEU4 could be important in the formation of protein-protein interactions, we carried out cross-linking experiments also with N4LnoP. Cross-linking with PFA results in the assembly of a multi-protein complex with a molecular mass similar to that observed for the wild-type form. Since Pro-rich deletion does not significantly affect neither the association of NEU4 to the membranes nor the formation of protein-protein interactions, we assume that the Pro-rich loop is not directly responsible for the interaction of NEU4 with the proteins

putatively involved in its anchorage to membranes. However, further experiments will be necessary to clarify whether the lack of the Pro-rich region impairs the interaction of NEU4 with some specific proteins, likely not responsible for NEU4 membrane association. To this purpose, purification of NEU4 containing complexes and their subsequent analysis by mass spectrometry will be made, following the method reported by Vasilescu and coworkers[327].

Proline residues are frequently found in the loop regions of proteins thus being accessible for protein interactions. Moreover, proline-rich sequences are binding motifs for a variety of protein modules[336]. Due to the rapid but non-specific nature of the interaction, proline-rich regions are often involved in complex protein association phenomena[324,337]. Protein-protein interactions occurring via the recognition of short peptide sequences by modular interaction domains play a central role in the assembly of signaling protein complexes. Thus, protein interaction domains participate in and regulate almost all essential cellular functions, including cell growth, differentiation, motility, polarity and apoptosis[338,339]. Therefore, we hypothesized an involvement of NEU4 Pro-rich region in interaction with signaling pathway components.

Studies performed in collaboration with Department of Medical Chemistry, Biochemistry and Biotechnology (L.I.T.A.) of the University of Milano evaluated the effect of NEU4 long expression in human neuroblastoma SK-N-BE cells. SK-N-BE cell line is known to possess the amplication of MYCN (v-myc myelocytomatosis viral related oncogene, neuroblastoma derived), an oncogene involved in rapid progression, poor prognosis and therapy resistance of tumours, including neuroblastoma[340,341]. Similarly, we produced stable SK-N-BE clones transfected with cDNA coding for the mutated form of NEU4 long (N4LnoP). N4LnoP clones were isolated and analyzed for mRNA content by both RT-PCR and real time PCR, in order to select the cell clone expressing a N4LnoP mRNA level similar to that of the wild-type (N4L). Stable transfection was also confirmed by western blot analysis.

In order to understand the effect of stable transfection of NEU4 cDNA, either wild-type or mutated, in SK-N-BE cells, we checked mRNA levels of the other sialidases as well. Results indicated that transfection of wild-type NEU4 long cDNA caused slight changes in NEU3 mRNA only. Conversely, transfection with NEU4 long mutant was associated with a downregulation of both NEU1 and NEU3 transcript levels. However, although reduction of NEU1 and NEU3 transcription is significant, we cannot assume that these mRNA changes observed in N4L or N4LnoP expressing clones cause a significant decrease in NEU1 and NEU3 protein level as well. Further experiments using NEU1 and NEU3 antibodies will be necessary to validate these data.

With regard to the enzymatic properties of NEU4 long mutant, a reduced specific enzymatic activity compared to the wild-type form was observed in SK-N-BE cell line, as already found in COS-7. Thus, the proline-rich region may be involved in interactions between NEU4 sialidase and its endogenous substrates.

Since we postulate an involvement of the proline-rich region in protein-protein interactions, we focused our attention on sialoglycoproteins. When the ability of NEU4, either wild-type or mutated, to hydrolyze sialylated glycoproteins was tested, many variations were observed in cytosolic proteins containing both α2-3- and α2-6-linked sialic acid residues only in NEU4 long expressing cells. On the contrary, transfection of NEU4 mutant did not cause any change in sialylation levels of glycoproteins, showing a sialylation pattern similar to that of control mock cells. In particular, in NEU4 expressing cells glycoproteins with a molecular weight of about 70-75 kDa underwent a marked loss of sialic acid, with both α2-3- and α2-6-linkage, indicating that the proline-rich loop may be essential for NEU4 sialidase activity towards these specific cytosolic glycoproteins. Therefore, we suggest a role for NEU4 Pro-rich region in recognition and/or binding of some glycoprotein substrates.

Subsequently, the proliferation rate of our stable transfected SK-N-BE clones was tested with different approaches. Results indicated that NEU4 long expression results in a significant increase in proliferation as compared to mock cells, as demonstrated by both trypan blue exclusion and MTT viability assays. On the other hand, the expression of N4LnoP did not confer any growth advantage in SK-N-BE cells, suggesting that the increase in cell proliferation rate is directly mediated by NEU4 proline-rich region. Thus, we suggest that the improved proliferation ability of NEU4 expressing cells is related to the enhanced activity of NEU4 towards its glycoprotein substrates.

To further analyze the function of NEU4 and its proline-rich region in SK-N-BE cells, we decided to undertake the following experiments under undifferentiated as well as differentiated conditions. To induce cell differentiation, SK-N-BE neuroblastoma cells were treated with retinoic acid (RA) in a low serum medium (1% FBS). As a control, SK-N-BE cells were left untreated in the same serum-starved conditions. First of all, we analyzed NEU4 mRNA level by real time PCR after 1 and 2 days of RA treatment. Although a slight increase in NEU4 mRNA level was observed in untreated cells during their grown in a low serum medium, the stronger upregulation in NEU4 mRNA level was detected in both N4L and N4LnoP clones upon stimulation with retinoic acid. In all SK-N-BE clones, the higher level induction in NEU4 transcription in response to RA stimulation was already obtained after 1 day of treatment. The enhanced level of both exogenous N4L and N4LnoP transcripts upon RA treatment was also confirmed by RT-PCR analysis, leading to selective amplification of myc-tagged N4L or N4LnoP cDNAs. These findings were also confirmed by western blotting results, indicating an enhanced level of myc-tagged NEU4 protein, either wild-type or mutated, in cell lysates of SK-N-BE clones grown under RA stimulation. In our system, retinoic acid is able to increase both the transcription and the expression of exogenous NEU4 in SK-N-BE cells. A possible explanation of this induction may be the presence of RA response elements (RARE) in the CMV promoter contained in the vector used for expression in mammalian cells, as reported by Nakamura et al.[333].

In order to check the ability of SK-N-BE cells to acquire a differentiated neuronal-like phenotype in response to retinoic acid, we measured acetylcholinesterase activity, a well-known neuronal marker, after

2 and 5 days of treatment. As expected, a significant increase in acetylcholinesterase activity was observed in RA treated cells, confirming that SK-N-BE cells undergo a neuronal differentiation under our differentiating conditions. Conversely, the level of this neuronal marker remained unchanged in untreated conditions. In particular, in the presence of retinoic acid in the culture medium, a strong upregulation of acetylcholinesterase activity was observed in all SK-N-BE clones after 5 days of treatment. Interestingly, only the expression of wild-type NEU4 long was able to significantly increase acetlycholinesterase activity already after 2 days of treatment. On the other hand, the activity of this enzyme in cells expressing NEU4 mutant is similar to control mock cells, suggesting a role for NEU4 Pro-rich region in the early phases of neuronal differentiation process. Furthermore, the induction of neuronal phenotype accomplished by RA treatment was also evaluated as morphological changes in SK-N-BE cells. Both morphological analysis and neurite outgrowth quantification are consistent with acetylcholinesterase activity data, indicating a role for NEU4 long and its Pro-rich region in the early phases of retinoic acid induced neuronal differentiation process. In the absence of RA, SK-N-BE cells maintained an undifferentiated morphology at all time points analyzed, while neurite formation was clearly observed in all SK-N-BE cells already after 1 or 2 days of RA exposure. These morphological changes occurring during RA induced neuronal differentiation are more pronounced in NEU4 long expressing cells, also at early time points. Interestingly, wild-type NEU4 long expressing cells showed an increased formation of neurites even in the absence of RA treatment. However, a 2 day treatment with RA is able to significantly increases the percentage of cells bearing neurites. In addition, NEU4 long expressing cells increased their neurite length already after 1 day of treatment with RA. On the contrary, no or very scant neurite outgrowth was observed in both mock and N4LnoP cells at this time point. However, in NEU4 mutant expressing cells, a significant increase in the neurite length, as well as in the number of cells bearing neurites, was detected after 2 day RA stimulation. On the whole, our results suggest that NEU4 long is involved in retinoic acid induced neuronal differentiation process. Moreover, the proline-rich region of NEU4 seems to be crucial to promote a significant acceleration in neuronal differentiation in RA treated SK-N-BE cells.

Interestingly, the extent of RA induction up to 7 days demonstrates that serum deprivation in the culture medium by itself is able to induce a differentiated phenotype in SK-N-BE cells, as already shown in other neuroblastoma cells[342,343]. However, the differentiation process is accomplished in a longer time respect to RA stimulation. Interestingly, expression of exogenous NEU4, either wild-type or mutated, seems to partially impair the ability of SK-N-BE cells to spontaneously extend neurites after 7 day culture in serum-starved conditions, although the percentage of cells bearing neurites does not significantly change. Conversely, treated SK-N-BE clones maintained a differentiated phenotype also after 7 days, showing a strong increase in both the number of cells bearing neurites and neurite length. Since no significant differences among stable transfected cells were observed after such a long RA treatment, we assume a role for NEU4 long mainly in the early phases of neuronal differentiation process.

Our findings seem to be in contrast with data previously reported for the short murine NEU4 enzyme. In fact, Shiozaki and coworkers[319] observed that murine NEU4, unlike NEU3[254], was downregulated during retinoic acid induced differentiation in Neuro2a cells. Overexpression of the short form of murine NEU4 (NEU4b) resulted in suppression of neurite formation, whereas its knock-down showed an acceleration. Thus, they claimed that mouse NEU4b plays an important role in the negative regulation of neurite formation, probably through desialylation of glycoproteins. These contradictory results may be explained by the different enzymatic and molecular properties of human and murine NEU4 sialidases, as previously reported by the same authors[280].

Analyzing NEU4 aminoacid sequence with Scansite program, consensus motifs for both Akt and Erk1/2 kinases were identified in NEU4 proline-rich region. Since these kinases have been reported to be involved in neuronal differentiation process[344,345], we decided to study both phosphatidylinositol 3-kinase (PI3K)/Akt and mitogen-activated protein kinase (MAPK) signaling pathways in N4L and N4LnoP expressing SK-N-BE cells. Experiments were carried out on cells cultured in serum starved conditions, in the presence or in the absence of retinoic acid. Untreated SK-N-BE cells cultured under normal growth conditions showed a basal activation of both PI3K and Erk1/2 signaling pathways. This is well in accordance with other studies, that indicate PI3K/Akt and Erk1/2 MAP kinases as the main proliferative pathways in SK-N-BE neuroblastoma cells (brodeur 2003). However, no significant differences in the basal level of Akt and Erk1/2 phosphorylation were observed among our cell clones. On the other hand, the switching to a serum starved condition caused a decrease in Akt activation in a time-dependent manner in SK-N-BE cells, along with an upregulation of PTEN protein level, a major negative regulator of the PI3K/Akt signaling pathway. Accordingly, the main substrates of PTEN are inositol phospholipids generated by the activation of the phosphoinositide 3-kinase (PI3K)[334]. Thus, the lower Akt activation observed in low serum conditions might be partially explained by the corresponding increase in PTEN. In addition, SK-N-BE cells cultured in a low serum medium exhibit a reduction in Erk1/2 phosphorylation. Interestingly, expression of NEU4, either wild-type or mutated, does not affect the response of these cells to serum withdrawal, with regard to the activation state of both PI3/Akt and Erk1/2 MAPK pathways. Conversely, RA stimulation significantly and rapidly activates both these pathways, as already reported for SH-SY5Y neuroblastoma cell line[344,345]. Our results show that the expression of NEU4, both wild-type and mutated, does not significantly affect RA induced activation of both PI3K/Akt and Erk1/2 pathways in SK-N-BE cells. Thus, we propose a downstream localization of NEU4 in these signaling pathways during neuronal differentiation.

In order to ascertain if NEU4 is a target for Akt or Erk1/2 kinases, working as a downstream effector for both Akt and Erk1/2 pathways, interactions between these kinases and NEU4 long were investigated by co-immunoprecipitation (co-IP) experiments. To this purpose, SK-N-BE cells were transiently transfected with cDNA coding for NEU4 long, either wild-type or mutated, and cultured under normal growth conditions for 2 days. No

interactions were found between wild-type NEU4 long and Erk1/2 kinase in these experimental conditions, indicating that NEU4 is not a substrate of this kinase. Conversely, when exogenously expressed wild-type NEU4 long was immunoprecipitated with an anti-myc antibody from whole-cell lysates of N4L expressing cells, Akt was identified by western blotting and vice versa. Interestingly, the deletion of the proline-rich region totally impairs the formation of NEU4-Akt complex, demonstrating that the interaction between these two proteins is mediated by proline-rich loop. We assume that Akt kinase interacts with NEU4 recognizing the Akt consensus motif located in the Pro-rich region, as previously suggested by *in silico* analysis. As a target of Akt kinase, NEU4 may be potentially phosphorylated in S307 site.

Finally, since our data demonstrate that NEU4 improves RA induced neuronal differentiation, as well as that NEU4 interacts with Akt kinase, we tested whether Akt activation mediates RA induced neuronal differentiation in SK-N-BE cells, as previously suggested for other neuroblastoma cell lines[344,345]. Our results demonstrate that activation of the PI3K/Akt signaling pathway by RA is required for neuronal differentiation of SK-N-BE cell line, since inhibition of PI3K by its specific inhibitor LY294002 resulted in a significant block of neurite outgrowth. Along with a reduction in Akt phosphorylation, a dose-dependent impairment of neurite extention was observed in RA treated cells upon pretreatment with LY294002 inhibitor. Since co-immunoprecipitation results indicate NEU4 as a possible substrate of Akt kinase, further experiments will be performed to check whether inhibition of Akt is able to prevent the interaction between Akt kinase and NEU4.

In conclusion, our data demonstrate that NEU4 long expression is able to improve neuronal differentiation induced by retinoic acid in SK-N-BE neuroblastoma cell line. This effect is clearly detectable in the early phases of the differentiation process, and it is mediated by the proline-rich region. Moreover, we found that the activation of PI3K/Akt signaling pathway upon RA stimulation is essential for neurite extension in SK-N-BE cells. Finally, NEU4 long seems to be a target of Akt kinase, interacting with Akt through the recognition motif located in its proline-rich loop. On the whole, these findings indicate NEU4 as a downstream effector in PI3K/Akt signaling pathway required for RA induced differentiation in SK-N-BE neuroblastoma cell line.

6. References

1. Schauer, R., Kamerling, J.P., J. Montreuil, J.F.G.V. & Schachter, H. Chapter 11 Chemistry, Biochemistry and Biology of Sialic Acids. in *New Comprehensive Biochemistry*, Vol. Volume 29, Part 2 243-402 (Elsevier, 1997).
2. Varki, A. Diversity in the sialic acids. *Glycobiology* **2**, 25-40 (1992).
3. Schauer, R. Biosynthesis and function of N- and O-substituted sialic acids. *Glycobiology* **1**, 449-452 (1991).
4. Traving, C. & Schauer, R. Structure, function and metabolism of sialic acids. *Cell Mol Life Sci* **54**, 1330-1349 (1998).
5. Schauer, R. Chemistry, metabolism, and biological functions of sialic acids. *Adv Carbohydr Chem Biochem* **40**, 131-234 (1982).
6. Roth, J., Kempf, A., Reuter, G., Schauer, R. & Gehring, W.J. Occurrence of sialic acids in Drosophila melanogaster. *Science* **256**, 673-675 (1992).
7. Reuter, G. & Gabius, H.J. Sialic acids structure-analysis-metabolism-occurrence-recognition. *Biol Chem Hoppe Seyler* **377**, 325-342 (1996).
8. Corfield, A.P., Wember, M., Schauer, R. & Rott, R. The specificity of viral sialidases. The use of oligosaccharide substrates to probe enzymic characteristics and strain-specific differences. *Eur J Biochem* **124**, 521-525 (1982).
9. Bourbouze, R., Akiki, C., Chardonloriaux, I. & Percheron, F. THE EVIDENCE FOR NEURAMINIC ACID-DERIVATIVES IN VEGETABLE GLYCOPROTEINS. *Carbohydrate Research* **106**, 21-30 (1982).
10. Barry, G.T. Detection of sialic acid in various Escherichia coli strains and in other species of bacteria. *Nature* **183**, 117-118 (1959).
11. Yamasaki, R., Griffiss, J.M., Quinn, K.P. & Mandrell, R.E. Neuraminic acid is alpha 2-->3 linked in the lipooligosaccharide of Neisseria meningitidis serogroup B strain 6275. *J Bacteriol* **175**, 4565-4568 (1993).
12. Kelm, S. & Schauer, R. Sialic acids in molecular and cellular interactions. *Int Rev Cytol* **175**, 137-240 (1997).
13. Schauer, R. Sialic acids and their role as biological masks. *Trends in Biochemical Sciences* **10**, 357-360 (1985).
14. Miyagi, T.*, et al.* Human sialidase as a cancer marker. *Proteomics* **8**, 3303-3311 (2008).
15. Muller, H.E. [Pathogenetic significance of microbial neuraminidases]. *Dtsch Med Wochenschr* **99**, 1933-1940 (1974).
16. Bratosin, D.*, et al.* Flow cytofluorimetric analysis of young and senescent human erythrocytes probed with lectins. Evidence that sialic acids control their life span. *Glycoconj J* **12**, 258-267 (1995).
17. Wieser, R.J., Baumann, C.E. & Oesch, F. Cell-contact mediated modulation of the sialylation of contactinhibin. *Glycoconj J* **12**, 672-679 (1995).
18. Jarvis, G.A. Recognition and control of neisserial infection by antibody and complement. *Trends Microbiol* **3**, 198-201 (1995).
19. Crocker, P.R.*, et al.* Siglecs: a family of sialic-acid binding lectins. *Glycobiology* **8**, v (1998).
20. Kelm, S., Schauer, R. & Crocker, P.R. The Sialoadhesins--a family of sialic acid-dependent cellular recognition molecules within the immunoglobulin superfamily. *Glycoconj J* **13**, 913-926 (1996).
21. Klein, A. & Roussel, P. O-acetylation of sialic acids. *Biochimie* **80**, 49-57 (1998).
22. Taylor, G. Sialidases: structures, biological significance and therapeutic potential. *Curr Opin Struct Biol* **6**, 830-837 (1996).
23. Frasch, A.C. Trans-sialidase, SAPA amino acid repeats and the relationship between Trypanosoma cruzi and the mammalian host. *Parasitology* **108 Suppl**, S37-44 (1994).

24. Schauer, R., Reuter, G., Muhlpfordt, H., Andrade, A.F. & Pereira, M.E. The occurrence of N-acetyl- and N-glycoloylneuraminic acid in Trypanosoma cruzi. *Hoppe Seylers Z Physiol Chem* **364**, 1053-1057 (1983).
25. Previato, J.O., Andrade, A.F., Pessolani, M.C. & Mendonca-Previato, L. Incorporation of sialic acid into Trypanosoma cruzi macromolecules. A proposal for a new metabolic route. *Mol Biochem Parasitol* **16**, 85-96 (1985).
26. Schenkman, S., Jiang, M.S., Hart, G.W. & Nussenzweig, V. A novel cell surface trans-sialidase of Trypanosoma cruzi generates a stage-specific epitope required for invasion of mammalian cells. *Cell* **65**, 1117-1125 (1991).
27. Engstler, M. & Schauer, R. Sialidases from African trypanosomes. *Parasitol Today* **9**, 222-225 (1993).
28. Engstler, M., Schauer, R. & Brun, R. Distribution of developmentally regulated trans-sialidases in the Kinetoplastida and characterization of a shed trans-sialidase activity from procyclic Trypanosoma congolense. *Acta Trop* **59**, 117-129 (1995).
29. Engstler, M., Reuter, G. & Schauer, R. The developmentally regulated trans-sialidase from Trypanosoma brucei sialylates the procyclic acidic repetitive protein. *Mol Biochem Parasitol* **61**, 1-13 (1993).
30. Smith, L.E. & Eichinger, D. Directed mutagenesis of the Trypanosoma cruzi trans-sialidase enzyme identifies two domains involved in its sialyltransferase activity. *Glycobiology* **7**, 445-451 (1997).
31. Chou, M.Y., Li, S.C. & Li, Y.T. Cloning and expression of sialidase L, a NeuAcalpha2-->3Gal-specific sialidase from the leech, Macrobdella decora. *J Biol Chem* **271**, 19219-19224 (1996).
32. Terada, T.*, et al.* Catalysis by a new sialidase, deaminoneuraminic acid residue-cleaving enzyme (KDNase Sm), initially forms a less stable alpha-anomer of 3-deoxy-D-glycero-D-galacto-nonulosonic acid and is strongly inhibited by the transition state analogue, 2-deoxy-2, 3-didehydro-D-glycero-D-galacto-2-nonulopyranosonic acid, but not by 2-deoxy-2,3-didehydro-N-acetylneuraminic acid. *J Biol Chem* **272**, 5452-5456 (1997).
33. Pavlova, N.V.*, et al.* 2-Keto-3-deoxy-D-glycero-D-galacto-nononic acid (KDN)- and N-acetylneuraminic acid-cleaving sialidase (KDN-sialidase) and KDN-cleaving hydrolase (KDNase) from the hepatopancreas of oyster, Crassostrea virginica. *J Biol Chem* **274**, 31974-31980 (1999).
34. Burmeister, W.P., Henrissat, B., Bosso, C., Cusack, S. & Ruigrok, R.W. Influenza B virus neuraminidase can synthesize its own inhibitor. *Structure* **1**, 19-26 (1993).
35. Burnet, F.M., Mc, C.J. & Stone, J.D. Modification of human red cells by virus action; the receptor gradient for virus action in human red cells. *Br J Exp Pathol* **27**, 228-236 (1946).
36. Heimer, R. & Meyer, K. STUDIES ON SIALIC ACID OF SUBMAXILLARY MUCOID. *Proc Natl Acad Sci U S A* **42**, 728-734 (1956).
37. Gottschalk, A. Neuraminidase: the specific enzyme of influenza virus and Vibrio cholerae. *Biochim Biophys Acta* **23**, 645-646 (1957).
38. Cabezas, J.A., Reglero, A. & Calvo, P. Glycosidases. (Fucosidases, galactosidases, glucosidases, hexosaminidases and glucuronidase from some molluscs and vertebrates, and neuraminidase from virus). *Int J Biochem* **15**, 243-259 (1983).
39. Gubareva, L.V., Kaiser, L. & Hayden, F.G. Influenza virus neuraminidase inhibitors. *Lancet* **355**, 827-835 (2000).
40. Roggentin, P., Schauer, R., Hoyer, L.L. & Vimr, E.R. The sialidase superfamily and its spread by horizontal gene transfer. *Mol Microbiol* **9**, 915-921 (1993).
41. Roggentin, P.*, et al.* Conserved sequences in bacterial and viral sialidases. *Glycoconj J* **6**, 349-353 (1989).

42. Crennell, S.J., Garman, E.F., Laver, W.G., Vimr, E.R. & Taylor, G.L. Crystal structure of a bacterial sialidase (from Salmonella typhimurium LT2) shows the same fold as an influenza virus neuraminidase. *Proc Natl Acad Sci U S A* **90**, 9852-9856 (1993).
43. Chong, A.K., Pegg, M.S., Taylor, N.R. & von Itzstein, M. Evidence for a sialosyl cation transition-state complex in the reaction of sialidase from influenza virus. *Eur J Biochem* **207**, 335-343 (1992).
44. Crennell, S.J.*, et al.* The structures of Salmonella typhimurium LT2 neuraminidase and its complexes with three inhibitors at high resolution. *J Mol Biol* **259**, 264-280 (1996).
45. Achyuthan, K.E. & Achyuthan, A.M. Comparative enzymology, biochemistry and pathophysiology of human exo-alpha-sialidases (neuraminidases). *Comp Biochem Physiol B Biochem Mol Biol* **129**, 29-64 (2001).
46. Comb, D.G., Watson, D.R. & Roseman, S. The sialic acids. IX. Isolation of cytidine 5'-monophospho-N-acetylneuraminic acid from Escherichia coli K-235. *J Biol Chem* **241**, 5637-5642 (1966).
47. Huang, R.T. & Orlich, M. Substrate specificities of the neuraminidases of Newcastle disease and fowl plague viruses. *Hoppe Seylers Z Physiol Chem* **353**, 318-322 (1972).
48. Yu, R.K. & Ledeen, R. Configuration of the ketosidic bond of sialic acid. *J Biol Chem* **244**, 1306-1313 (1969).
49. Holzer, C.T.*, et al.* Inhibition of sialidases from viral, bacterial and mammalian sources by analogues of 2-deoxy-2,3-didehydro-N-acetylneuraminic acid modified at the C-4 position. *Glycoconj J* **10**, 40-44 (1993).
50. Brossmer, R. & Nebelin, E. Synthesis of N-formyl- and N-succinyl-D-neuraminic acid on the specificity of neuraminidase. *FEBS Lett* **4**, 335-336 (1969).
51. von Itzstein, M. & Colman, P. Design and synthesis of carbohydrate-based inhibitors of protein-carbohydrate interactions. *Curr Opin Struct Biol* **6**, 703-709 (1996).
52. Wade, R.C. 'Flu' and structure-based drug design. *Structure* **5**, 1139-1145 (1997).
53. Fingerhut, R., van der Horst, G.T., Verheijen, F.W. & Conzelmann, E. Degradation of gangliosides by the lysosomal sialidase requires an activator protein. *Eur J Biochem* **208**, 623-629 (1992).
54. von Itzstein, M.*, et al.* Rational design of potent sialidase-based inhibitors of influenza virus replication. *Nature* **363**, 418-423 (1993).
55. Roggentin, T., Kleineidam, R.G., Schauer, R. & Roggentin, P. Effects of site-specific mutations on the enzymatic properties of a sialidase from Clostridium perfringens. *Glycoconj J* **9**, 235-240 (1992).
56. Taylor, N.R. & von Itzstein, M. Molecular modeling studies on ligand binding to sialidase from influenza virus and the mechanism of catalysis. *J Med Chem* **37**, 616-624 (1994).
57. Hayden, F.G.*, et al.* Efficacy and safety of the neuraminidase inhibitor zanamivir in the treatment of influenzavirus infections. GG167 Influenza Study Group. *N Engl J Med* **337**, 874-880 (1997).
58. Hoyer, L.L., Hamilton, A.C., Steenbergen, S.M. & Vimr, E.R. Cloning, sequencing and distribution of the Salmonella typhimurium LT2 sialidase gene, nanH, provides evidence for interspecies gene transfer. *Mol Microbiol* **6**, 873-884 (1992).
59. Roggentin, P., Rothe, B., Lottspeich, F. & Schauer, R. Cloning and sequencing of a Clostridium perfringens sialidase gene. *FEBS Lett* **238**, 31-34 (1988).

60. Rothe, B., Roggentin, P., Frank, R., Blocker, H. & Schauer, R. Cloning, sequencing and expression of a sialidase gene from Clostridium sordellii G12. *J Gen Microbiol* **135**, 3087-3096 (1989).
61. Traving, C., Schauer, R. & Roggentin, P. Gene structure of the 'large' sialidase isoenzyme from Clostridium perfringens A99 and its relationship with other clostridial nanH proteins. *Glycoconj J* **11**, 141-151 (1994).
62. Rothe, B., Roggentin, P. & Schauer, R. The sialidase gene from Clostridium septicum: cloning, sequencing, expression in Escherichia coli and identification of conserved sequences in sialidases and other proteins. *Mol Gen Genet* **226**, 190-197 (1991).
63. Traving, C., Roggentin, P. & Schauer, R. Cloning, sequencing and expression of the acylneuraminate lyase gene from Clostridium perfringens A99. *Glycoconj J* **14**, 821-830 (1997).
64. Roseman, S. The synthesis of complex carbohydrates by multiglycosyltransferase systems and their potential function in intercellular adhesion. *Chem Phys Lipids* **5**, 270-297 (1970).
65. Keenan, T.W., Morre, D.J. & Basu, S. Ganglioside biosynthesis. Concentration of glycosphingolipid glycosyltransferases in Golgi apparatus from rat liver. *J Biol Chem* **249**, 310-315 (1974).
66. Caputto, R., Maccioni, H.J. & Arce, A. Biosynthesis of brain gangliosides. *Mol Cell Biochem* **4**, 97-106 (1974).
67. van Echten, G. & Sandhoff, K. Ganglioside metabolism. Enzymology, Topology, and regulation. *J Biol Chem* **268**, 5341-5344 (1993).
68. van Echten-Deckert, G., Giannis, A., Schwarz, A., Futerman, A.H. & Sandhoff, K. 1-Methylthiodihydroceramide, a novel analog of dihydroceramide, stimulates sphinganine degradation resulting in decreased de novo sphingolipid biosynthesis. *J Biol Chem* **273**, 1184-1191 (1998).
69. Gillard, B.K., Clement, R.G. & Marcus, D.M. Variations among cell lines in the synthesis of sphingolipids in de novo and recycling pathways. *Glycobiology* **8**, 885-890 (1998).
70. Yu, R.K. Development regulation of ganglioside metabolism. *Prog Brain Res* **101**, 31-44 (1994).
71. Kotani, M., Kawashima, I., Ozawa, H., Terashima, T. & Tai, T. Differential distribution of major gangliosides in rat central nervous system detected by specific monoclonal antibodies. *Glycobiology* **3**, 137-146 (1993).
72. Hakomori, S. & Igarashi, Y. Functional role of glycosphingolipids in cell recognition and signaling. *J Biochem* **118**, 1091-1103 (1995).
73. Zhou, Q., Hakomori, S., Kitamura, K. & Igarashi, Y. GM3 directly inhibits tyrosine phosphorylation and de-N-acetyl-GM3 directly enhances serine phosphorylation of epidermal growth factor receptor, independently of receptor-receptor interaction. *J Biol Chem* **269**, 1959-1965 (1994).
74. Mutoh, T., Tokuda, A., Miyadai, T., Hamaguchi, M. & Fujiki, N. Ganglioside GM1 binds to the Trk protein and regulates receptor function. *Proc Natl Acad Sci U S A* **92**, 5087-5091 (1995).
75. Nojiri, H., Stroud, M. & Hakomori, S. A specific type of ganglioside as a modulator of insulin-dependent cell growth and insulin receptor tyrosine kinase activity. Possible association of ganglioside-induced inhibition of insulin receptor function and monocytic differentiation induction in HL-60 cells. *J Biol Chem* **266**, 4531-4537 (1991).
76. Brown, D.A. & London, E. Structure and function of sphingolipid- and cholesterol-rich membrane rafts. *J Biol Chem* **275**, 17221-17224 (2000).
77. Riboni, L., Viani, P., Bassi, R., Prinetti, A. & Tettamanti, G. The role of sphingolipids in the process of signal transduction. *Prog Lipid Res* **36**, 153-195 (1997).

78. Mukhopadhyay, G., Doherty, P., Walsh, F.S., Crocker, P.R. & Filbin, M.T. A novel role for myelin-associated glycoprotein as an inhibitor of axonal regeneration. *Neuron* **13**, 757-767 (1994).
79. Chen, M.S.*, et al.* Nogo-A is a myelin-associated neurite outgrowth inhibitor and an antigen for monoclonal antibody IN-1. *Nature* **403**, 434-439 (2000).
80. Prinjha, R.*, et al.* Inhibitor of neurite outgrowth in humans. *Nature* **403**, 383-384 (2000).
81. Crocker, P.R. & Varki, A. Siglecs in the immune system. *Immunology* **103**, 137-145 (2001).
82. Schachner, M. & Bartsch, U. Multiple functions of the myelin-associated glycoprotein MAG (siglec-4a) in formation and maintenance of myelin. *Glia* **29**, 154-165 (2000).
83. Crocker, P.R.*, et al.* Sialoadhesin and related cellular recognition molecules of the immunoglobulin superfamily. *Biochem Soc Trans* **24**, 150-156 (1996).
84. Sheikh, K.A.*, et al.* Mice lacking complex gangliosides develop Wallerian degeneration and myelination defects. *Proc Natl Acad Sci U S A* **96**, 7532-7537 (1999).
85. Hakomori, S. Glycosphingolipids in cellular interaction, differentiation, and oncogenesis. *Annu Rev Biochem* **50**, 733-764 (1981).
86. Hakomori, S. Cancer-associated glycosphingolipid antigens: their structure, organization, and function. *Acta Anat (Basel)* **161**, 79-90 (1998).
87. Hakomori, S., Handa, K., Iwabuchi, K., Yamamura, S. & Prinetti, A. New insights in glycosphingolipid function: "glycosignaling domain," a cell surface assembly of glycosphingolipids with signal transducer molecules,involved in cell adhesion coupled with signaling. *Glycobiology* **8**, xi-xix (1998).
88. Okada, Y., Mugnai, G., Bremer, E.G. & Hakomori, S. Glycosphingolipids in detergent-insoluble substrate attachment matrix (DISAM) prepared from substrate attachment material (SAM). Their possible role in regulating cell adhesion. *Exp Cell Res* **155**, 448-456 (1984).
89. Brown, D.A. & London, E. Structure of detergent-resistant membrane domains: does phase separation occur in biological membranes? *Biochem Biophys Res Commun* **240**, 1-7 (1997).
90. Hakomori, S. Glycosylation defining cancer malignancy: new wine in an old bottle. *Proc Natl Acad Sci U S A* **99**, 10231-10233 (2002).
91. Hakomori, S. Glycosynapses: microdomains controlling carbohydrate-dependent cell adhesion and signaling. *An Acad Bras Cienc* **76**, 553-572 (2004).
92. Bremer, E.G., Hakomori, S., Bowen-Pope, D.F., Raines, E. & Ross, R. Ganglioside-mediated modulation of cell growth, growth factor binding, and receptor phosphorylation. *J Biol Chem* **259**, 6818-6825 (1984).
93. Bremer, E.G., Schlessinger, J. & Hakomori, S. Ganglioside-mediated modulation of cell growth. Specific effects of GM3 on tyrosine phosphorylation of the epidermal growth factor receptor. *J Biol Chem* **261**, 2434-2440 (1986).
94. Stefanova, I., Horejsi, V., Ansotegui, I.J., Knapp, W. & Stockinger, H. GPI-anchored cell-surface molecules complexed to protein tyrosine kinases. *Science* **254**, 1016-1019 (1991).
95. Krummel, M.F. & Davis, M.M. Dynamics of the immunological synapse: finding, establishing and solidifying a connection. *Curr Opin Immunol* **14**, 66-74 (2002).
96. Regina Todeschini, A. & Hakomori, S.I. Functional role of glycosphingolipids and gangliosides in control of cell adhesion, motility, and growth, through glycosynaptic microdomains. *Biochim Biophys Acta* **1780**, 421-433 (2008).

97. Mintz, B. & Illmensee, K. Normal genetically mosaic mice produced from malignant teratocarcinoma cells. *Proc Natl Acad Sci U S A* **72**, 3585-3589 (1975).
98. Illmensee, K. & Mintz, B. Totipotency and normal differentiation of single teratocarcinoma cells cloned by injection into blastocysts. *Proc Natl Acad Sci U S A* **73**, 549-553 (1976).
99. Wang, F.*, et al.* Phenotypic reversion or death of cancer cells by altering signaling pathways in three-dimensional contexts. *J Natl Cancer Inst* **94**, 1494-1503 (2002).
100. Kenny, P.A. & Bissell, M.J. Tumor reversion: correction of malignant behavior by microenvironmental cues. *Int J Cancer* **107**, 688-695 (2003).
101. Iwabuchi, K.*, et al.* Reconstitution of membranes simulating "glycosignaling domain" and their susceptibility to lyso-GM3. *J Biol Chem* **275**, 15174-15181 (2000).
102. Saito, M. & Yu, R.K. Possible role of myelin-associated neuraminidase in membrane adhesion. *J Neurosci Res* **36**, 127-132 (1993).
103. Godoy, V.G., Dallas, M.M., Russo, T.A. & Malamy, M.H. A role for Bacteroides fragilis neuraminidase in bacterial growth in two model systems. *Infect Immun* **61**, 4415-4426 (1993).
104. Nees, S., Veh, R.W. & Schauer, R. Purification and characterization of neuraminidase from Clostridium perfringens. *Hoppe Seylers Z Physiol Chem* **356**, 1027-1042 (1975).
105. Corfield, T. Bacterial sialidases--roles in pathogenicity and nutrition. *Glycobiology* **2**, 509-521 (1992).
106. Muller, H.E. [Neuraminidase as a pathogenicity factor in microbial infections (proceedings)]. *Zentralbl Bakteriol Orig A* **235**, 106-110 (1976).
107. Galen, J.E.*, et al.* Role of Vibrio cholerae neuraminidase in the function of cholera toxin. *Infect Immun* **60**, 406-415 (1992).
108. Crennell, S., Garman, E., Laver, G., Vimr, E. & Taylor, G. Crystal structure of Vibrio cholerae neuraminidase reveals dual lectin-like domains in addition to the catalytic domain. *Structure* **2**, 535-544 (1994).
109. Gaskell, A., Crennell, S. & Taylor, G. The three domains of a bacterial sialidase: a beta-propeller, an immunoglobulin module and a galactose-binding jelly-roll. *Structure* **3**, 1197-1205 (1995).
110. Roggentin, P., Kleineidam, R.G. & Schauer, R. Diversity in the properties of two sialidase isoenzymes produced by Clostridium perfringens spp. *Biol Chem Hoppe Seyler* **376**, 569-575 (1995).
111. Li, Y.T.*, et al.* A novel sialidase capable of cleaving 3-deoxy-D-glycero-D-galacto-2-nonulosonic acid (KDN). *Arch Biochem Biophys* **310**, 243-246 (1994).
112. Angata, T.*, et al.* Identification, developmental expression and tissue distribution of deaminoneuraminate hydrolase (KDNase) activity in rainbow trout. *Glycobiology* **4**, 517-523 (1994).
113. Iriyama, N.*, et al.* Enzymatic properties of sialidase from the ovary of the starfish, Asterina pectinifera. *Comparative Biochemistry and Physiology B-Biochemistry & Molecular Biology* **126**, 561-569 (2000).
114. Pshezhetsky, A.V.*, et al.* Cloning, expression and chromosomal mapping of human lysosomal sialidase and characterization of mutations in sialidosis. *Nat Genet* **15**, 316-320 (1997).
115. Vinogradova, M.V.*, et al.* Molecular mechanism of lysosomal sialidase deficiency in galactosialidosis involves its rapid degradation. *Biochem J* **330 (Pt 2)**, 641-650 (1998).
116. Bousse, T., Takimoto, T. & Portner, A. A single amino acid changes enhances the fusion promotion activity of human parainfluenza virus type 1 hemagglutinin-neuraminidase glycoprotein. *Virology* **209**, 654-657 (1995).

117. Parks, G.D. & Pohlmann, S. Structural requirements in the membrane-spanning domain of the paramyxovirus HN protein for the formation of a stable tetramer. *Virology* **213**, 263-270 (1995).
118. Colman, P.M., Hoyne, P.A. & Lawrence, M.C. Sequence and structure alignment of paramyxovirus hemagglutinin-neuraminidase with influenza virus neuraminidase. *J Virol* **67**, 2972-2980 (1993).
119. Tang, H.B.*, et al.* Contribution of specific Pseudomonas aeruginosa virulence factors to pathogenesis of pneumonia in a neonatal mouse model of infection. *Infect Immun* **64**, 37-43 (1996).
120. Dwarakanath, A.D.*, et al.* The production of neuraminidase and fucosidase by Helicobacter pylori: their possible relationship to pathogenicity. *FEMS Immunol Med Microbiol* **12**, 213-216 (1995).
121. Camara, M., Boulnois, G.J., Andrew, P.W. & Mitchell, T.J. A neuraminidase from Streptococcus pneumoniae has the features of a surface protein. *Infect Immun* **62**, 3688-3695 (1994).
122. Schenkman, S. & Eichinger, D. Trypanosoma cruzi trans-sialidase and cell invasion. *Parasitol Today* **9**, 218-222 (1993).
123. Engstler, M., Reuter, G. & Schauer, R. Purification and characterization of a novel sialidase found in procyclic culture forms of Trypanosoma brucei. *Mol Biochem Parasitol* **54**, 21-30 (1992).
124. Uemura, H., Schenkman, S., Nussenzweig, V. & Eichinger, D. Only some members of a gene family in Trypanosoma cruzi encode proteins that express both trans-sialidase and neuraminidase activities. *EMBO J* **11**, 3837-3844 (1992).
125. Ming, M., Chuenkova, M., Ortega-Barria, E. & Pereira, M.E. Mediation of Trypanosoma cruzi invasion by sialic acid on the host cell and trans-sialidase on the trypanosome. *Mol Biochem Parasitol* **59**, 243-252 (1993).
126. Pereira, M.E., Mejia, J.S., Ortega-Barria, E., Matzilevich, D. & Prioli, R.P. The Trypanosoma cruzi neuraminidase contains sequences similar to bacterial neuraminidases, YWTD repeats of the low density lipoprotein receptor, and type III modules of fibronectin. *J Exp Med* **174**, 179-191 (1991).
127. Vandekerckhove, F.*, et al.* Substrate specificity of the Trypanosoma cruzi trans-sialidase. *Glycobiology* **2**, 541-548 (1992).
128. Chuenkova, M. & Pereira, M.E. Trypanosoma cruzi trans-sialidase: enhancement of virulence in a murine model of Chagas' disease. *J Exp Med* **181**, 1693-1703 (1995).
129. Clough, B.*, et al.* Plasmodium falciparum lacks sialidase and trans-sialidase activity. *Parasitology* **112 (Pt 5)**, 443-449 (1996).
130. Long, G.S., Bryant, J.M., Taylor, P.W. & Luzio, J.P. Complete nucleotide sequence of the gene encoding bacteriophage E endosialidase: implications for K1E endosialidase structure and function. *Biochem J* **309 (Pt 2)**, 543-550 (1995).
131. Petter, J.G. & Vimr, E.R. Complete nucleotide sequence of the bacteriophage K1F tail gene encoding endo-N-acylneuraminidase (endo-N) and comparison to an endo-N homolog in bacteriophage PK1E. *J Bacteriol* **175**, 4354-4363 (1993).
132. Monti, E., Preti, A., Venerando, B. & Borsani, G. Recent development in mammalian sialidase molecular biology. *Neurochem Res* **27**, 649-663 (2002).
133. Warren, L. & Spearing, C.W. Mammalian sialidase (neuraminidase). *Biochem Biophys Res Commun* **3**, 489-492 (1960).
134. Morgan, E.H. & Laurell, C.B. Neuraminidase in Mammalian Brain. *Nature* **197**, 921-922 (1963).
135. Ghosh, N.K., Kotowitz, L. & Fishman, W.H. Neuraminidase in human intestinal mucosa. *Biochim Biophys Acta* **167**, 201-204 (1968).

136. Fukui, Y., Fukui, K. & Moriyama, T. Source of neuraminidase in human whole saliva. *Infect Immun* **8**, 329-334 (1973).
137. Ohman, R., Rosenberg, A. & Svennerholm, L. Human brain sialidase. *Biochemistry* **9**, 3774-3782 (1970).
138. Ohman, R. & Svennerholm, L. The activity of ganglioside sialidase in the developing human brain. *J Neurochem* **18**, 79-87 (1971).
139. Murphy, J.V. & Craig, L. Effect of human cerebral neuraminidase on hexosaminidase A. *Clin Chim Acta* **51**, 67-73 (1974).
140. Tettamanti, G., Venerando, B., Cestaro, B. & Preti, A. Brain neuraminidases and gangliosides. *Adv Exp Med Biol* **71**, 65-79 (1976).
141. Minami, R., Kudoh, T., Oyanagi, K. & Nakao, T. Neuraminidase activity in liver and brain from patients with I-cell disease. *Clin Chim Acta* **96**, 107-111 (1979).
142. Kopitz, J., Muhl, C., Ehemann, V., Lehmann, C. & Cantz, M. Effects of cell surface ganglioside sialidase inhibition on growth control and differentiation of human neuroblastoma cells. *Eur J Cell Biol* **73**, 1-9 (1997).
143. Kopitz, J., Sinz, K., Brossmer, R. & Cantz, M. Partial characterization and enrichment of a membrane-bound sialidase specific for gangliosides from human brain tissue. *Eur J Biochem* **248**, 527-534 (1997).
144. Kopitz, J., von Reitzenstein, C., Burchert, M., Cantz, M. & Gabius, H.J. Galectin-1 is a major receptor for ganglioside GM1, a product of the growth-controlling activity of a cell surface ganglioside sialidase, on human neuroblastoma cells in culture. *J Biol Chem* **273**, 11205-11211 (1998).
145. Miyagi, T.*, et al.* Molecular cloning and characterization of a plasma membrane-associated sialidase specific for gangliosides. *J Biol Chem* **274**, 5004-5011 (1999).
146. Igdoura, S.A., Mertineit, C., Trasler, J.M. & Gravel, R.A. Sialidase-mediated depletion of GM2 ganglioside in Tay-Sachs neuroglia cells. *Hum Mol Genet* **8**, 1111-1116 (1999).
147. Michalski, J.C., Corfield, A.P. & Schauer, R. Solubilization and affinity chromatography of a sialidase from human liver. *Hoppe Seylers Z Physiol Chem* **363**, 1097-1102 (1982).
148. Meyer, D.M., Lemonnier, M. & Bourrillon, R. Human liver neuraminidase. *Biochem Biophys Res Commun* **103**, 1302-1309 (1981).
149. Michalski, J.C., Corfield, A.P. & Schauer, R. Properties of human liver lysosomal sialidase. *Biol Chem Hoppe Seyler* **367**, 715-722 (1986).
150. Spaltro, J. & Alhadeff, J.A. Cellular localization and substrate specificity of isoelectric forms of human liver neuraminidase activity. *Biochem J* **241**, 137-143 (1987).
151. Verheijen, F.W., Palmeri, S., Hoogeveen, A.T. & Galjaard, H. Human placental neuraminidase. Activation, stabilization and association with beta-galactosidase and its protective protein. *Eur J Biochem* **149**, 315-321 (1985).
152. Verheijen, F.W., Palmeri, S. & Galjaard, H. Purification and partial characterization of lysosomal neuraminidase from human placenta. *Eur J Biochem* **162**, 63-67 (1987).
153. McNamara, D.*, et al.* Characterization of human placental neuraminidases. Stability, substrate specificity and molecular weight. *Biochem J* **205**, 345-351 (1982).
154. den Tandt, W.R. & Scharpe, S. Methylumbelliferyl-N-acetylneuraminic acid sialidase in human liver. *Biochem Med* **31**, 287-293 (1984).
155. Mier, P.D., van Rennes, H., van Erp, P.E. & Roelfzema, H. Cutaneous sialidase. *J Invest Dermatol* **78**, 267-269 (1982).
156. Mutton, T., Resnick, M.I. & Boyce, W.H. Human renal neuraminidase. *Invest Urol* **15**, 419-421 (1978).

157. Pogorelova, T.N., Drukker, N.A., Orvol, V.I. & Krukier, II. [Prognostic value of neuraminidase activity in mammary gland secretion in fetal death]. *Klin Lab Diagn*, 23-24 (1997).
158. Petushkova, N.A., Tsvetkova, I.V. & Rozenfel'd, E.L. [Properties of human chorion neuraminidase]. *Biokhimiia* **50**, 645-651 (1985).
159. Sonmez, H., Suer, S., Gungor, Z., Baloglu, H. & Kokoglu, E. Tissue and serum sialidase levels in breast cancer. *Cancer Lett* **136**, 75-78 (1999).
160. Marchesini, S., Cestaro, B., Lombardo, A., Sciorelli, G. & Preti, A. Human blood cells sialidases. *Biochem Int* **8**, 151-158 (1984).
161. Katoh, S.*, et al.* Cutting edge: an inducible sialidase regulates the hyaluronic acid binding ability of CD44-bearing human monocytes. *J Immunol* **162**, 5058-5061 (1999).
162. Madoulet, C.*, et al.* Evidence for sialidase activity in K 562 cells: inhibition by adriamycin treatment. *Cancer Biochem Biophys* **9**, 15-23 (1986).
163. Venerando, B., Fiorilli, A., Croci, G.L. & Tettamanti, G. Presence in human erythrocyte membranes of a novel form of sialidase acting optimally at neutral pH. *Blood* **90**, 2047-2056 (1997).
164. Chiarini, A., Fiorilli, A., Di Francesco, L., Venerando, B. & Tettamanti, G. Human erythrocyte sialidase is linked to the plasma membrane by a glycosylphosphatidylinositol anchor and partly located on the outer surface. *Glycoconj J* **10**, 64-71 (1993).
165. Greffard, A.*, et al.* Initial characterization of human thymocyte sialidase activity: evidence that this enzymatic system is not altered during the course of T-cell maturation. *Int J Biochem* **26**, 769-776 (1994).
166. Cross, A.S. & Wright, D.G. Mobilization of sialidase from intracellular stores to the surface of human neutrophils and its role in stimulated adhesion responses of these cells. *J Clin Invest* **88**, 2067-2076 (1991).
167. Yeh, A.K., Tulsiani, D.R. & Carubelli, R. Neuraminidase activity in human leukocytes. *J Lab Clin Med* **78**, 771-778 (1971).
168. Waters, P.J., Corfield, A.P., Eisenthal, R. & Pennock, C.A. Freeze-stable sialidase activity in human leucocytes: substrate specificity, inhibitor susceptibility, detergent requirements and subcellular localization. *Biochem J* **301 (Pt 3)**, 777-784 (1994).
169. Tsuji, S., Yamada, T., Tsutsumi, A. & Miyatake, T. Neuraminidase deficiency and accumulation of sialic acid in lymphocytes in adult type sialidosis with partial beta-galactosidase deficiency. *Ann Neurol* **11**, 541-543 (1982).
170. Yamada, T., Tsuji, S., Ariga, T. & Miyatake, T. Lysosomal sialidase deficiency in sialidosis with partial beta-galactosidase deficiency. *Biochim Biophys Acta* **755**, 106-111 (1983).
171. Warner, T.G. & O'Brien, J.S. Synthesis of 2'-(4-methylumbelliferyl)-alpha-D-N-acetylneuraminic acid and detection of skin fibroblast neuraminidase in normal humans and in sialidosis. *Biochemistry* **18**, 2783-2787 (1979).
172. Ben-Yoseph, Y., Momoi, T., Baylerian, M.S. & Nadler, H.L. Km defect in neuraminidase of dysmorphic type sialidosis with and without beta-galactosidase deficiency. *Clin Chim Acta* **123**, 233-240 (1982).
173. Mendla, K. & Cantz, M. Specificity studies on the oligosaccharide neuraminidase of human fibroblasts. *Biochem J* **218**, 625-628 (1984).
174. Schneider-Jakob, H.R. & Cantz, M. Lysosomal and plasma membrane ganglioside GM3 sialidases of cultured human fibroblasts. Differentiation by detergents and inhibitors. *Biol Chem Hoppe Seyler* **372**, 443-450 (1991).
175. Usuki, S. & Sweeley, C.C. Consideration of a functional role of an extracellular sialidase secreted by cultured fibroblasts. *Indian J Biochem Biophys* **25**, 102-105 (1988).
176. Miyagi, T.*, et al.* Molecular cloning and expression of cDNA encoding rat skeletal muscle cytosolic sialidase. *J Biol Chem* **268**, 26435-26440 (1993).

177. Ferrari, J., Harris, R. & Warner, T.G. Cloning and expression of a soluble sialidase from Chinese hamster ovary cells: sequence alignment similarities to bacterial sialidases. *Glycobiology* **4**, 367-373 (1994).
178. Bonten, E., van der Spoel, A., Fornerod, M., Grosveld, G. & d'Azzo, A. Characterization of human lysosomal neuraminidase defines the molecular basis of the metabolic storage disorder sialidosis. *Genes Dev* **10**, 3156-3169 (1996).
179. Milner, C.M*., et al.* Identification of a sialidase encoded in the human major histocompatibility complex. *J Biol Chem* **272**, 4549-4558 (1997).
180. Womack, J.E., Yan, D.L. & Potier, M. Gene for neuraminidase activity on mouse chromosome 17 near h-2: pleiotropic effects on multiple hydrolases. *Science* **212**, 63-65 (1981).
181. Samollow, P.B., VandeBerg, J.L., Ford, A.L., Douglas, T.C. & David, C.S. Electrophoretic analysis of liver neuraminidase-1 variation in mice and additional evidence concerning the location of NEU-1. *J Immunogenet* **13**, 29-39 (1986).
182. Harada, F*., et al.* The patient with combined deficiency of neuraminidase and 21-hydroxylase. *Hum Genet* **75**, 91-92 (1987).
183. Boguski, M.S. & Schuler, G.D. ESTablishing a human transcript map. *Nat Genet* **10**, 369-371 (1995).
184. Igdoura, S.A*., et al.* Cloning of the cDNA and gene encoding mouse lysosomal sialidase and correction of sialidase deficiency in human sialidosis and mouse SM/J fibroblasts. *Hum Mol Genet* **7**, 115-121 (1998).
185. Rottier, R.J., Bonten, E. & d'Azzo, A. A point mutation in the neu-1 locus causes the neuraminidase defect in the SM/J mouse. *Hum Mol Genet* **7**, 313-321 (1998).
186. Monti, E., Preti, A., Rossi, E., Ballabio, A. & Borsani, G. Cloning and characterization of NEU2, a human gene homologous to rodent soluble sialidases. *Genomics* **57**, 137-143 (1999).
187. Sato, K. & Miyagi, T. Genomic organization and the 5'-upstream sequence of the rat cytosolic sialidase gene. *Glycobiology* **5**, 511-516 (1995).
188. Hata, K., Wada, T., Hasegawa, A., Kiso, M. & Miyagi, T. Purification and characterization of a membrane-associated ganglioside sialidase from bovine brain. *J Biochem* **123**, 899-905 (1998).
189. Wada, T*., et al.* Cloning, expression, and chromosomal mapping of a human ganglioside sialidase. *Biochem Biophys Res Commun* **261**, 21-27 (1999).
190. Monti, E*., et al.* Identification and expression of NEU3, a novel human sialidase associated to the plasma membrane. *Biochem J* **349**, 343-351 (2000).
191. Fronda, C.L., Zeng, G., Gao, L. & Yu, R.K. Molecular cloning and expression of mouse brain sialidase. *Biochem Biophys Res Commun* **258**, 727-731 (1999).
192. Hasegawa, T*., et al.* Molecular cloning of mouse ganglioside sialidase and its increased expression in neuro2a cell differentiation. *J Biol Chem* **275**, 14778 (2000).
193. Hasegawa, T., Feijoo Carnero, C., Wada, T., Itoyama, Y. & Miyagi, T. Differential expression of three sialidase genes in rat development. *Biochem Biophys Res Commun* **280**, 726-732 (2001).
194. Monti, E*., et al.* Molecular cloning and characterization of NEU4, the fourth member of the human sialidase gene family. *Genomics* **83**, 445-453 (2004).
195. Monti, E., Preti, A., Nesti, C., Ballabio, A. & Borsani, G. Expression of a novel human sialidase encoded by the NEU2 gene. *Glycobiology* **9**, 1313-1321 (1999).
196. Carrillo, M.B., Milner, C.M., Ball, S.T., Snoek, M. & Campbell, R.D. Cloning and characterization of a sialidase from the murine histocompatibility-2

complex: low levels of mRNA and a single amino acid mutation are responsible for reduced sialidase activity in mice carrying the Neu1a allele. *Glycobiology* **7**, 975-986 (1997).
197. Naganawa, Y.*, et al.* Molecular and structural studies of Japanese patients with sialidosis type 1. *J Hum Genet* **45**, 241-249 (2000).
198. Meuillet, E.J.*, et al.* Sialidase gene transfection enhances epidermal growth factor receptor activity in an epidermoid carcinoma cell line, A431. *Cancer Res* **59**, 234-240 (1999).
199. Lukong, K.E.*, et al.* Characterization of the sialidase molecular defects in sialidosis patients suggests the structural organization of the lysosomal multienzyme complex. *Hum Mol Genet* **9**, 1075-1085 (2000).
200. Bonten, E.J.*, et al.* Novel mutations in lysosomal neuraminidase identify functional domains and determine clinical severity in sialidosis. *Hum Mol Genet* **9**, 2715-2725 (2000).
201. Varghese, J.N., Laver, W.G. & Colman, P.M. Structure of the influenza virus glycoprotein antigen neuraminidase at 2.9 A resolution. *Nature* **303**, 35-40 (1983).
202. Burmeister, W.P., Ruigrok, R.W. & Cusack, S. The 2.2 A resolution crystal structure of influenza B neuraminidase and its complex with sialic acid. *EMBO J* **11**, 49-56 (1992).
203. Crennell, S., Takimoto, T., Portner, A. & Taylor, G. Crystal structure of the multifunctional paramyxovirus hemagglutinin-neuraminidase. *Nat Struct Biol* **7**, 1068-1074 (2000).
204. Chavas, L.M.*, et al.* Crystal structure of the human cytosolic sialidase Neu2. Evidence for the dynamic nature of substrate recognition. *J Biol Chem* **280**, 469-475 (2005).
205. Magesh, S., Suzuki, T., Miyagi, T., Ishida, H. & Kiso, M. Homology modeling of human sialidase enzymes NEU1, NEU3 and NEU4 based on the crystal structure of NEU2: hints for the design of selective NEU3 inhibitors. *J Mol Graph Model* **25**, 196-207 (2006).
206. Vimr, E.R. Microbial sialidases: does bigger always mean better? *Trends Microbiol* **2**, 271-277 (1994).
207. Amino, R., Serrano, A.A., Morita, O.M., Pereira-Chioccola, V.L. & Schenkman, S. A sialidase activity in the midgut of the insect Triatoma infestans is responsible for the low levels of sialic acid in Trypanosoma cruzi growing in the insect vector. *Glycobiology* **5**, 625-631 (1995).
208. Aquino, A. & Gabor, A.J. Movement-induced seizures in nonketotic hyperglycemia. *Neurology* **30**, 600-604 (1980).
209. Jung, S., Rutka, J.T. & Hinek, A. Tropoelastin and elastin degradation products promote proliferation of human astrocytoma cell lines. *J Neuropathol Exp Neurol* **57**, 439-448 (1998).
210. Schauer, R. Chemistry and biology of the acylneuraminic acids. *Angew Chem Int Ed Engl* **12**, 127-138 (1973).
211. Warren, L., Buck, C.A. & Tuszynski, G.P. Glycopeptide changes and malignant transformation. A possible role for carbohydrate in malignant behavior. *Biochim Biophys Acta* **516**, 97-127 (1978).
212. Warner, T.G.*, et al.* Isolation and properties of a soluble sialidase from the culture fluid of Chinese hamster ovary cells. *Glycobiology* **3**, 455-463 (1993).
213. Usuki, S., Lyu, S.C. & Sweeley, C.C. Sialidase activities of cultured human fibroblasts and the metabolism of GM3 ganglioside. *J Biol Chem* **263**, 6847-6853 (1988).
214. Usuki, S., Hoops, P. & Sweeley, C.C. Growth control of human foreskin fibroblasts and inhibition of extracellular sialidase activity by 2-deoxy-2,3-dehydro-N-acetylneuraminic acid. *J Biol Chem* **263**, 10595-10599 (1988).
215. Sweeley, C.C. Extracellular sialidases. *Adv Lipid Res* **26**, 235-252 (1993).

216. Datta, A.K. & Paulson, J.C. Sialylmotifs of sialyltransferases. *Indian J Biochem Biophys* **34**, 157-165 (1997).
217. Ogura, K. & Sweeley, C.C. Mitogenic effects of bacterial neuroaminidase and lactosylceramide on human cultured fibroblasts. *Exp Cell Res* **199**, 169-173 (1992).
218. Hong, V.N.*, et al.* Studies on the sialidoses: properties of human leucocyte neuraminidases. *Biochim Biophys Acta* **616**, 259-270 (1980).
219. Verheijen, F.W.*, et al.* Two genetically different MU-NANA neuraminidases in human leucocytes. *Biochem Biophys Res Commun* **117**, 470-478 (1983).
220. Hoogeveen, A.T., Verheijen, F.W. & Galjaard, H. The relation between human lysosomal beta-galactosidase and its protective protein. *J Biol Chem* **258**, 12143-12146 (1983).
221. Galjaard, H.*, et al.* Molecular heterogeneity in human beta-galactosidase and neuraminidase deficiency. *Enzyme* **38**, 132-143 (1987).
222. van der Horst, G.T., Galjart, N.J., d'Azzo, A., Galjaard, H. & Verheijen, F.W. Identification and in vitro reconstitution of lysosomal neuraminidase from human placenta. *J Biol Chem* **264**, 1317-1322 (1989).
223. Potier, M., Michaud, L., Tranchemontagne, J. & Thauvette, L. Structure of the lysosomal neuraminidase-beta-galactosidase-carboxypeptidase multienzymic complex. *Biochem J* **267**, 197-202 (1990).
224. Pshezhetsky, A.V. & Potier, M. Association of N-acetylgalactosamine-6-sulfate sulfatase with the multienzyme lysosomal complex of beta-galactosidase, cathepsin A, and neuraminidase. Possible implication for intralysosomal catabolism of keratan sulfate. *J Biol Chem* **271**, 28359-28365 (1996).
225. Hiraiwa, M.*, et al.* Protective protein in the bovine lysosomal beta-galactosidase complex. *Biochim Biophys Acta* **1341**, 189-199 (1997).
226. Bonten, E.J. & d'Azzo, A. Lysosomal neuraminidase. Catalytic activation in insect cells is controlled by the protective protein/cathepsin A. *J Biol Chem* **275**, 37657-37663 (2000).
227. van der Spoel, A., Bonten, E. & d'Azzo, A. Transport of human lysosomal neuraminidase to mature lysosomes requires protective protein/cathepsin A. *EMBO J* **17**, 1588-1597 (1998).
228. Penzel, R.*, et al.* Splice donor site mutation in the lysosomal neuraminidase gene causing exon skipping and complete loss of enzyme activity in a sialidosis patient. *FEBS Lett* **501**, 135-138 (2001).
229. Lowden, J.A. & O'Brien, J.S. Sialidosis: a review of human neuraminidase deficiency. *Am J Hum Genet* **31**, 1-18 (1979).
230. Lieser, M., Harms, E., Kern, H., Bach, G. & Cantz, M. Ganglioside GM3 sialidase activity in fibroblasts of normal individuals and of patients with sialidosis and mucolipidosis IV. Subcellular distribution and and some properties. *Biochem J* **260**, 69-74 (1989).
231. Mueller, O.T. & Wenger, D.A. Mucolipidosis I: studies of sialidase activity and a prenatal diagnosis. *Clin Chim Acta* **109**, 313-324 (1981).
232. Okamura-Oho, Y., Zhang, S. & Callahan, J.W. The biochemistry and clinical features of galactosialidosis. *Biochim Biophys Acta* **1225**, 244-254 (1994).
233. Suzuki, Y. [Lysosomal enzymes, sphingolipid activator proteins, and protective protein]. *Nippon Rinsho* **53**, 2887-2891 (1995).
234. Rudenko, G., Bonten, E., Dazzo, A. & Hol, W.G.J. 3-DIMENSIONAL STRUCTURE OF THE HUMAN PROTECTIVE PROTEIN - STRUCTURE OF THE PRECURSOR FORM SUGGESTS A COMPLEX ACTIVATION MECHANISM. *Structure* **3**, 1249-1259 (1995).
235. Arai, Y., Edwards, V., Takashima, S. & Becker, L.E. Vascular pathology in galactosialidosis. *Ultrastruct Pathol* **23**, 369-374 (1999).

236. D'Azzo, A., Hoogeveen, A., Reuser, A.J., Robinson, D. & Galjaard, H. Molecular defect in combined beta-galactosidase and neuraminidase deficiency in man. *Proc Natl Acad Sci U S A* **79**, 4535-4539 (1982).
237. Mueller, O.T.*, et al.* Sialidosis and galactosialidosis: chromosomal assignment of two genes associated with neuraminidase-deficiency disorders. *Proc Natl Acad Sci U S A* **83**, 1817-1821 (1986).
238. Wiegant, J., Galjart, N.J., Raap, A.K. & d'Azzo, A. The gene encoding human protective protein (PPGB) is on chromosome 20. *Genomics* **10**, 345-349 (1991).
239. Naganawa, Y.*, et al.* Stable expression of protective protein/cathepsin A-green fluorescent protein fusion genes in a fibroblastic cell line from a galactosialidosis patient. Model system for revealing the intracellular transport of normal and mutated lysosomal enzymes. *Biochem J* **340 (Pt 2)**, 467-474 (1999).
240. Kleijer, W.J.*, et al.* Prenatal diagnosis of sialidosis with combined neuraminidase and beta-galactosidase deficiency. *Clin Genet* **16**, 60-61 (1979).
241. Sewell, A.C. & Pontz, B.F. Prenatal diagnosis of galactosialidosis. *Prenat Diagn* **8**, 151-155 (1988).
242. Olson, E.N. & Klein, W.H. bHLH factors in muscle development: dead lines and commitments, what to leave in and what to leave out. *Genes Dev* **8**, 1-8 (1994).
243. Sato, K. & Miyagi, T. Involvement of an endogenous sialidase in skeletal muscle cell differentiation. *Biochem Biophys Res Commun* **221**, 826-830 (1996).
244. Akita, H., Miyagi, T., Hata, K. & Kagayama, M. Immunohistochemical evidence for the existence of rat cytosolic sialidase in rat skeletal muscles. *Histochem Cell Biol* **107**, 495-503 (1997).
245. Tettamanti, G. & Riboni, L. Gangliosides and modulation of the function of neural cells. *Adv Lipid Res* **25**, 235-267 (1993).
246. Kopitz, J., von Reitzenstein, C., Muhl, C. & Cantz, M. Role of plasma membrane ganglioside sialidase of human neuroblastoma cells in growth control and differentiation. *Biochem Biophys Res Commun* **199**, 1188-1193 (1994).
247. Kopitz, J., von Reitzenstein, C., Sinz, K. & Cantz, M. Selective ganglioside desialylation in the plasma membrane of human neuroblastoma cells. *Glycobiology* **6**, 367-376 (1996).
248. Kopitz, J., Oehler, C. & Cantz, M. Desialylation of extracellular GD1a-neoganglioprotein suggests cell surface orientation of the plasma membrane-bound ganglioside sialidase activity in human neuroblastoma cells. *FEBS Lett* **491**, 233-236 (2001).
249. Simons, K. & Ikonen, E. Functional rafts in cell membranes. *Nature* **387**, 569-572 (1997).
250. Saito, M. & Yu, R.K. Role of myelin-associated neuraminidase in the ganglioside metabolism of rat brain myelin. *J Neurochem* **58**, 83-87 (1992).
251. Pitto, M., Chigorno, V., Giglioni, A., Valsecchi, M. & Tettamanti, G. Sialidase in cerebellar granule cells differentiating in culture. *J Neurochem* **53**, 1464-1470 (1989).
252. Wu, G. & Ledeen, R.W. Stimulation of neurite outgrowth in neuroblastoma cells by neuraminidase: putative role of GM1 ganglioside in differentiation. *J Neurochem* **56**, 95-104 (1991).
253. Saito, M., Tanaka, Y., Tang, C.P., Yu, R.K. & Ando, S. Characterization of sialidase activity in mouse synaptic plasma membranes and its age-related changes. *J Neurosci Res* **40**, 401-406 (1995).

254. Rodriguez, J.A., Piddini, E., Hasegawa, T., Miyagi, T. & Dotti, C.G. Plasma membrane ganglioside sialidase regulates axonal growth and regeneration in hippocampal neurons in culture. *J Neurosci* **21**, 8387-8395 (2001).
255. Farooqui, T., Franklin, T., Pearl, D.K. & Yates, A.J. Ganglioside GM1 enhances induction by nerve growth factor of a putative dimer of TrkA. *J Neurochem* **68**, 2348-2355 (1997).
256. Proshin, S., Yamaguchi, K., Wada, T. & Miyagi, T. Modulation of neuritogenesis by ganglioside-specific sialidase (Neu 3) in human neuroblastoma NB-1 cells. *Neurochem Res* **27**, 841-846 (2002).
257. Valaperta, R.*, et al.* Induction of axonal differentiation by silencing plasma membrane-associated sialidase Neu3 in neuroblastoma cells. *J Neurochem* **100**, 708-719 (2007).
258. von Reitzenstein, C., Kopitz, J., Schuhmann, V. & Cantz, M. Differential functional relevance of a plasma membrane ganglioside sialidase in cholinergic and adrenergic neuroblastoma cell lines. *Eur J Biochem* **268**, 326-333 (2001).
259. Kalka, D., von Reitzenstein, C., Kopitz, J. & Cantz, M. The plasma membrane ganglioside sialidase cofractionates with markers of lipid rafts. *Biochem Biophys Res Commun* **283**, 989-993 (2001).
260. Da Silva, J.S., Hasegawa, T., Miyagi, T., Dotti, C.G. & Abad-Rodriguez, J. Asymmetric membrane ganglioside sialidase activity specifies axonal fate. *Nat Neurosci* **8**, 606-615 (2005).
261. Yang, L.J.*, et al.* Sialidase enhances spinal axon outgrowth in vivo. *Proc Natl Acad Sci U S A* **103**, 11057-11062 (2006).
262. Dennis, J.W. & Laferte, S. Tumor cell surface carbohydrate and the metastatic phenotype. *Cancer Metastasis Rev* **5**, 185-204 (1987).
263. Hakomori, S. Tumor malignancy defined by aberrant glycosylation and sphingo(glyco)lipid metabolism. *Cancer Res* **56**, 5309-5318 (1996).
264. Hakomori, S. & Handa, K. Glycosphingolipid-dependent cross-talk between glycosynapses interfacing tumor cells with their host cells: essential basis to define tumor malignancy. *FEBS Lett* **531**, 88-92 (2002).
265. Yogeeswaran, G. & Salk, P.L. Metastatic potential is positively correlated with cell surface sialylation of cultured murine tumor cell lines. *Science* **212**, 1514-1516 (1981).
266. Fogel, M., Altevogt, P. & Schirrmacher, V. Metastatic potential severely altered by changes in tumor cell adhesiveness and cell-surface sialylation. *J Exp Med* **157**, 371-376 (1983).
267. Passaniti, A. & Hart, G.W. Cell surface sialylation and tumor metastasis. Metastatic potential of B16 melanoma variants correlates with their relative numbers of specific penultimate oligosaccharide structures. *J Biol Chem* **263**, 7591-7603 (1988).
268. Dennis, J.W., Granovsky, M. & Warren, C.E. Glycoprotein glycosylation and cancer progression. *Biochim Biophys Acta* **1473**, 21-34 (1999).
269. Schengrund, C.L., Lausch, R.N. & Rosenberg, A. Sialidase activity in transformed cells. *J Biol Chem* **248**, 4424-4428 (1973).
270. Yogeeswaran, G. & Hakomori, S. Cell contact-dependent ganglioside changes in mouse 3T3 gibroblasts and a suppressed sialidase activity on cell contact. *Biochemistry* **14**, 2151-2156 (1975).
271. Bosmann, H.B. & Hall, T.C. Enzyme activity in invasive tumors of human breast and colon. *Proc Natl Acad Sci U S A* **71**, 1833-1837 (1974).
272. Nojiri, N., Takaku, F., Tetsuka, T. & Saito, M. Stimulation of sialidase activity during cell differentiation of human promyelocytic leukemia cell line HL-60. *Biochem Biophys Res Commun* **104**, 1239-1246 (1982).

273. Miyagi, T., Konno, K., Sagawa, J. & Tsuiki, S. Neoplastic alteration of a membrane-associated sialidase of rat liver. *Jpn J Cancer Res* **81**, 915-919 (1990).
274. Miyagi, T., Sagawa, J., Kuroki, T., Matsuya, Y. & Tsuiki, S. Tumor-promoting phorbol ester induces alterations of sialidase and sialyltransferase activities of JB6 cells. *Jpn J Cancer Res* **81**, 1286-1292 (1990).
275. Miyagi, T., Sato, K., Hata, K. & Taniguchi, S. Metastatic potential of transformed rat 3Y1 cell lines is inversely correlated with lysosomal-type sialidase activity. *FEBS Lett* **349**, 255-259 (1994).
276. Sawada, M.*, et al.* Reduced sialidase expression in highly metastatic variants of mouse colon adenocarcinoma 26 and retardation of their metastatic ability by sialidase overexpression. *Int J Cancer* **97**, 180-185 (2002).
277. Tokuyama, S.*, et al.* Suppression of pulmonary metastasis in murine B16 melanoma cells by transfection of a sialidase cDNA. *Int J Cancer* **73**, 410-415 (1997).
278. Tringali, C.*, et al.* Expression of sialidase Neu2 in leukemic K562 cells induces apoptosis by impairing Bcr-Abl/Src kinases signaling. *J Biol Chem* **282**, 14364-14372 (2007).
279. Kato, T.*, et al.* Overexpression of lysosomal-type sialidase leads to suppression of metastasis associated with reversion of malignant phenotype in murine B16 melanoma cells. *Int J Cancer* **92**, 797-804 (2001).
280. Yamaguchi, K.*, et al.* Evidence for mitochondrial localization of a novel human sialidase (NEU4). *Biochem J* **390**, 85-93 (2005).
281. Uemura, T.*, et al.* Contribution of sialidase NEU1 to suppression of metastasis of human colon cancer cells through desialylation of integrin beta4. *Oncogene* **28**, 1218-1229 (2009).
282. Kakugawa, Y.*, et al.* Up-regulation of plasma membrane-associated ganglioside sialidase (Neu3) in human colon cancer and its involvement in apoptosis suppression. *Proc Natl Acad Sci U S A* **99**, 10718-10723 (2002).
283. Kato, K.*, et al.* Plasma-membrane-associated sialidase (NEU3) differentially regulates integrin-mediated cell proliferation through laminin- and fibronectin-derived signalling. *Biochem J* **394**, 647-656 (2006).
284. Ueno, S.*, et al.* Plasma membrane-associated sialidase is up-regulated in renal cell carcinoma and promotes interleukin-6-induced apoptosis suppression and cell motility. *J Biol Chem* **281**, 7756-7764 (2006).
285. Nomura, H.*, et al.* Expression of NEU3 (plasma membrane-associated sialidase) in clear cell adenocarcinoma of the ovary: its relationship with T factor of pTNM classification. *Oncol Res* **16**, 289-297 (2006).
286. Wada, T.*, et al.* A crucial role of plasma membrane-associated sialidase in the survival of human cancer cells. *Oncogene* **26**, 2483-2490 (2007).
287. Tringali, C.*, et al.* Silencing of membrane-associated sialidase Neu3 diminishes apoptosis resistance and triggers megakaryocytic differentiation of chronic myeloid leukemic cells K562 through the increase of ganglioside GM3. *Cell Death Differ* **16**, 164-174 (2009).
288. Yoon, S.J., Nakayama, K., Hikita, T., Handa, K. & Hakomori, S.I. Epidermal growth factor receptor tyrosine kinase is modulated by GM3 interaction with N-linked GlcNAc termini of the receptor. *Proc Natl Acad Sci U S A* **103**, 18987-18991 (2006).
289. Anastasia, L.*, et al.* NEU3 sialidase strictly modulates GM3 levels in skeletal myoblasts C2C12 thus favoring their differentiation and protecting them from apoptosis. *J Biol Chem* **283**, 36265-36271 (2008).
290. Toledo, M.S., Suzuki, E., Handa, K. & Hakomori, S. Effect of ganglioside and tetraspanins in microdomains on interaction of integrins with fibroblast growth factor receptor. *J Biol Chem* **280**, 16227-16234 (2005).

291. Gopalakrishna, P., Rangaraj, N. & Pande, G. Cholesterol alters the interaction of glycosphingolipid GM3 with alpha5beta1 integrin and increases integrin-mediated cell adhesion to fibronectin. *Exp Cell Res* **300**, 43-53 (2004).
292. Yamanami, H.*, et al.* Down-regulation of sialidase NEU4 may contribute to invasive properties of human colon cancers. *Cancer Sci* **98**, 299-307 (2007).
293. Comelli, E.M., Amado, M., Lustig, S.R. & Paulson, J.C. Identification and expression of Neu4, a novel murine sialidase. *Gene* **321**, 155-161 (2003).
294. Claros, M.G. & Vincens, P. Computational method to predict mitochondrially imported proteins and their targeting sequences. *Eur J Biochem* **241**, 779-786 (1996).
295. Kobayashi, T., Ito, M., Ikeda, K., Tanaka, K. & Saito, M. Purification and characterization of a membrane-bound sialidase from pig liver. *J Biochem* **127**, 569-575 (2000).
296. Seyrantepe, V.*, et al.* Neu4, a novel human lysosomal lumen sialidase, confers normal phenotype to sialidosis and galactosialidosis cells. *J Biol Chem* **279**, 37021-37029 (2004).
297. Sasaki, A.*, et al.* Overexpression of plasma membrane-associated sialidase attenuates insulin signaling in transgenic mice. *J Biol Chem* **278**, 27896-27902 (2003).
298. Seyrantepe, V.*, et al.* Molecular pathology of NEU1 gene in sialidosis. *Hum Mutat* **22**, 343-352 (2003).
299. Lukong, K.E.*, et al.* Intracellular distribution of lysosomal sialidase is controlled by the internalization signal in its cytoplasmic tail. *J Biol Chem* **276**, 46172-46181 (2001).
300. Hiraiwa, M., Uda, Y., Nishizawa, M. & Miyatake, T. Human placental sialidase: partial purification and characterization. *J Biochem* **101**, 1273-1279 (1987).
301. Hiraiwa, M., Nishizawa, M., Uda, Y., Nakajima, T. & Miyatake, T. Human placental sialidase: further purification and characterization. *J Biochem* **103**, 86-90 (1988).
302. Zhou, X.Y.*, et al.* Mouse model for the lysosomal disorder galactosialidosis and correction of the phenotype with overexpressing erythroid precursor cells. *Genes Dev* **9**, 2623-2634 (1995).
303. Neufeld, E.F. Lysosomal storage diseases. *Annu Rev Biochem* **60**, 257-280 (1991).
304. Seyrantepe, V.*, et al.* Mice deficient in Neu4 sialidase exhibit abnormal ganglioside catabolism and lysosomal storage. *Hum Mol Genet* **17**, 1556-1568 (2008).
305. Phaneuf, D.*, et al.* Dramatically different phenotypes in mouse models of human Tay-Sachs and Sandhoff diseases. *Hum Mol Genet* **5**, 1-14 (1996).
306. Sango, K.*, et al.* Mouse models of Tay-Sachs and Sandhoff diseases differ in neurologic phenotype and ganglioside metabolism. *Nat Genet* **11**, 170-176 (1995).
307. Miklyaeva, E.I.*, et al.* Late onset Tay-Sachs disease in mice with targeted disruption of the Hexa gene: behavioral changes and pathology of the central nervous system. *Brain Res* **1001**, 37-50 (2004).
308. Seyrantepe, V.*, et al.* Mice doubly-deficient in lysosomal hexosaminidase A and neuraminidase 4 show epileptic crises and rapid neuronal loss. *PLoS Genet* **6**.
309. Malisan, F. & Testi, R. GD3 ganglioside and apoptosis. *Biochim Biophys Acta* **1585**, 179-187 (2002).
310. Castro-Palomino, J.C., Simon, B., Speer, O., Leist, M. & Schmidt, R.R. Synthesis of ganglioside GD3 and its comparison with bovine GD3 with

regard to oligodendrocyte apoptosis mitochondrial damage. *Chemistry* **7**, 2178-2184 (2001).
311. De Maria, R.*, et al.* Requirement for GD3 ganglioside in CD95- and ceramide-induced apoptosis. *Science* **277**, 1652-1655 (1997).
312. Rippo, M.R.*, et al.* GD3 ganglioside directly targets mitochondria in a bcl-2-controlled fashion. *FASEB J* **14**, 2047-2054 (2000).
313. Garcia-Ruiz, C.*, et al.* Trafficking of ganglioside GD3 to mitochondria by tumor necrosis factor-alpha. *J Biol Chem* **277**, 36443-36448 (2002).
314. Hasegawa, T.*, et al.* Role of Neu4L sialidase and its substrate ganglioside GD3 in neuronal apoptosis induced by catechol metabolites. *FEBS Lett* **581**, 406-412 (2007).
315. Sallusto, F. & Lanzavecchia, A. Efficient presentation of soluble antigen by cultured human dendritic cells is maintained by granulocyte/macrophage colony-stimulating factor plus interleukin 4 and downregulated by tumor necrosis factor alpha. *J Exp Med* **179**, 1109-1118 (1994).
316. Stamatos, N.M.*, et al.* LPS-induced cytokine production in human dendritic cells is regulated by sialidase activity. *J Leukoc Biol*.
317. Stamatos, N.M.*, et al.* Differential expression of endogenous sialidases of human monocytes during cellular differentiation into macrophages. *FEBS J* **272**, 2545-2556 (2005).
318. Finlay, T.M.*, et al.* Thymoquinone from nutraceutical black cumin oil activates Neu4 sialidase in live macrophage, dendritic, and normal and type I sialidosis human fibroblast cells via GPCR Galphai proteins and matrix metalloproteinase-9. *Glycoconj J* **27**, 329-348.
319. Shiozaki, K.*, et al.* Developmental change of sialidase neu4 expression in murine brain and its involvement in the regulation of neuronal cell differentiation. *J Biol Chem* **284**, 21157-21164 (2009).
320. Tran, S.E., Holmstrom, T.H., Ahonen, M., Kahari, V.M. & Eriksson, J.E. MAPK/ERK overrides the apoptotic signaling from Fas, TNF, and TRAIL receptors. *J Biol Chem* **276**, 16484-16490 (2001).
321. Hollingsworth, M.A. & Swanson, B.J. Mucins in cancer: protection and control of the cell surface. *Nat Rev Cancer* **4**, 45-60 (2004).
322. Wei, X., Xu, H. & Kufe, D. Human MUC1 oncoprotein regulates p53-responsive gene transcription in the genotoxic stress response. *Cancer Cell* **7**, 167-178 (2005).
323. Holmstrom, T.H.*, et al.* Inhibition of mitogen-activated kinase signaling sensitizes HeLa cells to Fas receptor-mediated apoptosis. *Mol Cell Biol* **19**, 5991-6002 (1999).
324. Gu, W. & Helms, V. Dynamical binding of proline-rich peptides to their recognition domains. *Biochim Biophys Acta* **1754**, 232-238 (2005).
325. Soding, J., Biegert, A. & Lupas, A.N. The HHpred interactive server for protein homology detection and structure prediction. *Nucleic Acids Res* **33**, W244-248 (2005).
326. Fujiki, Y., Hubbard, A.L., Fowler, S. & Lazarow, P.B. Isolation of intracellular membranes by means of sodium carbonate treatment: application to endoplasmic reticulum. *J Cell Biol* **93**, 97-102 (1982).
327. Vasilescu, J., Guo, X. & Kast, J. Identification of protein-protein interactions using in vivo cross-linking and mass spectrometry. *Proteomics* **4**, 3845-3854 (2004).
328. Opheim, D.J. & Touster, O. alpha-D-Mannosidase from rat liver lysosomes. *Methods Enzymol* **50**, 494-500 (1978).
329. Noma, T.*, et al.* Structure and expression of human mitochondrial adenylate kinase targeted to the mitochondrial matrix. *Biochem J* **358**, 225-232 (2001).

330. Ellman, G.L., Courtney, K.D., Andres, V., Jr. & Feather-Stone, R.M. A new and rapid colorimetric determination of acetylcholinesterase activity. *Biochem Pharmacol* **7**, 88-95 (1961).
331. Bradford, M.M. A rapid and sensitive method for the quantitation of microgram quantities of protein utilizing the principle of protein-dye binding. *Anal Biochem* **72**, 248-254 (1976).
332. Zanchetti, G.*, et al.* Sialidase NEU3 is a peripheral membrane protein localized on the cell surface and in endosomal structures. *Biochem J* **408**, 211-219 (2007).
333. Nakamura, Y., Ozaki, T., Ichimiya, S., Nakagawara, A. & Sakiyama, S. Ectopic expression of DAN enhances the retinoic acid-induced neuronal differentiation in human neuroblastoma cell lines. *Biochem Biophys Res Commun* **243**, 722-726 (1998).
334. Myers, M.P.*, et al.* The lipid phosphatase activity of PTEN is critical for its tumor supressor function. *Proc Natl Acad Sci U S A* **95**, 13513-13518 (1998).
335. de Geest, N.*, et al.* Systemic and neurologic abnormalities distinguish the lysosomal disorders sialidosis and galactosialidosis in mice. *Hum Mol Genet* **11**, 1455-1464 (2002).
336. Songyang, Z. Recognition and regulation of primary-sequence motifs by signaling modular domains. *Prog Biophys Mol Biol* **71**, 359-372 (1999).
337. Williamson, M.P. The structure and function of proline-rich regions in proteins. *Biochem J* **297 (Pt 2)**, 249-260 (1994).
338. Pawson, T. & Nash, P. Assembly of cell regulatory systems through protein interaction domains. *Science* **300**, 445-452 (2003).
339. Pawson, T. & Scott, J.D. Signaling through scaffold, anchoring, and adaptor proteins. *Science* **278**, 2075-2080 (1997).
340. Schwab, M. Human neuroblastoma: amplification of the N-myc oncogene and loss of a putative cancer-preventing gene on chromosome 1p. *Recent Results Cancer Res* **135**, 7-16 (1994).
341. Schwab, M., Varmus, H.E. & Bishop, J.M. Human N-myc gene contributes to neoplastic transformation of mammalian cells in culture. *Nature* **316**, 160-162 (1985).
342. Schubert, D., Humphreys, S., Baroni, C. & Cohn, M. In vitro differentiation of a mouse neuroblastoma. *Proc Natl Acad Sci U S A* **64**, 316-323 (1969).
343. Seeds, N.W., Gilman, A.G., Amano, T. & Nirenberg, M.W. Regulation of axon formation by clonal lines of a neural tumor. *Proc Natl Acad Sci U S A* **66**, 160-167 (1970).
344. Lopez-Carballo, G., Moreno, L., Masia, S., Perez, P. & Barettino, D. Activation of the phosphatidylinositol 3-kinase/Akt signaling pathway by retinoic acid is required for neural differentiation of SH-SY5Y human neuroblastoma cells. *J Biol Chem* **277**, 25297-25304 (2002).
345. Masia, S., Alvarez, S., de Lera, A.R. & Barettino, D. Rapid, nongenomic actions of retinoic acid on phosphatidylinositol-3-kinase signaling pathway mediated by the retinoic acid receptor. *Mol Endocrinol* **21**, 2391-2402 (2007).

Glycobiology Advance Access published September 30, 2009

doi: 10.1093/glycob/cwp156

Human sialidase NEU4 long and short are extrinsic proteins bound to outer mitochondrial membrane and the endoplasmic reticulum, respectively

Alessandra Bigi[1], Lavinia Morosi[1], Chiara Pozzi[1], Matilde Forcella[1], Guido Tettamanti[2], Bruno Venerando[3], Eugenio Monti[4], and Paola Fusi[1]

[1]Department of Biotechnologies and Biosciences, University of Milan-Bicocca, Piazza della Scienza, 2, 20126, Milano. [2]Laboratory of Stem Cells for Tissue Engineering, IRCCS Policlinico San Donato, 20097 San Donato Milanese [3]Department of Medical Chemistry, Biochemistry and Biotechnology, L.I.T.A.-Segrate, University of Milan, Via F.lli Cervi, 93, 20090 Segrate. [4]Department of Biomedical Sciences and Biotechnology, University of Brescia, Viale Europa, 11, 25123 Brescia, Italy

Corresponding author: Paola Fusi, Department of Biotechnologies and Biosciences, University of Milan-Bicocca, Piazza della Scienza, 2, 20126, Milano. Phone: +390264483405; fax: +390264483565; e-mail: paola.fusi@unimib.it.

Running title: Studies on human NEU4 isoforms subcellular localization

Keywords: endoplasmic reticulum / long and short isoforms / mitochondrial membrane / peripheral membrane protein / sialidase NEU4

Supplementary data:

Supplementary Figures Legends

Supplementary Figure S1

Supplementary Figure S2

Received: 29-Apr-2009; Accepted: 27-Sep-2009

Abstract

Sialidases are widely distributed glycohydrolytic enzymes removing sialic acid residues from glycoconjugates. In mammals, several sialidases with different subcellular localizations and biochemical features have been described. NEU4, the most recently identified member of the human sialidase family, is found in two forms, NEU4 long and NEU4 short, differing in the presence of a 12 aminoacid sequence at the N-terminus. Contradictory data are present in the literature about the subcellular distribution of these enzymes, their membrane anchoring mechanism being still unclear.

In this work we investigate human NEU4 long and NEU4 short membrane anchoring mechanism and their subcellular localization. Protein extraction with Triton X-114 and sodium carbonate and cross-linking experiments demonstrate that both forms of NEU4 are extrinsic membrane proteins, anchored via protein-protein interactions. Moreover, through confocal microscopy and subcellular fractionation, we show that the long form localizes in mitochondria, while the short form is also associated with the endoplasmic reticulum. Finally, mitochondria subfractionation experiments suggest that NEU4 long is bound to the outer mitochondrial membrane.

Introduction

Sialidases (EC 3.2.1.18), hydrolases cleaving sialic acid residues from sialylated glycoconjugates, are widely distributed in nature, from microorganisms to mammals (Saito and Yu 1995). Since 1993 several mammalian sialidases have been cloned (Monti *et al.* 2002): a lysosomal form (NEU1), a cytosolic form (NEU2), a plasma membrane associated form (NEU3) and another form, also bound to intracellular membranes, called NEU4 (Monti *et al.* 2004). These sialidases show important similarities in their primary structures, such as the F(Y)RIP motif, Asp boxes, as well as some common aminoacids constituting the catalytic site and a β-propeller structure, with the catalytic site lying in a deep cleft on one side of the molecule (Crennell *et al.* 1993, Taylor 1996). However, they also show different biochemical properties, as regards substrate specificity and subcellular localization. The three dimensional structure of human sialidase NEU2 has recently been solved, showing that the enzyme possesses the well-known β-propeller 3D structure already described in viral, microbial and tripanosomal sialidases (Chavas *et al.* 2005).

NEU4, the fourth member of the sialidase family in mammals, was identified by searching sequence databases for entries showing similarities to the human cytosolic sialidase NEU2 (Monti *et al.* 2004). Its activity on different sialoglycoconjugates, including the artificial substrate 4MU-NeuAc, is optimal at very acidic pH (3.2). Different authors have investigated NEU4 subcellular localization. Monti and colleagues demonstrated the association of NEU4 with the inner cellular membranes (Monti *et al.* 2004), through Western-blot analysis and immunofluorescence staining. More recently, Seyrantepe and colleagues (Seyrantepe *et al.* 2004) showed that human NEU4 is targeted to the lysosomes. On the other hand, Yamaguchi and coworkers (Yamaguchi *et al.* 2005) isolated a cDNA fragment coding for two NEU4 isoforms which differ for the presence, in the long form, of an additional 12 aminoacids N-terminal sequence. These authors also showed that the two isoforms were not distinguishable

in substrate specificity, but exhibited different subcellular localizations, the long form being targeted mainly to mitochondria and the short form to intracellular membranes.

This work was undertaken with the aim of accurately assessing the subcellular localization of both forms of NEU4 and to provide more details on its membrane anchoring mechanism. Analysis of NEU4 primary structure rules out the possibility of it being a transmembrane protein, since the only potential transmembrane domain is incompatible with the β-propeller sialidase structure; moreover no membrane anchoring motifs, such as GPI anchors, palmitoylation or myristoylation sites, are present on NEU4 aminoacidic sequence, leaving the mechanism through which NEU4 binds to membranes still an open question. To this purpose we expressed both long (HsNEU4 long) and short (HsNEU4 short) forms of human NEU4 in COS-7 cells, both carrying a C-terminal c-myc tag. Solubilisation experiments, carried out with Triton X-114 and sodium carbonate, showed that both NEU4 long and NEU4 short are extrinsic membrane proteins; cross-linking experiments also strongly suggested an association to the membrane through protein-protein interactions. Moreover, subcellular localization studies, performed through confocal microscopy and subcellular fractionation, showed that NEU4 long resides in the outer mitochondrial membrane, while the short form is bound to the endoplasmic reticulum.

Results

Triton X-114 phase separation shows that both NEU4 long and NEU4 short are hydrophilic proteins

Transmembrane regions prediction methods, such as TMPred and TMHMM, suggest the existence of a potential transmembrane domain in NEU4 primary structure. However, the presence of such a domain is not compatible with the typical sialidase β-propeller three dimensional structure, yielded by homology modelling (Magesh *et al.* 2006). On the other

hand, no membrane anchoring motifs, such as GPI anchors, palmitoylation or myristoylation sites, are present on NEU4 aminoacidic sequence. In order to gain insight into the mechanism through which NEU4 long and NEU4 short bind to the membranes, we undertook protein extraction with Triton X-114 followed by temperature-induced phase separation, as previously performed for sialidase NEU3 (Zanchetti *et al.* 2007). This detergent allows protein solubilisation with phase-separation of hydrophilic from amphiphilic membrane proteins. Crude extracts, obtained from COS-7 cells transiently expressing either HsNEU4 long or short form as fusion proteins carrying a C-terminal c-myc epitope, were initially treated with Triton X-114 and then subjected to aqueous/detergent phase separation. Western-blot analysis showed that both forms of HsNEU4 were totally extracted in the aqueous phase (Figure 1), as well as Protein Disulfide Isomerase (PDI), which is a hydrophilic protein loosely bound to ER membranes. On the other hand Caveolin-1 (Cav-1), a protein associated to the lipid bilayer by a hydrophobic domain and palmitoylation, was extracted by Triton X-114 and then totally recovered in the detergent phase. These phase-partitioning results prompted us to affirm that both forms of NEU4 are hydrophilic proteins, as already suggested by primary structure analysis. Moreover, no sialidase activity was detected in both aqueous and detergent fractions (data not shown).

Carbonate extraction suggests that both NEU4 long and NEU4 short are extrinsic membrane proteins

In order to assess whether NEU4 is a peripheral membrane protein, the membrane fractions obtained from COS-7 cells expressing either HsNEU4 long or HsNEU4 short were brought to pH 11.5 with sodium carbonate and incubated for 30 min on ice. A subsequent ultracentrifugation yielded a soluble fraction and a membrane fraction, which were brought to pH 7.5 and subjected to SDS-PAGE followed by Western-blotting (Figure 2A). NEU4

detection was performed with an anti c-myc antibody. In addition, Early Endosome Antigen 1 (EEA1) and Caveolin-1 (Cav-1) were used as controls for peripheral and intrinsic membrane proteins, respectively. As expected, both the long and the short form of HsNEU4 were found in the particulate fraction of untreated samples, as confirmed by sialidase activity assay using 4MU-NeuAc as a substrate (Figure 2C). Partial recovery of both NEU4 long and NEU4 short in the soluble fraction in control samples is due to minor protein release during collection and manipulation of membranes samples. Both long and short forms of NEU4 were partially solubilised by sodium carbonate treatment. A densitometric analysis of the bands showed that about 30% and 50% of HsNEU4 short and HsNEU4 long, respectively, were solubilised upon carbonate treatment (Figure 2B). As expected, after treatment with sodium carbonate, the peripheral membrane protein EEA1 was completely recovered in the soluble fraction, while Cav-1, an integral membrane protein, was not solubilised at all, thus demonstrating that carbonate treatment extracts peripheral proteins without affecting membrane integrity. After sodium carbonate treatment no appreciable sialidase activity could be recorded in any fraction (data not shown), presumably due to alkaline denaturation or inactivation of the enzyme, as previously reported for sialidase NEU3 (Zanchetti *et al.* 2007). In addition, treatment of the membrane fraction prepared from COS-7 expressing either HsNEU4 long or HsNEU4 short with a high ionic strength buffer, containing 1.5 M NaCl, did not cause any NEU4 release (data not shown), suggesting that this sialidase is a peripheral protein strongly associated to membranes.

Reversible cross-linking shows that HsNEU4 long and HsNEU4 short are anchored to membranes through protein-protein interactions

Since our data showed that both forms of HsNEU4 are extrinsic membrane proteins, we performed cross-linking experiments in order to assess whether these sialidases might be

anchored to the membrane via protein-protein interactions. The lack of any motif for membrane anchoring through prenylation, acylation or GPI on NEU4 aminoacidic sequence suggested protein-protein interactions as the most likely membrane associating mechanism. Paraformaldehyde (PFA) is known to form covalent bonds between chemical groups not further apart than 2 Å, which can readily be reversed by heat treatment at 95°C. COS-7 cells transiently expressing either HsNEU4 long or HsNEU4 short were supplemented in the medium with PFA, as reported in Material and methods. Crude cell extracts were then subjected to SDS-PAGE and Western-blotting in order to assess the presence of NEU4 complexes. Both HsNEU4 forms and their complexes were detected with an anti-c-myc antibody. Initially, COS-7 cells expressing either long or short form of HsNEU4 were treated for different times with various concentrations of PFA (data not shown). These preliminary tests showed that 20 min incubation with 0.25% (w/v) PFA was sufficient to obtain cross-linking of both HsNEU4 long and HsNEU4 short to adjacent membrane proteins; longer incubation times or higher PFA concentrations resulted in smeared electrophoretic bands, indicative of aspecific cross-linking. As shown in Figure 3, after PFA treatment, NEU4 was detected only as a high Mr complex (higher than 250 kDa), which hardly entered into the running gel. Cross-linking reversion, obtained by incubation at 95°C for 20 min, led to the disappearance of NEU4 complex and to the reappearance of bands corresponding to HsNEU4 long and HsNEU4 short molecular masses. This experiment confirmed that both forms of NEU4 interact with other proteins likely involved in their anchorage to membranes.

Confocal microscopy and subcellular fractionation show that the long form of HsNEU4 localizes in mitochondria, while the short form is bound to the endoplasmic reticulum

The existence of contradictory data in literature (Monti *et al.* 2004, Seyrantepe *et al.* 2004, Yamaguchi *et al.* 2005) about NEU4 subcellular localization prompted us to further

investigate this issue, both through confocal microscopy and subcellular fractionation studies. Colocalization experiments were carried out in COS-7 cells, transiently expressing either HsNEU4 long or HsNEU4 short as fusion proteins carrying a C-terminal c-myc epitope. Markers of different cellular compartments, such as cytochrome *c* (cyt *c*) for mitochondria, Lysosome-Associated Membrane Protein-1 (LAMP-1) for lysosomes and Calnexin (Cnx) for endoplasmic reticulum, were also used. 24 h after transfection, cells were fixed, permeabilized and analysed by confocal microscopy. Results, reported in Figure 4, showed that HsNEU4 long colocalizes with the mitochondrial marker cyt *c* (Figure 4A panel f), as reported by Yamaguchi and colleagues (Yamaguchi *et al.* 2005), but not with the lysosomal marker LAMP-1 (Figura 4B panel f), as claimed by Seyrantepe and coworkers (Seyrantepe *et al.* 2004). Moreover, while colocalization of HsNEU4 short with either of these markers could not be observed (Figure 4A panel e and 4B panel e), superimposition with Cnx diffused fluorescent signal, shown in Figure 4C panel e, suggested that HsNEU4 short can be bound to the endoplasmic reticulum. Colocalization of HsNEU4 long or HsNEU4 short with the subcellular markers was confirmed by Z-stack analyses, performed on confocal microscopy images (data not shown).

In order to check the possibility that the observed subcellular localization of both HsNEU4 forms might be an artifact due to protein transient over-expression, HsNEU4 subcellular localization was evaluated at different post-transfection times. No differences in subcellular localization of both HsNEU4 forms was observed when fixing and analysing the cells 5, 10, 24 and 36 h after transfection (Supplementary data, Figure S1). HsNEU4 short appeared to be diffusely localized inside the cells at all times, its signal only slightly superimposing with cyt c. On the other hand, HsNEU4 long exhibited the already observed complete colocalization with the mitochondrial marker. Moreover, a total and partial mitochondrial colocalization of HsNEU4 long and HsNEU4 short, respectively, was also observed in HeLa cells,

demonstrating that this subcellular distribution is not restricted to a particular cell type (Supplementary data, Figure S2).

Finally, to assess the difference in subcellular localization between the short and long form of HsNEU4, we performed cotransfection experiments with both c-myc-tagged HsNEU4 long and HA-tagged HsNEU4 short expressing vectors. Results are shown in Figure 5: HsNEU4 short showed a diffused intracellular label both in COS-7 and in HeLa cells, while a more localized distribution, closely mirroring the one observed in single transfection experiments, was found for HsNEU4 long in both cell types. The overlay confirms the results obtained by separate transfections, showing only a partial colocalization for HsNEU4 long and HsNEU4 short.

Results obtained by confocal microscopy were confirmed in subcellular fractionation experiments, shown in Figure 6, yielding a mitochondrial, a microsomal and a cytosolic fraction. HsNEU4 long was found only in the mitochondrial fraction, while the short form was found also in the microsomal fraction, enriched in endoplasmic reticulum membranes. As expected, none of the two proteins was found in the cytosolic fraction. Detection of COX IV, Cnx and 3-phosphoglycerate kinase (PGK) confirmed fractionation efficiency. In order to quantify the relative abundance of HsNEU4 long and HsNEU4 short in mitochondria, these organelles were purified from crude extracts transiently expressing each form of HsNEU4, as described in Materials and methods. This procedure allowed to obtain a highly purified fraction containing heavy mitochondria; only 3.5% of total lysosomes were found in this fraction, as confirmed by activity assay of the lysosomal α-mannosidase (Figure 7C). Western-blot analysis performed with an anti c-myc antibody, showed that only HsNEU4 long is abundantly recovered in the mitochondrial fraction (Figure 7A). A densitometric analysis showed that 66% of HsNEU4 long is found in mitochondria, while only 13% of HsNEU4 short is recovered in this fraction (Figure 7B). The partial recovery of HsNEU4 long

is accounted for by the fact that most of the small mitochondria are normally lost in the supernatant during the centrifugation. The inner mitochondrial membrane complex COX IV was used as a loading control for mitochondrial fraction and to normalize densitometric data. The apparently high content of HsNEU4 short in the mitochondrial fraction shown in Figure 6 is due to the fact that the same quantities of total proteins of all subcellular fractions were loaded onto the gel. However, when the same volumes of total extract and purified mitochondria were evaluated for both the short and the long form, as done in the experiment reported in Figure 7, results clearly showed that most HsNEU4 long is found in mitochondria, while only a small fraction of HsNEU4 short localizes in these organelles. The different amount of mitochondria analysed in these two experiments was also indicated by intensity of COX IV band, which is higher in Figure 6 than in Figure 7.

Submitochondrial fractionation shows that HsNEU4 long is bound to the outer mitochondrial membrane

To further analyse the submitochondrial localization of HsNEU4 long, heavy mitochondria from COS-7 cells expressing this sialidase were purified as described above and then lysed with 2% CHAPS, yielding a pellet containing the mitochondrial membranes and a supernatant representing the soluble fraction. These samples were subsequently subjected to SDS-PAGE, followed by Western-blotting with an anti c-myc antibody. Results, reported in Figure 8A, showed that HsNEU4 long form is bound to mitochondrial membranes. The presence of VDAC1, a porin which is found inside the outer mitochondrial membrane, demonstrated that mitochondria are purified undamaged, carrying both outer and inner membranes. Moreover, sialidase activity performed on the same mitochondrial fractions showed that about 95% of the total enzyme activity is membrane associated (Figure 8B).

In order to assess in which of the two mitochondrial membranes HsNEU4 long is located, isolated intact mitochondria were subjected to osmotic shock (OS) and treated with trypsin at different concentrations. This treatment partially removes the outer mitochondrial membrane, as previously demonstrated (Noma *et al.* 2001). Crude extracts obtained from whole mitochondria (- OS) and mitoplasts (+ OS) were subjected to SDS-PAGE followed by Western-blotting (Figures 8C and 8D). The peripheral outer membrane protein TOMM22, the peripheral inner membrane protein TIMM50 and the mitochondrial matrix enzyme SOD2 were used as controls. As expected for a peripheral outer membrane protein, Figure 8D shows that there is a decrease in intensity for TOMM22 band already in the presence of 10 µg/ml trypsin in intact mitochondria (- OS) as well as in mitoplasts (+ OS). Moreover, a fragment is also detectable in the case of TOMM22 as a result of a partial trypsin digestion. HsNEU4 long was proteolysed in the same manner in intact (- OS) as well as in osmotically shocked (+ OS) mitochondria, highlighting a behaviour similar to TOMM22.

On the other hand, peripheral inner membrane protein TIMM50, due to its localization, appeared to be less susceptible to trypsin treatment in intact mitochondria, showing a decrease in band intensity only at 25 µg/ml trypsin. When trypsin treatment was performed on mitoplasts, TIMM50 became more accessible to the protease and was found to be already degraded at 10 µg/ml trypsin. Moreover, in agreement with its localization in the matrix, SOD2 was found to be unaffected by tryptic digestion in all conditions. Finally, as shown in Figure 8C, both TOMM22 and HsNEU4 long showed the same behaviour in being partially released during osmotic shock and recovered in the supernatant, unlike TIMM50. On the whole HsNEU4 long behaviour closely mirrored that of the outer membrane protein TOMM22, strongly suggesting an outer mitochondrial membrane localization for this sialidase.

Discussion

Although all human sialidases share a high primary structure similarity (ranging from 42 to 70%), some (the lysosomal sialidase NEU1 complex and the cytosolic sialidase NEU2) are soluble, while others (NEU4 and NEU3) are membrane associated. However, no apparent structural differences account for their different subcellular localizations and solubilities. No membrane binding motives, such as GPI anchors, miristoylation or palmitoylation sites, are evident from NEU4 and NEU3 primary structure analysis. Moreover, a potential transmembrane domain, predicted in NEU4 primary structure by TMPred and TMHMM servers, cannot fit into the β-propeller three dimensional structure, yielded by homology modelling (Magesh *et al.* 2006), performed using HsNEU2 crystallographic structure as a template (Chavas *et al.* 2005). Therefore the mechanism through which sialidases HsNEU3 and HsNEU4 are anchored to the membrane is still unclear. Moreover, as regards human sialidase NEU4, different and contrasting subcellular localizations had been previously suggested for its two forms (Monti *et al.* 2004, Seyrantepe *et al.* 2004, Yamaguchi *et al.* 2005). Yamaguchi and colleagues demonstrated mitochondrial localization for NEU4 long and intracellular membrane localization for NEU4 short (Yamaguchi *et al.* 2005). On the other hand Seyrantepe and colleagues (Seyrantepe *et al.* 2004) claimed that NEU4 is a lysosomal enzyme and recently showed that mice deficient in NEU4 exhibit abnormal ganglioside catabolism and lysosomal storage (Seyrantepe *et al.* 2008).

We therefore undertook this work with the aim of elucidating membrane anchoring and subcellular localization of NEU4 long and NEU4 short and gain some insight into the function of this sialidase.

In the first part of this work, we showed that NEU4 is recovered in the aqueous phase after treatment with Triton X-114, clearly ruling out the possibility of it being an integral membrane protein. This result indirectly confirms that HsNEU4 folds into a β-propeller

structure, which disrupts the only possible transmembrane domain. Moreover, NEU4 complete solubilisation in the aqueous phase also rules out any possible interaction with membrane lipids, in accordance with primary structure analysis, suggesting that membrane proteins are involved in NEU4 anchoring. This is well in accordance with NEU4 partial solubilisation obtained after alkaline treatment with sodium carbonate, that shows it to be, at least in part, an extrinsic membrane protein, as already demonstrated for HsNEU3 (Zanchetti *et al.* 2007). However its interaction with the membrane is apparently stronger than that of the EEA1 protein, which is readily and completely solubilised by carbonate treatment. Reversible cross-linking experiments with PFA strongly suggests that both forms of HsNEU4 are associated to the membrane through protein-protein interactions. All these experiments yielded the same results for both NEU4 long and NEU4 short, showing that both forms interact with the membrane through the same anchoring mechanism, despite their different subcellular localizations. This in turn shows that the first 12 aminoacids, which are lacking in NEU4 short, are not responsible for membrane anchoring, although they might play a role in cellular sorting.

The confocal microscopy studies on COS-7 cells transiently transfected with HsNEU4 long, reported in this work, clearly show that this enzyme colocalizes with mitochondria, as previously suggested by Yamaguchi and coworkers (Yamaguchi *et al.* 2005). Instead, in contrast to what reported by Seyrantepe (Seyrantepe *et al.* 2004, Seyrantepe *et al.* 2008), no appreciable colocalization with lysosomes was observed in our experiments. Using the same experimental approach, we also showed that HsNEU4 short is found in intracellular membranes, but does not colocalize with lysosomes. A diffused intracellular fluorescence, well superimposing with Calnexin fluorescence strongly suggests that this enzyme is located in the endoplasmic reticulum, as previously suggested (Monti *et al.* 2004, Yamaguchi *et al.* 2005). The different subcellular localizations of the two forms is not restricted to a single

cellular type, as shown by experiments performed on HeLa cells. Moreover, it not due to an over-expression artifact, as demonstrated by the fact that it does not change when both NEU4 forms are coexpressed, nor when each of them is expressed at lower levels, after shorter post-transfection times.

Our subcellular fractionation experiments confirmed confocal microscopy results: HsNEU4 long was found in the mitochondrial fraction, while HsNEU4 short was also detected in the microsomal fraction. None of these two sialidases was detected in the cytosolic fraction. In order to remove contaminating lysosomes as much as possible, Western-blottings were performed also on isolated mitochondria. The employed fractionation procedure has been reported to yield a highly purified mitochondrial fraction and control enzyme activity assays showed the presence of only 3.5% contaminant lysosomes. Thus, although HsNEU4 long presence in lysosomes cannot be completely ruled out, its predominant localization is beyond any doubt in mitochondria. Our data are therefore in contrast with those of Seyrantepe and coworkers (Seyrantepe *et al.* 2004, Seyrantepe *et al.* 2008), who found a predominantly lysosomal localization of NEU4, although their activity assays performed after subfractionation of transfected COS-7 cells, also showed a partial colocalization with mitochondrial and microsomal fractions. These authors also found (Seyrantepe *et al.* 2008) that transfection of cells from sialidosis patients with NEU4 expression vectors decreased lysosomal storage, yielding a 25% of transfected cells with normal lysosomes. Moreover they observed a only 30% reduction of sialidase activity in lysosomes from NEU4 knock-out mice and a lysosomal storage phenotype only in lungs and spleen cells. Although these results may suggest a role for NEU4 in lysosomal degradation of gangliosides, the lack of NEU1 involvement in the process cannot be easily explained. In fact, NEU4 knock-out mice still possess a functional lysosomal NEU1 complex, actively degrading sialic acid containing

compounds. Moreover, mutations of this enzyme only have been demonstrated beyond any reasonable doubt to cause sialidosis (de Geest *et al.* 2002).

Although our data suggest that HsNEU4 short is found primarily in the endoplasmic reticulum, a partial localization at mitochondrial level is also apparent; the first 12 aminoacids seem likely to be involved in mitochondrial sorting, as already suggested (Yamaguchi *et al.* 2005), although a longer tract, approximately 30 aminoacids from the N-terminus, would be required for this localization, according to the prediction programs MITOPROT and signalP. On the whole it can be said that the sequence required for correct mitochondrial localization is probably longer than 12 aminoacids, but the lack of the first 12 aminoacids is sufficient to impair translocation to mitochondria.

When isolated mitochondria were subfractionated into a soluble fraction and a membranes containing pellet, HsNEU4 long was found only in the pellet, confirming its features of membrane bound enzyme. In addition, the application of a further mitochondrial subfractionation provided evidence for HsNEU4 long localization in the outer mitochondrial membrane, since this enzyme behaves exactly as the outer mitochondrial membrane protein TOMM22. When mitoplasts were prepared through osmotic shock removing the outer mitochondrial membrane, both proteins were partially solubilised. Moreover, the fact that they were degraded by trypsin to the same extent in whole mitochondria and in mitoplasts suggests that NEU4 long accessibility to this protease does not change upon removal of the outer mitochondrial membrane. Moreover, incomplete degradation of HsNEU4 long by trypsin both in whole mitochondria and in mitoplasts suggests that this sialidase is tightly anchored to the membrane and only partially accessible to trypsin. On the contrary, a different behaviour was observed in the case of the inner mitochondrial membrane protein TIMM50, which, unlike fully accessible TOMM22, was found to be susceptible to trypsin treatment only when the outer membrane was partially destroyed after osmotic shock. Our data are

consistent with those obtained by Yamaguchi and coworkers (Yamaguchi *et al.* 2005) in Percoll density gradient centrifugation, where about 70% of sialidase activity was recovered in the outer mitochondrial membrane fraction. Cross-linking experiments, performed in this work, will be the basis for a future purification and characterization of membrane proteins interacting with NEU4.

Another issue still to be elucidated is the role of NEU4 sialidase. It seems likely that this lowly expressed, selectively located sialidase must have a specific function, different from the main degradative role of the lysosomal sialidase NEU1. A role in signal transduction connected to apoptosis has been already proposed for mitochondrial NEU4 (Yamaguchi *et al.* 2005), as a modulator of GD3 levels. Moreover, Hasegawa and coworkers (Hasegawa *et al.* 2007) demonstrated that in SH-SY 5Y cell lines HsNEU4 long expression was decreased prior to catechol metabolites induced apoptosis, that ganglioside GD3 was targeted to mitochondria during apoptosis and that an inhibitor of glucosylceramide synthase was able to partially recover cell viability. The same research group found that NEU4 expression was markedly decreased in colon cancer, while it was subjected to an early up-regulation during apoptosis (Yamanami *et al.* 2007). More recently, a paper has been published showing that mouse Neu4 plays an important regulatory role in neurite formation, likely through desialylation of glycoproteins (Shiozaki, K *et al.* 2009). All these data suggest a role in apoptosis for NEU4, through its action on GD3 ganglioside, as well as in neurite differentiation.

Still obscure is the role of the short form of this enzyme. An accurate characterization of the kinetic properties of both the short and the long form of the enzyme, when affecting gangliosidic and glycoproteic substrates, will be necessary to shed light on this point.

Materials and methods

Antibodies

Mouse anti-c-myc mAb and rabbit anti-Caveolin-1 pAb, for Western-blotting experiments, were purchased from Santa Cruz Biotechnology. Mouse anti-PDI mAb was from Stressgene and mouse anti-EEA1 mAb from BD Biosciences. Rabbit anti-Calnexin, anti-VDAC1/Porin, anti-COX IV and anti-Superoxide Dismutase 2 pAbs, goat anti-TIMM50 pAb and mouse anti-TOMM22 [1C9-2] mAb were obtained from Abcam. Mouse anti-PGK mAb was purchased from Molecular Probes. Goat anti-mouse and rabbit anti-goat IgG HRP-conjugated antibodies were from Calbiochem. Goat anti-rabbit IgG HRP-conjugated antibody was from Biorad. For immunofluorescence staining, mouse anti-HA mAb was from Santa Cruz Biotechnology, rabbit anti-c-myc pAb from Sigma and mouse anti-cytochrome *c* mAb from Promega Corporation. Mouse anti-LAMP1 and anti-Calnexin mAbs were from BD Biosciences. Donkey anti-rabbit Cy3- and anti-mouse Cy2-conjugated antibodies were purchased from Jackson ImmunoResearch Laboratories. Dulbecco's Modified Eagle's Medium (DMEM), fetal bovine serum (FBS), L-glutamine, penicillin and streptomycin were obtained from Lonza. All other reagents were purchased from Sigma.

Vectors

cDNA encoding the long form of HsNEU4 was amplified by PCR using oligonucleotide primers HNEU4-EcoRI-F (5'-GGAATTCATGATGAGCTCTGCAGCCTTCC-3') and HNEU4-XbaI-R (5'-GTCTAGAGGAGGGCCAGCAGCACCC-3'), *Pfu* Turbo DNA-polymerase (Stratagene) and HsNEU4 long in pCDNA3x(+)HA (Invitrogen) as template. The resulting PCR product was subcloned into pcDNA3.1/*myc*-His expression vector (Invitrogen) to obtain HsNEU4 long fused in C-terminal with c-myc epitope and a polyhistidine tag, to be used for recognition purposes. HsNEU4 short cDNA was generated by PCR deletion of the

sequence encoding the additional 12 amino acid residues at N-terminal of NEU4 long form. Mutagenesis was performed using Quick-Change Site-directed Mutagenesis Kit (Stratagene), according to the manufacturer's guidelines; specific primers were used, together with pcDNA3.1/*myc*-His-HsNEU4 long or pCDNA3x(+)HA-HsNEU4 long plasmid as a template, in order to obtain HsNEU4 short fused in C-terminal with c-myc epitope and a polyhistidine tag or in N-terminal with HA epitope, respectively. HsNEU4 long and HsNEU4 short sequences were confirmed by automated sequencing using vector and gene-specific primers (T7 and BGH for plasmid and NEU4-INT 5'-CGCCGCGCGCCTCTGCTG-3' for NEU4 insert).

Cell cultures and transfection

COS-7 and HeLa cells were cultured using DMEM supplemented with 10% (v/v) FBS, 4 mM L-glutamine, 100 U/ml penicillin and 100 µg/ml streptomycin and maintained at 37°C in a humidified 5% CO_2 incubator. Cells, cultured in 100 mm cell culture dishes (seeded at 6×10^5 cells/dish) or onto glass coverslips (seeded at 2.5×10^4 cells/coverslip), were transiently transfected with NEU4 expressing vectors in serum-free medium using FuGene6 reagent (Roche), according to the manufacturer's instructions. After transfection, cells were grown for 24-36 h in complete medium and then processed for NEU4 expression analysis. Cell viability before and after transfection was carried out using MTT assay (Sigma), according to the manufacturer's protocol. Transfection efficiency was evaluated with beta-galactosidase assay, according to the manufacturer's protocol.

Triton X-114 phase separation

Membrane solubilisation with Triton X-114 was performed as described (Bordier 1981). Briefly, 24 h after transfection, COS-7 cells were washed twice with cold PBS, harvested by

scraping and collected at 800 *g* for 10 min at 4°C. Cells were lysed by 5 sec probe sonication (Bandelin Sonoplus 2070 sonicator) in 10 mM Tris-HCl, pH 7.4, 150 mM NaCl, supplemented with proteases inhibitor cocktail (Roche), and then centrifuged at 800 *g* for 10 min at 4°C. The resulting crude extract was diluted in 100 µl of the above buffer to yield a final protein concentration of 1.0 mg/ml. Protein extraction was performed by addition to the sample of a corresponding volume of 2% (v/v) precondensed Triton X-114 in 10 mM Tris-HCl, pH 7.4, 150 mM NaCl, followed by incubation for 1 h on ice. Detergent-extracted samples (200 µl) were then layered onto a cushion of 6% (w/v) sucrose, 10 mM Tris-HCl, pH 7.4, 150 mM NaCl, 0.06% (v/v) Triton X-114 (300 µl), incubated 3 min at 30°C and centrifuged at 300 *g* for 3 min at room temperature. After centrifugation, the upper aqueous phase was removed and treated again with 1% (v/v) fresh Triton X-114. A second phase separation was then performed as above using the same sucrose cushion. Finally, the detergent and aqueous phases were adjusted to the same final volume with 10 mM Tris-HCl, pH 7.4, 150 mM NaCl. Aliquots of the starting sample and separated phases were subjected to sialidase activity assay and analysed by Western-blotting for detection of HsNEU4 and endogenous protein markers, Caveolin-1 (as an integral membrane protein) and PDI (as a soluble protein).

Sodium carbonate extraction

Sodium carbonate extractions were performed as described (Fujiki *et al.* 1982). Briefly, 36 h after transfection, COS-7 cells were washed twice with cold PBS, harvested by scraping and then collected by centrifugation at 800 *g* for 10 min at 4°C. Cells were suspended in ice-cold 10 mM Tris-HCl, pH 7.5, containing a proteases inhibitor cocktail (Roche) and sonicated at the minimum setting for 5 sec. After centrifugation at 800 *g* for 10 min at 4°C, the supernatant (crude extract) was centrifuged at 100,000 *g* for 1 h at 4°C to collect total cell membranes.

The pellet was resuspended in lysis buffer and then split into identical aliquots. To obtain peripheral protein extraction, membrane samples were then treated with an equal volume either of ice-cold 0.2 M Na_2CO_3, pH 12.0 or 10 mM Tris-HCl, pH 7.5, 3 M NaCl or lysis buffer alone, as a control, and incubated for 30 min on ice. After centrifugation at 100,000 *g*, pellets were resuspended in the appropriate buffer to yield the membrane fractions, while the supernatants represented the soluble fractions. Samples containing sodium carbonate were quickly brought to pH 7.5 by the addition of acetic acid. Finally, soluble and membrane fractions were adjusted to the same final volume and then subjected to sialidase activity assay and Western-blotting for detection of HsNEU4 and endogenous markers, Caveolin-1 (as an integral membrane protein) and EEA1 (as a peripheral membrane protein).

Cross-linking with paraformaldehyde

Paraformaldehyde cross-linking was performed in transfected cells as described (Vasilescu *et al.* 2004). Briefly, 24 h after transfection, COS-7 cells were treated with 0.25-1.0% (w/v) paraformaldehyde (PFA) in PBS for 5-60 min at 37°C. The cross-linking reaction was quenched with glycine to a final concentration of 125 mM, for 5 min at room temperature. Cells harvested by scraping were collected at 800 *g* for 10 min at 4°C, washed twice with PBS and resuspended in lysis buffer (50 mM Tris pH 7.5, 150 mM NaCl, 10% glycerol, 1% NP-40, 5 mM EDTA) containing the Roche proteases inhibitor cocktail. After an incubation of 30 min on ice, cell lysate was centrifuged at 18,000 *g*, to pellet cell debris. Prior to SDS-PAGE, cell extract was heated in Sample Buffer for 10 min at 65°C for complexes analysis or boiled for 20 min at 95°C to reverse the formaldehyde cross-links. Aliquots of PFA-treated cell extracts, before and after subjecting them to cross-link reversal condition, were analysed by Western-blotting with anti-c-myc antibody for detection of HsNEU4.

Confocal immunofluorescence microscopy

For indirect immunofluorescence staining, COS-7 and HeLa cells were cultured onto glass-coverslips and transfected with NEU4 expressing vectors; 24 h after transfection, cells were briefly washed in PBS, fixed with 3% (w/v) paraformaldehyde (PFA) in PBS for 20 min at room temperature or in methanol for 5 min at -20°C. PFA reaction was quenched by treatment with 50 mM NH_4Cl in PBS for 30 min. Fixed cells were washed three times with PBS and then permeabilized with 0.3% Saponin (w/v) in PBS (PBS-Sap) for 20 min and double-stained at room temperature with anti-c-myc and anti-cytochrome *c*, anti-LAMP1 or anti-Calnexin antibodies at appropriated dilutions in PBS-Sap for 1 h. After incubation, cells were washed three times in the same buffer and then double-stained with Cy2- and Cy3-conjugated secondary antibodies as above. After washes with PBS-Sap and PBS, coverslips were mounted using DakoCytomation Fluorescent Mounting Medium (DAKO). Slides were examined with a Leica Mod. TCS-SP2 (Leica Microsystem) confocal microscopy and images were processed with Leica Confocal software (LCS.EXE) and Adobe Photoshop software.

Subcellular fractionation

36 h after transfection, COS-7 cells were washed twice with cold PBS and lysed on plate using fractionation buffer (20 mM HEPES, pH 7.4, 250 mM sucrose, 10 mM KCl, 1.5 mM $MgCl_2$, 1 mM EDTA and 1 mM EGTA), containing a proteases inhibitor cocktail (Roche) and 1 mM DTT. Cell lysate was then passed through a 25 G needle 10 times, leaved for 20 min on ice and centrifuged at 800 *g* for 5 min at 4°C to remove nuclei and unbroken cells. The post-nuclear supernatant was centrifuged at 10,000 *g* for 15 min at 4°C to collect mitochondria and then at 100,000 *g* for 1 h to obtain microsomal and cytosolic fractions. Mitochondrial and microsomal pellets were washed with fractionation buffer, resuspended by pipetting, passed through a 25 G needle 10 times and then recentrifuged as above. After centrifugation, wash

buffer was removed and pellets were resuspended in buffer containing 10% glycerol and 0.1% SDS. Mitochondrial, microsomal and cytosolic fractions were subjected to Western-blotting for detection of HsNEU4 and endogenous markers, COX IV (as mitochondrial protein), Calnexin (as ER protein) and PGK (as cytosolic protein).

Mitochondria extraction and fractionation

24 h after transfection, COS-7 cells (2×10^7) were washed twice with cold PBS, harvested by scraping and collected at 800 *g* for 10 min at 4°C. Mitochondria isolation was performed using Mitochondria Isolation Kit for Cultured Cells (Pierce) following the reagent-based method, according to the manufacturer's instructions. Briefly, the post-nuclear supernatant (total extract), obtained after cell lysis, was centrifuged at 3,000 *g* for 15 min at 4°C to collect a purified fraction of mitochondria. The mitochondrial pellet was lysed with 2% CHAPS in PBS by vortexing and centrifuged at maximum speed to obtain membrane (pellet) and soluble (supernatant) fractions. Aliquots of the post-nuclear supernatant, total mitochondria and submitochondrial fractions were analysed by Western-blotting for detection of HsNEU4 and mitochondrial markers, VDAC1/Porin (outer membrane), COX IV (inner membrane) and SOD2 (matrix). To assess the purity of the mitochondrial fraction, lysosomal α-mannosidase was assayed as described (Opheim and Touster 1978).

Mitoplasts isolation and protease treatment

Submitochondrial fractionation was performed as described (Noma *et al.* 2001). For preparation of mitoplasts (mitochondria devoid of their external membrane), intact mitochondria were subjected to osmotic shock, by resuspension in 20 mM Hepes/KOH, pH 7.4 followed by incubation for 30 min on ice. Mitoplasts were recovered by centrifugation at 4,000 *g* and then resuspended in 10 mM Hepes/KOH, pH 7.4, 220 mM mannitol, 70 mM

sucrose. As a control, whole mitochondria were incubated in an isotonic buffer (10 mM Hepes/KOH, pH 7.4, 220 mM mannitol, 70 mM sucrose) for 30 min on ice and centrifuged as described above. Samples of mitochondria and mitoplasts were treated with trypsin at a final concentration of 0, 10 and 25 µg/ml for 20 min on ice. Reactions were stopped by adding PMSF at a final concentration of 0.4 mg/ml and a proteases inhibitor cocktail. After incubation for 5 min on ice, the samples were centrifuged at 12,000 *g* for 10 min at 4°C, and the pellets were analysed by Western-blotting for detection of HsNEU4 and mitochondrial markers, TOMM22 (outer membrane), TIMM50 (inner membrane) and SOD2 (matrix).

SDS-PAGE and Western-blotting

Protein concentration of samples was determined by the Bradford assay (Bradford 1976) using Coomassie Plus - The Better Bradford™ Assay Kit (Pierce). Protein samples were separated by 12% SDS-PAGE and transferred to a PVDF Immobilon-P (Millipore) membrane. Membranes were blocked with 5% (w/v) dried milk in PBS for 30 min at room temperature and then incubated overnight at 4°C with appropriate dilutions of antibodies in 1% (w/v) dried milk in PBS (for anti-c-myc, anti-EEA1, anti-Cav-1 and anti-PDI antibodies) or 5% (w/v) bovine serum albumin (BSA) in PBS (for anti-Cnx, anti-PGK, anti-VDAC1, anti-SOD2, anti-COX IV, anti-TOMM22 and anti-TIMM50 antibodies). After three washes (10 min each) with PBS containing 0.1% (v/v) Tween 20 (PBS-T), membranes were treated for 1 h at room temperature with HRP-conjugated secondary antibody diluted in 1% (w/v) dried milk in PBS-T (for anti-mouse antibody) or 5% (w/v) dried milk in PBS (for anti-rabbit and anti-goat antibodies). After three washes in PBS-T, detection was performed using ECL plus detection system (Millipore). Protein levels were quantified by densitometry of immunoblots using the NIH Image-based software Scion Image (Scion Corporation).

Sialidase activity assay

NEU4 enzymatic activity was determined with 4MU-NeuAc (Sigma) as a substrate (Monti *et al.* 2004). Briefly, reactions were set up in triplicate using 30 µg of total proteins in 25 mM Na citrate/phosphate buffer, pH 3.2, 0.1 mM 4MU-NeuAc, 6 mg/ml BSA, in a final volume of 100 µl. After incubation for 30 min at 37°C, reactions were stopped by adding 1.5 ml of 0.2 M Glycine/NaOH, pH 10.8. The amount of sialic acid released was evaluated by spectrofluorimetric measurement of the 4-methylumbelliferone released.

Funding

This work was supported by MIUR-PRIN (grant 2006) to G.T., E.M. and P.F. and *Fondazione Cariplo* (grant 2006) to E.M.

Acknowledgements

We thank Dr. Gabriele Zanchetti (University of Brescia) for his technical support in the solubilisation experiments, and Prof. Roberto Bresciani (University of Brescia) and Dr. Anna Maria Villa (University of Milan-Bicocca) for guidance in the confocal microscopy experiments.

Abbreviations

4MU-NeuAc, 4-methylumbelliferyl-N-acetyl-α-D-neuraminic acid; BSA, bovine serum albumin; Cav-1, Caveolin-1; CHAPS, 3-[(3-Cholamidopropyl)dimethylammonio]-1-propanesulfonate; Cnx, Calnexin; COX IV, cytochrome *c* oxidase; cyt *c*, cytochrome *c*; DAKO, DakoCytomation Fluorescent Mounting Medium; DMEM, Dulbecco's Modified Eagle's Medium; ECL, Enhanced Chemioluminescence; EDTA, ethylenediaminetetraacetic acid; EEA1, Early Endosomal Antigen 1; EGTA, ethylene glycol tetraacetic acid; DTT, dithiothreitol; FBS, fetal bovine serum; GPI, glycosylphosphatidylinositol; HRP, horseradish peroxidase; HsNEU1, Homo sapiens sialidase NEU1; HsNEU2, Homo sapiens sialidase NEU2; HsNEU3, Homo sapiens sialidase NEU3; HsNEU4, Homo sapiens sialidase NEU4; LAMP-1, Lysosome-Associated Membrane Protein 1; MTT, [3-(4,5-dimethylthiazol-2-yl)-2,5-diphenyl tetrazolium bromide]; PBS, phosphate buffered saline; PBS-Sap, 0.3% saponin in PBS; PBS-T, PBS containing 0.1% Tween 20; PDI, Protein Disulfide-Isomerase; PFA, paraformaldehyde; PGK, 3-phosphoglycerate kinase ; PMSF, phenylmethylsulfonyl fluoride; PVDF, polyvinylidine difluoride; SDS-PAGE, sodium dodecyl sulfate-polyacrylamide gel electrophoresis; SOD2, Superoxide Dismutase 2; TIMM50, Translocase of Inner Mitochondrial Membrane, subunit 50; TOMM22, Translocase of Outer Mitochondrial Membrane, subunit 22; VDAC1/Porin, Voltage-Dependent Anion Channel.

References

Bordier C. 1981. Phase separation of integral membrane proteins in Triton X-114 solution. *J Biol Chem.* 256(4):1604-1607.

Bradford MM. 1976. A rapid and sensitive method for the quantitation of microgram quantities of protein utilizing the principle of protein-dye binding. *Anal Biochem.* 72:248-254.

Chavas LM, Tringali C, Fusi P, Venerando B, Tettamanti G, Kato R, Monti E, Wakatsuki S. 2005. Crystal structure of the human cytosolic sialidase Neu2. Evidence for the dynamic nature of substrate recognition. *J Biol Chem.* 280(1):469-475.

Crennell SJ, Garman EF, Laver WG, Vimr ER, Taylor GL. 1993. Crystal structure of a bacterial sialidase (from Salmonella typhimurium LT2) shows the same fold as an influenza virus neuraminidase. *Proc Natl Acad Sci U S A.* 90(21):9852-9856.

de Geest N, Bonten E, Mann L, de Sousa-Hitzler J, Hahn C, d'Azzo A. 2002. Systemic and neurologic abnormalities distinguish the lysosomal disorders sialidosis and galactosialidosis in mice. *Hum Mol Genet.* 11(12):1455-1464.

Fang Y, Wu G, Xie X, Lu ZH, Ledeen RW. 2000. Endogenous GM1 ganglioside of the plasma membrane promotes neuritogenesis by two mechanisms. *Neurochem Res.* 25(7):931-940.

Fujiki Y, Hubbard AL, Fowler S, Lazarow PB. 1982. Isolation of intracellular membranes by means of sodium carbonate treatment: application to endoplasmic reticulum. *J Cell Biol.* 93(1):97-102.

Hasegawa T, Yamaguchi K, Wada T, Takeda A, Itoyama Y, Miyagi T. 2000. Molecular cloning of mouse ganglioside sialidase and its increased expression in neuro2a cell differentiation. *J Biol Chem.* 275(11):8007-8015.

Hasegawa T, Sugeno N, Takeda A, Matsuzaki-Kobayashi M, Kikuchi A, Furukawa K, Miyagi T, Itoyama Y. 2007. Role of Neu4L sialidase and its substrate ganglioside GD3 in neuronal apoptosis induced by catechol metabolites. *FEBS Lett.* 581(3):406-412.

Kakugawa Y, Wada T, Yamaguchi K, Yamanami H, Ouchi K, Sato I, Miyagi T. 2002. Up-regulation of plasma membrane-associated ganglioside sialidase (Neu3) in human colon cancer and its involvement in apoptosis suppression. *Proc Natl Acad Sci U S A.* 99(16):10718-10723.

Kopitz J, Muhl C, Ehemann V, Lehmann C, Cantz M. 1997. Effects of cell surface ganglioside sialidase inhibition on growth control and differentiation of human neuroblastoma cells. *Eur J Cell Biol.* 73(1):1-9.

Magesh S, Suzuki T, Miyagi T, Ishida H, Kiso M. 2006. Homology modeling of human sialidase enzymes NEU1, NEU3 and NEU4 based on the crystal structure of NEU2: Hints for the design of selective NEU3 inhibitors. *J Mol Graph Model.* 25(2):196-207.

Monti E, Bassi MT, Papini N, Riboni M, Manzoni M, Venerando B, Croci G, Preti A, Ballabio A, Tettamanti G, Borsani G. 2000. Identification and expression of NEU3, a novel human sialidase associated to the plasma membrane. *Biochem J.* 349(Pt 1):343-351.

Monti E, Preti A, Venerando B, Borsani G. 2002. Recent development in mammalian sialidase molecular biology. *Neurochem Res.* 27(7-8):649-663.

Monti E, Bassi MT, Bresciani R, Civini S, Croci GL, Papini N, Riboni M, Zanchetti G, Ballabio A, Preti A, Tettamanti G, Venerando B, Borsani G. 2004. Molecular cloning and characterization of NEU4, the fourth member of the human sialidase gene family. *Genomics.* 83(3):445-453.

Mu FT, Callaghan JM, Steele-Mortimer O, Stenmark H, Parton RG, Campbell PL, McCluskey J, Yeo JP, Tock EP, Toh BH. 1995. EEA1, an early endosome-associated protein. EEA1 is a conserved alpha-helical peripheral membrane protein flanked by cysteine "fingers" and contains a calmodulin-binding IQ motif. *J Biol Chem.* 270(22):13503-13511.

Noma T, Fujisawa K, Yamashiro Y, Shinohara M, Nakazawa A, Gondo T, Ishihara T, Yoshinobu K. 2001. Structure and expression of human mitochondrial adenylate kinase targeted to the mitochondrial matrix. *Biochem J.* 358(Pt 1):225-232.

Opheim DJ, Touster O. 1978. Lysosomal α-D-mannosidase of rat liver. Purification and comparison with the golgi and cytosolic alpha-D-mannosidases. *J Biol Chem.* 253(4):1017-1023.

Rodriguez JA, Piddini E, Hasegawa T, Miyagi T, Dotti CG. 2001. Plasma membrane ganglioside sialidase regulates axonal growth and regeneration in hippocampal neurons in culture. *J Neurosci.* 21(21):8387-8395.

Saito M, Yu RK. 1995. Biochemistry and function of Sialidases. In: Rosenberg A editor. Biology of the Sialic Acids. New York (NY): Plenum Press. p. 261-313.

Sasaki A, Hata K, Suzuki S, Sawada M, Wada T, Yamaguchi K, Obinata M, Tateno H, Suzuki H, Miyagi T. 2003. Over-expression of plasma membrane-associated sialidase attenuates insulin signaling in transgenic mice. *J Biol Chem.* 278(30):27896-27902.

Seyrantepe V, Landry K, Trudel S, Hassan JA, Morales CR, Pshezhetsky AV. 2004. Neu4, a novel human lysosomal lumen sialidase, confers normal phenotype to sialidosis and galactosialidosis cells. *J Biol Chem.* 279(35):37021-37029.

Seyrantepe V, Canuel M, Carpentier S, Landry K, Durand S, Feng L, Zeng J, Caqueret A, Gravel RA, Marchesini S, Zwingmann C, Michaud J, Morales CR, Levade T,

Pshezhetsky AV. 2008. Mice deficient in Neu4 sialidase exhibit abnormal ganglioside catabolism and lysosomal storage. *Hum Mol Genet.* 17(11):1556-1568.

Shiozaki K, Koseki K, Yamaguchi K, Shiozaki M, Narimatsu H, Miyagi T. 2009. Developmental change of sialidase NEU4 expression in murine brain and its involvement in the regulation of neuronal cell differentiation. *J Biol Chem.* 284(32):21157-21164.

Taylor G. 1996. Sialidases: structures, biological significance and therapeutic potential. *Curr Opin Struct Biol.* 6(6):830-837.

Vasilescu J, Guo X, Kast J. 2004. Identification of protein-protein interactions using in vivo cross-linking and mass spectrometry. *Proteomics*. 4(12):3845-3854.

Yamaguchi K, Hata K, Koseki K, Shiozaki K, Akita H, Wada T, Moriya S, Miyagi T. 2005. Evidence for mitochondrial localization of a novel human sialidase (NEU4). *Biochem J*. 390(Pt 1):85-93.

Yamanami H, Shiozaki K, Wada T, Yamaguchi K, Uemura T, Kakugawa Y, Hujiya, Miyagi T. 2007. Down-regulation of sialidase NEU4 may contribute to invasive properties of human colon cancers. *Cancer Sci*. 98(3):299-307.

Zanchetti G, Colombi P, Manzoni M, Anastasia L, Caimi L, Borsani G, Venerando B, Tettamanti G, Preti A, Monti E, Bresciani R. 2007. Sialidase NEU3 is a peripheral membrane protein localized on the cell surface and in endosomal structures. *Biochem J*. 408(2):211-219.

Legends to figures

Fig. 1. Partition of HsNEU4 long and HsNEU4 short proteins during Triton X-114 phase separation. COS-7 cells expressing NEU4 long or short were lysed and total cell extracts were subjected to phase separation with Triton X-114. Aliquots of total extract (T), aqueous phase (AP) and detergent phase (DP) were separated by SDS-PAGE and analysed by Western-blotting. Both NEU4 forms were detected using anti-c-myc antibody. To check separation, antibodies directed against hydrophilic Protein Disulfide Isomerase (PDI) and integral membrane protein Caveolin-1 (Cav-1) were used.

Fig. 2. Extraction of HsNEU4 short and HsNEU4 long upon sodium carbonate treatment. COS-7 cells expressing HsNEU4 long or short were lysed and cell membranes were treated with Tris buffer (Carbonate -) as a control or with sodium carbonate (Carbonate +). **(A)** Equal volumes of input cell membranes (T), membranes (P) and soluble (S) fractions were separated by SDS-PAGE and subjected to Western-blot analysis. NEU4 was detected using anti-c-myc antibody. To assess the accuracy of extraction, antibodies directed against peripheral membrane protein Early Endosomal Antigen 1 (EEA1) and integral membrane protein Caveolin-1 (Cav-1) were used. **(B)** Relative quantification of NEU4 protein level in each fraction compared with input sample. Densitometric analysis was performed using NIH Image-based software Scion Image (Scion Corporation). Quantification data are representative of three independent experiments. **(C)** Sialidase activity determined with 4MU-NeuAc under control condition. Values are means ± SD of three independent experiments.

Fig. 3. Cross-linking with paraformaldehyde and analysis of HsNEU4 containing complexes. COS-7 cells expressing HsNEU4 long or short were treated with 0.25% paraformaldehyde (PFA) for 20 min. In order to assess the presence of NEU4 complexes, cell lysates were

separated by SDS-PAGE, before and after subjecting them to cross-link reversal condition, and then analysed by Western-blotting with anti-c-myc antibody.

Fig. 4. Subcellular localization of HsNEU4 long and HsNEU4 short determined by indirect immunofluorescence staining. COS-7 cells were transiently transfected with HsNEU4 long or short and subjected to immunofluorescence staining and confocal microscopy analysis. **(A)** To analyse mitochondrial localization, COS-7 cells were double-stained with anti-c-myc antibody, for detection of NEU4 short (panel a) or long (panel d), and anti-cytochrome *c* (cyt *c*) antibody (panels b and e) as mitochondrial marker. Overlay images are shown in panels c and f. Scale bars: 20 μm (panel a), 25 μm (panel d). **(B)** To analyse lysosomal localization, COS-7 cells were double-stained with anti-c-myc antibody, for detection of NEU4 short (panel a) or long (panel d), and anti-LAMP-1 antibody (panels b and e) as lysosomal marker. Overlay images are shown in panels c and f. Scale bars: 30 μm (panel a), 15 μm (panel d). **(C)** COS-7 cells were double-stained with anti-c-myc antibody for detection of NEU4 short (panel a) and anti-Calnexin (Cnx) antibody (panel b) as ER marker. Overlay image is shown in panel c. Scale bar: 25 μm.

Fig. 5. Coexpression of HsNEU4 long and HsNEU4 short in COS-7 and HeLa cells evaluated by indirect immunofluorescence staining. COS-7 and HeLa cells were transiently cotransfected with c-myc-tagged HsNEU4 long and HA-tagged HsNEU4 short and subjected to immunofluorescence staining and confocal microscopy analysis. Cells were double-stained with anti-HA and anti-c-myc antibodies, for detection of NEU4 short (panels a and d) or long (panel b and e), respectively. Overlay images are shown in panels c and f. Scale bars: 30 μm (panel a), 25 μm (panel d).

Fig. 6. Intracellular distribution of HsNEU4 long and HsNEU4 short evaluated by subcellular fractionation. COS-7 cells expressing HsNEU4 long or short were lysed and subfractionated in mitochondrial (Mit), microsomal (Mic) and cytosolic (Cyt) fractions. Equal amount of protein were subjected to SDS-PAGE and Western-blotting. Both NEU4 forms were detected using anti-c-myc antibody. Antibody directed against cytochrome *c* oxidase (COX IV), Calnexin (Cnx) and 3-phosphoglycerate kinase (PGK) were used as mitochondrial, microsomal and cytosolic marker, respectively.

Fig. 7. Recovery of HsNEU4 long or HsNEU4 short in a purified heavy mitochondrial fraction. COS-7 cells expressing HsNEU4 long or short were lysed and processed to isolate heavy mitochondrial fraction. **(A)** Aliquots of total extract (TE) and mitochondrial fraction (MF) were subjected to SDS-PAGE and Western-blotting. NEU4 short and long were detected using anti-c-myc antibody. COX IV was used as mitochondrial loading control. **(B)** Relative quantification of NEU4 protein level in mitochondrial fraction compared with total cell extract. NEU4 levels in each fraction were normalized to the corresponding COX IV level. Densitometric analysis was performed using NIH Image-based software Scion Image (Scion Corporation). Quantification data are representative of three independent experiments. **(C)** Lysosomal α-mannosidase activity assayed in total extract (TE) and mitochondrial fraction (MF). Values are expressed as a percentage of enzyme activity as compared with the input crude extract. Data are representative of three independent experiments.

Fig. 8. Submitochondrial localization of the long form of HsNEU4. **(A)** COS-7 cells expressing HsNEU4 long were lysed and processed to isolate heavy mitochondrial fraction. Intact mitochondria were lysed with 2% CHAPS in PBS and then subfractionated to obtain a membrane (P) and a soluble (S) fraction. Aliquots of fractions were subjected to SDS-PAGE

and Western-blotting with anti-c-myc antibody, for NEU4 detection. To control subfractionation, antibodies directed against outer mitochondrial membrane protein VDAC1 and mitochondrial matrix protein SOD2 were used. **(B)** Sialidase activity using 4MU-NeuAc as a substrate assayed in the above submitochondrial fractions. Values are expressed as a percentage of enzyme activity recovered in each fraction as compared with the input sample of mitochondria. Data are representative of three independent experiments. **(C)** Intact heavy mitochondria isolated from COS-7 cells expressing HsNEU4 long were subjected to osmotic shock (OS) in 20 mM Hepes/KOH, pH 7.4, as reported in Materials and methods. Mitochondria (- OS) or mitoplasts (+ OS) are collected through centrifugation and supernatants were analysed by immunoblotting, performed with anti-c-myc antibody. TOMM22 and TIMM50 were used as outer and inner mitochondrial membrane markers, respectively. **(D)** Aliquots of intact (- OS) and osmotically shocked (+ OS) mitochondria were treated with various concentrations (0, 10 and 25 μg/ml) of trypsin. After centrifugation at 12,000 *g*, samples were analysed by SDS-PAGE and Western-blotting with anti-c-myc antibody for NEU4 long detection. TOMM22, TIMM50 and SOD2 were also probed with specific antibodies and used as outer membrane, inner membrane and matrix protein controls, respectively.

Figure 1

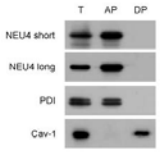

Figure 2

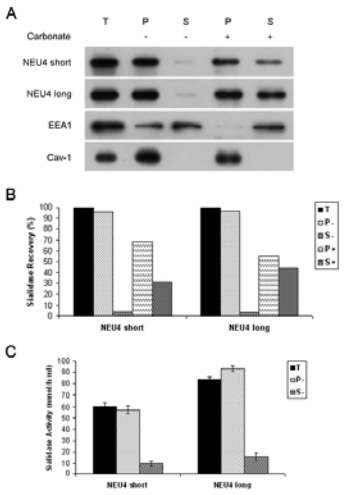
A
T
P
S
P
S
Carbonate
-
-
+
+
NEU4 short
NEU4 long
EEA1
Cav-1
B
Sialidase Recovery (%)
100
90
80
70
60
50
40
30
20
10
0
T
P-
S-
P+
S+
NEU4 short
NEU4 long
C
Sialidase Activity (nmol/h/ml)
100
90
80
70
60
50
40
30
20
10
0
T
P-
S-
NEU4 short
NEU4 long

Figure 3

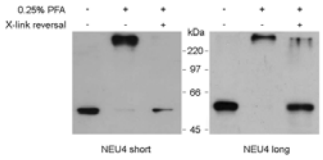

Figure 4

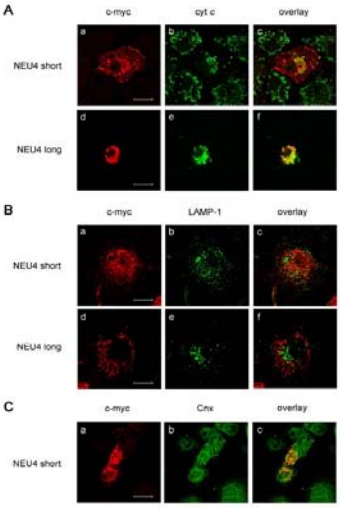
A
c-myc
cyt c
overlay
a
b
c
NEU4 short
d
e
f
NEU4 long
B
c-myc
LAMP-1
overlay
a
b
c
NEU4 short
d
e
f
NEU4 long
C
c-myc
Cnx
overlay
a
b
c
NEU4 short

Figure 5

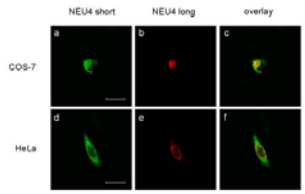

Figure 6

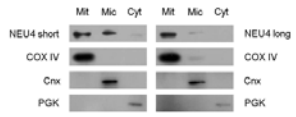
Mit
Mic
Cyt
Mit
Mic
Cyt
NEU4 short
COX IV
Cnx
PGK
NEU4 long
COX IV
Cnx
PGK

Figure 7

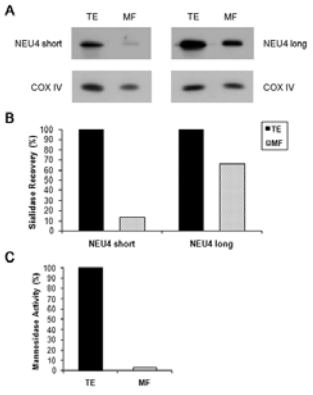
A
TE
MF
TE
MF
NEU4 short
NEU4 long
COX IV
COX IV
B
Sialidase Recovery (%)
TE
MF
NEU4 short
NEU4 long
C
Mannosidase Activity (%)
TE
MF

Figure 8

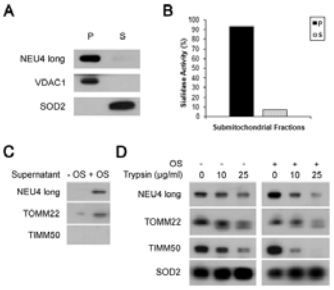
A
P
S
NEU4 long
VDAC1
SOD2
B
Sialidase Activity (%)
Subsitochondrial Fractions
C
Supernatant
- OS
+ OS
NEU4 long
TOMM22
TIMM50
D
OS
Trypsin (µg/ml)
0
10
25
NEU4 long
TOMM22
TIMM50
SOD2